ESKLEROSI ANIZKOITZAREN IL22RA SUSZEPTIBILITATE-GENEAREN ANALISIA

ANALYSIS OF THE MULTIPLE SCLEROSIS SUSCEPTIBILITY GENE IL22RA2

Andoni Urtasun Arricaberri

2023

eman ta zabal zazu

Universidad del País Vasco

Euskal Herriko Unibertsitatea

AURKIBIDEA

Irudien zerrenda

Taulen zerrenda

Laburduren zerrenda

Laburdura	**Esanahia**
1,25(OH)2VD	1,25-dihydroxyvitamin D
AA	amino acid
ANOVA	analysis of variance
AP	acetone precipitation
APC	antigen presenting cell
BBB	blood brain barrier
CDNA	complementary deoxyribonucleic acid
CL	cell lysate
CM	culture medium
CNS	central nervous system
co-IP	co-immunoprecipitation
CSA	cyclosporine A
DAPI	4',5-diamidino-2-phenylindole
DC	dendritic cell
DM	moDC differentiation medium
DMSO	dimethyl sulfoxide
DMT	disease-modifying therapies
DNA	deoxyribonucleic acid
dNTPs	deoxynucleoside triphosphates
DSP	dithiobis succinimidyl propionate
dsRNA	double stranded RNA
EAE	experimental allergic/autoimmune encephalomyelitis
EBI3	Epstein-Barr virus induced gene 3
EBV	Epstein-Barr virus
EDSS	Expanded Disability Status Scale
EDTA	ethylenediamine tetraacetic acid
ELISA	enzyme-linked immunosorbent assay
ER	endoplasmic reticulum
ERAD	endoplasmic reticulum-associated degradation
EST	expressed sequence tag
EV	empty vector
FACS	fluorescence-activated cells sorting
FBS	fetal bovine serum
FSC	forward scatter
FW	forward primer

GA	glatiramer acetate
GBD	Global Burden Disease
GWAS	genome-wide association studies
HERVs	human endogenous retroviruses
HLA	human leucocyte antigen
HRP	horseradish peroxidase
i.e.	in example
ICC	immunocytochemistry
IFNΓ	interferon gamma
IHC	immunohistochemistry
IL	interleukin
IL12A	human interleukin-12 alpha gene
Il12a	mice interleukin-12 alpha gene
IL17SP	signal peptide of interleukin 17A
IL-22BP	human interleukin-22 binding protein
IL-22BPi1	human interleukin-22 binding protein isoform 1
IL-22BPi2	human interleukin-22 binding protein isoform 2
IL-22BPi3	human interleukin-22 binding protein isoform 3
IL22RA2	human interleukin-22 receptor alpha 2 gene
Il22ra2	mice interleukin-22 receptor alpha 2 gene
*IL22RA2*v1	human interleukin-22 receptor alpha 2 gene variant 1
*IL22RA2*v2	human interleukin-22 receptor alpha 2 gene variant 2
*IL22RA2*v3	human interleukin-22 receptor alpha 2 gene variant 3
IMSGC	International MS Genetics Consortium
IP	immunoprecipitation
kDa	kilodalton
KO	knockout
LPS	lipopolysaccharide
M	million
mAb	monoclonal antibodies
MACS	magnetic-activated cell sorting
MD	middle domain
MHC	major histocompatibility complex
MODCS	monocyte-derived dendritic cells
MRNA	messenger ribonucleic acid
MS	multiple sclerosis
m-subAB	mutant subtilase cytotoxine
NBD	nucleotide binding domain
NK	natural killer
ORF	open reading frame
PBMC	peripheral mononuclear cell
PBS	phosphate buffer saline
PCR	polymerase chain reaction

PFA	paraformaldehyde
PPI	peptidyl-porolyl cis-trans isomerase
PPIA	cyclophilins A
PPIB	cyclophilins B
PPIC	cyclophilins C
PPMS	primary progressive multiple sclerosis
qPCR	quantitative polymerase chain reaction
RA	retinoic acid
RNA	ribonucleic acid
RRMS	relapsing-remitting multiple sclerosis
RT-PCR	reverse transcription polymerase chain reaction
RV	reverse primer
SBD	substrate binding domain
SEM	standard error of the mean
SFM	serum free medium
siRNA	small interfering RNA
SNP	single nucleotide polymorphism
SPMS	secondary progressive multiple sclerosis
SSC	side scatter
STAT	signal transducer and activator of transcription
subAB	subtilase cytotoxine
Ta	annealing temperature
TBST	tris-buffered saline, 0.1% Tween 20
Th	T helper
Tm	melting temperature
TNFα	tumor necrosis factor alpha
TR	transfection reagent
TSL	transcript support level
UVA	ultraviolet radiation A
UVB	ultraviolet radiation B
UVC	ultraviolet radiation C
UVR	ultraviolet radiation
vD	vitamin D
WB	western blot

1. ABSTRACT

Multiple sclerosis (MS) is a chronic inflammatory neurological disease whose underlying cause remains uncertain. It is the most common non-traumatic disabling disease affecting young adults and can be influenced by different environmental and genetic factors. We have studied two MS-susceptibility genes, *IL22RA2* and *IL12A*, to better understand their regulation and relationship to MS. We demonstrated that the *IL22RA2* gene gives rise to three isoforms in monocyte-derived dendritic cells (moDCs). Expression of all three isoforms was increased during moDC differentiation and decreased by different maturation stimuli. We also found that $CD14^{++}/CD16^{+}$ intermediate monocytes produced higher levels of *IL22RA2* mRNA than classical and non-classical monocytes. Using transfected human cell lines, we demonstrated that the protein product of *IL22RA2* variant 1 (*IL22RA2v1*), the IL-22BP isoform 1 (IL-22BPi1), was poorly secreted and largely retained in the endoplasmic reticulum (ER). IL-22BPi1 differs from IL-22BPi2 by an in-frame 32-amino acid (AA) insertion encoded by an alternatively spliced exon. We therefore hypothesized that this insertion is important for the retention of IL-22BPi1 in the ER. Adding the 32 AA insertion to an unrelated cytokine, IL-2, resulted in reduced IL-2 secretion and increased ER retention, similar to IL-22bp1. We performed interactome analysis to uncover the mechanism underlying the ER retention of IL-22BPi1 and identified ER chaperones GRP78, GRP94, GRP170 and calnexin as main interactors. Structure-function analysis revealed that, like IL-22BPi2, IL-22BPi1 binds to the substrate-binding domain of GRP78 as well as to the middle domain of GRP94, and thus, we have demonstrated the domain of interaction of IL-22BPi1 and IL-22BPi2 with GRP78 and GRP94. However, only IL-22BPi1 overexpression activated an unfolded protein response (UPR) resulting in increased protein levels of GRP78 and GRP94. Upon silencing of *IL22RA2* expression in moDC, GRP78 levels were significantly reduced, suggesting that native *IL22RA2* expression naturally contributes to upregulated GRP78 levels in these cells. The *IL22RA2* alternatively spliced exon was reported to be recruited through a single mutation in the proto-splice site of a Long Terminal Repeat retrotransposon sequence in the ape lineage. Our work suggests that positive selection of IL-22BPi1 was not driven by IL-22

antagonism, as is the case for IL-22BPi2 and IL-22BPi3, but by capacity for induction of an UPR response. Finally, we demonstrated that another variant apart from the canonical *IL12A* was expressed in moDCs and in different immune and epithelial cells lines. Altogether, our work highlights the relevance of the study of splicing variants of MS susceptibility genes for a better understanding of the effect of the genetic factors in the disease.

2. SARRERA

2.1. Multiple sclerosis

Sarrera honen helburua esklerosi anizkoitza (ingeleraz, multiple sclerosis (MS)) eta lan hau ulertzeko funtsezkoak diren hainbat alderdi azaltzea da. Esklerosi anizkoitzaren izaeratik hasi eta munduan zehar dituen eragin eta prebalentzia, berau pairatzeko arriskua areagotzen duten ingurumen-faktoreen, ibilbide klinikoaren eta egungo tratamenduen azalpeneraino. Azken atalak MS suszeptibilitate-geneen analisi funtzionala dakar. Gaixotasunaren osagai genetikoaren garrantzia eta komunitate zientifikoaren ahaleginak eta lorpenak deskribatzen ditu. Orain arte, mutazioen MSrekiko lotura 231 gene baino gehiagotan frogatu dute, gehienak zelula immuneetan adieraziak.

MS gaixotasun neurologiko inflamatorio kronikoa da, eta helduei eragiten dien gaixotasun ez-traumatiko arruntena (GBD 2016 Esklerosi Anizkoitzaren Laguntzaileak, 2019; Kobelt et al., 2017). Esklerosi anizkoitza garatzeko arriskua hainbat ingurumen-faktorek eta sentiberatasun genetikok alda badezakete ere, sakoneko kausa zalantzazkoa da oraindik.

2.1.1. Prebalentzia eta lotutako ingurugiro eta bizimodu arriskuak

Esklerosi anizkoitzaren tratamenduen kostuaren igoera mundu mailako arazoa da (Hartung et al., 2015; San-Juan-Rodriguez et al., 2019). Osasun holistikoa (botikak, errehabilitazioa, diziplina anitzeko zaintzak) jasotzeko aukera bermatu behar da gaixotasunaren abiadura moteltzeko eta modu honetan desgaitasunaren aurrerapena eta esklerosi anizkoitzaren gaixoen autonomia. Hau, Europako eta Ipar Amerikako multiple esklerosidun gaixoen zahartze prozesuren erronkan are garrantzitsua da.(GBD 2016 Multiple Sclerosis Collaborators, 2019).

Erronka handituz doa, izan ere, mundua mailako intzidentzia eta prebalentzia handituz doaz (Bezzini et al., 2020; Etemadifar et al., 2020; Koch-Henriksen & Magyari, 2021; Y. Liu & Tang, 2018; Wallin et al., 2019; Walton et al., 2020; Wijeratne et al., 2022). Esklerosi anizkoitzaren mundu mailako egoerari buruzko lanik sakonetako bat “Global Burden Disease (GBD) 2016 Multiple Sclerosis collaborators” taldeak eginikoa da (GBD 2016 Multiple Sclerosis Collaborators, 2019). Egileen arabera adinaren araberako prebalentzia Ipar Amerikan eta Europako iparraldeko zenbait herrialdeetan 120 kasu 100.000 biztanlekoa da, Europa eta australasiako beste herrialdeetan ertaina (60-120 kasu 100.000 biztanleko) eta baxuena (<60 kasu 100.000 biztanleko) Asian, Afrikan, Latinoamerikan, Ekialde Hurbilean eta Ozeanian. Bere lanetik ateratako 2.1. Figuren herrialdeen araberako datuak ikus daitezke. Azpimarratzekoa da prebalentzia baxuko eskualdeetan, herrialde askok ez dutela daturik eta eredu matematikoaren araberako estimazioak erabili direla. Era beran, Groenlandiako datuak biztanleria lagin txikitik eratorriak dira.

Prebalentzia datuen mapak esklerosi anizkoitzarekin estuen lotutako ingurune faktorera hurbiltzen gaitu: latitude. GBD taldearen modeloaren arabera, ekuatorea eta biztanleria gehien bizi den latitudearen (74.7º) artean bederatzi biderreko aldea dago (GBD 2016 Multiple Sclerosis Collaborators, 2019).

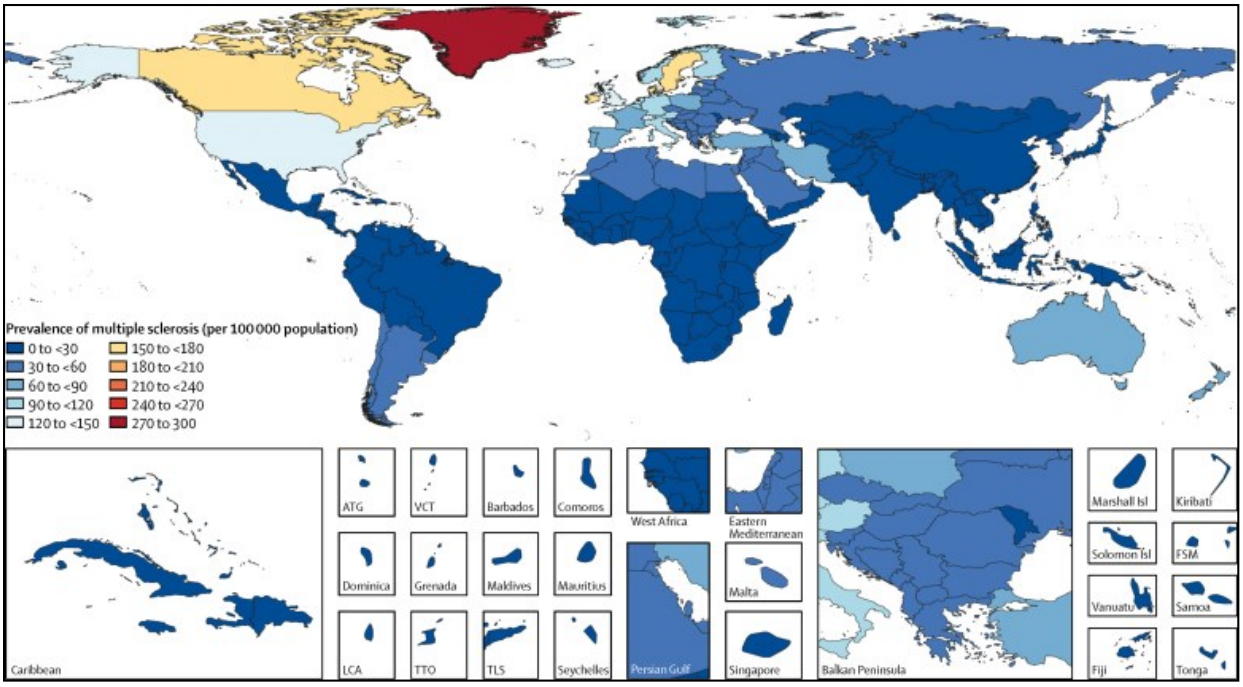

Figure 2.1. Esklerosi anitzaren prebalentzia 100.000 biztanleko 2016ean bi sexuendako eta herrialdeka. ATG=Antigua eta Barbuda. Isl=Irlak LCA=Saint Lucia. VCT=Saint Vincent eta Granadinak. TTO=Trinidad eta Tobago. TLS= Ekialdeko Timor. FSM= Mikronesiako estatu federatuak. *Iturria:* (GBD 2016 Multiple Sclerosis Collaborators, 2019)

Desberdintasun geografikoa inguruko erradiazio ultrabioletaren (ingeleraz ambient ultraviolet radiation, UVR) neurriaren islapena bezala ulertu izan da. Inguruko erradiazio ultrabioleta D bitaminaren (ingeleraz vitamin D, vD) iturri nagusiena da gizakiongan (Ascherio et al., 2010) eta erradiazio maila baxuek D bitaminaren nahikotasun mailan eragina dute. Inguruko erradiazio ultrabioleta hiru zatitan banatu daiteke: A (UVA), B (UVB) eta C (UVC). UVC ozono geruzak eta atmosferak xurgatzen dute, gizakion larruazalean UVA eta UVB bakarrik dute eragina. UVB D bitaminaren azaleko sintesiaren eragile nagusia da (Sallander et al., 2013). D bitamina maila baxuak esklerosi anizkoitzari lotuta egon dira 70 hamarkadatik (Goldberg, 1974) eta azken ikerketen arabera, D bitamina mila baxuen eta esklerosi anitza pairatzeko arriskuaren artean kausa-efektu erlazioa dagoela ematen du (Sintzel et al., 2017). Azpimarratzekoa da, vD baxuak elikadurarekin (D bitaminaren beste iturria) eta polimorfismo genetikoekin lotuta dagoela (Dobson & Giovannoni, 2019). vDren forma aktiboak, 1,25 D dihidroxibitamina (1,25 (OH) 2vD),

funtzio garrantzitsuak ditu immunitate-sistemaren barruan. Makrofagoen eta monozitoen jarduera antimikrobianoak indartzen ditu modu autokrinoan, zelula antigoalekoen bereizketa eta funtzioak modulatzen ditu, heldugabeak eta tolerogenikoagoak izatera bultzatuz, eta horrek egoera proinflamatoriotik tolerogenoagora igarotzea dakar, T linfozitoen ugaritzea ezabatuz eta haien bereizketa eta ekoizpen zitokinikoa modulatuz (Charoenngam & Holick, 2020). Guztira, vDk babes-efektua eragiten du MSn, hantura-egoera murriztuz.

Hala ere, Japoniako ikertzaile talde batek MSean latitudeak UVB-k baino eragin handiagoa duela frogatu zuen (Kinoshita et al., 2015). Hau latitudeak beste arrisku faktore garrantzitsu batekin duen loturarengatik izan daiteke. Epstein-Barr birusaren (ingeleraz, Epstein-Barr virus, EBV) infekzioa esklerosi anitzaren aldez aurreko baldintzatzat hartua izan da (Pakpoor et al., 2013), eta infekzio tasa latitudearekin batera handitu egiten da (Disanto et al., 2013).

Kohorte baten luzetarako azterketa batek, estatu batuetako indar armatuetan zerbitzu aktiboan zeuden 10 milioi gazte helduk baino gehiagok osatua, horietatik 955i MS diagnostikatu zitzaien, EBV MS garatzeko eragile bezala inplikatzen duten datu sinesgarriak emanez (Bjornevik et al., 2022). EBVren kasuan bezain harreman estua aurkitu ez bada ere, beste birus batzuk ere erlazionatu dira MSaekin. EBVren kasuan bezala, birus horiek prebalentzia handia dute populazio helduetan, eta bizialdi osoko infekzioak ezar ditzakete berraktibazio-aldiekin. Horien artean, aipa daitezke Herpesviridae familiako beste kide batzuk, hala nola barizela – zoster birusa, zitomegalobirusa (CMV) eta giza birusa (Tarlinton et al., 2020). Herpes ez diren birusen artean, John Cunningham birusa eta giza erretrobirus endogenoak (ingeleraz, human endogenous retroviruses (HERVs)) daude. HERVak giza genoman integratutako atzerabirus-probidentzia akastunak dira. HERVs-H eta W MS diagnostiko batekin lotuta daudela frogatu da, eta gero eta datu gehiago daude adierazteko proteinen adierazpenak aktibazio immunologikoa eta hantura dakarrela (Tarlinton et al., 2020).

Latitudearekin lotura ez duten ingurune faktoren artean erretzea dago. Hau faktore garrantzitsuen artean sahiesterrazena da eta esklerosi anizkoitzaren garapen eta progresioarekin estuki lotuta izan da (Degelman & Herman, 2017). Erretzearen efektua, biriken irritazio eta inflamazioari lotuta dago, izan ere, nikotina esklerosi anitzaren ereduetan efektu neurobabeslea erakutsi izan du (Gao et al., 2014) eta aho-tabakoa ez dago esklerosi anizkoitzaren arriskuari lotuta (Hedström et al., 2013). Oro har, MSn erretzearen ondorio ezabagarriak adierazten dituzten ebidentzia zientifikoak biriketako narritadura eta hantura ez-espezifikoekin lotuta daude.

Ongi oinarritutako beste arrisku faktore bat, aipatutako latitude altuak, eguzki esposizio baxua, D bitamina baila baxuak, EBV infekzioa eta erretzeaz gaindi, sexua da. Haurtzaroan esklerosi anizkoitzaren prebalentzia bi sexuetan antzekoa bada ere, nebazaroan, bien kurba banatzen joaten da, emakumezkoengan duen hazkunde handia izanik, gizonenganako prebalentzia bitik bat izatera iristeraino (2.2. Irudia; (GBD 2016 Multiple Sclerosis Collaborators, 2019)). Saguei buruzko hainbat ikerketek MS suszeptibilitatean eta desgaitasunaren progresioan dauden sexu-desberdintasunak salatzen dituzte. Desberdintasun horiek sistema immunologikoaren edo nerbio-sistema zentralaren (CNS) eta sexu-hormonen sexu-adierazpen kromosomikoaren aldakuntzaren ondorio izan daitezke. (Voskuhl, 2020). Horri dagokionez, testosterona eta estradiol hormonen propietate neurobabesleak jakinarazi dira (Mansilla et al., 2021). MSren eragina handiagoa da emakumeetan gizonetan baino. MS sintomak haurdunaldi berantiarrean hobetu ohi dira, estriol maila altuekin batera. Aldiz, gizonek joera handiagoa dute MS mota batzuk geroago garatzeko bizitzan, testosteronaren gainbehera fisiologikoarekin lotuz adinarekin (Mansilla et al., 2021).

Beste arrisku faktore batzuk ere ikertuak izan dira, hala nola, elikadura, obesitatea, hesteetako mikrobiotaren aldaketak, airearen kutsadura eta haurdunaldia. Esklerosi anizkoitzaren arriskua mugatzen duten faktore gutxi batzuen berri ere eman izan da,

zitomegalobirusaren infekzioa, kafe kontsumo altua, alkohola eta nikotina esaterako (Olsson et al., 2017).

Guztira, ikerketek erakutsi dute esklerosi anizkoitza gaixotasun desafiatzailea dela, eta haren eragina eta prebalentzia gero eta handiagoa dela. Kontuan hartuta MS gaixotasun larria dela heldu gazteei eragiten diena, ikuspegi terapeutiko holistiko bat behar da, medikazioa, errehabilitazioa eta diziplina anitzeko arreta barne, MSko pazienteei laguntzeko.

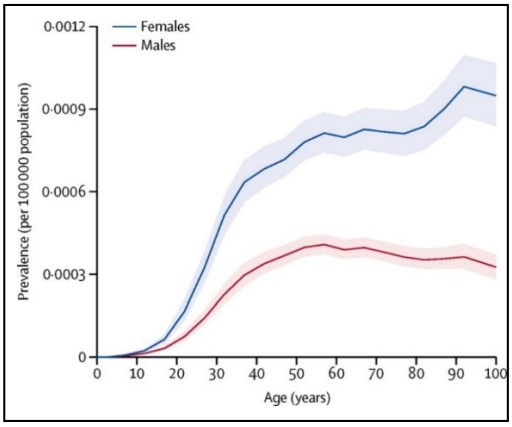

Figure 2.2. Esklerosi anizkoitzaren prebalentzia adina eta sexuaren arabera 2016ean. Itzalek %95eko ziurgabetasun interbaloak adierazten dituzte. *Iturria:* (GBD 2016 Multiple Sclerosis Collaborators, 2019).

2.1.2. Histologia

MS patologia XIX. mendearen bigarren erdialdean deskribatu zen, Jean-Martin Charcot neurologo frantsesa izan zen gaixotasunaren deskribapen zehatza egin zuen lehen egilea (Charcot, 1868), eta bertan, plaka esklerosatuak deskribatu zituen, inguru perientrikularrean, pons eta bizkarrezur muinean. Hortik aurrera, gaixotasunari buruzko gure ezagutza zabaldu egin da; ulertu ahal izan dugu plaka esklerosatuen edo lesioen izaera, haien motak eta gaixotasunaren progresioa. Animalien ereduek lagunduta, gaixotasun autoimmune honen oinarri immunologikoak ezartzen ari dira eta tratamendu ezberdinak garatu dira.

Charcot deitutako “plakak” esklerosi anizkoitza plaka desizoztaileak dira, eta ondoriozko orbain glialak, CNSren aurkako eraso autoimmuneen ondorio direnak. Hasiera batean, lesioek CNSko materia zuriari bakarrik eragiten ziotela uste zen, baina materia grisean 60ko hamarkadaren hasieratik daudela frogatu da (Brownell & Hughes, 1962; Lassmann, 2018). Hanturazko lesio horiek handitu egiten dira CNSn sartzen diren zelula inflamatorioen uhinekin (Olsson et al., 2017). CNSko neuronak mielina-zorroz estalita daude, oligodendrozitoak sortuta (2.3. Figure, ezkerrean), eta globulu immuneen infiltrazioak odoleko garuneko hesian zehar (BBB) inflamazioa eragiten du oligodendrozitoei kalte eginez eta desmielinizazioa eraginez, eta, azkenik, axoi-lesioa (2.3 Figure, eskuinean)

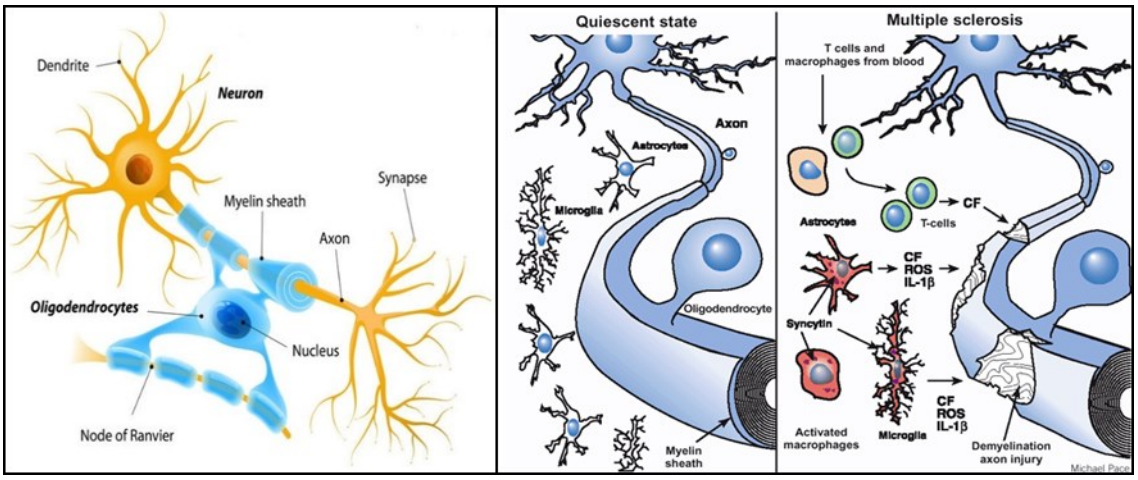

Figure 2.3. Nerbio-sistema zentralean neuronek duten mielinizazioa (eskuinean) eta esklerosi anizkoitzaren eragina (eskuinean). Oligodendrozitoek axoiak babesten dituzten mielina sortzen dute, nerbio kinaden igorpena ahalbidetzeko. Esklerosi anizkoitzaren garapenak dakarren inflamazio eta desmielinizazioa urteetan pilatu egiten da nerbioren endekapena eraginez.. Iturria: (Electrospinning Company, 2022; Mattson & Taub, 2004)

Zelula immunitarioak nerbio-sistema zentralean sartzearen arrazoia ezezaguna da. Infiltrazio inflamatorioetan zelula ezberdinak egoten dira, hala nola, linfozitoak (T eta B zelulak), monozitoak eta plasmako beste zelula batzuk. T zelulen kopuru handiak inflamazioaren eragile nagusitzat hartua izatera eraman ditu, baina atxikimendu molekulen, txemokina eta zitokinen

gainerregulazioa ez da bakarrik infiltratutako zeluletan ematen, bertako astrozito eta mikroglian ere ematen da (Lassmann, 2013).

Lesio desberdinak daude gai zurian edo grisean ematen diren arabera, baina gai zuriko lesioek dute inflamazio maila altuena (Peterson et al., 2001). Lesioak inflamazio fasearen arabera, aktibo, inaktibo, zabaltze mantsoan eta bermielinizatzen direnen artean bereizi daitezke.

Lesio aktiboaren ezaugarria zelula fagozitikoen, aktibatutako mikroglia eta makrofagoen, dentsitate haundia da. Lesio aktibo klasikoan, mikroglia desmielinizazio lesioaren kanpoaldean nabarmentzen da, lesioaren erdigunerantz bere kopurua txikitzen delarik eta makrofagoena handitu (Prineas et al., 2001). T eta B zelulak lesioaren hasieratik egon ohi dira eta ehunaren desmielinizazio eta kalteak, inflamazioaren bigarren fasea eragiten dut, makrofago eta mikroglia adierazle nagusien dituelarik.

Lesio inaktiboak, burmuinean ohikoagoak izaten dira eta ingurua zehazki markatuta izaten dute gliosi erreaktiboak sortutako orbain ehunarengatik (Lassmann, 2018). Zelula fagozitikoen kopurua, eta orohar, inflamazioa baxua izaten den baina axoien kalteak jarraitu egiten du (Kornek et al., 2000).

Mantso zabaltzen diren lesioek, aktiboek baino inflamazio maila askoz baxuagoa izaten dute. Inaktiboa den erdigunea erakusten dute eta ertz estuan mikroglia aktibazioa eta makrofagoen infiltrazioa (Prineas et al., 2001).

Lesio batzuetan bermielinizazio partziala edo orokorra gertatu daiteke, baina sortutako mielina garapenean sortutako mielinarenganako desberdina da kualitatiboki (Wooliscroft et al., 2019). Lesio hauek “itzal plaka” izena jasotzen dute eta euren ezaugarria internodo motzak dituzten mielina zakuez osatutako axoiak dira (Popescu et al., 2013; Prineas et al., 1993). Bermielinizazioa oso aldakorra da gaixo desberdinen artean eta lesioaren kokapenaren

araberakoa da (Lassmann, 2013). Eremu hauek, bigarren inflamazioa pairatzeko sentikortasun handiagoa dute itxura normaleko gai zuriak baino eta arrisku gehiago dute epe luzeko desmielinizazioa eta axoien endekapena garatzeko (Bramow et al., 2010).

2.1.3. Garapen klinikoa

Lesioak garatzen eta pilatzen doaz, gaixotasunaren garapenean zehar; gaixotasuna bera bidai bat da, arriskuan egotetik, asintomatiko, prodromal, eta sintomatiko izateraino (Dobson & Giovannoni, 2019) 2.4. Irudian ikus daitekeen bezala. Esklerosi anizkoitzaren gaixo askok lesioak erakusten dituzte gaixotasuna adierazten denerako, esklerosi anizkoitzaren fase asintomatikoa edo subklinikoa deritzona eta hainbat urtez luzatu daitekeena (Olsson et al., 2017). Lesio “asintomatiko” hauek gaixotasunean zehar gertatzen jarraitzen dute, hamar bat arazo kliniko bakoitzeko (Dobson & Giovannoni, 2019). Sintomatologia lesioaren kokapen eta tamainaren araberakoa izaten da. Neuritis optikoa, ikusmen nerbioaren lesioaren ondorioz, izan ohi da esklerosi anizkoitzaren aurkezpen ohikoena (Toosy et al., 2014).

Gaixoen gehiengo zabalak (%80-90) esklerosi anizkoitz errepikari-atzekaria (ingeleraz, relapsing-remitting multiple sclerosis, RRMS) pairatzen dute. Agerraldiek, desgaitasun neurologikoko gertaera akutuak, orokorrean orduan edota egunak ematen dituzte oharkabean garatzen, haste batzuk ematen dituzte egonkortuta eta azkenean errekuperazioa ematen da. Hasierako faseetan, errekuperazioa ia osoa da baina kaltea metatu egiten da denboran zehar. Dena den, agerraldi klinikoak izebergaren punta baino ez dira esklerosi anizkoitzaren aktibitatean (Dobson & Giovannoni, 2019). Esklerosi anizkoitz errepikari-atzekariaren agerpenetik hamar-hamabost urtera, esklerosi anizkoitza sekundarioki progresioa (ingeleraz, secondary progressive multiple sclerosis, SPMS) gertatzen da eta agerraldiak beharrean endekapen progresioa ematen

da. Beste kasuetan, endekapen progresiboa hasieratik gertatzen da, esklerosi anizkoitz primarioki progresiboa (ingeleraz, primary progressive multiple sclerosis,PPMS).

Lesio aktiboak esklerosi anizkoitza errepikari-atzekarian gailentzen dira, mantso zabaltzen diren lesioak forma progresiboetan komunagoak direlarik. Bermielinizazioa fase guztietan gertatzen da, bereziki fase progresiboetan (Lassmann, 2013) eta neuroendekapena sintomatologia klinikoaren hastapenetik (Dobson & Giovannoni, 2019). Ez dago histologia mailako berezitasunik esklerosi anizkoitzaren motaren arabera, horren ordez, ezaugarri bereziko eremuen proportzioan jarraipen bat ematen da. Hau, gaixotasunaren garapen kliniko mailakatuarekin bat dator, esklerosi anizkoitza errepikari-atzerakaritik sekundarioki progresibora pasatuz urteen poderioz (Dobson & Giovannoni, 2019).

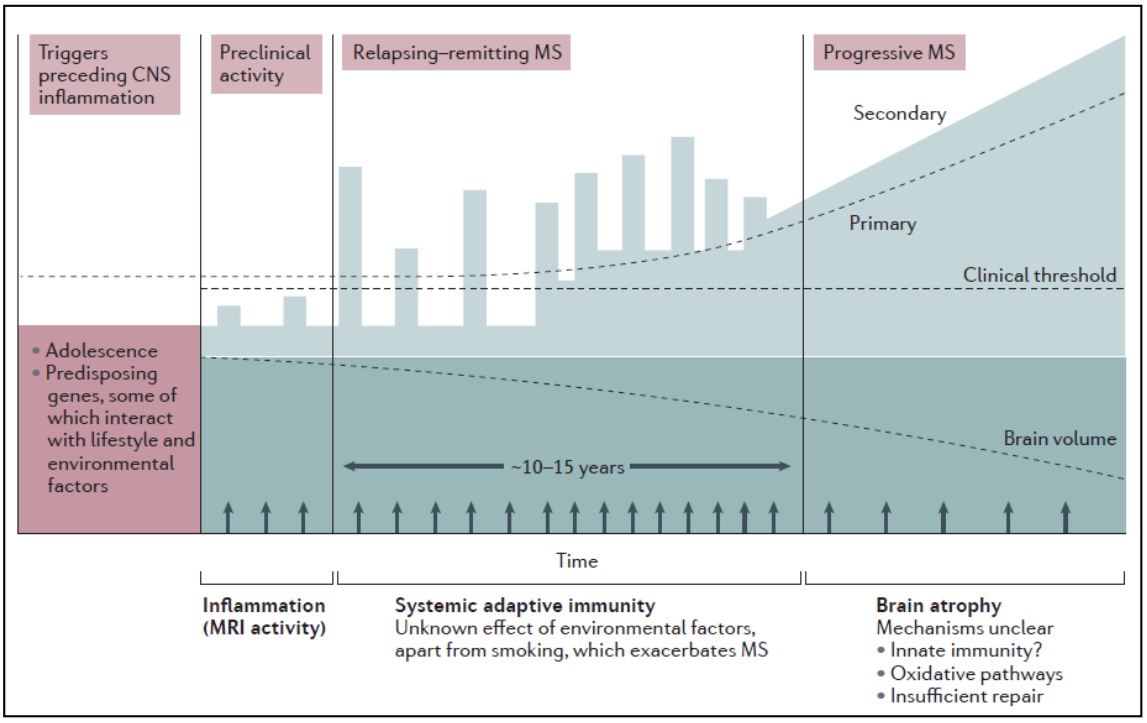

Figure 2.4. Esklerosi anizkoitza gaixotasunaren garapena. Urdin argiak esklerosi anizkoitzaren garapena adierazten dut eta zutabeek nerbio-sistema zentralean agerraldiek eragindako kalte inflammatorioa, batzuetan maila klinikora iristen ez dena. Geziek erresonantzia magnetiko irudi (ingeleraz, magnetic resonance image, MRI) bide neurtutako nerbio-sistema zentral gertatuko inflamazio berriak

adierazten dituzte eta agerraldi klinikoak baino asko ere maizago ematen dira. (Olsson et al., 2017)-tik moldatua.

MS pazienteen desgaitasun-maila neurologo batek Hedatutako Desgaitasunaren Egoeraren Eskalaren bidez egiten da (EDSS; ikus Figure 2.5), aurkezpen klinikoan eta erresonantzia magnetikoaren jardueran oinarrituta, McDonald-en irizpideak erabiliz (2022 By Deborah Clark & Shelley Jones). McDonalden irizpideak erabiltzen dira MSren diagnostikorako, eta W. Ian McDonald neurologoaren izena dute, nazioarteko talde bat zuzendu zuena Ameriketako Esklerosi Anizkoitzaren Elkarte Nazionalarekin lankidetzan. 2017an berrikusi zituzten azken aldiz (Thompson et al., 2018).

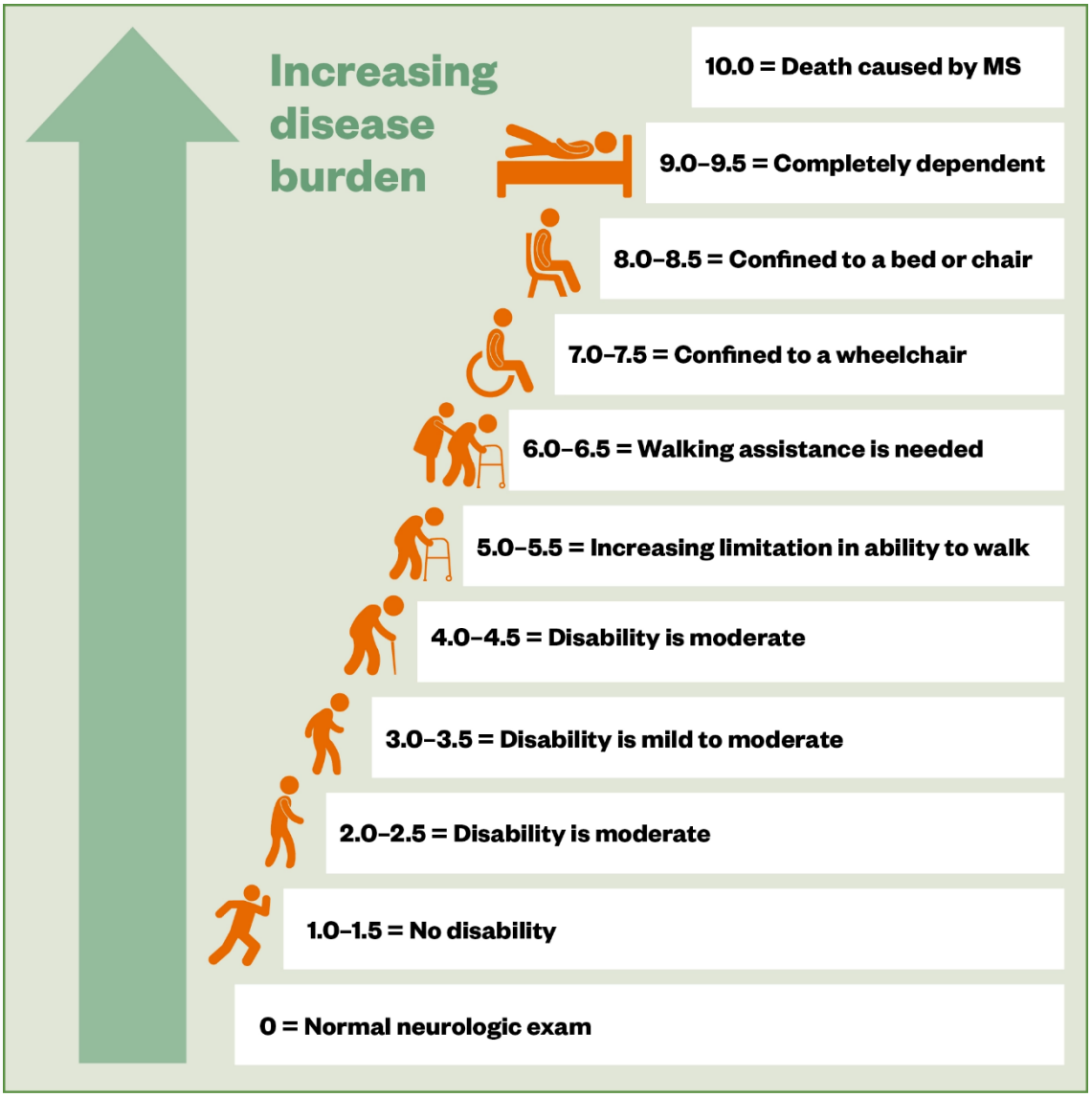

Figure 2.5. EDSS eskala. John Kurtzke neurologoak garatu zuen 1983an (Kurtzke, 1983) eta 0tik 10era doa 0,5 unitateko gehikuntzetan. Desgaitasunaren neurri nagusi gisa ibiltzean oinarritzen da, EDSSren 1,0 eta 4,5 arteko mailekin, laguntzarik gabe ibiltzeko gai direnak, eta 5,0 eta 9,5 arteko mailekin, oinez ibiltzeko eragozpenak definitzen dituenak. *Iturria: (Clark & Shelley Jones, 2022)*

2.1.4. Etiopatologia

Erantzun immunologiko eta inflammatorioa oso konplexua da esklerosi anitzen eta gaixotasunaren ikerkuntzaren erdigunean egon da betidanik. Esklerosi anizkoitzaren immunopatologia hobe lurtzeko animali ereduak garatu izan dira. Ez dago benetako esklerosi anitzarekiko animali eredurik baina enzefalitis alergiko/autoimune experimentala (EAE; ingeleraz, experimental allergic/autoimmune encephalomyelitis, EAE) da eredurik erabilgarriena. Sentikortasuna dute animali barietatetan nerbio-sistema zentraleko mielina edo mielinaren osagai diren glikoproteina (ingeleraz, myelin oligodendrocyte glycoprotein, MOG) proteina basikoa (ingeleraz, myelin basic protein, MBP), eta proteina proteolipidikoaren bitartez inmunizatzean datza. Horretarako adjubante gogorrak erabili behar dira. Animaliaren barietate eta immunizazio protokoloaren arabera, ezaugarri klinikoak, monobasiko, agerraldiko, edo progresiboak izan daitezke (A. P. Robinson et al., 2014). Animali eredu hauek ere oso lagungarriak dira esklerosi anizkoitzaren tratamenduen eraginkortasun terapeutikoa aztertzeko.

Animali esperimentaziotik eta datu klinikoetatik eratorritako jakintza uztartuz, inflamazioa prozesuaren eredu patogenikoan deskribatu izan da non T zelula laguntzaile (ingeleraz, T helper (Th) cells) edo CD4+ T zelulek, eta antigenoak aurkezten dituzten zelulek, mikroglia eta makrofagoak kasu, berebiziko garrantzia duten. Antigenoak aurkezten dituzten zelulek T zelula laguntzaileei antigenoak eman eta zitokina ingurune bereizia sortzen dute T zelulak polarizatuz. Antigeno aurkezten dituzten zelulen zitokinen arabera T zelula laguntzaile desberdinak deskribatu izan dira, inflamazioaren aldeko (Th1, Th17, Th22), kontrako (Th2, Th9) edo erregulatzeko (Treg) profilarekin (2.6. Irudia).

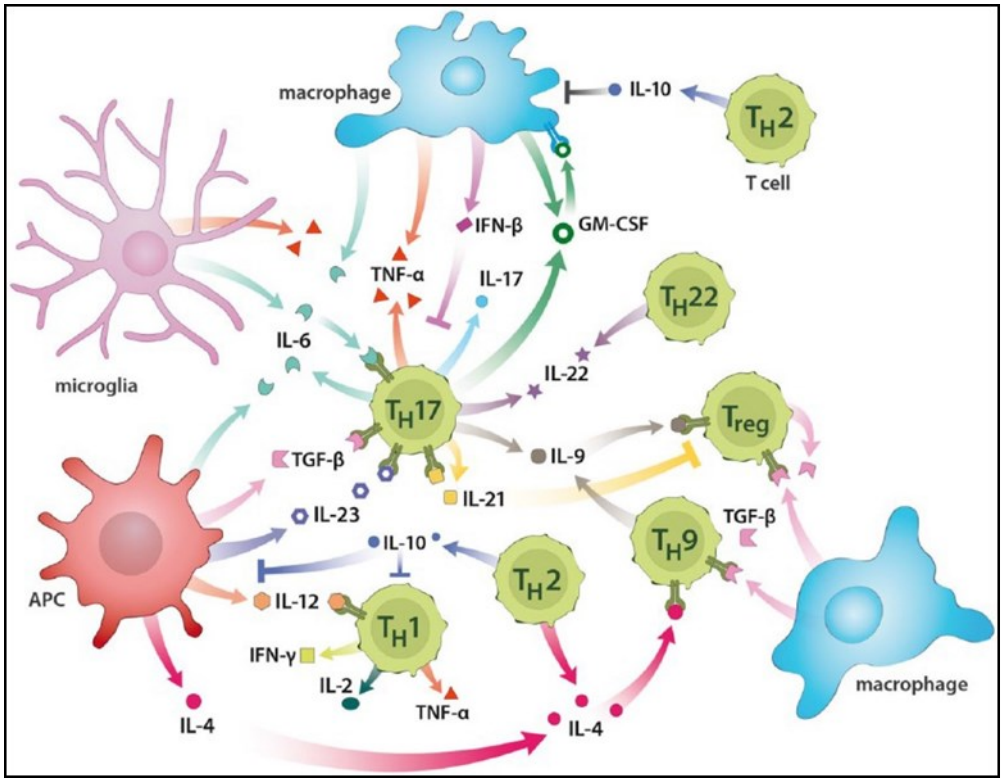

Figure 2.6. T zelula laguntzaile azpimotak. T zelula laguntzaile bakunak antigenoak aurkezten dituzten zelulek aktibatzen dituzte, eta zitokina inguruaren arabera T zelula laguntzaile desberdinak sortzen dira, bakoitzak zitokina desberdinak jariatzeko gaitasunarekin. Zitokina hauek T zelulen azpimoten oreka mantenduko dute eta antigenoak aurkezten dituzten zelulen gaineko eragina dute, denbora beran interakzio sare konplexua eraikiz. *Iturria: (Göbel et al., 2018)*

MS eta EAE ereduaren kontestuan, antigenoak aurkezten dituzten zelula espezializatu batzuk, zelula dendritikoak (ingeleraz, dendritic cells, DC), dira mielina Th zelulei periferiako gangoil linfatikoetan aurkezten dizkietenak. Zelula dendritikoen inflamazioaren aldeko zitokinek Th zelulak Th1 (IL-12) edota Th17 (IL-6, IL-23) azpimultzo inflamatorioetan desberdintzera bultzatzen dituzten. Gero, nerbio-sistema zentralean sartzen dira muga hematoentzefalikoa igaroz eta bertako antigeno aurkezle diren zelulak, mikrogliak nagusi, berriro aktibatzen dituzte. Nerbio-sistema zentralean aktibo daudenean inflamazioa sustatzen dute euren zitokinen bidez: Th1en kasuan interferon gamma (IFNγ) eta tumore nekrosi faktorea (ingeleraz, tumor necrosis factor alpha, TNFα), eta interleukina-17 (IL-17), IL-21, IL-22 eta TNFα Th17ren kasuan. Zitokina hauek inflamazioaren aldekoak dira eta, berezko eta hartutako immunitate erantzuna bultzaten

dute eta inflamazio lekura zelula gehiago erreklutatzen dituzte. Makrofago eta mikrogliak ez dituzte antigenoak bakarrik aurkezten, T zelulen zitokinen eraginpean produktu asko sortzen dituzte TNFα, IL-1, glutamatoa, proteasak, oxigenoaren espezie erreaktiboak eta oxido nitrikoa esaterako. Gauza bera gertatzen da astrozitoen kasuan, hauek ere gaitasuna dute zitokina, oxigenoaren espezie erreaktiboak eta oxido nitrikoa jariatzeko. oxigenoaren espezie erreaktiboak eta oxido nitrikoak garrantzi handia dute oligodendrozito eta neuronenganako zitotoxizitatean (Ohl et al., 2016). Prozesuaren xehetasunen ulermenak abian jarraitzen du, adierazpen eskematikoa 2.7. Irudian ikus daiteke. Animali ereduek zitokinen eraginaren nondik norakoen ulermenerako oso baliagarriak izan dira, zitokinek esklerosi anizkoitzean duten eraginaren zehaztasunak ezagutzeko ikusi “Cytokine signaling in multiple sclerosis: Lost in translation” (Göbel et al., 2018).

Ikerketa oso berri batek, EBVa MS (Bjornevik et al., 2022) garatzeko eragile gisa inplikatu zuen luzetarako ikerketa baten ildotik, mimetismo molekular bat erakutsi du EBVren transkripzio-faktorearen (EBVren antigeno nuklearra 1) eta CNS proteinaren glia-zelulen atxikipen-molekularen artean, zeinak azal bailezake MSn ikusitako mielinaren aurkako erantzun immunea (Lanz et al., 2022).

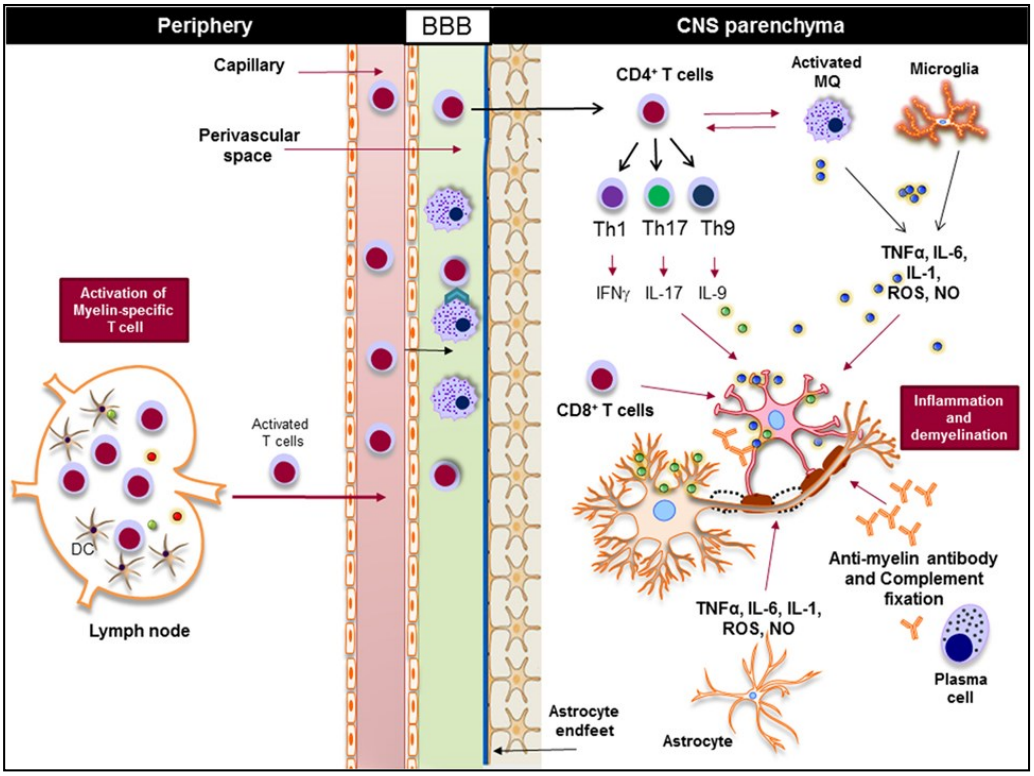

Figure 2.7. Esklerosi anizkoitzaren immunopatologiaren diagrama. Mielina espezifikoak diren T zelulak aktibatuak dira zelula dendritikoengatik (DC) eta nerbio-sistema zentralera mugitzen dira. Bertan, euren jariatutako zitokina desberdinek, makrofago, mikroglia, astrozito eta plasma zelulak aktibatzen dituzte inflamazio prozesua sortuz eta desmielinizazioa eta neurotoxizitatea eraginez. Source (Gharagozloo et al., 2018)

2.1.5. Tratamendua

MSarendako sendabiderik ez dagoen arren, MSaren tratamendua azkeneko bi hamarkadetan hobetu egin da botika berrien bidez, denak gaixotasunaren alderdi inflamatorioei lotuta. Horien artean gaixotasuna aldatzen duten terapiak (ingeleraz, disease-modifying therapies, DMTs). Lesioen inflamatorioen prebentzioa, agerraldi klinikoen kopuru eta larritasuna mugatzea eta ezgaitasunaren metaketaren moteltzea eragiten dute (Giovannoni et al., 2016).

Immunomodulatorioak, immunosupresiboak eta berreraikuntza immunologikoak bezala sailkatu daitezke.

90ko hamarkada, bi DMT immunodulatorio injektagarri garatu ziren: Interferon-β (1993) eta Glatiramer Acetate (GA; 1997). Interferon-β zelula immunitario desberdinek sortzen dute eta muga hematoentzefalikoaren egonkortzea, T eta B zelulen funtzioa baldintzatu eta zitokinen espresioa aldatu ditzake (Haji Abdolvahab et al., 2016). GA, lau amino azidoren (AA) nahasketaren ondorioz sortutako polimeroa da, mielinari erantzuten dioten T zelulak blokeatu eta GAri erantzuten dioten Th2 motako zelula supresore erregulatzaileak sortzen dituena (Ruggieri et al., 2007). Berriki, aho bidezko DMT immunomodulatorioak ere garatu izan dira, Teriflunomide (2013) eta dimethilfumarate (2014) adibidez.

Beste DMT garrantzitsu batzuk immunosupresoreak dira. Horien artean Fingolimod, estatu batuetako FDA agentziak 2011an MSarendako onartutako aho bidezko botika, gangoil linfatikoetatik T zelulen migrazioa ekiditzen duena. Beste immunosupresore batzuk, humanizatutako antigorputz monoklonaletan (ingelera, Monoklonala antibody, mAb) oinarritzen dira, adibidez Natalizumab (2006) eta Ocrelizumab (2017). Lehendabizikoak, anti-VLA4, inflamazio zelulen migrazioa ekiditzen du muga hematoentzefalikoan; bigarrenak, anti-CD20, B zelulak suntsitzen ditu (Dobson & Giovannoni, 2019).

Berreraikuntza immunologikoko terapiek, sistema immunitarioaren aldaketa iraunkorra eragiten dituzte, eta teorikoki, gaixotasunaren aktibitaterik gabeko tarte luzeak. Gaur egun erabiltzen diren botiken artean Mitoxantrone (2000), Alemtuzumab (2013; mAb anti-CD52) eta Cladribrine (2017) daude, denek zelula immunitarioen suntsiketan oinarritzen dira (Le Page & Edan, 2018).

Botiken erabileran bi estrategia erabiltzen dira: eskalada eta indukzioa (2.8. Irudia). Eskalada estrategian lehen lerroko tratamenduekin hasten da (eraginkortasun ertaina dute DMT

Immunomodulatorioak) eta “eskalatu” egiten da eraginkortasun gehiagoko (baina arrisku gehiago eta garestiago diren) botiketara (DMT immunosupresoreak). Gaixotasunaren oso aktiboa bada edo bere garapena oso azkarra, estrategia hau behar bada ez da eraginkorrena. Kasu horietan, indukzio estrategia erabiltzen da, hasieratik eraginkortasun handiko terapiak erabiliz, natalizumab (imumnosupresorea) edo alemtuzumab (berreraikuntza immunologikoko terapia). Botikaren eraginkortasun handiagoak kontrako efektu larrien arriskua handitzen du (Thompson et al., 2018).

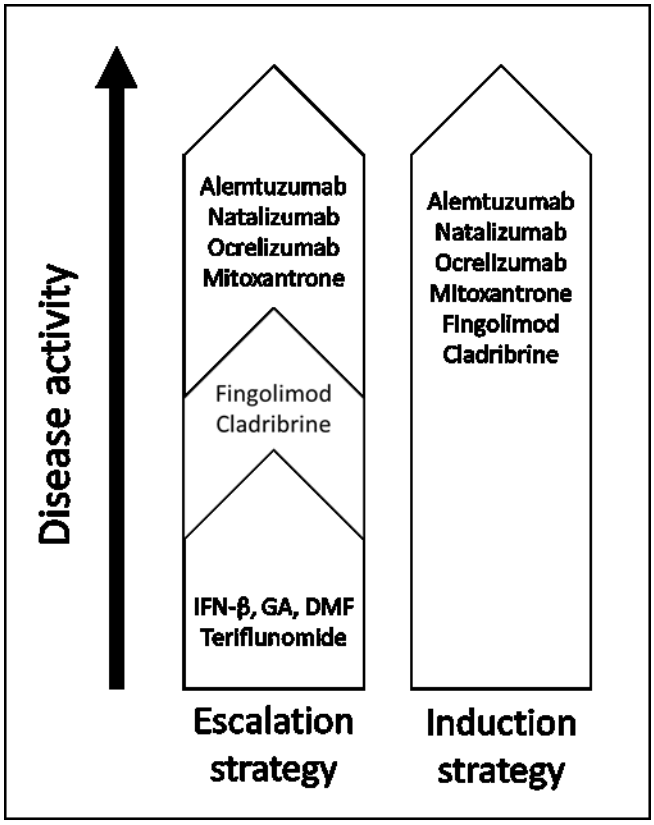

Figure 2.8. Esklerosi anizkoitzaren tratamendurako estrategiak. Eskalada estrategia, gaixotasunaren aktibitatearen arabera botika gogorragoak hartzean datza, eraginkortasuna eta arriskuak beharren arabera moldatuz. Garapen azkarreko gaixoen kasuan, hurbiltze agresiboagoa hartzen da, indukzio estrategia, eraginkortasun handieneko terapia hasieratik erabiliz. IFN-β: interferon-β; DMF: dimethilfumarate.

Dena den, gaur egungo tratamenduek, gaixotasunaren garapena atzeratu dezakete baina ez gelditu eta erabilgarriak dira esklerosi anizkoitz errepikari-atzerakarian baina ez mota

progresiboetan (Lassmann, 2013). Horregatik tratamendu berrien premia handia da esklerosi anizkoitzean (Thompson et al., 2018).

Azken ikerketek, esperantzarendako lehoia irekitzen duten hamarkada honetarako (Schweitzer et al., 2020) baina beharrezkoa da esklerosi anizkoitzaren mekanismoen ulermen zehatza, ahal den heinean arrisku genetiko eta bizimodua eta ingurugiro faktoreak uztartuz (Olsson et al., 2017)

2.1.6. Faktore genetikoak eta genoma mailako ikerketak

Ingurugiro faktoren garrantzia handia bada ere, faktore genetikoen eragina MSn oso garrantzitsua da. Gaixoen %12,6k, 8tik batek, esklerosi anizkoitzeko aitzindaria du familian (Harirchian et al., 2018).

Hala ere, ez da herentzia eredu sinplerik ematen ezaugarri Mendeliarren kasuan bezala. Bestalde, adostasun zabala dago gaixotasuna multifaktoriala dela eta esklerosi anizkoitzaren aldeko genotipoa hainbat gene independenteen interakzioren ondorio dela, arrisku gene bakoitza biztanlerian zabalduta dagoela eta bakoitzak eragin txikia edo ertaina duela (Hollenbach & Oksenberg, 2015).

Hainbat ikerketek esklerosi anizkoitzaren genetika aztertu dute, eta gaixotasunaren konplexutasuna kontuan hartuta, nazioarteko ahalegin konbinatuak garatu dira MS suszeptibilitatearekin lotutako geneei buruzko informazio eraginkorragoa biltzeko. Alde horretatik, nabarmendu da garrantzitsua dela histokonpatibilitate handiko geneak (MHC), beste 200 generekin batera, gehienak zelula immuneen bidez adieraziak. Ezin da herentziaren eredu sinple baten bidez MSa azaldu, ez errepikapen-tasak ez bikien desberdintasunek ez baitute ezaugarri

mendeliar baten presentziarik onartzen. Alderantziz, adostasun zabala dago gaixotasuna faktore anitzekoa dela eta MS-aldeko genotipoa gene polimorfiko independente edo elkarreragile anizkoitzetatik sortzen dela, populazioan ohikoak diren alelo arriskutsuekin eta bakoitzak arrisku orokorrari eragin txikia edo, gehienez ere, neurrizkoa egiten diolarik (Hollenbach & Oksenberg, 2015).

Gaixotasunaren lehen faktore genetikoan 1972an ezagutu ziren, MHC konplexua kodifikatzen duen Human Leucocyte Antigen (HLA) eremuan (Jersild et al., 1972, 1973; Naito et al., 1972).MHC I eta II motako proteinek osatzen dute. Proteina horiek funtzio garrantzitsua betetzen dute zelulen bidezko erantzun immunologiko egokitzaileetan. Peptidoak dituzte zelulen azalean CD8+ eta CD4 + T zeluletan, hurrenez hurren (beren mekanismoetara hurbiltzeko, ikus 2.9 Figure). MHC I klasearen kate astuna HLA-A, HLA-B eta HLA-C izeneko hiru genetatik adierazten da. MHC II klaseko α eta β kateak HLA-DR, HLA-DP eta DQ izeneko hiru gene bikoteren bidez adierazten dira (Abualrous et al., 2021).

HLA eremuan, 6p21 kromosomaren beso motzean, erantzun genetikoari lotutako leku asko daude (Campbell & Trowsdale, 1993). HLA geneak histokonpatibilitateari lotuta ezagutu ziren eta euren aldaketak gaixotasun eta minbizi mota askorekin lotuta daude (Trowsdale & Knight, 2013). I eta II motako HLA giza genomako lekurik polimorfikoenak eta bariazio genetikoaren ikerketarako eredu moduan erabiltzen dira osasun eta gaixotasunean (Vandiedonck & Knight, 2009).

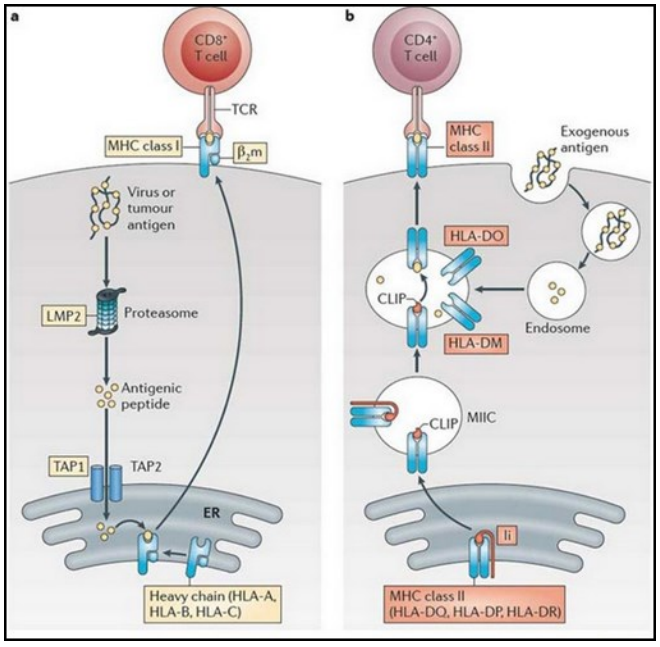

Figure 2.9. MHC klase I eta MHC klase II antigenoen aurkezteko moduak. MHC klaseko I eta II klaseetako aurkezpen-bideak. Histokonpatibilitate-konplexu nagusia (MHC) peptido-zatiak kargatzen dituzten azaleko proteina multzo bat da, T-zelulek antigenoa aurkez dezaten. Bi klase ezberdin daude, I eta II. MHC I klaseko aurkezpena (a) zelula eukarioto mota guztietan gertatzen da eta CD8+ T zelulek ezagutzen dute. Zelulen infekzioek antigeno intrazelularrek eragiten dituzte, antigenoak proteasoman digeritzen dira eta MHC molekuletara kargatzen dira azaleko migrazioaren aurretik. MHC II (b) klasearen aurkezpena APCetan bakarrik dago eta CD4+ T zelulek ezagutzen dute. Antigeno extrazelularrak harrapatzen dira, lisosometan digeritzen dira eta MHC molekuletara kargatzen dira endosoma berantiarretan, azaleko migrazioaren aurretik. *Iturria:* (K. S. Kobayashi & van den Elsen, 2012).

Esklerosi anizkoitzaren konplexutasuna dela eta, giza genetikoen ikerketaren eremuak urte asko behar izan ditu ikerketen diseinu eta balio estatistikoak zehazteko (Olsson et al., 2017). Horretarako esklerosi anizkoitzaren genetikaren nazioarteko kontsortzioa sortu zen (ingeleraz, International MS Genetics Consortium, IMSGC) 2003. urtean partehartze kolaboratzaile bat sustatzeko esklerosi anizkoitzaren arrisku genetikoen bilaketan. IMSGCk genoma osoko asoziazio ikerketak bultzatzen ditu esklerosi anizkoitzaren garapenean eragiten duten geneak identifikatzeko. Euren azken lana (IMSGC, 2019b), (IMSGC, 2019b), esklerosi anizkoitzaren genetikan egindako analisirik

handiena da, 47.429 gaixo eta 68.374 kontrol erabili dituzte. Deskribatutako esklerosi anizkoitzaren mapa genetikoan hurrengo proiektuen oinarria izan da, euren hitzetan “esklerosi anizkoitzaren ikerketan mugarria eta datozen ikerkuntzendako mapa”. Euren ikerkuntzak lehenago topatutako sentikortasun bereziko MHC aldaketak konfirmatu eta berriak topatu ditu, genoma mailan estatistikoki independenteak diren 31 efektu topatzeraino. MHC-tik kanpo 200 aldaketa topatu ditu esklerosi anizkoitzarekin lotutako 156 eremutan. Ere berean, X kromosoman esklerosi anizkoitzarekin lotutako lehen aldaki esanguratsua topatu dut, esklerosian sexuan duen eraginaren ulermenerako oinarrizko pausua emanez.

Emaitza guztiak aintzat hartuta, predisposizio genetikoaren %40 inguru azaldu dezakete balidatutako aleloen bitartez: %21a MHC eremuan ta %18 bertatik kanpoko genoma mailako asoziazioetan (2.10. Irudia). Beste %9,3 aldaki iradokitzaileei dagokie, egungo ikerketan muga pasa ez dutenak bain hurrengo ikerketetan esanguratsu izateko aukera asko dituztenak. Esklerosi anizkoitzari lotutako sentikortasun genetiko hauek kasuen %19,2 erantzule zuzentzan hartzen dira.

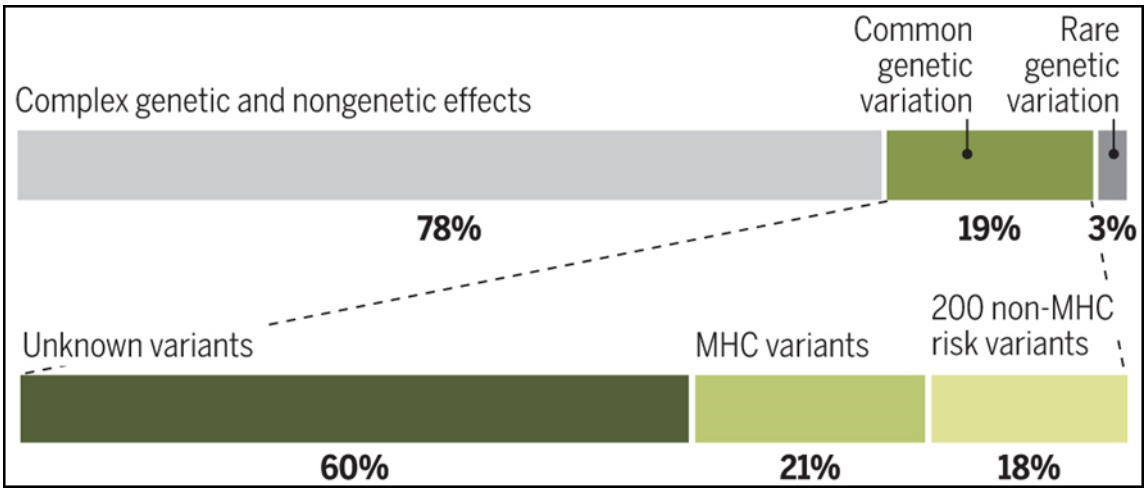

Figure 2.10 Esklerosi anizkoitzaren arriskuaren faktoreak. Esklerosi multiplean aldaketa genetiko komunen eta arraroen efektuak, arriskuaren %19,2 eta %3,2 azaltzen ditu hurrenez hurren. Aldaketa genetiko komunen %39,7 MHCko aldakiek eta bertatik kanpoko beste 200 aldakiek azaltzen dituzte. Source: (Briggs, 2019)

MHCtik kanpoko 200 aldakii dagokienez, zelula eta ehun immunologikoei lotutakoak nagusitzen ziren eta ez bakarri T zeluletan, baizik eta B zelulan, natural killer (NK) zeluletan, zelula dendritikoetan eta monozitoetan. Ehunei dagokionez timoa gailentzen da, bertan ematen den T zelula autoerreaktiboen garrantzia azpimarratuz. Nerbio-sistema zentralari dagokionez, mikroglian bereziki eta ez astrozito edo neuronetan. Aipagarria da nerbio-sistema zentraleko genen aldaketak urriagoak izatea, esklerosi anizkoitzaren sentikortasun genetikoek erantzun inmunologikoaren erregulazioan sortutako kalteek hamarkadetan eragina sortzen dutelarik sintoma klinikoak agertu aurretik (IMSGC, 2019b).

Hala ere, aipatutako gene asko zelula mota desberdinetan parte hartzen dute. Honek aldaki bakoitzak zelula mota batean eragina duen edo denetan duen eragina den bere efektuaren arrazoia den dudan jartzen du. Kontestuaren garrantzia analisi funtzionaletan ikertu beharrekoa da.

Bariazio genetikoek bakarrik ez dute esklerosi anizkoitzaren konplexutasuna azaltzen eta horregatik bariazio genetikoen eta ingurugiroaren arteko efektu gehigarrien ikerketan interesa handituz doa. Horrelako ikerketetan, momentuz HLA genetara mugatzen direnak, erretzeak, EBV infekzioak, mononukleosiak eta nebazaroko obesitatea ikertu dituzte (Olsson et al., 2017). Horietako batean (Hedström et al., 2017), HLA-DRB1*15 mutazioa duten eta HLA-A*02 ez duten erretzaileek 13 aldiz arrisku gehiago dute genotipo berdina duten ez erretzaileek baino, erretzeak esklerosi anizkoitza jasateko arriskua T zelulenganako eraginean gertatzen dera iradokiz.

Batera hartuta, IMSGCk egindako ahaleginek MSri laguntzen dioten faktore genetikoen ulermenik sakonena eman dute, eta nabarmendu dute immunitate-zeluletan adierazitako geneetan aldaera genetikoek duten garrantzia gaixotasun autoimmune horren elementu nagusi gisa. Mutazioei eta ingurumen-faktoreekin dituzten harremanei buruzko analisi funtzionalak funtsezkoak izan daitezke etorkizuneko aurrerapenak bideratzeko.

2.2. IL22RA2 eta IL12A geneak

2.2.1. Sarrera

Lehen aipatutako aldakiak nukleotido bakarreko polimorfismoak (ingeleraz, single nucleotide polymorphisms, SNPs) dira, DNA sekuentzian sortzen den nukleotido bakarreko aldaketak. Nukleotido bakarrak ordezkatuak, ezabatuak edo gehituak izan daitezke. SNP batek polipeptidoaren sekuentzia aldatzen ez duenean aldaketa sinonimoa (mutazio isila) deitzen zaio eta aldaketa dakarrenean ez-sinonimoa. Aldaketa ez-sinonimoek aminoazido aldaketa (missense) edo polipeptidoaren sekuentzia etetea (nonsense) eragin dezakete.

Interluekina 22 hartzaile alpha 2 (*IL22RA2*) ematen diren SNPak historikoki esklerosi anizkoitzari lotutako arrisku genetikoarekin lotuta agertu da IMSGCren ikerketetan (IMSGC, 2019a, 2019a, 2019c; IMSGC et al., 2011, 2013). Eskandinavia (Beyeen et al., 2010) eta Euskal Herriko (Vandenbroeck et al., 2012) biztanlerietan deskribatua izen esklerosi anizkoitzaren arriskuari lotuta. Gure ikerketa taldeak esklerosi anizkoitzaren gene hau topatu izanak bere ulermenean sakontzeko ikerkuntzara bultzatu gaitu. Gure taldeak identifikatutako SNPa, rs28385692, *IL22RA2* geneak kodifikatutako interleukina 22 proteina lokailuan (ingeleraz, interlukin 22 binding protein) 16. amino azidoa Leuzinatik (Leu) to Prolinara (Pro) aldatzen du (Gómez-Fernández et al., 2020). *IL22RA2* 6 kromosoman kokatzen da, 6q23.3 eremuan zehazki eta gene homologoak ditu ikertuak izan diren beste ornodun guztietan (Cunningham et al., 2019).

Era beran, interleukina-12 (IL-12) ere, esklerosi anizkoitzean arrisku genetikoko faktore bezala aurkitua izan da (IMSGC, 2019a, 2019b, 2019c; IMSGC et al., 2011, 2013). Haien artean Interleukina-12 alpha (*IL12A*) genea gailentzen da. Gene hau 3 kromosoman kokatzen da, 3q25.33 bana zitogenetikoan, eta oso ongi kontserbatutako genea da ornodun guztietan

ortologoak dituelarik (Cunningham et al., 2019). Geroago azaltzen den moduan *IL12A* genea analisi funtzionala burutzeko hautagai ona da, izan ere, IL-12 eta IL-35 zitokinak eratzeko gaitasuna du eta kontrako efektuak eragiten dituzte, esklerosi anizkoitzean garrantzi handikoak direnak.

2.2.2. *IL22RA2* genea eta IL-22BP zitokina

IL22RA2 geneak IL-22BP proteina kodifikatzen du. Zelula mieloide desberdinek espresatzen dute: hestetako (Huber et al., 2012; Jinnohara et al., 2017; Martin et al., 2014) eta larruazaleko (Voglis et al., 2018) zelula dendritikoek, hesteko mukosako eosinofiloek (Martin et al., 2016), eta baita hestetik eratorritako CD4+ T zelula linfoideak ere (Pelczar et al., 2016). Orain dela gutxi, epidermiseko keratinozitoak azaleko IL-22BP iturri nagusia direla topatu izan da (Fukaya et al., 2018). Emakumezkoen bular ehunean ere espresio indartsua dauka (The Human Protein Atlas, 2022).

Gene honek hiru aldaki desberdin kodifikatzen ditu: *IL22RA2* 1 aldakia (IL22RAv1; IL-22BP 1 isoforma (IL-22BPi1) kodifikatzen duena), *IL22RA2v2* (IL-22BPi2), eta *IL22RA2v3* (IL-22BPi3). Monozitoetatik eratorritako zelula dendritikoetan (ingeleraz, monocyte derived dendritic cells,moDCs) hiruak espresatzen dira (Lim et al., 2016). Aldaerarik luzeena, IL22RA2v1, 2893 base pare (bp) luze da, IL22RA2v2 2797 bp eta IL22RA2v3 2627 bp. Aldaeren egitura exonikoari dagokionez, aldaerarik luzeenak sei exoi ditu, eta beste bietan 3. exoia falta da. Aldaerarik laburrenak ere ez du bosgarren exoia, eta seigarren exonaren eskean gelditzen da (1.11 Figure).

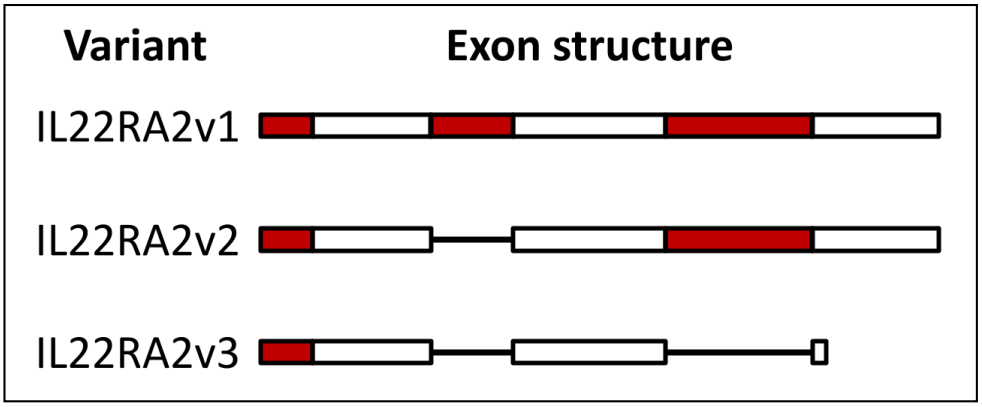

Figure 2.11. *IL22RA2* aldakien irudikapena exoien egituraren arabera. Giza *IL22RA2* geneak hiru barietate desberdin sortzen ditu MSan garrantzitsuak izan daitezkeenak. Exoiak gorri eta xuriz irudikatuta daude eta tamaina proportzionala dute. Exoien arteko marrek, barietate luzeenarekiko hutsuneak irudikatzen dituzte.

Isoforma motzetan kodifikatutako proteina motzagoa da: IL-22BP1k 263 aminoazido (AA); IL-22BPi2k 231 AA eta IL-22BPi3k 130 AA. Era beran xaguen gene homologoa de il22ra2 geneak, aldaki bakarra ekoitz dezake, gizakion *IL22RA2v2* homologoa dena (Wei et al., 2003; Weiss et al., 2004). Saguetan gizakion isoforma guztiak ez egoteak mugatu egin dezake animalia-modeloen gaitasuna IL22RA2ak MSn dituen ondorioak ulertzeko, eta, beraz, beharrezkoa da giza zelulekin eta ehunekin lan egitea.

Aipagarria da *IL22RA2v1*ren jatorria ikertua izan dela (Piriyapongsa et al., 2007). 96 nukleotidoko exoi bat gehiago dauka *IL22RA2v2* aldakiak baino, eta amaierako errepikapen luzeko (ingeleraz, log terminal repeat, LTR) erretrotransposoi baten intsertzioaren ondorio da. Intsertzioa primate eta mundu berriko tximinoen banaketaren aurretik geratu zen (orain 25 milioi urte) eta mutazio bakarra, mozketarako lekuan mutazioa gertatu zen gizaki eta orangutanen banaketaren aurretik (orain 14 milioi urte) LTR transposoia exoiean bihurtuz eta *IL22RA2v1* sortuz.

Izenak dioen bezala, IL-22BPk, interleukina-22 (IL-22) lotzeko gaitasuna dauka. IL-22 IL-10 zitokina familiaren parte da eta barrera gainazalen erregulazio immunologikoan bereziki parte

hartzen du (Sonnenberg et al., 2011) gaixotasun askotan parte hartze duelarik (Ahlfors et al., 2014; Che et al., 2020; Hernandez et al., 2018; Kulkarni et al., 2014; Mizoguchi et al., 2018). IL-22ren seinalizazioa IL-22R1/IL-10R2 heterodimeroak osatutako mintza hartzailearen bidez gertatzen da. Ehunen birsortze eta defentsan parte hartzen du molekula antimikrobialak, eta proliferazioaren aldeko eta apoptosiaren kontrako seinaleak areagotuz (Sabat et al., 2014a). Jokabide bikoitza – inflamazioaren kontrako eta aldeko efektuak egokitu izan zaizkio (Zenewicz, 2018; Zenewicz & Flavell, 2011); are gehiago, IL-22 minbiziaren sustatzaile bezala identifikatua izan da (Lim & Savan, 2014; Markota et al., 2018). Batez ere sistema immunologiko hainbat zelulek sortzen dute, CD4+ Th17 eta Th22 zelula linfoideek (Jia & Wu, 2014; Plank et al., 2017) eta neutrofiloek (Zindl et al., 2013). Seinalizazio hartzailea, interleukin-22 receptor 1 (IL-22R1), orohar zelula ez immunitarioetara mugatzen da, zelula epitelialak eta hepatozitoak kasu (Savan et al., 2011).

IL-22BP Il-10 familian jariatutako hartzaile bakarra eta IL-22rekin daukan afinitatea ikertua izan da IL-22BPi2ren kasuan (Figure 2.12; (Jones et al., 2008; Wolk et al., 2007)). Ikerketa hauek,IL-22BPi2k IL-22ren aktibitate biologikoa neutralizatzen duela erakutsi dute, IL-22rekin konplexu bereziki estua eratuz (Dumoutier et al., 2001; Jones et al., 2008; Kotenko et al., 2001; Xu et al., 2001). Gainazaleko hartzaile disolbagarriarekin, sIL-22R1, alderatuta, disoziazio denbora erdiaren (t½) balioa asko luzeagoa a IL-22/IL-22BPi2 konplexuarendako (≈4.7 egun IL-22/IL-22BPi2endako eta 7min IL-22/sIL-22R1 konplexuarentzat). Gauzak horrela, IL-22BPi2k mintzeko hartzaileak baino askoz afinitate handiago erakusten du IL-22rengatik (Jones et al., 2008). Bestalde, IL-22BPi3k afinitate baxuagoa erakusten du, IL-22/sIL-22R1 konplexuaren antzekoa (Jones et al., 2008), eta ez da IL-22ren bioaktibitatea mugatzen horren eraginkorra (Lim et al., 2016). IL-22BPi1k 32 amino azidoko intsertzioa dauka IL-22BPi2ren 67. Posizioan, 4. Exon berezi baten bidez, eta bere funtzio biologikoa lan honen baitan ikertua izan da.

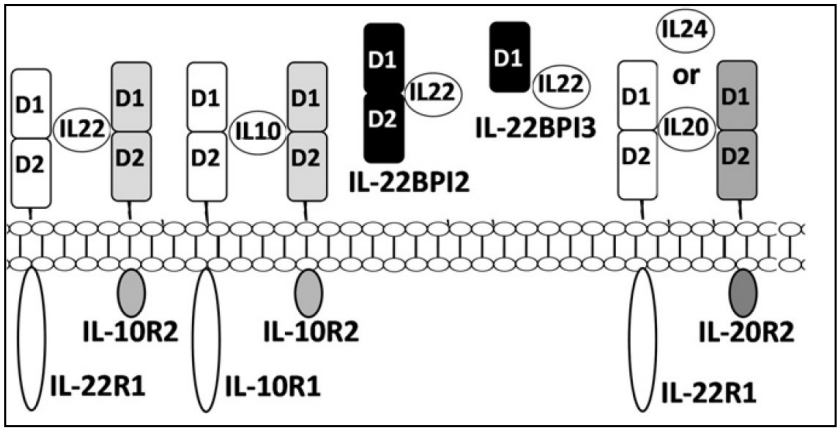

Figure 2.12. IL-22 hartzailearen azpiunitateek sortutako proteinen adierazpena. IL-22 hartzaileak bi azpiunitate ditu IL-22R1 eta IL-10R2. IL-22R1 IL-20 eta IL-24 seinalizazioan parte hartzen dtu. IL-10R2 IL-10 hartzailearen azpiunitatea da. IL-22BPi2 eta IL-22BPi3k IL-22 blokeatu dezakete. D = dominioa. *Iturria:* (Jones et al., 2008).

IL-22BP gaixotasunetan duen parte hartzea, batez ere IL-22BPk xaguan duen eraginaren bitartez ikertzen ari da batik bat. IL-22ren kasuan bezala, inflamazioaren aldeko eta kontrako zereginei lotua izan da. Inflamazioak eragindako koloneko minbiziaren sagu eredu batean, kolonean zelula dendritikoek sortutako IL-22BPk parte hartze babeslea izan zuen tumorigenesia eta epitelioko zelulen proliferazioa kontrolatuz (Huber et al., 2012). Bestalde, IL-22BP produkzioa Chron-en gaixotasuneko inflamazioan handitu egiten da eta kolitis ultzeradunean IL-22 babeslearen blokeoaren bidez efektu patogenikoak ditu (Martin et al., 2016; Pelczar et al., 2016). IL-22BP ezabatuta (ingleraz, knock out, KO) duten saguetan, psoriasiaren larriagotzea gertatzen da IL-22rekin lotutako peptido antimikrobialak direla eta, IL-22BP antigorputzen bidez neutralizatuz ere efektua errepikatu zen (Martin et al., 2017). IL-22BP espresioa saguen hesteetako Peyerren plaketako zelula dendritikoetan ikertua izan da, bertan bakterio hartzea sustatzen du genen espresioa modulatuz eta folikuluarekin lotutako epitelioan (Jinnohara et al., 2017). Saguei sepsiaren indukzioaren aurretik IL-22BPi2 errekonbinantea, rIL-22BPi2, administratzeak karga bakterianoaren eta organo hutsegiteak arinketa dakar (Weber et al., 2007). IL-22BPren efektuaren anbibalentziarekin jarraituz, azkeneko ikerketek IL-22BP saguen gripean

bakterioen superfinfekziora laguntzen duela (Abood et al., 2019) eta gibeleko hutsegitean babesten duela erakutsi dute (Schwarzkopf et al., 2019). *IL22RA2* aldakii dagokienez, eskistoma infekzioaekin eta Hepatitsi C birusak eragindako fibrosi eta zirrosisarekin lotu izan dira (Sertorio et al., 2015) eta baita minibiziarekin ere, prognosian hobekuntza ereaginez, 5 urteko progresiorik gabeko biziraupena hiru aldiz handituz leukemia linfozitiko kronikoan (Wade et al., 2011).

EAEren testuinguruan, MSrako sagu-ereduan, Il22ra2 genea ezabatzeak, partzialki arindu zuen fenotipoaren larritasuna (Laaksonen et al., 2014). Horren ildotik, Il22ra2 espeziearen aldaera genetiko natural bat duten arratoiek, IL-22BP esamolde txikiagoa dutenak, eta genea erabat ezabatzen duten saguek, gaixotasun ez hain larria dute (Beyeen et al., 2010; Huber et al., 2012). Il22ra2 KO EAE saguek CNSren hantura eta demielizazio murritzagoa zuten, eta CNSen infiltratuetako monocyte inflamatorioen proportzioa nabarmen txikiagoa izan zen, neutrofiloen edo IFNp3+, IL-17+ edo Foxp3+ T zelulen artean alde esanguratsurik ez zegoen bitartean. IL-22 eta IL-22BP-reik ez zuten sagueetan, ikerketak ondorioztatu zuen, halaber, IL-22BP– ezabatutako saguen gaixotasunaren larritasun murriztua IL-22 seinaleztapen desinhibizatuaren ondorioa dela. Txosten horretan bertan, Il22ren adierazpena gainerregulatuta dagoela eta Il22ra2rena, berriz, murriztuta bizkarrezur-muinean, hanturaren gainean (Lindahl et al., 2019).

Perriard et al. (Perriard et al., 2015) frogatu zuten IL-22 eta IL-22BP espresioa diserregulatuta daudela MS pazienteetan, IL-22 espresioa handituta dago kontrol osasuntsuekin alderatuta serum eta PBMCetan, eta IL-22 maila altuagoa dela gaixotasun aktiboa duten pazienteetan gaixotasun ez-aktiboa dutenetan baino. Arriskuko SNPek geneen transkripzioen adierazpen orokorreko mailei eragin diezaiekete edo transkripzio alternatiboen lotura areagotu (Edwards et al., 2013). IL22RA2 arrisku-genotipoaren kasuan (rs17066096) frogatu da arrisku-genotipoaren eramaileek IL22RA2 gehiago adierazten dutela beste genotipoaren eramaileek baino *in vitro* egindako ikerketan (Lindahl et al., 2019)

Ikerketa gehiago egin behar da IL22RA2 eta IL22-BPren rol fisiologikoan SNP arriskutsuek zenbateraino eragiten duten ulertzeko.

2.2.3. *IL12A* genea eta IL-12 eta IL-35 zitokinak

IL12A geneak IL-12A proteina kodifikatzen du, inflamazioaren aldeko IL-12 zitokina heterodimerkoaren p35 (35 kilo Dalton, kDa) azpiunitatea, IL-12p35, kodifikatzen du. IL12B geneak, IL-12p40 kodifikatzen du, p40 (40kDa) IL-12p35ekin lotzen da IL-12 sortzeko baina IL-23 ere sortu dezake IL23A geneak kodifikatutako IL-23p19 azpiunitatearekin.

IL-12 (p35 + p40) bere familiako lehen zitokina izan zen (Kobayashi et al., 1989; Trinchieri et al., 2003) IL-23 baino hamar urte lehenago (p19 + p40) (Oppmann et al., 2000). Hala ere, IL-23ren aurkikuntza baino lehenago, 1996ean IL-12p40aren antzekoa den Epstein-Barr virus-induced gene 3 (Ebi3) proteinaren aurkikuntzak (Devergne et al., 1996) IL-12p35arekin lotutako beste interleukina baten aurkikuntza ekarri zuen: IL-35 (p35 + EBI3) (Devergne et al., 1997). Ordutik beste bi interleukina gehiago topatu dira IL-12 familian, bietan EBI3 dagoelarik: IL-27 (p28 + Ebi3) 2002an (Pflanz et al., 2002) eta IL-39 (p19 + Ebi3) 2016ean (X. Wang et al., 2016). IL-12 familia osatzen duten interleukinak 1.13. Irudian aurkezten dira.

IL-12ri dagokionez, zelula berean IL-12p35 eta IL-12p40 espresatzea beharrezkoa da bioaktiboa den IL-12p70 zitokina jariatzeko (Jalah et al., 2013), IL-12 errezeptorearekin (hau ere bi unitatez osatua: IL-12Rβ1/IL-12Rβ2) lotzeko gai dena eta zelula dendritikoetan eta NK eta T zeluletan aktibatuetan espresatzen dena (Sun et al., 2015).

IL-12 zelula desberdinek sortzen dute, hala nola B linfozitoek eta neutrofiloek, baina ekoizle fisiologikorik nagusienak antigenoak aurkezten dituzten zelulak dira, zelula dendritikoak

eta makrofagoak (Oppenheim, 2020). Ezinbestekoa da IFN-γren sekreziorako, eta CD8 T zelulak zelula zitotoxiko efektore bihurtzeko prozesuan beharrezkoa da eta Th1 memoria/efektore zelula sortu eta mantentzeko (Jordan & Baxter, 2020).

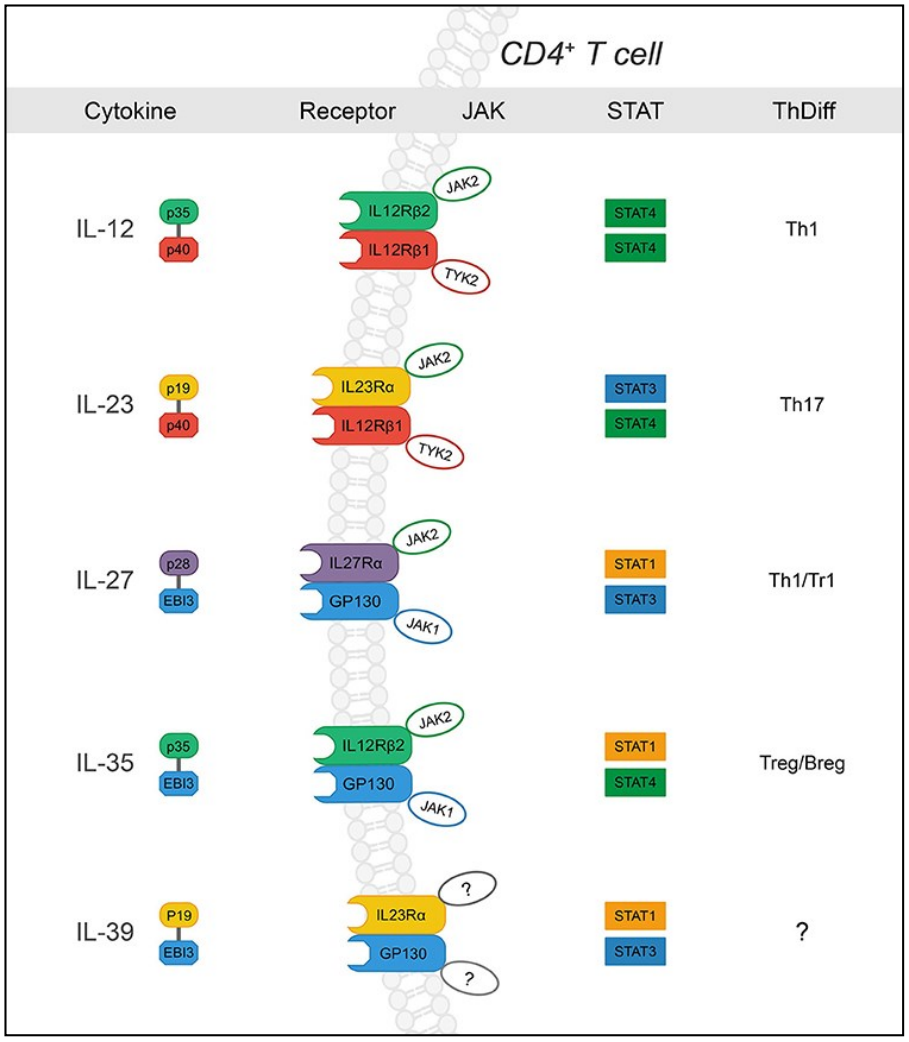

Figure 2.13. IL-12 zitokina familia. IL-12 zitokina familia partaide guztiek bi azpiunitate dituzte: α eta β azpiunitate bana. IL-12p35 α azpiunitatea da, p19 eta p28 bezala; β azpiunitateak aldiz, IL-12p40 eta Ebi3 dira. Bi azpiunitate mota hauen konbinazioak zitokina desberdinak sortzen ditu, eta hartzaile heterodimerikoak ere partekatzen dituzte. IL12A gure intereseko genearen kasuan, IL-12 eta IL-35en α azpiunitatea kodifikatzen du. Zitokina horiek CD4+ T zeluletako errezeptoreetan STAT* proteina desberdinen bidez. *Signal transducer and activator of transcription (STAT). (Bastian et al., 2019)-etik moldatua.

IL-12k parte hartze garrantzitsua du esklerosi anizkoitzean, espresio maila altuak gaixotasunaren garapenarekin orain dela 20 urte lotu zirelarik (Balashov et al., 1997; Comabella et al., 1998) eta efektuan denboran zehar konfirmatu izan direlarik, Th1 eta Th17 zelulen diferentziazio prozesuaren indukzioa esaterako (Lasek et al., 2014). IL-12 maila altuak eta Th1 zelulak hainbat gaixotasunetan ere atzeman egin dira, hala nola, artritis erreumatoidea, non gaixotasunaren garapenari lotuta dagoen (Pope & Shahrara, 2013) ubeitis autoinmunean (begi barneko gaitz inflamatorio talde bat; (El-Shabrawi et al., 1998)). *IL12A* aldakii dagokienez, gaixotasun zeliakoarekin (Dubois et al., 2010), Sjögren-en sindromearekin (Lessard et al., 2013), esklerosi sistemikoarekin (Mayes et al., 2014) zirrosi biliario primariaren (J. Z. Liu et al., 2012) eta beste gaixotasun batzuekin lotua izan dira.

Sagu ereduen ikerkuntzek, EAEn eta uveoretinitis autoinmune esperimentalean (gizakion ubeitisaren animali eredua, ingeleraz, experimental autoimmune uveoretinitis, EAU) IL-12 eta Th1 mailen handiagotze esanguratsuak erakutsi dituzte, nerbio-sistema zentraleko patogenesian IL-12k duen parte hartza azpimarratuz (Bright et al., 1998; Tarrant et al., 1998). Are gehiago, Th1 zelulek sortutako IFN-eta M1 makrofagoen espantsioa bultzatzen du (Dungan et al., 2014) eta oxido nitrikoaren sintasa entzimaren espresioa handitu, makrofago eta mikrogliaren nitrogeno oxido sintesia sustatuz (Xiao et al., 2008). Ikerketek IL-12ak eragindako Th1 zelulen desberdintzea organo-espezifiko gaixotasun autoinmneetan duen garrantzia erakusten dute.

EAEn erabilitako duseztatze genetiko ereduetan, IL-12p40 ez duten saguak EAErekiko erresistentean diren bitartean IL-12p35 faltan dutenek suszeptibilitate handiagoa dute, IL-12p40k inflamazioan duen eragin bikoitza adieraziz eta burmineko inflamazio autoinmunearen garapenean IL-23 (IL-12p40/IL-23p19) IL-12 baino garrantzitsuagoa izan daitekeela iradokiz (Gaffen et al., 2014). Hala ere, Ustekinumab, IL-12p40ren aurkako antigorputz monoklonala, psoriarian, artritis prosiartikoan eta Chron gaixotasunerako tratamendurako onartua badago ere (Lu et al., 2020) ez zuen efikaziarik erakutsi esklerosi anizkoitz errepikari-atzekarian bigarren

faseko froga klinikoetanal (Segal et al., 2008). Era beran, IL23A, IL-23p19 kodifikatzen duen genearen aldakiak psoriasia sufritzeko arriskuarekin lotu dira (Tsoi et al., 2017) baina ez dago ebidetizarik esklerosi anizkoitzaren kasuan (IMSGC, 2019b).

IL-35k ere gaitasun eta propietate interesgarriak ditu. Lau hartzaile konbinazio desberdin aktibatu ditzake, eta STAT1 eta STAT4 proteinen fosforilazioa eragiten du T zeluletan eta B zeluletan berriz, STAT1 eta STAT3 JAK1 eta JAK2 entzimen bidez (Bastian et al., 2019). CD4+ Foxp3+ T zelula erregulatorioek (ingeleraz, T regulatory cell, T reg) eta B zelula erregulatorioek (ingeleraz, regulatory B cells, Breg) ekoitzitako zitokina erregulatorio gisa funtzionatzen du inflamazioa arinduz eta ondorioz, hainbat gaixoatsun autoinmune eta infekziosoen larritasuna murriztuz (Garbers et al., 2012; Shen et al., 2014). Heste hodian tolerantziaren mantenimenduarekin (Shen et al., 2014; Wirtz et al., 2011) eta diabetes autoinmunaren babesarekin ere lotua izan da (Bettini et al., 2012; Mondanelli et al., 2015). IL-35 espresio maila ez-ohikoak hainba gaixotasun inmunologoreetan antzeman dira (Su et al., 2018) esklerosi anizkoitza tarteko (Jafarzadeh et al., 2015)

Bere efektu tolergonekoa dela eta, garrantzitsua da ere minibizian duen parte hartzeagatik. Jakina da EBI3 giza minibizietan adierazten dela, hala nola Hodgkin linfoman eta suduerfaringeko kartzinoman (Larousserie et al., 2005; Niedobitek et al., 2002). IL-35ek tumoren hazkuntza sustatzeko gaitasuna duela ere ikusi da. Tumoretik eratorritako IL-35k tumoreen hazkundea laguntzen du zelula mieloideen akumulazioa eta angiogenesia sustatuz (Z. Wang et al., 2013). T zeluletatik eratorritako IL-35ak leukemia mieloidearen hazkuntza laguntzen du eta (Tao et al., 2015) eta IL-35 mailak birika minbizian iragarle txarrak dira (Gu et al., 2015).

Regarding MS, different studies have highlighted its relevance as well. A study (J.-Q. Liu et al., 2012) using the EBI3 subunit knockout mice showed that EBI3 reduces EAE disease severity by suppressing Th17 responses. The addition of the exogenous p35 itself is able to

improve EAE by promoting Tregs and Bregs cells expansion that are IL-35 positive (Choi et al., 2017). Another group studied the effects of IL-35 expression in B cells and showed that IL-35, but not IL-12 or IL-27, is required for recovery of EAE (Shen et al., 2014). A Swiss study (Haller et al., 2017) created a IL-35 expressing DC line that exhibits tolerogenic properties such us an inhibitory effect on T cells. Vaccination with IL-35+ DCs promoted tumor growth in line with previous reports and very excitingly, vaccination IL-35+ DCs were also able to ameliorate EAE. Overall, animal studies suggest a strong protective role of IL-35 in EAE.

MSri dagokionez, ikerketa ezberdinek ere bere garrantzia nabarmendu dute. Ikerketa batek (J.-Q. Liu et al., 2012) EBI3 azpi-unitateko knockout saguak erabiliz frogatu zuen EBI3k EAEren gaixotasunaren larritasuna murrizten duela Th17ren erantzunak ezabatuz. P35 exogenoa gehituta, EAE hobetu daiteke Tregs eta Bregs zelulen hedapena sustatuz, IL-35 positiboak direnak (Choi et al., 2017). Beste talde batek IL-35 adierazpenaren ondorioak aztertu zituen B zeluletan, eta frogatu zuen IL-35, baina ez IL-12 edo IL-27, beharrezkoa dela EAE berreskuratzeko (Shen et al., 2014). Suitzako ikerketa batek (Haller et al., 2017) IL-35 adierazten zuten zelula dendritikoak sortu zituen, propietate tolerogenikoan zituztenak, TLR estimulazioaren aurrean erantzun arina emanez. IL-35+ DC hauek T zelulen proliferazio eta funtzipa inhibitu zuten *in vitro* eta *in vivo*, eta ez zen IL-35aren jariapenaren ondorioa solik baizik eta zelula dendritikoen fenotipo tolerogenikoarena. IL-35+ DC hauek tumoreen azkundea suspertzen dute, baina oso interesgarria da EAE hobetzeko gaitasuna era badutela.

MSko pazienteekin egindako ikerketek IL-35aren serum maila nabarmen baxuagoa erregistratu dute MSko pazienteetan, pertsona osasuntsuetan baino, eta horiek gora egiten dute tratatzean; beraz, tratamenduaren ondorio onuragarriak partzialki IL-35 upregulazioaren bidez gerta daitezkeela adierazten dute (Jafarzadeh et al., 2015). Horrekin lotuta, ikerketa batek erakutsi zuen gaixotasunaren progresioarekin lotutako IL-35 serumaren beheranzko mailaren erlazioa (Badihian et al., 2018), eta ikerketa handiago batek baieztatu zuen IL-35 serumaren

mailak nabarmen txikiagoak zirela pazienteetan kontrol osasungarrietan baino (Eslami et al., 2022). Aitzitik, pazienteen IL-35 maila handiagoa erakusten duen txosten bat ere badago (Kamal et al., 2021), pazienteen egoera klinikoak azal dezakeena. Azkenik, helminto-infekzioak dituzten eta gaixotasun-jarduera murriztua duten MS pazienteekin egindako ikerketa batek eragin hori IL-35 maila handiagoekin lotu zuen, zeinak immunorregulazio-ondorioak baititu bai Breg zeluletan, bai Treg zeluletan (Correale et al., 2021). Oro har, IL-35ek animalia-ereduetan eta giza pazienteetan duen babes-rolaren ebidentzia gero eta handiagoa da

3. HIPOTESIA ETA HELBURUAK

MS gaixotasun neurologikoa da, eta hantura kronikoa du ezaugarri. Gaixotasun ez-traumatiko ohikoena da heldu gazteei artean. Bere kausa zehatza ezezaguna da, baina ingurumen- eta genetika-faktore desberdinak deskribatu dira gaixotasuna areagotzen dutenak.

Gaixotasun konplexu honen inplikazio genetikoak ulertzeko asmoz, 2003an IMSGC bat sortu zen. Eskala handiko genoma osoen elkartzeari buruzko ikerketek arrisku autosomikoko 231 aldaera identifikatu dituzte, MSri modu esanguratsuan lotuak. Aldaera horiek zelula immunologiko mota eta ehun askotan adierazten diren geneekin lotuta daude, monozitoak eta DCak barne.

231 arrisku-aldaeren artean, IL22RA2 eta IL12A geneak daude. Bi geneek zitokinoak kodetzen dituzte, bitartekari immunologiko garrantzitsuak, eta zelula mieloideetan adierazten dira, hau da, monozitoetan eta/edo DCetan. Bi geneek transkribatutako isoforma ezberdinak sortzen dituztela diote, baina ez dira sakon aztertu.

Hipotetizatzen dugu IL22RA2 eta IL12A adierazpen-mailak eta -aldaerak eta horien kodifikatutako proteinak aztertzeak areagotu egingo duela MS duten papera ulertzea. Horregatik lan honen helburuak hauek dira:.

- Lehen mailako giza zeluletan eta giza zelulen lerroetan zelula-iturriak eta IL22RA2 eta IL12A adierazpen-mailak eta aldaerak ezaugarritzea.

- IL22RA2 proteina-isoformeen funtzioa ulertzea.

Horretarako, azpipopulazio monozito, moDC eta giza zelulen lerro ezberdinak erabiliko ditugu, biologia molekularreko teknika ezberdinak aplikatuz gene horien eta haien proteina eratorrien adierazpena detektatu eta aldatzeko.

MS gaixotasunaren progresioari dagokionez zitokinen transkribapen osteko erregulazio eta funtzioaren inguruan jakintza zabaltze aldera, Stanfordeko Unibertsitateko Rando Laborategian ikerketa-egonaldi bat egin nuen (eranskina). Rando laborategiak transkripzio faktore garrantzitsu baten isoforma ezberdinak aurkitu zituen muskuluetako zelula amentzat, eta bat egin nuen Pax3 isoformeen funtzioa aztertzeko MuSCen funtzioan saguetan in vivo.

4. MATERIALAK ETA METODOAK

4.1. Geneen espresioaren analisia

Gene-adierazpenaren analisia geneak proteinak eta RNA espezie funtzionalak bezalako produktu funtzionalak sintetizatzeko nola transkribatzen diren aztertzean datza. Horretarako, beharrezkoa da RNA isolatzea. RNA isolatu ondoren, RNAren transkripzioa cDNA egonkorragora egiten da. Polimeras-katearen erreakzio (ingeleraz, polymerase chan reaction, PCR) konbentzional eta kuantitatiboa erabiliz, zeluletan dagoen RNA kopurua analizatu eta kuantifikatu daiteke. Ikerketa honetan, IL22RA2 eta IL12A zitokina-geneen aldakien buruzko azterketa egin da, beste zitokina-gene batzuekin batera, haien gene-adierazpenaren profil argia izateko zelula-mota eta -baldintza desberdinetan.

4.1.1. RNAren isolamendua eta bere kalitatearen baliospena

RNA isolamendua TRI reagent (Sigma, T9424) erabiliz egin izan da ekoizlearen instrukzioen arabera. Motzean:

I) Laginaren prestaketa

a Zelulak Eppendorf batean bildu eta zentriguatu (500G 5’ RT) pikor bat lortzeko.

b Pikorra hiru aldiz garbitu 1X PBSarekin.

c Pikorraren lisia TRI Reagent erabiliz gauzatu pipetarekin nahastuz. TRI reagent militro (mL) bat nahiko da bost-hamar miloi animali zelularentzako. Zelulak behin TRI reagentean homogenizatu ostean -70ºC gordeak izan dira hilabete bat baino gutxiagoan.

II) Faseen banaketa:

a Laginak bost minutuz inguru tenperaturan (ingeleraz, room tenperature, RT) mantentzen dira nucleoprotein konplexuen disoziazio osoa bermatzeko.

b 0.1 mL 1-bromo-3-kloropropan gehitu erabilitako TRI Reagent mL bakoitzeko.

c Lagina ongi estali, 15 segunduz ongi nahastu eta 15 minutuz inguru tenperaturan mantendu.

d Lortutako emaitza zentrifugatu 12,000 × *g* 15 minutuz 2–8 °C artean. Zentrifugazioak hiru fase azaleratzen ditu (2.1. Irudia): fase gorri organikoa (proteinen fasea), interfasea (DNA daukana) eta kolorerik abeko goiko fase urtsua (RNA daukana).

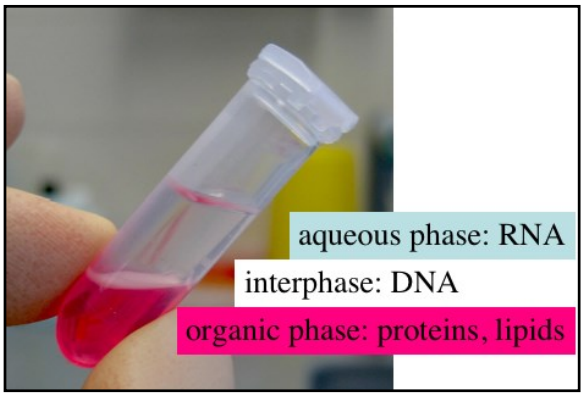

Figure 4.1. TRI reagentaren bidezko faseak. *Iturria:* https://openwetware.org/

III) RNAren isolamendua

a Fase urtsua Eppendorf berry batera pasa eta 0.5 mL 2-propanol gehitu laginari gehitutako TRI Reagent mL bakoitzeko.

b Lagina 10 minutuz inguru tenperaturan eduki.

c Zentriguatu 12,000 × *g* 10 minutuz 4 °C-tan. RNAk tutuaren oinarrian pikor bat osatuko du.

d Fase likidoa kendu eta RNA pikorra %75eko etanol mililitro bat erabiliz TRI Reagent mililitro bakoitzeko.

e Lagina nahastu eta zentrifugatu 7,500 × *g* 5 minutuz 4°C-tan.

f RNA pikorra lehortzen utzi. Ez utzi guztiz lehortzen berriro solubilizatzeko zailtasunak eragiten baititu.

g Beharrezkoa den ur bolumena gehitu RNA pikorrari. Disoluzioa errezteko pipeta erabili eta lagina 55-60ºko tenperaturan eduki 10-15 minutuz.

IV) RNAren kuantifikazioa

RNAren kantitate eta purutasuna neurtzeko Nanodrop 2000c spectrophotometer (Thermo Scientific) gailua erabili zen. A_{260}/A_{280} ratioa ≥1.7 handiagoko lagina haintzat hartu ziren anplifikazioa egiteko.

4.1.2. RT-PCR

Reverse transcription polymerase chain reaction (RT-PCR) biologia molekularreko teknika bat da RNA ezegonkorra DNA konplementarioan (ingeleraz, conplementary DNA, cDNA) bihurtzeko. Lortutako RNA laginak cDNAn bihurtu ziren High-Capacity cDNA Reverse Transcription Kits (Thermo Scientific, 4368814) erabiliz ekoizlaren instrukzioen arabera. Hurrengo tauletan, erabilitako erreaktibo (4.1. Taula) eta erreakzio baldintzak (4.2 Taula) azaltzen dira. Erreakzioa Verity Thermocycler (Applied Biosystems) aparatuan burutu zen..

Osagaia	Kantitatea erreakzioko
10X RT BUFFER	2 uL
10X RT RANDOM PRIMERS	2 uL
25X dNTP MIX (100nm)	0,8 uL
RNase Inhibitor	1 uL
MultiScribe Reverse Transcriptase, 50U/uL	1 uL
DNase and RNase freeH20	13,2 uL-X*uL
RNA (500ng)	X* uL

Table 4.1. RT-PCR erreakzioaren osagaiak. ***RNA bolumena konzentrazioaren araberako da eta beraz lagin bakoitzean desberdina da.**

Baldintzak	Lehen pausua	Bigarren pausua	Hirugarren pausua	Laugaren pausua
Tenperatura (ºC)	25	37	85	4
Denbora (minutuak)	10	120	5	∞

Table 4.2. RT-PCR erreakzioaren baldintzak.

4.1.3. PCR konbentzionala

PCR konbentzionalak 100 eta 1000 pare base (ingeleraz, base pair, bp) inguruko DNA sekuentzien erreplikazioa ahalbidetzen du. DNA eredua behar izaten du, helburu den sekuentzia daukana, DNA helburu den sekuentziaren konplemenatario diren primerak, beroa irauten duen DNA polimerasa, nukleotidoak (ingeleraz, deoxynucleoside triphosphates, dNTP) eta buffer soluzioa. PCRa tenperatura aldaketa zikloetan bidez gauzatzen da, DNA ereduaren desnaturalizazioa (DNAren helize bikoitza bi hari bakanetan bereiztea), primerak DNA eredura lotzea (primarren araberakoa da) eta luzapena (polimerasaren araberako pausoa da eta primerretik hasita polimerasak erdua jarraituz dNTP berriak lotzen ditu 3'tik 5'rako norantzean). DNA eredua ziklen baitan logaritmikoki handitzen doa eta sortutako DNA konplementario zatiari anplikoia deritzo (anplifikatutako produktua). Ziko bakoitza bat eta hiru minutu artean irauten ditu eta prozesu osoa 45 minuttik bi ordutara.

PCR mota desberdinak daude. PCR konbentzionala deskribatutako prozesuan datza. PCR mutiplexa primer desberdinekin lagin beran anpliko desberdinak batera anplifikatzean datza. Kabi PCRan, bi erreakzio ematen dira, lehengoan bilatzen den anplikoia baino handiago den sekuentzia anplifikatzen da eta bigarrengoan bilatzen den anplikoia, modu honetan anplikoi zailen anplifikazioa egiten da.

PCR erreakzioak Verity Thermocycler (Applied Biosystems) aparatuan gauzatu ziren erreakzio bakoitzaren araberako balditzetan. Erreakzioetan Taq DNA polymerase (#10342020, Thermo Fisher Scientific) polimerasa erabili zen eta dNTPak (#10297018, Thermo Fisher Scientific). PCR produktuak %2 (pisua/volumena) agarosadun (A9539, Sigma) gelean Tris acetate-EDTA buferra eta SYBR Safe (#S33102, Thermo Fisher Scientific) erabiliz ikusi ziren ChemiDoc Imaging System (Bio-Rad) erabiliz.

4.1.4. Quantitative PCR

Denbora errealeko (ingeleraz, real time, RT) edo kuantitaboa (ingeleraz, quantitative, q) PCRa teknika azkar eta sentikorra da, anplifikatutako produkuaren kantitatea denbora errealean neurtzea ahal bidetzen duena. qPCR hauek 7500 Fast Real Time PCR System (Applied Biosystems) gailuan burutu egin ziren. Bi sistema erabili ziren horretrako, anplikoia tindatzen duten tindatzaileak eta froga fluoreszenteak.

Indatzadaile bidezko PCR kuantitatiboa markatu gabeko primerren bidez egiten da eta bilatzen den anplikoia (normalean 50-200 bp artekoa) hari bikoitzeko DNAri lotzeko gai den tindatzailea erabiliz markatzen da, kasu honetan Syber Green (Thermo Scientific, 4385616). DNA genomikoaren kontaminazioa ekiditzeko primerrak exoi desberdinetan kokatzen dira, RNAren zatiketa ematen dakoan bakarrik anplifikatzeko (zehaztasun gehiagorako 2.2.1. IL22RA2 adakiak ikusi). Hurrengo taulan (4.3. Taula) erabilitako Syber Green primerren zerrenda dago.

Genea	Identifikazio kodea	Ekoizlea
ACTB	Hs. PT.39a.22214847	IDT
CHOP	Hs.PT.58.3400360	IDT
CHOP	Hs.PT.58.3400360	IDT
ERDj3	QT00042560	Qiagen
ERP44	Hs.PT.58.4529248	IDT
ERP44	Hs.PT.58.4529248	IDT
GRP170	QT00046214	Qiagen
GRP78	Hs.PT.58.22715160	IDT
GRP78	Hs.PT.58.22715160	IDT
GRP94	QT01848273	Qiagen
HERP	Hs.PT.58.21409911	IDT
HERP	Hs.PT.58.21409911	IDT
HPRT1	Hs.PT.58v.45621572	IDT
HPRT1	Hs.PT.58v.45621572	IDT
IL18	Hs.PT.58.25675872	IDT
IL22RA2	Hs.PT.58.40811	IDT

IL22RA2 (aldaki guztiak)	Hs.PT.58.40811	IDT
PPIB	Hs.PT.58.40291667	IDT
PPIB	Hs.PT.58.40291667	IDT
TGF-B	Hs. PT.58.22563137	IDT

Table 4.3. Lan honetan erabilitako Syber Green primerren zerrenda.

Froga bidezko PCR kuantitatiboan primerrek fluoroforo bat atxikita daramate eta hari bikoitzeko DNA osatzen ari duenean disdira egiten du. Lan honetan FAM eta VIC fluoroforoak erabili izan dira, denak Thermo Scientific konpainiatik eskurtatua, Taqman Assays izena hartzen dutelarik. Hurrengo taulean (4.4. Taula) erabilitako Taqman Assays guztiak agertzen dira.

Gene	Assay ID	Dye
ACTB	Hs99999903_m1	VIC
IFNB	Hs01077958_s	FAM
IL10	Hs00961622_m1	FAM
IL12A	Hs00168405_m1	FAM
IL12B	Hs01011519_m1	FAM
IL19	Hs00604657_m1	FAM
IL19	Hs00604657_m1	FAM
IL20	Hs00218888_m1	FAM
IL20	Hs00218888_m1	FAM
IL22	Hs01574154_m1	FAM
IL22RA2 (aldaki guztiak)	Hs00364814_m1	FAM
IL23A	Hs00900828_g1	FAM
IL24	Hs01114274_m1	FAM
IL26	Hs00218189_m1	FAM
IL28A	Hs00820125_g1	FAM
IL28B	Hs04193047_gH	FAM

IL29	Hs00601677_g1	FAM
IL4	Hs99999030_m1	FAM
IL6	Hs00174131_m1	FAM

Table 4.4. Lan honetan erabilitako Taqman Assays guztien zerrenda.

4.2. Primerren diseinua

4.2.1. Sarrera

Lehenago deskribatu bezala, PCRa primerrak rebiliz gauzatzen da, primerrak nukleotido sekuentzia motzak dira, anplifikatu nahi den sekuentziarekiko konplementarioak, eta polimerasaren atxikimendua ahalbidetzen dute anplifikazio sekuentzia osoa ekoizteko. Primerren diseinuan euren propietate fisiko eta kimikoak kontuan izan behar dira eta noski, interesekoa den sekuentziaren ikuskatzen sakona. Hainbat faktore hartu behar dira kontutan:

- **Primerraren luzeera:** pnukleotido gehiago dituzten primerrak espezifikoagoak dira; baina primerra gero eta motza izan gero eta errezago lotzen da DNAri polimerasaren atximendua ahlbidetzeko. 20 bat (18 eta 24 artean) nukleotido dituzten primerak oreka ona dute espezifizitate eta lotze efizientziaren artean.

- **Tenperatura:** fusio tenperatura (ingeleraz, melting temperature, Tm), primerra DNA oinarrira lotzeko gehienezko tenperatura, berebiziko garrantzia da eta 56-62ºC aretane egotea gomendatzen da, 65ºC-tik gorako fusio tenperaturek nahi ez diren atxikitzea eragin ditzazketelako. Bi primerrek antzeko fusio tenperatura (2-5ºC desberdintasuna gehienez) izan behar dute atxikitze tenperatura (primerrak lotzen diren tenperatura;ingeleraz, annealing tenperature, Ta) berdina izan dezaten. Fusio tenperatura horrela kalkulatu daiteke:

  Tm = 2ºC x (A edo T nucleotido kopurua) + 4ºC (C edo G nukleotido kopurua)

- **GC edukia:** tenperaturan deskribatu bezalak, C eta G nucleotidoek Tm %100 gehiago handitzen dute A eta Tk baino. Era beran GC metaketa (lau G edota C jarraian baino

gehiago) ekiditzea gomendatzen da. Horregatik primerren GC eduki optimoa primerraren %30-60 bitartekoa da.P

- **Primerren amaierak:** primerraren 3' ertzeko azken 5-6 nukleotidoak ezinbestekoak dira atxikitze egokiarendako. Edozein hustegite ekiditu eta C eta Gak erabiltzea gomendatzen da espezifizitatea handitzeko. 5' ertzak malgutasun handiaoga du eta sekuentzia ez konplementarioak gehitu daitezke.

- **Egitura errepikakor eta sekundarioak:** errepikatutako nukleotido patroiek biribilkaketak eta autoatxikitzeak sortu ditzazkete; primerrak euren artean konplementarioak badiera elkar atxikituz. Egitura hauek ekiditu behar dira.

- **Produktuaren luzeera:** produktua gero eta luzeago denan efizientzia txikiagoa da. Profuktuaren luzzerak produktua ekoizteko denboran ere eragina dauka. Produktu txikiagoak hobeak izan ohi dira. qPCRaren kasuan, produktu motzak gomendatzen dira, 80 eta 200 nukleotidko arteko produktuak dira egokienak.

- **Atxikite gurutzatuak:** genoman zehar antzeko sekuentziak eman daitezke eta beraz, beharrezkoa da erabiltzen dugun primerraren sekuentzia gure intereseko sekuentzian bakarrik dagoela nahi ez dugu sekuentzietara ez atxikitzeko edo behintzat gure laginean ez egotea.

Diseinatutako primerrak aipatuato gomendio hauek jarraitua tentuz diseinatu dira, ahalik eta primer bikote hoberenak lortzeko

4.2.2. *IL22RA2* aldakiak

Sarreran azaldu bezala, IL22RA2 geneak hiru aldaki ezberdin ekoizten ditu. Bakoitzarendako primer espezifikoak diseinatzeko, proteina kodifikatzen duen sekuentziak batera jarri ziren Clustal O (https://www.ebi.ac.uk/Tools/msa/clustalo/) programaren bidez. Lerrokatutako oinarri onen bidez primerak diseinatu ziren (4.2. Irudia). Diseinua egin zenean, IL22RA2 1 aldakia, IL22RA2v1, ez zegoen literaturan deskribatuta giza plazentatik kanpo. Primer desberdinak diseinatu ziren aldaki guztiak atzemateko. Erabilitako primerren zerrenda 4.5. Taulan dago, eta euren posizioa sekuentzia lerrokatuan (4.2. Irudian) eta 4.3. irudiko diagraman.

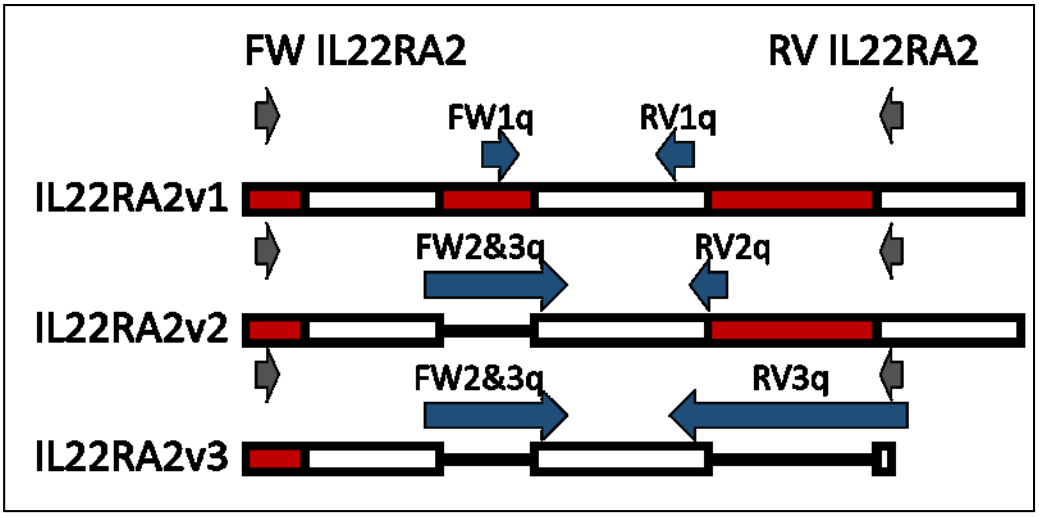

Figure 4.2. *IL22RA2*en aldakien exoien primerren atxikitze lekuak.

	Sequence (5'->3')
FW IL22RA2	TGCTTTCTAGGCTTCCTCATC
RV IL22RA2	TGAGCCCCTTCATAAACCTT
FW 1q	ATTTTGCAATGGCAGCCTG
RV 1q	GCCTGGGAAGTTACAAGAAATG
FW 2&3q	GTGCAGTACAAAATATATGGACAGA
RV 2q	GAGGATCTATTTTGTTTCCCACC
RV 3q	CTTTTGCTCTTTCCCACCAG

Table 4.5. IL22RA2 aldaki desberdinak detektatzeko diseinatutako primerrak. FW: forward primer; RV: reverse primer; q: qPCR primer. Kolorea 2.2. Irudian primerrak duen posizioarekin bat egiten du.

CLUSTAL O (1.2.1) sekuentzia anizkoitzen lerrokatzea (IL22RA2 sekuentzia)

```
IL22RA2     ATGATGCCTAAACATTGCTTTCTAGGCTTCCTCATCAGTTTCTTCCTTACTGGTGTAGC

IL22RA2     AGGAACTCAGTCAACGCATGAGTCTCTGAAGCCTCAGAGGGTACAATTTCAGTCCCGAAA

IL22RA2     TTTTCACAACATTTTGCAATGGCAGCCTGGGAGGGCACTTACTGGCAACAGCAGTGTCTA


IL22RA2-001 TTTTGTGCAGTACAAAATCATGTTCTCATGCAGCATGAAAAGCTCTCACCAGAAGCCAAG
IL22RA2-002 TTTTGTGCAGTACAAAAT----------------------------------------------------------------------
IL22RA2-003 TTTTGTGCAGTACAAAAT----------------------------------------------------------------------

IL22RA2-001 TGGATGCTGGCAGCACATTTCTTGTAACTTCCCAGGCTGCAGAACATTGGCTAAATATGG
IL22RA2-002 ------------------------------------------------------------------------------------ATATGG
IL22RA2-003 ------------------------------------------------------------------------------------ATATGG

IL22RA2     ACAGAGACAATGGAAAAATAAAGAAGACTGTTGGGGTACTCAAGAACTCTCTTGTGACCT

IL22RA2     TACCAGTGAAACCTCAGACATACAGGAACCTTATTACGGGAGGGTGAGGGCGGCCTCGGC

IL22RA2-001 TGGGAGCTACTCAGAATGGAGCATGACGCCGCGGTTCACTCCCTGGTGGGAAACAAAAAT
IL22RA2-002 TGGGAGCTACTCAGAATGGAGCATGACGCCGCGGTTCACTCCCTGGTGGGAAACAAAAAT
IL22RA2-003 TGGGAGCTACTCAGAATGGAGCATGACGCCGCGGTTCACTCCCTGGTGGGAAA----------

IL22RA2-001 AGATCCTCCAGTCATGAATATAACCCAAGTCAATGGCTCTTTGTTGGTAATTCTCCATGC
IL22RA2-002 AGATCCTCCAGTCATGAATATAACCCAAGTCAATGGCTCTTTGTTGGTAATTCTCCATGC
IL22RA2-003 ----------------------------------------------------------------------------------------
IL22RA2-001 TCCAAATTTACCATATAGATACCAAAAGGAAAAAAATGTATCTATAGAAGATTACTATGA

IL22RA2-002 TCCAAATTTACCATATAGATACCAAAAGGAAAAAAATGTATCTATAGAAGATTACTATGA
IL22RA2-003 ----------------------------------------------------------------------------------------

IL22RA2-001 ACTACTATACCGAGTTTTTATAATTAACAATTCACTAGAAAAGGAGCAAAAGGTTTATGA
IL22RA2-002 ACTACTATACCGAGTTTTTATAATTAACAATTCACTAGAAAAGGAGCAAAAGGTTTATGA
IL22RA2-003 ----------------------------------------------------------GGAGCAAAAGGTTTATGA

IL22RA2     AGGGGCTCACAGAGCGGTTGAAATTGAAGCTCTAACACCACACTCCAGCTACTGTGTAGT

IL22RA2     GGCTGAAATATATCAGCCCATGTTAGACAGAAGAAGTCAGAGAAGTGAAGAGAGATGTGT
```

Figure 4.3. CLUSTAL O(1.2.1) sekuentzia anizzkoitzen lerrokatzea IL22RA2 barainteen proteina kodifikazio sekuentzietan. Hiru aldakiek sekuentzia berdina duten eremuetan bakarra adieratzen da, exoien artean atzeko kolorea aldatzen da. Kolorea 2.5. Taulako primerrei dagokie.

4.2.3. *IL12A* aldakiak

IL12A geneak 6 aldaki ezerdin sortzeko gai bada ere informazio gutxi dago euren inguruan, batez ere 3 kromosomaren analisitk datorrena (Muzny et al., 2006). Bakarrik aldaki kanonikoa, IL12A-001 aldakia, 253 AAko proteina kodifikatzen duena, izan da sakonki aztertua. Beste aldakiek transkriptoen euskarri maila (aldakien euskarritasun maila aztertzeko metodoa; ingeleraz, transcript support level, TSL) baxuagoa dute. TSL metodo bat da, datu primarioetan oinarritzen dena, luzera osoko transkripzio egiturari eusteko: mRNA eta adierazitako sekuentzia etiketa (EST) lerrokatzea, Kaliforniako Santa Cruz eta Ensembl unibertsitateek emana. IL12A kanonikoak TSL1 (altuena) duen bitartean, IL-12A-203K TSL2 puntuazioa du, non mRNA euskarri onena susmagarritzat jotzen den edo euskarria EST anitzekoa den, eta gainerakoak TSL3 puntuazioa, non euskarri bakarra EST bakarrekoa den.

Aldakin desberdinen artean, bik, IL12A-202 eta IL12A-205, aldaki kanonikoak duen exoietako bat faltan dute eta 239 eta 214 AAko proteinak kofikatzen dituztela uste da. Hala ere badira, beste hiru aldaki gehiago, IL22RA2v1k bezala atxikitako introiak dituztena: IL12A-203, IL12A-206 and IL12A-204. IL12A-203K introi asko gordetzen ditu, eta bere ebidentzia maila eskasak kanonikoaren aurrepausoa dela pentsatzera narama. IL-12A-206ek gordetzen du IL22RA2v1ekin antzekotasunik hurbilena, atxikitutako introi bakarra dauka, 100 bp baino gutxiagoa eta proteinaren kodifikazioan irakurketa aldatuko ez lukeena. IL12A-204 aldaki motza da bigarren introia atxiktuta darama eta 20 base geroago gelditzen da. Aldaki bakoitzarendako primer espezifikoak disenaiatzeko proteina kodifikatzen duen sekuentziak lerrokatu eta aztertu egin ziren 4.6. eta 4.7 tauletan eta 4.4 Irudian agertzen den bezala. Gutxienezko lehengai kopurua erabiltzen duten isoforma ezberdinak bereizteko, 5 primer diseinatu ziren aldakin guztiak anplifikatzeko, IL12A-204 izan ezik (4.4 Figure). Hiru PCR desberdin diseinatu ziren aldaki desberdinak amplifikatzeko: FW1 eta RV1 primerrak 203, 206, 201 eta 205 aldakiak

anplifikatzeko; FW1 eta RV1.1. 203 eta 206 aldakiak anplifikatzeko; eta FW2 eta RV2 203, 206, 201 eta 202 aldakiak anplifikatzeko. Lehendabiziko PCRean, FW1 eta RV1 primerrak erabiltzen direnan, 203 eta 206 aldakien anplifikazio produktua berdina da, baina 1.1 PCRean, FW1 eta RV1.1. erabiliz, 206 aldakia anplifikatu daiteke 201 aldaki kanonikoa anplifikatu gabe. Are gehiago, bigarren PCRean, FW2 eta RV2 primerrekin, biak elkarrekin anplifikatu daitezke tamaina desberdineko produktuak sortzen dituztelarik. Testuan azaltzen den bezala, hau da aldakiak primer kopuru txikienarekin desberdintzeko estrategia efizienteena baina 204 aldakia ezin da anplifikatu. Azkenik, aipatzekoa da, 203 aldakiaren tamaina dela eta, besteak baino anplifikazio efizientzia gutxiago izan dezakeela, 1.1. PCRaren helburuan bere anplifikazioa erraztea da, izan ere, bakarrik beste aldaki bat, 206 aldakia, anplifikatzeko gaitazuna du. IL12A-204 aldakin moztu bat da, eta alde batera utzi genuen beste isoformak aztertzeko. Primer guztiak IDT enpresak ekoitzi zituen.

	IL12A ISOFORM	*203*	*206*	*204*	*201*	*202*	*205*
EXOIAK (bp)	1	**314**	**305**	**339**	**221**	**425**	**221**
	2	**146**	**146**	**146**	**146**	**146**	**146**
	ATXIKITUTAKO INTROIA 2			**20**			
	3	**114**	**114**		**114**	**114**	
	ATXIKITUTAKO INTROIA 3	**325**					
		42	**42**		**42**		**42**
	4	**75**	**75**				
	ATXIKITUTAKO INTROIA 4	**42**	**42**		**42**	**42**	**42**
	5	**91**					
	ATXIKITUTAKO INTROIA 5	**144**	**144**		**144**	**144**	**144**
	6	**616**	**268**		**616**	**609**	**268**

Table 4.6. IL12A aldaki kanonikoaren, IL12A-201en, eta beste aldakien sekuentziaren egitura. bp: nukletoido base pareak.

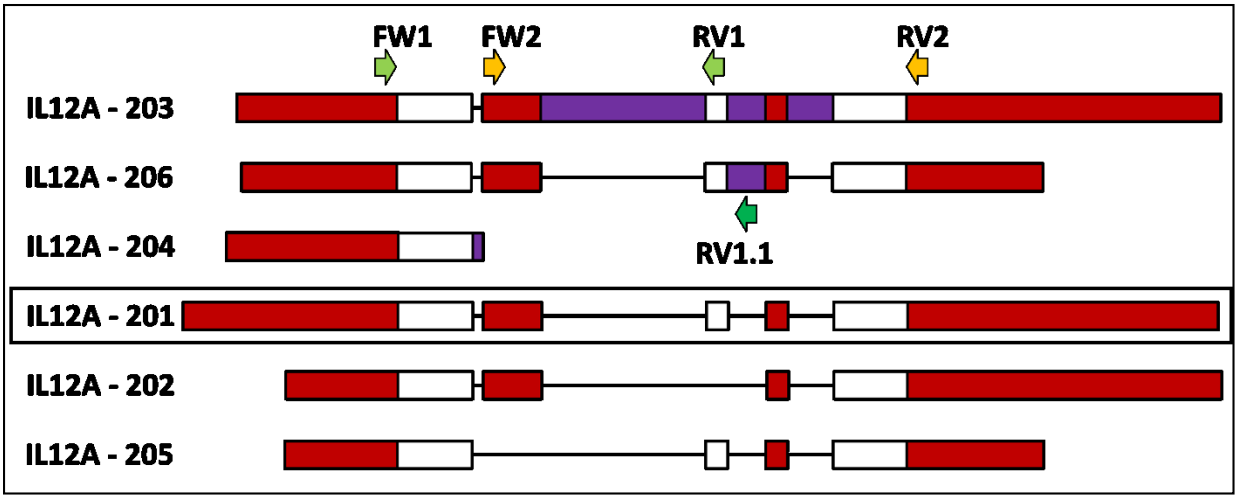

Figure 4.4. *IL22RA2*en aldakien exoien primerren atxikitze lekuak.

	Sekuentzia (5'->3')
IL12A FW 1	GCTCAGCATGTGTCCAG
IL12A RV 1	GGTCTCTCTGGAATTTAGGC
IL12 RV 1.1	TAATCAGACATCAGTGATATGAAT
IL12A FW 2	ACAAAAGATAAAACCAGCACAGTG
IL12A RV 2	GTCTTCATAAATACTACTAAGGCACA

Table 4.7. PCR konbentzionalaren bidez IL12Aren aldaki desberdinak atzemateko primerrak.

4.3. DNA birkonbinatzilearen klonazioa

DNA birkonbinatzailea naturan ez dauden DNA zatien konbinazioa da. DNA birkonbinatzailearen klonazioa DNA errekonbinatzailea duen bektore bat sortzeko erabiltzen den teknika multzoa da. Bektorearen laguntzarekin, DNA errekonbinatzaileak zelula objektiboetan duen proteina adieraz daiteke. Ikerketa honetan, bi klonazio ezberdin aurkitu ditugu, IL22RA2 genearen RNA kodifikazioaren sekuentzia ezberdinen ondorioak hobeto ulertu ahal izateko produktuaren proteinan, beste zitokinetako efektua alderatuz.

4.3.1. IL22RA2 IL17Aren seinale peptidoarekin pCMV6-Entry bektorean

4.3.1.1. Helburua eta arrazonamendua

Proiektuaren lehen uneetan, eta artearen momentuko egoerarekin bat etorriz, nahiko zaila zen jariatutako proteina antzematea. Gainera, sarreran aipatu den bezala, SNP rs28385692 kodifikazio-transkripzioaren aldaera arraro bat da, leuzinare ordez prolina bat jartzen duena IL22RA2 transkripzio guztien seinale-peptidoan 16 posizioan, proteinen sekrezioan eragina izan dezakeena. Klonazio honen helburua IL22RA2 beste seinale peptido batekin klonatzea zen. IL-17 proteina ondo aztertu eta ondo jariatua izanik, jariakinaren alde nagusiak seinale-peptidoak banatzen ote zituen probatzeko hautagai ezin hobea egiten zuen, edo, aitzitik, proteinaren egitura zen jariatze-dinamikaren eragilea. Klonazio honen oinarria IL17A (IL17SP) seinalearen peptidoak IL-22BPren jariaketan duen eragina aztertzea izan zen, funtsezko osagaia baita biologia zelularra eta gaixotasunaren gaineko papera ulertzeko.

4.3.1.2. Klonazio estrategia

Klonazio estrategia gauzatzeko, bilatzen diren fusio proteinaren ezaugarriak finkatu behar dira, klonazioa erabiliko diren errestrikzio lekuak eta proteina antzemateko etiketa. Horretarako lehendabizi erabiliko diren geneak eta bektoreak aztertu behar dira eta beharrezkoak diren beste elementu guztiak finkatu (4.5 Irudia).

- **Kozac kontsensu sekuentzia**
  5′-GCCACCATGG-3′

  1978an Kozakek (Kozak et al., 1987) gehienetan egoten zen (kontsensu) sekuentizia zegoela translazioaren hasiera laguntzen zuena, eta ordutik oso erabilia da klonazioetan.

- **Gelditze kodoia**

  5′-TAA-3′

- **Etiketen gehitzea**

  - Myc EQKLISEEDL (1202 Da)
    5'-GAG CAG AAA CTC ATC TCA GAA GAG GAT CTG-3'

    Atzekoz aurrera doan primerrean etiketa gehitzen denz, sekuentziaren complementarioa atze aurrera behar da:

    3'-CAG ATC CTC TTC TGA GAT GAG TTT CTG CTC-5'

  - Flag DYKDDDDK (1012 Da)
    5'-GAT TAC AAG GAT GAC GAC GAT AAG-3'

    Since we add the flag in the reverse primer we need the complementary:

    3'-CTT ATC GTC GTC ATC CTT GTA ATC-3'

Figure 4.5. Klonaziorako beharrezkoak diren elementuak.

Kasu honetan, bektore interesgarriak induzibleak (pTRe3g-Bi-mCherry) eta eratzaileak (pcDNA3.1) ziren, eta haien murrizketa-mapek 4 murriztapen-gune desberdin erakusten zituzten, eta ez zeuden txertatzean (Apa I, BamH I, Not I eta EcoR V). Digestio-entzima horietatik EcoRV baztertu egin zen ertz kamutsak izateagatik. Apa I ere baztertu egin zen inkubazio-tenperatura (25ºC, 37ºC izan beharrean) eta buffer optimoa (CutSmart versus NEBuffer3.1) desberdinak dituelako BamH I eta Not I.ekin konparatuta. Beraz, BamH I eta Not I klonatzeko hautagai posibleak ziren.

Beste aukera bat zen klonazioa, hasieran behintzat, etxeko bektore batean egitea, pCMV6-Entry Sgf I eta Mlu I erabiliz. Behin klonazioa lortuz gero, intereseko bektoreetara aldatuz.

Hala ere errestrikzio lekuen azterteak hiru aukera utzi zizkigun IL17SP eta IL22RA2 sekuentziak batera sortzeko:

1. BamH I eta Not I-en erabilera intereseko bektoreetan (pTRe3g-Bi-mCherry eta pcDNA3.1.).

2. BamH I erabilera bakarik intereseko bektoreetan.

3. pCMV6-Entry bektorean klonazioa burutzea, *IL22RA2* zeogen bektorea hain zuzen, Myc eta Flag etiketa dituena SgfI and MluI errestrikzio lekuen bidez (*IL22RA2* kendu eta IL17SP+*IL22RA2* jarri).

Bigarren aukera ere arazo bat dauka, entzima bakarrarekin digestioa eginez gero zaila da sartutako gehigarria norantza onean dagoen jakitea.

Azkeneko aukera klonazioa egitea ahalbidetuko liguke baina solik pCMV6-Entry bektorean Sgf I and MluI erabiliz. Hau izan zen aukeratuakoa, klonazio epe laburrenean lortze aldera.

Azkeneko aukera klonazioa egitea ahalbidetuko liguke baina solik pCMV6-Entry bektorean Sgf I and MluI erabiliz. Hau izan zen aukeratuakoa, klonazio epe laburrenean lortze aldera.

Aztertuako alderdiez gain, klonazio honen aspektu nagusiena, klonazioa bi DNA zati desberdinen bidez (IL17A seinale peptidoa eta IL22RA2ren irakurketa irekia (ingeleraz, open reading frame (ORF)) eratutako gehigarria sortzea da. Hori lortzeko Koen Vandenbroeck-en aurretiazko esperientiza erabili zen, gaingartzeko estensio estrategia erabilitz (4.6. Irudia).

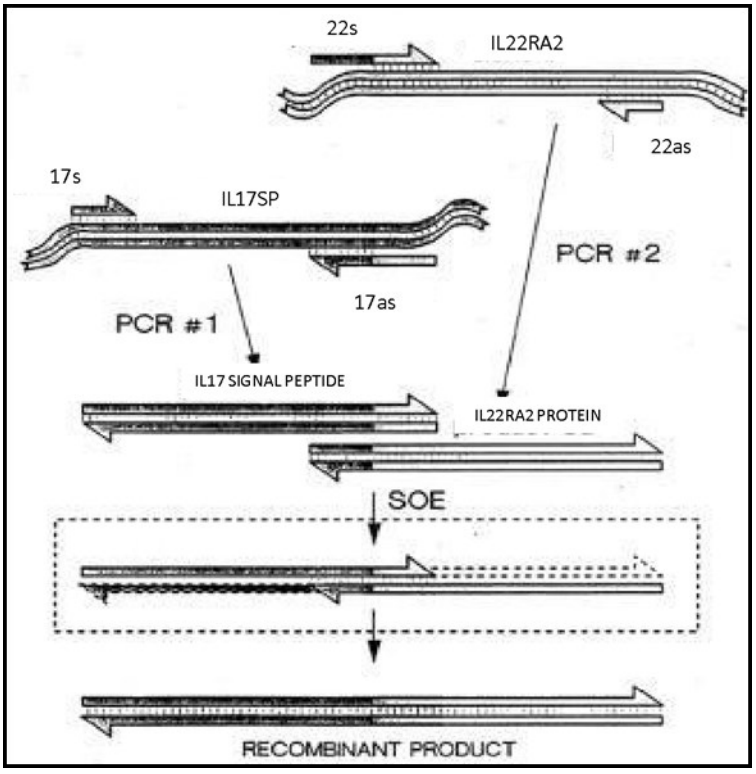

Figure 4.6. Klonazio estrategiaren adierazpen orokorra. Nabarmentzekoa da, 17s eta 22as primerren hasiera (17s) edo bukaera (22as) ez datorrela bat anplifikatzen den produktuarekin eta errestrikzio lekuei dagokiela. (Horton et al., 2013):-etik moldatua.

4.3.1.3. Deskribapen orokorra

Estrategia honek pausu desberdinak ditu:

I. Primerren diseina

II. Beharrezkoak diren zatiak ekoiztea. Bi PCR:

a. IL17SP zatia sortu 17s (Fw) eta17as (Rv) primerren bidez.

b. *IL22RA2* proteinaren amaiera sortu 22s (Fw) eta 22as (Rv) primerren bidez.

III. Zatien hibirdazioa eta 5'tik 3'rako luzapena. Primerrik gabeko PCRa.

IV. Bilatzen den produktuaren anplifikazioa. Behin zatiak elkarrekin daudenan 17s (Fw) eta 22as (Rv) primerren bidez.

V. Sartu nahi den gehiagarriaren eta bektorearen digestioa. Pauso honetan sortutako arazoek, estrategia moldatzera behartu gintuzten klonazioa lehendabizi TOPO TA sisteman eginez eta gero pCMV6 bektorera pasaz.

VII. Transformazioa.

VIII. Kolonien konfirmazioa

4.3.1.4. Primerren diseinua

Estrategia erabakitakoan, primerrak beharren arabera diseiantu ziren. Ez zen beharrezkoa inongo etiekta edo gelditzen kodonik gehitzea helmuga betorean daudelako. Era berean, Kozak kontsentsu sekuetzia eta errestrikzio entzimen lekuak oinarri zen DNA sekuentziatik hartu zitezkeen. Hurrengo irudietan (4.7 iruditik 4.10 irudira) disenatutatko primerak deskribatzen dira.

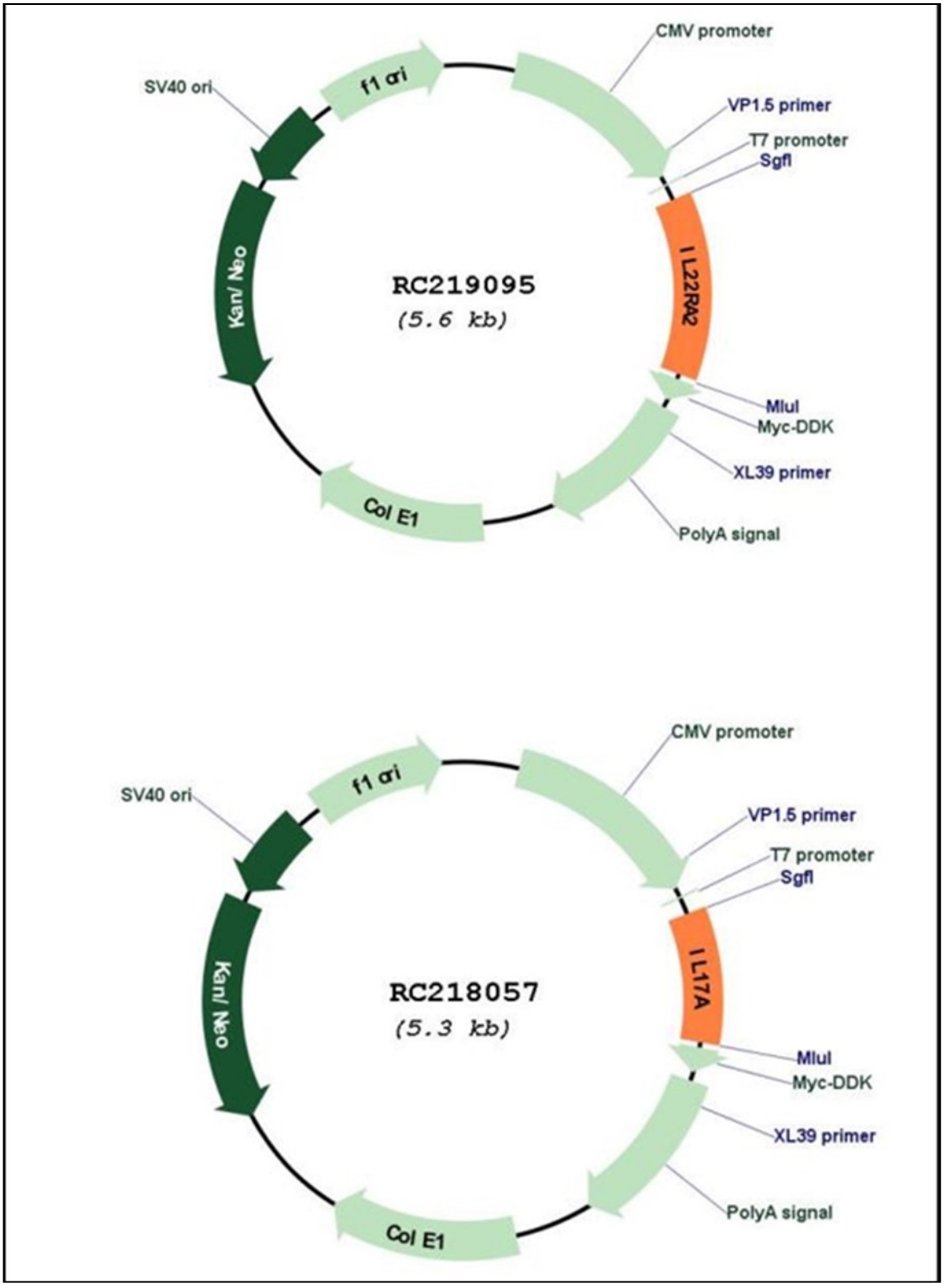

Figure 4.7. IL17A (RC218057) eta IL22RA2 (RC219095) bektoreen mapak. *Iturria: ekoizlearen webgunea; https://www.origene.com/.*

IL17A vector's sequence of interest for cloning

Red=Kozak consensu sequence Green = Sgf I restriction site Blue= IL17A ORF
Yellow = signal peptide Grey=4aa after the signal peptide Red = Sgf I restriction site
Green= Myc and DDK tags

ATAGGGCGGCCGGGAATTCGTCGACTGGATCCGGTACCGAGGAGATCTGCCGCC
GCGATCGCC

ATGACTCCTGGGAAGACCTCATTGGTATCACTGCTACTGCTGCTGAGCCTGGAG
GCCATAGTGAAGGCAGGAATCACAATCCCACGAAATCCAGGATGCCCAAATTCT
GAGGACAAGAACTTCCCCCGGACTGTGATGGTCAACCTGAACATCCATAACCGG
AATACCAATACCAATCCCAAAAGGTCCTCAGATTACTACAACCGATCCACCTCAC
CTTGGAATCTCCACCGCAATGAGGACCCTGAGAGATATCCCTCTGTGATCTGGGA
GGCAAAGTGCCGCCACTTGGGCTGCATCAACGCTGATGGGAACGTGGACTACCA
CATGAACTCTGTCCCCATCCAGCAAGAGATCCTGGTCCTGCGCAGGGAGCCTCC
ACACTGCCCCAACTCCTTCCGGCTGGAGAAGATACTGGTGTCCGTGGGCTGCAC
CTGTGTCACCCCGATTGTCCACCATGTGGCC

ACGCGTACGCGGCCGCTCGAGCAGAAACTCATCTCAGAAGAGGATCTGGCAGC
AAATGATATCCTGGATTACAAGGATGACGACGATAAGCTTTAA

Primers sequence necessary for the generation of IL17SP amplification

ATAGGGCGGCCGGGAATTCGTCGACTGGATCCGGTACCGAGGAGATCTGCGCC
GCGATCGCC

ATGACTCCTGGGAAGACCTCATTGGTATCACTGCTACTGCTGCTGAGCCTGGAG
GCCATAGTGAAGGCAGGAATCACAATCCCACGAAATCCAGGATGCCCAAATTCT
GAGGACAAGAACTTCCCCCGGACTGTGATGGTCAACCTGAACATCCATAACCGG
AATACCAATACCAATCCCAAAAGGTCCTCAGATTACTACAACCGATCCACCTCAC
CTTGGAATCTCCACCGCAATGAGGACCCTGAGAGATATCCCTCTGTGATCTGGGA
GGCAAAGTGCCGCCACTTGGGCTGCATCAACGCTGATGGGAACGTGGACTACCA
CATGAACTCTGTCCCCATCCAGCAAGAGATCCTGGTCCTGCGCAGGGAGCCTCC
ACACTGCCCCAACTCCTTCCGGCTGGAGAAGATACTGGTGTCCGTGGGCTGCAC
CTGTGTCACCCCGATTGTCCACCATGTGGCC

ACGCGTACGCGGCCGCTCGAGCAGAAACTCATCTCAGAAGAGGATCTGGCAGC
AAATGATATCCTGGATTACAAGGATGACGACGATAAGGTTTAA

Figure 4.8. *IL17*ko primerrendako sekuentziak.

IL22RA2 vector's sequence of interest for cloning

Red=Kozak consensu sequence Green = Sgf I restriction site Blue= IL22RA2 ORF
Yellow= signal peptide Grey=4aa after the signal peptide Red = Sgf I restriction site
Green=Myc and DDK tags

ATAGGGCGGCCGGGAATTCGTCGACTGGATCCGGTACCGAGGAGATCTGCCGCCGC
GATCGCC

ATGATGCCTAAACATTGCTTTCTAGGCTTCCTCATCAGTTTCTTCCTTACTGGTGTAG
CAGGAACTCAGTCAACGCATGAGTCTCTGAAGCCTCAGAGGGTACAATTTCAGTCC
CGAAATTTTCACAACATTTTGCAATGGCAGCCTGGGAGGGCACTTACTGGCAACAG
CAGTGTCTATTTTGTGCAGTACAAAATATATGGACAGAGACAATGGAAAAATAAAGA
AGACTGTTGGGGTACTCAAGAACTCTCTTGTGACCTTACCAGTGAAACCTCAGACA
TACAGGAACCTTATTACGGGAGGGTGAGGGCGGCCTCGGCTGGGAGCTACTCAGAA
TGGAGCATGACGCCGCGGTTCACTCCCTGGTGGGAAACAAAAATAGATCCTCCAGT
CATGAATATAACCCAAGTCAATGGCTCTTTGTTGGTAATTCTCCATGCTCCAAATTTA
CCATATAGATACCAAAAGGAAAAAAATGTATCTATAGAAGATTACTATGAACTACTA
ACCGAGTTTTTATAATTAACAATTCACTAGAAAAGGAGCAAAAGGTTTATGAAGGGG
CTCACAGAGCGGTTGAAATTGAAGCTCTAACACCACACTCCAGCTACTGTGTAGTG
GCTGAAATATATCAGCCCATGTTAGACAGAAGAAGTCAGAGAAGTGAAGAGAGATG
TGTGGAAATTCCA

ACGCGTACGCGGCCGCTCGAGCAGAAACTCATCTCAGAAGAGGATCTGGCAGCAA
ATGATATCCTGGATTACAAGGATGACGACGATAAGGTTTAA

Primers sequence necessary for the generation of IL22RA2 without signal peptide amplification

ATAGGGCGGCCGGGAATTCGTCGACTGGATCCGGTACCGAGGAGATCTGCCGCCGC
GATCGCC

ATGATGCCTAAACATTGCTTTCTAGGCTTCCTCATCAGTTTCTTCCTTACTGGTGTAG
CAGGAACTCAGTCAACGCATGAGTCTCTGAAGCCTCAGAGGGTACAATTTCAGTCC
CGAAATTTTCACAACATTTTGCAATGGCAGCCTGGGAGGGCACTTACTGGCAACAG
CAGTGTCTATTTTGTGCAGTACAAAATATATGGACAGAGACAATGGAAAAATAAAGA
AGACTGTTGGGGTACTCAAGAACTCTCTTGTGACCTTACCAGTGAAACCTCAGACA
TACAGGAACCTTATTACGGGAGGGTGAGGGCGGCCTCGGCTGGGAGCTACTCAGAA
TGGAGCATGACGCCGCGGTTCACTCCCTGGTGGGAAACAAAAATAGATCCTCCAGT
CATGAATATAACCCAAGTCAATGGCTCTTGTTGGTAATTCTCCATGCTCCAAATTTA
CCATATAGATACCAAAAGGAAAAAAATGTATCTATAGAAGATTACTATGAACTACTA
ACCGAGTTTTTATAATTAACAATTCACTAGAAAAGGAGCAAAAGGTTTATGAAGGGG
CTCACAGAGCGGTTGAAATTGAAGCTCTAACACCACACTCCAGCTACTGTGTAGTG
GCTGAAATATATCAGCCCATGTTAGACAGAAGAAGTCAGAGAAGTGAAGAGAGATG
TGTGGAAATTCCA

ACGCGTACGCGGCCGCTCGAGCAGAAACTCATCTCAGAAGAGGATCTGGCAGCAA
ATGATATCCTGGATTACAAGGATGACGACGATAAGGTTTAA

Figure 4.9. *IL22RA2*ko primerrendako sekuentziak.

Sequence and product of the primers for IL-17 signal peptide amplification

- Forward primer (17S) structure and sequence (30 bases; melting Tª 69.8)

3 bases before restriction site + Restriction site (Sgf I) + Kozak consense secuence of the vector fragment+ IL17SP start

5'- GCCGCGATCGCCATGACTCCTGGGAAGACC

- Forward primer (17AS) structure and sequence (37 bases; melting Tª 67.1)

IL22RA2 mature protein start +4 aa + IL17 SP end

5'AGGCTTCAGAGACTCATGCGTTGACTGAGTGATTGTGATTCCTGCCTTCACTATGGCCTCCAGGCTC

- Generated IL17SP fragment: 93 + 30 = 123 bp

GCCGCGATCGCCATGACTCCTGGGAAGACCTCATTGGTATCACTGCTACTGCTGCTGAGCCTGGAGGCC
ATAGTGAAGGCAGGAATCACAATCACTCAGTCAACGCATGAGTCTCTGAAGCCT

Sequence and product of the primers for IL22RA2 without signal peptide amplification

- Forward primer (22S) structure and sequence (30 bases; melting Tª 63.9)

IL17 SP end + 4aa +IL22RA2 mature protein start

5'-GAGCCTGGAGGCCATAGTGAAGGCAGGAATCACAATCACTCAGTCAACGCATGAGCTCTGAAGCCT

- Forward primer (22AS) structure and sequence (33 bases; melting Tª 66.0)

6 bases before restriction site + Restriction site (Mlu I) + IL22RA2 mature protein end

5'- CCGCGTACGCGTTGGAATTTCCACACATCTCTC

- Generated IL22RA2 amplification product: 639 + 30 = 669 bp

GAGCCTGGAGGCCATAGTGAAGGCAGGAATCACAATCACTCAGTCAACGCATGAGTCTCTGAAGCCTC
AGAGGGTACAATTTCAGTCCCGAAATTTTCACAACATTTTGCAATGGCAGCCTGGGAGGGCACTTACTG
GCAACAGCAGTGTCTATTTTGTGCAGTACAAAATATATGGACAGAGACAATGGAAAAATAAAGAAGAC
TGTTGGGGTACTCAAGAACTCTCTTGTGACCTTACCAGTGAAACCTCAGACATACAGGAACCTTATTACG
GGAGGGTGAGGGCGGCCTCGGCTGGGAGCTACTCAGAATGGAGCATGACGCCGCGGTTCACTCCCTG
GTGGGAAACAAAAATAGATCCTCCAGTCATGAATATAACCCAAGTCAATGGCTCTTTGTTGGTAATTCTC
CATGCTCCAAATTTACCATATAGATACCAAAAGGAAAAAAATGTATCTATAGAAGATTACTATGAACTAC
TATACCGAGTTTTTATAATTAACAATTCACTAGAAAAGGAGCAAAAGGTTTATGAAGGGGCTCACAGAG
CGGTTGAAATTGAAGCTCTAACACCACACTCCAGCTACTGTGTAGTGGCTGAAATATATCAGCCCATGTT
AGACAGAAGAAGTCAGAGAAGTGAAGAGAGATGTGTGGAAATTCCAACGCGTACG

Figure 4.10. Diseinatutako primerren sekuentzia eta produktuak.

Sequence of the final desired overlapping product to be amplified and cloned

Combined fragment 93 + 639 = 722

GCCGCGATCGCCATGACTCCTGGGAAGACCTCATTGGTATCACTGCTACTGCTGCTGAGCCTGGAGGC
CATAGTGAAGGCAGGAATCACAATCACTCAGTCAACGCATGAGTCTCTGAAGCCTCAGAGGGTACAA
TTTCAGTCCCGAAATTTTCACAACATTTTGCAATGGCAGCCTGGGAGGGCACTTACTGGCAACAGCAG
TGTCTATTTTGTGCAGTACAAAATATATGGACAGAGACAATGGAAAAATAAAGAAGACTGTTGGGGT
ACTCAAGAACTCTCTTGTGACCTTACCAGTGAAACCTCAGACATACAGGAACCTTATTACGGGAGGGT
GAGGGCGGCCTCGGCTGGGAGCTACTCAGAATGGAGCATGACGCCGCGGTTCACTCCCTGGTGGGA
AACAAAAATAGATCCTCCAGTCATGAATATAACCCAAGTCAATGGCTCTTTGTTGGTAATTCTCCATGC
TCCAAATTTACCATATAGATACCAAAAGGAAAAAAATGTATCTATAGAAGATTACTATGAACTACTATA
CCGAGTTTTTATAATTAACAATTCACTAGAAAAGGAGCAAAAGGTTTATGAAGGGGCTCACAGAGCG
GTTGAAATTGAAGCTCTAACACCACACTCCAGCTACTGTGTAGTGGCTGAAATATATCAGCCCATGTTA
GACAGAAGAAGTCAGAGAAGTGAAGAGAGATGTGTGGAAATTCCAACGCGTACG

3 bases before restriction site + Restriction site (Sgf I) + Kozak consense secuence of the vector fragment+ IL17SP start+ IL17SP+IL17 SP end + 4aa +IL22RA2 mature protein start+ IL22RA2 mature protein+ IL22RA2 mature protein end + Restriction site (Mlu I) + bases after restriction site

Figure 4.11. Anplifikatu eta klonatu beharreko gainjarritako produktuaren sekuentzia.

4.3.2. IL22RA2ren 4. exoiaren klonazioa beste zitokinen adierazpen bektoreetan

4.3.2.1. Helburua eta arrazonamendua

IL22RA2 genearen aldaki luzeena (IL22RA2v1) erretikulu endoplasmatikoan pilatzen proteina kodifikatzen duela, eta IL22RA2v2 barianearekiko alde bakarra exoi gehiharria dela, beharrezkoa zen exoi hau beste zitokina batean klonatzean, exoiaren elemntuek zitokina horren jariapena mugatzeko gai diren ikertzeko.

4.3.2.2. Klonazio estrategia

Helburu honetarako, edozein zitokina erabilgarria zenez, baliabideen araberako hurbilketa egin zen. LaborategianIL-2, IL-4, IL-10 eta IL-17 zeuden eskuragai.

Zitokina hauen irakurtea patroia ikertu egin zen lau zitokina hauetan errestrikzio lekua topatzeko. Eskuragai zeuden entzimen zerrenda ere egin zen, errestrikzio lekuen kopurua mugatuz. Amaitzeko entzimek bektorea behin bakarrik mozteko gaitasuna aztertu zen (4.8. Taula) eta bi zitokinek betetzen zituzten betebehar guztiak.

Entzima		**Zitokinan mozteko lekua**				**Bektorearen mozketa lekuak**			
Izena	Mozketa mota	IL17	**IL10**	**IL4**	**IL2**	**IL17v**	**IL10v**	**IL4v**	**IL2v**
AciI	Itsaskorra			304		69 aldiz	67 aldiz	67 aldiz	67 aldiz
BglII	Itsaskorra		126			1008 p	1008 p	1008 p	1008 p
NheI	Itsaskorra			54		No	No	No	No
XbaI	Itsaskorra				234	No	No	No	No

AluI	Kamutsa			258		17 aldiz	22 aldiz	18 aldiz	18 aldiz
DpnI	Kamutsa				354	28 aldiz	28 aldiz	28 aldiz	28 aldiz
EcoRV	Kamutsa	253		84		1553 p	1622 p	1499 p	1547 p
HincII	Kamutsa	141				3 aldiz	2 aldiz	3 aldiz	3 aldiz
PvuII	Kamutsa			258		3 aldiz	5 aldiz	3 aldiz	3 aldiz

Table 4.8. Errestrikzio entzimen mozketa lekuak ikertutako bektoreetan. Restriction enzyme with cutting positions in the studied vectors. Euren aretan bi entzimek soilik, NheI eta XbaI, betetzen dituzte dituzte baldintzak (atzekalde iluna).

Gure helburua ahalik eta modu azkarrenean burutzeko IL-2 eta IL-4ean klonazioa paraleloan egitea erabaki genuen. Klonazio estrategiak, errestrikzio entzima bakarra erabiliz 4. Exoia sartzeko, amaierako produktuan errestrikzio lekua sartutako sekuentziaren bi alboetan egotea eraginko luke, IL-2 klonazio estrategian ikus daitekeen moduan (4.12 Irudia).

4.3.2.3. Deskribapen orokorra

Difinitutako estrategiak hurrengo pausoak ditu:

I. Primerren diseinua

II. Bilatzen den sekuentziaren ekoizpena diseinatutako primerrekin (PCR bakarra)

III. Sartuko den sekuetziaren eta bektorearen digestioa intereseko entzimaren bidez (2 digestio independiente)

IV. Bektore eta sekuentziaren ligazioa eta errekombinazioa

V. Transformazioa

VI. Kolonien konfirmazio PCR eta sekuentziazioa.

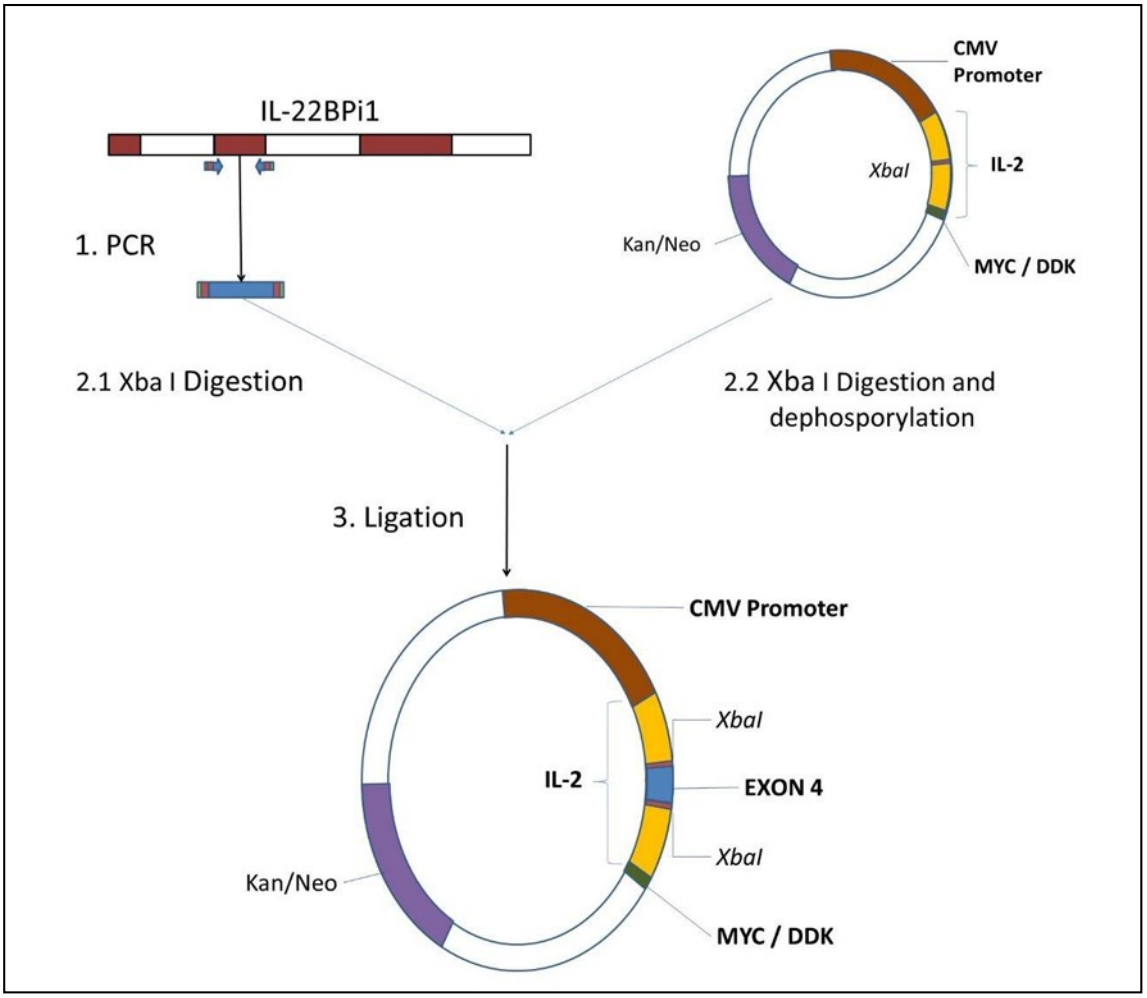

Figure 4.12. Klonazio estrategiaren adierazpen orokorra IL22RA2ren 4. exoia IL2 bektorean XbaI entzimarekin.

4.3.2.4. Primerren diseinua

IL22RA2 4. Exoiaren ikerketa, sekuentzia zaila dela erakutsi zuen bi arrazoirengatik: GC eduki baxua, fusio tenperatura baxuak eraginez, eta primerren arteko konplementarietate aundia exoia anplifikatzeko primerretan. Exoiaren azken 16 basetan oinarritutako primerrak fusio tenperatua baxuegiak eragingo lituzte (fusio tenperatura baxuek atxikimendu ez-espezifikoak handitzen dituzte). Base gehiago erabiliz egindako primerrek fusio tenperatura hobea emango lituzkete baina aurrekoaren kasuan, konplementarietate oso altua litzateke eta horrek anplifikazio efizientzia mugatuko luke. Fusio tenperatura eta konplementarietatearen arteko oreka bilatu

nahiean base gehigarri bakoitzaren eragina aztertu zen, baina zenbait konplementarietate arazo ekidiezinak ziren aurreko primerretan bai IL4 (4.13. Irudia) eta bai IL2 (4.14 Irudia) zitokinen kasuetan.

Cloning of Exon 4 of IL22RA2 in IL4 vector with Nhel restriction enzyme

- Vector´s sequence of interest for cloning (RC213286 representing NM_172348)
  Red=Cloning site Blue=ORF Green=Tags(s)

TTTTGTAATACGACTCACTATAGGGCGGCCGGGAATTCGTCGACTGGATCCGGTACCGAGGAGATCTGCC
GCCGCGATCGCC
ATG GGT CTC ACC TCC CAA CTG CTT CCC CCT CTG TTC TTC CTG/CTA GCA TGT GCC
GGC AAC TTT GTC CAC GGA CAC AAG TGC GAT ATC ACC TTA CAG GAG ATC ATC AAA
ACT TTG AAC AGC CTC ACA GAG CAG AAG AAC ACA ACT GAG AAG GAA ACC TTC TGC
AGG GCT GCG ACT GTG CTC CGG CAG TTC TAC AGC CAC CAT GAG AAG GAC ACT CGC
TGC CTG GGT GCG ACT GCA CAG CAG TTC CAC AGG CAC AAG CAG CTG ATC CGA TTC
CTG AAA CGG CTC GAC AGG AAC CTC TGG GGC CTG GCG GGC TTG AAT TCC TGT CCT
GTG AAG GAA GCC AAC CAG AGT ACG TTG GAA AAC TTC TTG GAA AGG CTA AAG ACG
ATC ATG AGA GAG AAA TAT TCA AAG TGT TCG AGC
ACGCGTACGCGGCCGCTCGAGCAGAAACTCATCTCAGAAGAGGATCTGGCAGCAAATGATATCCTGGATT
ACAAGGATGACGACGATAAGGTTTAA

- Restriction enzyme

Enzyme		Recognition sequence	Cut
Name	End type		
NheI	Sticky	5' GCTAGC	5' G CTAGC3'
		3' CGATCG	3' CGATC G5'

Enzyme	Oligo Sequence (recognition sequence in red)	Chain lenght	%Cleavage	
			2h	20hr
NheI	GGCTAGCC	8	0	0
	CGGCTAGCCG	10	10	25
	CTAGCTAGCTAG	12	10	50

- Need amplified fragment

Red=Enzyme recognition site Blue= necessary bases around recongnition site for cutting
Green= IL22RA2 Exon 4 sequence Dark Blue= necessary exon sequence primers

5'G GAC TAG/CTA GCA ATG TTC TCA TGC AGC ATG AAA AGC TCT CAC CAG AAG CCA AGT GGA TGC TGG CAG CAC ATT TCT TGT AAC TTC CCA GGC TGC AGA ACA TTG GCT AAA CTG/CTA GCT AGG TG 3'

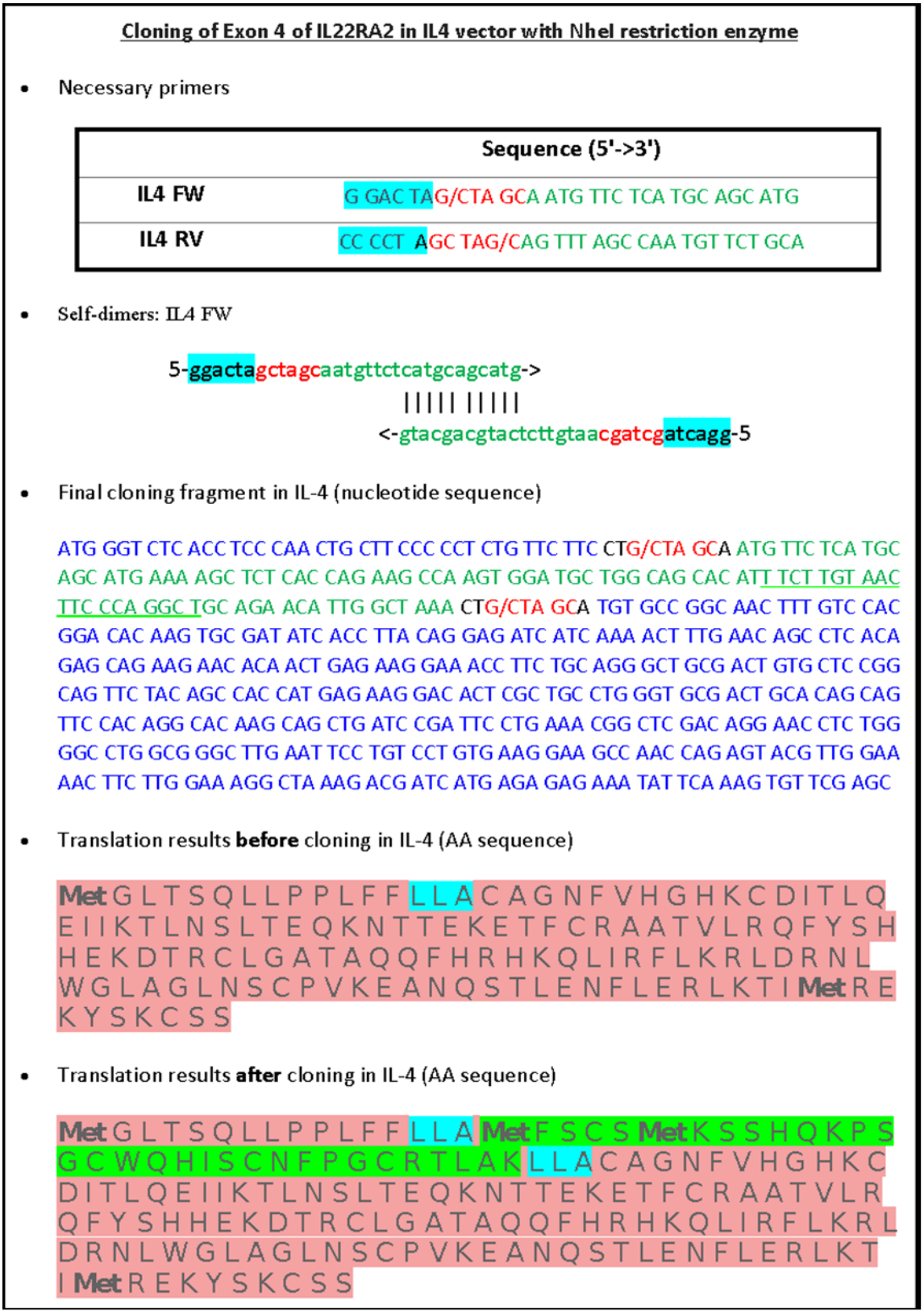

Cloning of Exon 4 of IL22RA2 in IL4 vector with Nhel restriction enzyme

- Necessary primers

	Sequence (5'->3')
IL4 FW	G GAC TAG/CTA GCA ATG TTC TCA TGC AGC ATG
IL4 RV	CC CCT AGC TAG/CAG TTT AGC CAA TGT TCT GCA

- Self-dimers: IL4 FW

5-ggactagctagcaatgttctcatgcagcatg->
||||| |||||
<-gtacgacgtactcttgtaacgatcgatcagg-5

- Final cloning fragment in IL-4 (nucleotide sequence)

ATG GGT CTC ACC TCC CAA CTG CTT CCC CCT CTG TTC TTC CTG/CTA GCA ATG TTC TCA TGC AGC ATG AAA AGC TCT CAC CAG AAG CCA AGT GGA TGC TGG CAG CAC ATT TCT TGT AAC TTC CCA GGC TGC AGA ACA TTG GCT AAA CTG/CTA GCA TGT GCC GGC AAC TTT GTC CAC GGA CAC AAG TGC GAT ATC ACC TTA CAG GAG ATC ATC AAA ACT TTG AAC AGC CTC ACA GAG CAG AAG AAC ACA ACT GAG AAG GAA ACC TTC TGC AGG GCT GCG ACT GTG CTC CGG CAG TTC TAC AGC CAC CAT GAG AAG GAC ACT CGC TGC CTG GGT GCG ACT GCA CAG CAG TTC CAC AGG CAC AAG CAG CTG ATC CGA TTC CTG AAA CGG CTC GAC AGG AAC CTC TGG GGC CTG GCG GGC TTG AAT TCC TGT CCT GTG AAG GAA GCC AAC CAG AGT ACG TTG GAA AAC TTC TTG GAA AGG CTA AAG ACG ATC ATG AGA GAG AAA TAT TCA AAG TGT TCG AGC

- Translation results **before** cloning in IL-4 (AA sequence)

Met G L T S Q L L P P L F F L L A C A G N F V H G H K C D I T L Q
E I I K T L N S L T E Q K N T T E K E T F C R A A T V L R Q F Y S H
H E K D T R C L G A T A Q Q F H R H K Q L I R F L K R L D R N L
W G L A G L N S C P V K E A N Q S T L E N F L E R L K T I Met R E
K Y S K C S S

- Translation results **after** cloning in IL-4 (AA sequence)

Met G L T S Q L L P P L F F L L A Met F S C S Met K S S H Q K P S
G C W Q H I S C N F P G C R T L A K L L A C A G N F V H G H K C
D I T L Q E I I K T L N S L T E Q K N T T E K E T F C R A A T V L R
Q F Y S H H E K D T R C L G A T A Q Q F H R H K Q L I R F L K R L
D R N L W G L A G L N S C P V K E A N Q S T L E N F L E R L K T
I Met R E K Y S K C S S

Figure 4.13. IL22RA2ren 4. Exoiaren klonaketa IL4 bektorean Nhel errestrikzio entzimaren bidez.

Cloning of Exon 4 of IL22RA2 in IL2 vector with NheI restriction enzyme

- Vector´s sequence of interest for cloning (RC210013 representing NM_00586)
  Red=Cloning site Blue=ORF Green=Tags(s)

TTTTGTAATACGACTCACTATAGGGCGGCCGGGAATTCGTCGACTGGATCCGGTACCGAGGAGATCTGCC
GCCGCGATCGCC

ATG TAC AGG ATG CAA CTC CTG TCT TGC ATT GCA CTA AGT CTT GCA CTT GTC ACA
AAC AGT GCA CCT ACT TCA AGT TCT ACA AAG AAA ACA CAG CTA CAA CTG GAG CAT
TTA CTG CTG GAT TTA CAG ATG ATT TTG AAT GGA ATT AAT AAT TAC AAG AAT CCC
AAA CTC ACC AGG ATG CTC ACA TTT AAG TTT TAC ATG CCC AAG AAG GCC ACA GAA
CTG AAA CAT CTT CAG TGT/CTA GAA GAA GAA CTC AAA CCT CTG GAG GAA GTG CTA
AAT TTA GCT CAA AGC AAA AAC TTT CAC TTA AGA CCC AGG GAC TTA ATC AGC AAT
ATC AAC GTA ATA GTT CTG GAA CTA AAG GGA TCT GAA ACA ACA TTC ATG TGT GAA
TAT GCT GAT GAG ACA GCA ACC ATT GTA GAA TTT CTG AAC AGA TGG ATT ACC TTT
TGT CAA AGC ATC ATC TCA ACA CTG ACT
ACGCGTACGCGGCCGCTCGAGCAGAAACTCATCTCAGAAGAGGATCTGGCAGCAAATGATATCCTGGATT
ACAAGGATGACGACGATAAGGTTTAA

- Restriction enzyme

Enzyme		Recognition sequence	Cut
Name	End type		
XbaI	Sticky	5' TCTAGA	5' ---T CTAGA--- 3'
		3' AGATCT	3' ---AGATC T--- 5'

Enzyme	Oligo Sequence (recognition sequence in red)	Chain lenght	%Cleavage	
			2h	20hr
NheI	GGCTAGCC	8	0	0
	CGGTCTAGAGC	10	>90	>90
	TGCGTCTAGAGCA	12	75	>90
	CTAGGTCTAGACTAG	14	75	>90

- Need amplified fragment

Red=Enzyme recognition site Blue= necessary bases around recongnition site for cutting
Green= IL22RA2 Exon 4 sequence Dark Blue= necessary exon sequence primers

5'C ATC GCT/CTA GAA ATG TTC TCA TGC AGC ATG AAA AGC TCT CAC CAG AAG
CCA AGT GGA TGC TGG CAG CAC ATT TCT TGT AAC TTC CCA GGC TGC AGA ACA
TTG GCT AAA TGT/CTA GAG CCG TC 3'

Cloning of Exon 4 of IL22RA2 in IL2 vector with Nhel restriction enzyme

- Necessary primers

	Sequence (5'->3')
IL4 FW	C ATC GCT/CTA GAA ATG TTC TCA TGC AGC ATG
IL4 RV	GA CGG CTC TAG/ACA TTT AGC CAA TGT TCT GCA

- Self-dimers: IL2 FW

5-catcgctctagaaatgttctcatgcagcatg->
||||| |||||
<-gtacgacgtactcttgtaaagatctcgctac-5

- Final cloning fragment in IL-4 (nucleotide sequence)

ATG TAC AGG ATG CAA CTC CTG TCT TGC ATT GCA CTA AGT CTT GCA CTT GTC ACA AAC AGT
GCA CCT ACT TCA AGT TCT ACA AAG AAA ACA CAG CTA CAA CTG GAG CAT TTA CTG CTG
GAT TTA CAG ATG ATT TTG AAT GGA ATT AAT AAT TAC AAG AAT CCC AAA CTC ACC AGG
ATG CTC ACA TTT AAG TTT TAC ATG CCC AAG AAG GCC ACA GAA CTG AAA CAT CTT CAG
TGT/CTA GAA ATG TTC TCA TGC AGC ATG AAA AGC TCT CAC CAG AAG CCA AGT GGA TGC
TGG CAG CAC ATT TCT TGT AAC TTC CCA GGC TGC AGA ACA TTG GCT AAA TGT/CTA GAA
GAA GAA CTC AAA CCT CTG GAG GAA GTG CTA AAT TTA GCT CAA AGC AAA AAC TTT CAC
TTA AGA CCC AGG GAC TTA ATC AGC AAT ATC AAC GTA ATA GTT CTG GAA CTA AAG GGA
TCT GAA ACA ACA TTC ATG TGT GAA TAT GCT GAT GAG ACA GCA ACC ATT GTA GAA TTT
CTG AAC AGA TGG ATT ACC TTT TGT CAA AGC ATC ATC TCA ACA CTG ACT

- Translation results **before** cloning in IL-4 (AA sequence)

Met Y R Met Q L L S C I A L S L A L V T N S A P T S S S T K K T Q L
Q L E H L L L D L Q Met I L N G I N N Y K N P K L T R Met L T F K F
Y Met P K K A T E L K H L Q C L E E E L K P L E E V L N L A Q S K
N F H L R P R D L I S N I N V I V L E L K G S E T T F Met C E Y A D
E T A T I V E F L N R W I T F C Q S I I S T L T

- Translation results **after** cloning in IL-4 (AA sequence)

Met Y R Met Q L L S C I A L S L A L V T N S A P T S S S T K K T Q L
Q L E H L L L D L Q Met I L N G I N N Y K N P K L T R Met L T F K F
Y Met P K K A T E L K H L Q C L E Met F S C S Met K S S H Q K P S
G C W Q H I S C N F P G C R T L A K C L E E E L K P L E E V L N L
A Q S K N F H L R P R D L I S N I N V I V L E L K G S E T T F Met C
E Y A D E T A T I V E F L N R W I T F C Q S I I S T L T

Figure 4.14. IL22RA2ren 4. Exoiaren klonaketa IL2 bektorean Xbal errestrikzio entzimaren bidez.

4.4. Zelulen isolatze eta kultiboa

For the understanding of *IL22RA2* and *IL12A* genes, and its protein products, different cell models were used. Apart from well-known cell lines for which there are established conditions of culture, primary cells were used. In the case of *IL22RA2*, its expression on moDCs generated from monocytes isolated from blood have been described as mentioned in the introduction. As their name indicates, moDCs are derived from monocytes, and monocytes are present in blood. Therefore, the first step is to obtain blood. The object of interest is not the whole blood but the peripheral mononuclear cells (PMBCs) among which are monocytes, and thus, PBMC isolation is required. PMBCs can easily be frozen to be used when necessary. A second isolation is necessary to purify the monocytes from the PBMCs to differentiate them into moDCs. This process is described in detail in the following sections.

IL22RA2 eta IL12A geneak eta bere proteina-produktuak ulertzeko, zelula-eredu desberdinak erabili ziren. Hazkuntza-baldintzak dituzten zelula-lerro ezagunez gain, lehen mailako zelulak erabili ziren. IL22RA2en kasuan, odoletik isolatutako monozitoek sortutako moDCk genea adierazten dutela deskribatu da sarreran aipatu bezala. Izenak dioen bezala, DCak monozitoetatik datoz, eta monozitoak odolean daude. Beraz, lehen urratsa odola lortzea da. Interesaren objektua ez da odol osoa, baizik eta zelula mononuklear periferikoak (ingeleraz peripheral mononuclear cells (PMBC)), zeinen artean monozitoak dauden, eta, beraz, PBMC isolamendua behar da. PMBCak erraz izoztu daitezke, behar denean erabiltzeko. Bigarren isolamendu bat behar da PBMCen monocyteak garbitzeko, moDCetan bereizteko. Prozesu hau hurrengo ataletan deskribatzen da zehatz-mehatz.

4.4.1. Odola lortzea eta PBMC isolaketa eta kriopreserbazioa

PBMC, ingelerazko perihperal blood mononuclear cell, odolean dauden zelula nukleobakarrek, monozito eta linfozitoek (NK, T eta B zelulek) osatzen dute. PMBCak bi moduz lortu ziren: odol osotik hasita eta bere zentrifugazioatik ertorrikako “buffy coat” deritzon geruzatik (4.15. Irudia). Laginaren arabera prozedua zertsobait aldatzen zen. Laginak Euskal Biobankotik (www.biobancovasco.org). zetozen, ospitale mailako ehun plataforma, ikerkuntza basikoa laguntzea helburu duena.

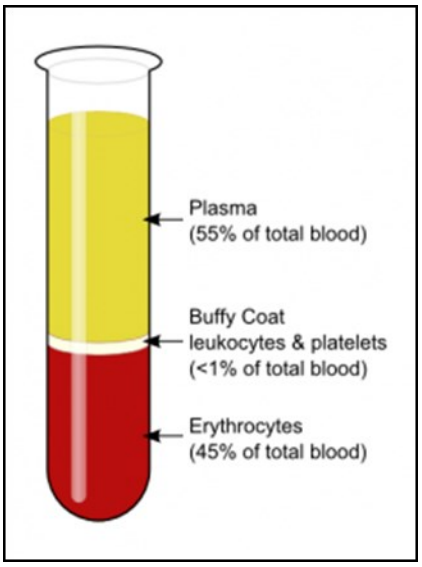

Figure 4.15. Odol osoaren fase desberdinen irudikapena. Buffy coat, koagulatu gabeko odolaren fasea da zeinak zelula txuti eta paketa gehienak pilatzen dituena. *Iturria:*https://microbeonline.com/buffy-coat-definition-composition-preparation-uses/

PBMCak odol laginetatik ateratzeko teknika, bai odol osoaren eta bai buffy coat-aren kasuan, Ficoll erreaktiboan oinarritzen zen. Ficoll-Paque Ficoll PM400, masa moleulkar altuko (M 400,000) sukorsa eta epikoloridrin polimeroa sintetikoa, duen soluzio urtsua da. Polimeroaren molekulek beso asko dituzte eta esferikoak dira. Zelula populazio desberdinen densitatearen arabera, odol lagina Ficoll-Paque erreaktiboaren gainean jartzen da (nahastu gabe) eta

zentriguatu egiten da. Zelulen migrazio desberdinaren ondorioaz, zelula mota bakoitzarendako geruzak sortzen dira (4.16. Irudia). Gero, PMBCak dauden geruza aspiratu eta garbitu egiten da PMBCak lortzeko.

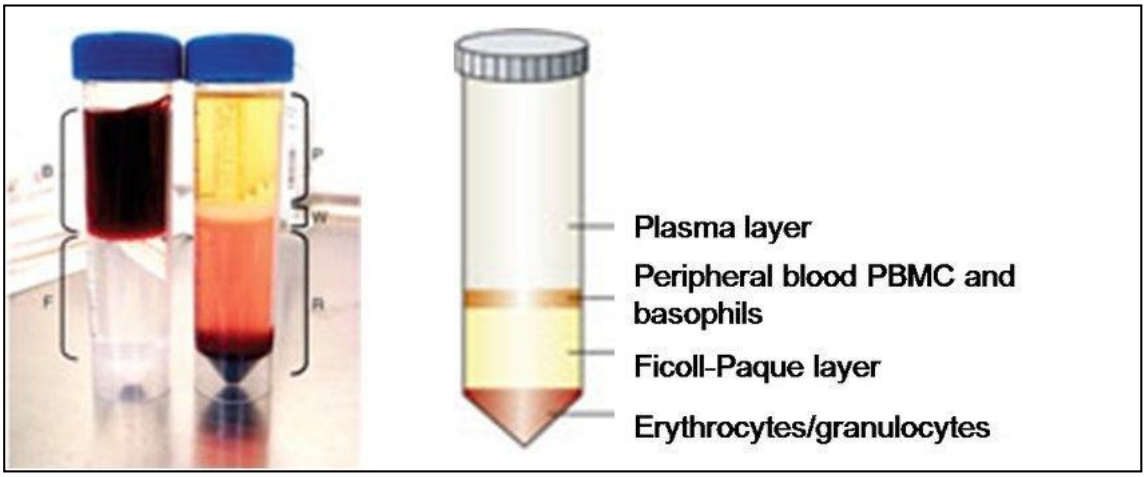

Figure 4.16. Ficoll aurretik eta ondoren ematen den fase banaketa. Ezkerraldean laginaren argazkia zentrifugatu aurretik. Eskuinalean, zentriguazioaren ostea eta geruza bakoitzeko populazioen deskribapena. *Iturria: ResearchGate. Available from: https://www.researchgate.net/figure/Separation-of-granulocytes-from-PBMC-and-basophils-by-Ficoll-Paque-centrifugation_fig3_50231000*

4.4.1.1. Whole blood

Odol osotik PMBCak isolatu eta kriopreserbatzeko protokoloa.

0. Hasi aurretik:

a. Fluxu ganbara garbitu.
b. PBS 1X esterilaba berotu 37ºCk bainuan.
c. Kriopreserbazioarko medioa prestatu 2x (DMSO %20)
d. Emaile bakoitzarendako, prestatu eta etiketatu:
    I. 50 mL bi 2 Falcon PBS 1X 10 mL-rekin (odola disolbatzeko).
    II. 50 mL bi 2 Falcon Ficoll 12.5mL-rekin.
    III. 15 mL Falcon bat PBS 1X 6mL-rekin (garbiketa).
    IV. 10 kriobial.

1. Odol tutuei zentrifugazio azkarra eman

Pauso honen bidez tapa odolik gelditzea ekiditzen da.

2. Odola diluitu

Fluxu ganbaran, tututen tapak kendu eta pipeta serologiko edo Pasteur bat erabiliz, antikoagulatutako 10 mL odols pasa 10 mL PBS dituen Falcon 50 tutura (2 tutu emaileko).

3. Ficollera pasa

Kontu handiz diluitutako odolaren 20 mL-ak 12.5 mL Ficoll dituen Falcon 50 tutura pasa TANTAKA, odola Ficollarekin nahastu dadin ekidituz (2 tutu emaileko).

4. Zentrifugatu

Zentriguatu FRENORIK GABE 400G 35 'RT
Zentrifugazio baldintzak: RFC 400 ACCEL 4 DECEL 0

5. PMBCak banatu

Poliki, goiko fale likidoa (plasma) eta Ficollaren aretan dagoen zelula mononuklearren geruza aspiratu 1000uL-ko pipetarekin. Zeulak PBSa daukan 15 mL-ko Falcon tutura pasa (2 tutu emaileko).

6. Zentrifugatu (lehen garbiketa)

Zentrifugatu 250-300G 10 'RT
Gainaldeko likidoa dekantatu behekaldeko pikorra puskatu gabe. Pausu hontan eta hurrengoan, PBMCen garbiketa dute helburu, egon daitezkeen plaketa eta plasma proteinak kenduz.

7. Bersuspentsioa eta kontaketa

PBS 1X mL-bat gehitu, pelleta bersuspenditu eta homogenizatu. Bi tutuak batean batu. Bolumena 8 mL-tara eraman PBS 1Xen bidez.
Eppendorf batean bersuspentsioaren 10 µL eta Trypan Blueren beste 10 µL jarri. Hiruzpalau minutu itxoin tindaketa eman dadin etan Neubauerren ganbaran zenbatu. Gehiegi badaude, alikuota berria hartu eta PBSean diluitu tindaketaren aurretik.

8. Zentrifugatu (bigarren garbiketa)

Zentrifugatu 250G 10 'RT
Gainaldeko likidoa dekantatu behekaldeko pikorra puskatu gabe. Saiatu 50 µL PBS baino gehiagorik ez uzten, baina pikorra lehor utzi gabe.

9. Bersuspenditu

Momentu hontatik aurrera lortutako PMBCak helburu desberdinetarako erabili daitezke:
Momentuan erabiltzeko
Kriopreservatuta gorde

10. Kriopreserbazioarako alikuotatzea

Bilatzen diren alikuotak 2 milioi (M) PBNC / 500 mL tutoko dira %10 DMSO daukan FBSan. Milioi bat PMBC daude odol soko mL bakoitzeko. Krioprserbazio soluzioak FBSa %10 DMSOarekin dauka. Emaitzak ikusita, 2X kriopreservazio soluzioa (%20 DMSO) prestatzen da eta FBSan bersuspenditutako zelulei gehintzen zai 1:1 proportzioan. Kriobialak Mr. Frosty izeneko edukiontziaren bidez (kongelazio abiadrua -1ºC / minutuko) izozten dira -80ºC-etan. Kalkuluak ikusteko, begiratu 2.15. Irudia.

11. PMBCen desizoztea eta garbiketa erabili aurretik

- 1X PBS esterlia berotu 37ºC-tara bainuan
- Bial bakoitza bainuan(37ºC) desizoztu bi minutuz.
- TANTAKA 1X PBS gehitu (0.5 mL)
- Falcon 15 batera pasa
- TANTAKA 15 mL arte bete
- Zentrifugatu 1800 rpm 10 'RT
- Gaineko likidoa bota
- Pikorra gelditzen den likoan bersupensidtu
- 10 mL PBS gehitu
- Zentrifugatu 2000 rpm 5 'RT
- Gaineko likido guztia bota
- Pikorra bersuspenditu

4.4.1.2. Buffy Coat

Buffy coat-etik PMBCak isolatu eta kriopreserbatzeko protokoloa.

0. Hasi aurretik:

a. Fluxu ganbara garbitu.
b. PBS 1X esterilaba berotu 37ºCk bainuan.
c. Kriopreserbazioarko medioa prestatu 2x (DMSO %20)
d. Emaile bakoitzarendako, prestatu eta etiketatu:
   I. 50 mL Falcon bat PBS 1X 40 mL-rekin (odola disolbatzeko).
   II. 50 mL bi Falcon Ficoll 10mL-rekin.
   III. 50 mL bi Falcon PBS 1X 40 mL-rekin (garbiketa).
   IV. 10 kriobial.

1. Buffy coat diluitu

Fluxu ganbaran,buffy coat-aren poltsatik odola atera eta PBS 1X-ean dilutiu 1:4 proportiozan (30 mL PBS 1X eta 10 mL buffy coat. Ongi nahastu.

3. Ficollera pasa

Kontu handiz diluitutako buffy coataren 20 mL 1o mL Ficoll dituen Falcon 50 tutura pasa TANTAKA, odola Ficollarekin nahastu dadin ekidituz (2 tutu emaileko).

4. Zentrifugatu

Zentriguatu FRENORIK GABE 400G 35 'RT
Zentrifugazio baldintzak: RFC 400 ACCEL 4 DECEL 0

5. PMBCak banatu

Poliki, goiko fale likidoa (plasma) eta Ficollaren aretan dagoen zelula mononuklearren geruza aspiratu 1000uL-ko pipetarekin. Zeulak PBSa daukan 50 mL-ko Falcon tutura pasa eta bete PBS-z (2 tutu emaileko).

6. Zentrifugatu (lehen garbiketak)

Zentrifugatu 250-300G 10 'RT
Gainaldeko likidoa dekantatu behekaldeko pikorra puskatu gabe. PBS 1X mL bat gehitu eta pikorra bersuspenditu. PBS 1X bete eta errepikatu.

7. Bersuspentsioa eta kontaketa

PBS 1X mL-bat gehitu, pelleta bersuspenditu eta homogenizatu. Bolumena 50 mL-tara eraman PBS 1Xen bidez. Eppendorf batean bersuspentsioaren 10 µL eta Trypan Blueren beste 10 µL jarri. Hiruzpalau minutu itxoin tindaketa eman dadin etan Neubauerren ganbaran zenbatu.

8. Zentrifugatu (bigarren garbiketa)

Zentrifugatu 250G 10 'RT

Gainaldeko likidoa dekantatu behekaldeko pikorra puskatu gabe. Saiatu 50 µL PBS baino gehiagorik ez uzten, baina pikorra lehor utzi gabe.

9. Bersuspenditu

Momentu hontatik aurrera lortutako PMBCak helburu desberdinetarako erabili daitezke:
Momentuan erabiltzeko
Kriopreservatuta gorde

10. Kriopreserbazioarako alikuotatzea

Bilatzen diren alikuotak 50 milioi (M) PBMC / 500 mL tutoko dira %10 DMSO daukan FBSan. Buffy coat batean 200 eta 600 M PMBC egon daitezke. Krioprserbazio soluzioak FBSa %10 DMSOarekin dauka. Emaitzak ikusita, 2X kriopreservazio soluzioa (%20 DMSO) prestatzen da eta FBSan bersuspenditutako zelulei gehintzen zai 1:1 proportzioan. Kriobialak Mr. Frosty izeneko edukiontziaren bidez (kongelazio abiadrua -1ºC / minutuko) izozten dira -80ºC-etan. Kalkuluak ikusteko, begiratu 2.15. Irudia.

11. PMBCen desizoztea eta garbiketa erabili aurretik

Prozedura odol osoaren berdina da.

Cryopreservation calculations

Whole blood: 2 M cells/ vial (500 uL)	Generic	Per blood sample (10mL)
Number of cells (millions):	x	20
Number of needed vials (2 million per vial):	x/2	10
Needed volume (0,5 mL per vial):	(0.5 x (x/2)) = 0.25x mL	5
Cryopreservation medium volume (half of the needed total volume):	(0.25x) /2 = 0,125x mL	2.5
Cryopreservation medium 2x (FBS 20% DMSO):		
FBS (Fetal Bovine Serum):	0.8 * (0.125x) mL	2
DMSO:	0.2 * (0.125x) mL	0.5
Buffy coat: 50 M cells/ vial (1000ul)		
Number of cells (millions):	x	400
Number of needed vials (50 million per vial):	x/50	8
Needed volume (1 mL per vial):	x/50 mL	8
Cryopreservation medium volume (half of the needed total volume):	(x/50) /2 = x/100 mL	4
Cryopreservation medium 2x (FBS 20% DMSO):		
FBS (Fetal Bovine Serum):	0.8 * (x/100) mL	3.2
DMSO:	0.2 * (x/100) mL	0.8

Figure 4.17. Buffy coat edo odol osotik lortutako PBMCen kriopreserbazioarako kalkuluak.

4.4.2. Monozitoen isolamendua

Monozitoak PBMCetatik isolatuak zian ziren, horretarako linfozitoak (NK, T eta B zelulak) kendu behar dira. Monozitoek PMBC-en %10-15a suposatzen dute eta CD14 gainazalean espresatzea dute komunean. Hala ere berriagoak diren ikerketek, monozitoen artean hiru azpipopulazio bereizten dituzte euren gainazaleko errezpetoren eta ezaugarri guntzionalengatik: monozito klasikoak (CD14++CD16-), tartekoak (CD14++CD16+) eta ez-klasikoak (CD14+CD16+). Monozito klasikoak gehiengoa (%85-95 inguru) diren bitartean tarteko eta ez-

klasikoen populazioa %5-10 ingurukoa da (2.18. Irudia) eta adinean aurrera joan ahala handitzen doa (Sadeghi et al., 1999; Seidler et al., 2010).

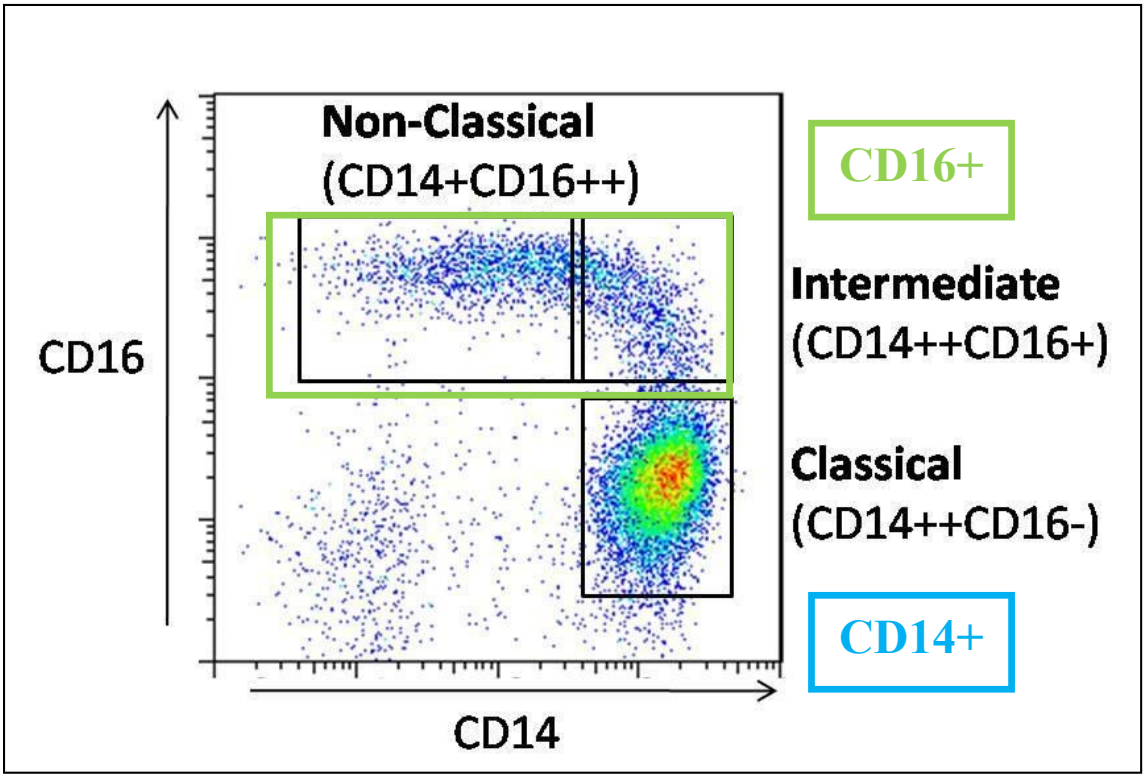

Figure 4.18. Monozitoen azpitalden adirazpena fluxuzko zitometrian CD14 and CD16 markatzaileak erabiliz. *Iturria: (Wong et al., 2012).*

Monozitoen isolamendua burutzeko helburuarekin bi teknologia deberdin erabili izan dira: magnetic-activated cell sorting (MACS) eta fluorescence-activated cells sorting (FACS). Bi teknologietan zelulak gainazaleko errezeptoreeen aurkako antigorputzen bidez markatu egtien dira (FACS teknologaren kasua zelula barruko markaketa ere posible da); MACS teknologiaren kasuan, antigorputzek partikula magnetikoak dituzte atxikita, eta FACSen kasuan partikula fluorescentea. Bien ezaugarriak deskribatzen dituen taula duzue hemen (4.9 Taula):

	MACS	FACS
Zelulen isolamenduko ezaugarri bereziak		
Zelulen markaketa	Magnetikoa	Fluoreszentziazkoa

Espezifizitatea	Altua	Altua
Hautaketa positiboa	Posiblea	Posiblea
Hautaketa negatiboa	Posiblea	Posiblea
Markaketa anitza	Mugatua	Posiblea
Espresio mailaren araberako banaketa	Ez da posiblea	Posiblea
Populazio desberdinak batera banatzeko aukera	Oso mugatua eta ez aldi berean	Posiblea
Zelula barruko protein araberako banaketa	Ez da posiblea	Posiblea
Ezaugarri orokorrak		
Zailtasun teknikoa	Baxua	Altua
Eskalagarritasuna	Erreza	Zaila
Prozesatze denbora	Ertaina	Luzea

Table 4.9. MACS eta FACS teknologien ezagarrien konparaketa. FACS teknologiak zelulen banaketarako aukera asko ematen dituen arren MACS, erabilerrezagoa, azkarragoa eta eskalagarriagoa da, zelula kopuru handiak denbora eta kostu efizientziaz banaketa errexean burutzeko gai.

MACS teknologia Miltenyik garatu zuen (Miltenyi et al., 1990), eta aipatutako moduan, zelulak gainazaleko errezeptoreen kontrako antibogorputzekin markatu eta eremu magnetiko indartsu batetik pasatzeean datza. Markatutako zeulak barruan gelditzen dira eta markatu gabeak pasau egitn dira. Hautaketa negatiboa egiten denean, pasatutako zelulak biltzen dira, eta hautaketa posititiboa egiterakoan, zutabea eremu magnetikotik atera behar da zelulak askatzeko (4.10 Taula).

	HAUTAKETA POSITIBOA		***HAUTAKETA NEGATIBOA***	
Markaketa	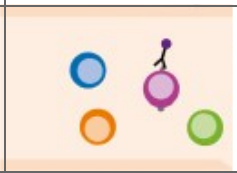	Interesezko zelulak magnetikoki markatzen dira Microbead-ak erabiliz	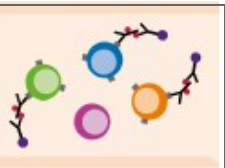	Helburu ez diren zelulak magnetikoki markatu egiten dira
Banaketa	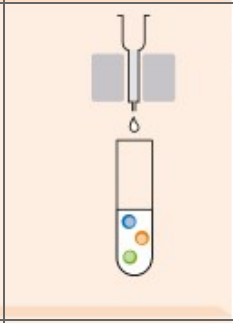	Zelulak Banatzaile batean jarritako zutabaren bidez banatzen dira. Zuzenean pasatzen den frakzio, helburu ez diren zelulak biltzen dira.	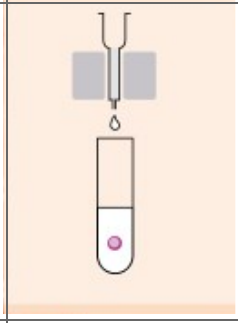	Helburu ez diren zelulak zutabean gelditzen dira. Helburu diren zelulak bakarrik pasatzen dira.
Eluzioa	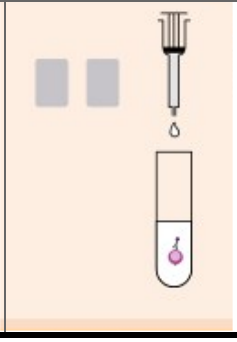	Zutabea banatzailetik kentzen da. Lotuta zeuden zelulak eluitu egiten dira frakzio aberastu eta markatu bezala.		

Table 4.10. MACS hautaketa positiboa eta negatiboaren arteko konparaketa. https://www.miltenyibiotec.com/US-en/ -tik moldatua.

FACS teknologia fluxuzko zitometrian oinarritzen da, eta 4.9 taula adierazi bezala, zelulen banaketa ahalbidetzen duen zelula nahasketa heterogenoetatik hasita. Prozesuaren oinarreiak hurrengoak dira (4.19 Irudia).

Zelula nahasketa likido (normalean PBS) korronte estu batean sartzen da, zelulak errenkadan jarri. Korrontea fluoreszentzia laser eta deketbore debesberdinetatik pasazten da: forward scatter (tamaina zehazten du), side scatter (konplexutasuna zehazten du) eta fluoreszentzia (tindaketak neurtzeko). Analisiaren ondoren, noozle izeneko abiadura handiko bibrazio mekanismoak, korrontea tantetan banatzen du, tanta bakoitzean zelula bat jarriz. Momentu zehatz horretan, tantak sortzen ari direnean, karga elektrikoa ematen zaiek aztertuako

ezaugarrien arabera. Kargatutako tantak, bi deflekzio plakek sortutako eremu elektrostatikoan zehar erortzen dira, kargaren arabera alde batera edo bestera eroriz.

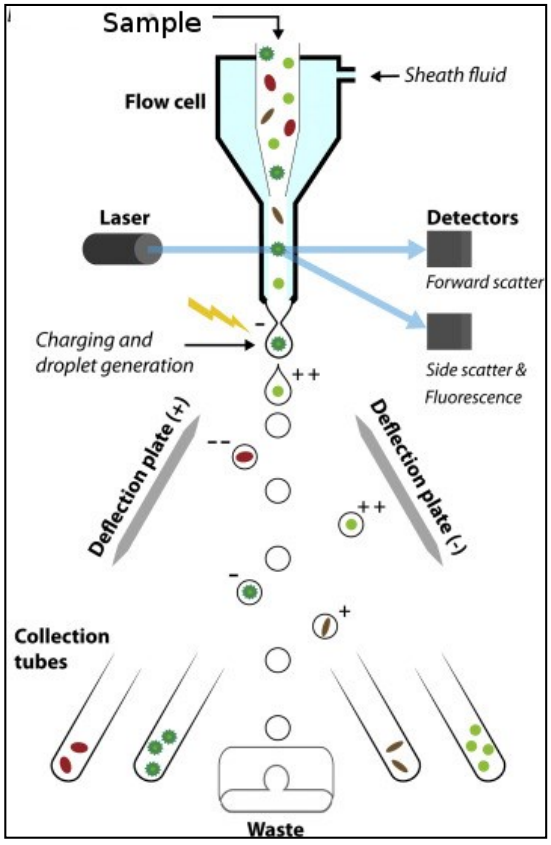

Figure 4.19. FACS teknologiaren irudikapen eskematikoa. *Iturria:* (Pereira et al., 2018)

4.4.2.1. CD14+ monozitoen isolaketa (MACS)

CD14+ monozitoak PBMCetatik isolatzeko MACS hautaketa positiboa erabili zen CD14aren bidezko markaketa erabiliz (#130-050-201, Miltenyi Biotec). Protokoloa hurrengoa da:

1. **Zelulen prestaketa**

a. Zelulen kopurua zehaztu Neubauer-en ganbera eta zitometroaren bidez.
b. Zentrifugatu 300×g 10 minutuz.
c. Gaineko likidoa pipetarekin kendu.

2. **Markaketa**

a. Zelula pikorra 80 µL bufferrean bersuspenditu 10^7 zelulako.
b. Gehitu CD14 MicroBeads-en 20 uL 10^7 zelulako.
c. Ongi nahastu eta 15 minutuz eduki 4−8 °C-tan.

d. Zelulak garbitu 1−2 mL buffer gehituz 10^7 zelulako eta zentrifugatu 300×g 10 minutuz. Gaineko likidoa pipetarekin kendu.
e. 10^8 zelula arte 500 µL buferrean bersuspenditu

3. **Banaketa**

a. MACS zutabea eremu magnetikoa eragiten duen banatzaile egokian jarri.
b. Zutabea prestatu bufferaren 500 µL pasaraziz.
c. Zelula nahasketa zutabean jarri.
d. Markatu gabeko zelulak gorde eta zutabea garbitu bufferaren 500 µL pasaraziz. Garbiketa buffera hiru aldiz pasaraziz burutu.

4. **Eluzioa**

a. Zutabea banatzailetik atera eta helburu diren zelulak biltzeko tutu egokia jarri.
b. mL bat buffer jarri zutabean. Pistoia zutabean jarri eta barruraino sakatu magnetikoki markatutako zelulak erauzteko.

4.4.2.2. CD16 + eta CD16-CD14+ monozioten isolaketa (MACS)

Monozitoen azpipopulazioen isolaketarak bi estrategia desberdin erabili ziren. CD16+ monozitoen (tarteko eta ez-klasiko) kopuru txikiakan kontutan hartua hasierako PBMC kopuru handiak beharrezkoak dira. Buffy coata erabili izan da beti PBMC kopuru handia hauek lortzeko (500 M zelula inguru). Gutxiengoa diren bi populazioak batera banatzetik hasi ginen desberdintasunik bazen aztertzeko.

Horretarako MACS teknologian oinarritutako Miltenyi enpresaren CD16+ Isolation kit (#130-091-765) erabili genuen. CD16+ monozitoen kit honek bi MACS banaketa egitean oinarritzen da. Lehendabizi MACS hautaketa negatiboa egiten da monozitoak ez diren baina CD16 espresatzen duten zelulak (granulozitoak, CD15+, eta NK zelulak, CD56+) baztertuz. Laginean CD16 espresatzen duten zelula bakarrak monozitoak direnean, MACS hautaketa positiboa egiten da. Monozito gehienak markatu gabe gelditzen dera eta CD14+ monozitoak isolatzeko hautaketa positiboa egiten da azkenik. Prozesu guztia fluxuzko zitometria bidez behatu zen (4.20. Irudia) hurrengo protokoloa erabiliz:

1. Zelulen prestaketa
   a. Zelulen kopurua zehaztu Neubauer-en ganbera eta zitometroaren bidez.
   b. Zentrifugatu 300×g 10 minutuz.
   c. Gaineko likidoa pipetarekin kendu.
2. CD15+ (granulozito) eta CD56+ (NK zelula) hautaketa negatiboa

2.1 Granulozito eta NK zelulen markaketa magnetikoa

a. Zelula pikorra 1350 uL bufferean bersuspenditu 5 x 10^8 zelulako.
b. Gehitu 450 uL FcR Blocking Reagent eta 450 uL of Non-Monocyte Depletion Cocktail 5 x 10^8 zelulako.
c. Ongi nahastu eta 15 minutuz eduki 4−8 °C-tan.
d. Zelulak garbitu 48,5 mL bufer gehituz 10^7 zelulako eta zentrifugatu 300×g 10 minutuz. Gaineko likidoa pipetarekin kendu.
a. 5 x 10^8 zelula arte 2000 µL buferrean bersuspenditu.

2.1 Banaketa magnetikoa: granulozito eta NK zelulen deplezioa

a. LD zutabea eremu magnetikoa eragiten duen banatzaile egokian jarri.
b. Zutabea prestatu 500 µL buffer pasaraziz.
c. Zelula nahasketa zutabean jarri.
d. Markatu gabeko zelulak gorde 15 mL Falcon batean.
e. Zurabea hiru aldiz garbitu buffearekin.
f. Bildu zutabetik pasatutako buffera.

2.3 Zelula kontaketa

a. Zeulak bufferrean birsuspenditu 15 mL-etaraino (tutuaren gaitasun maximoraino).
b. Eppendorf batean bersuspentsioaren 10 µL eta Trypan Blueren beste 10 µL jarri.
c. Bertsuspensioaren 50 uL-ri 450 uL buffer gehitu zitometroan zenbatzeko.

3. CD16+ monozitoen isolaketa

3.1 Aberastutako monozitoen markaketa

a. Zelula pikorra 2000 uL buferrean bersuspenditu 5 x 10^8 zelulako.
b. Gehitu CD16 Microbeads-en 450 uL.
c. Ongi nahastu eta 15 minutuz eduki 4−8 °C-tan.
d. Zelulak garbitu 13 mL buffer gehituz eta zentrifugatu 300×g 10 minutuz. Gaineko likidoa pipetarekin kendu.
e. 5 x 10^8 zelularte 2000 uL buferrean bersuspenditu.

3.2 Banaketa magnetikoa: CD16+ monozitoen hautaketa positiboa

a. LS zutabea eremu magnetikoa eragiten duen banatzaile egokian jarri.
b. Zutabea prestatu 3 mL buffer pasaraziz.
c. Zelula nahasketa zutabean jarri.
d. Markatu gabeko zelulak gorde 15 mL Falcon batean.
e. Zurabea hiru aldiz garbitu 3mL buffearekin; zutabea hustu arte itxoin berriro betetzeko.
f. Pasatako guztia gorde; hau CD16- frakzioa da CD14+ hautaketa egiteko.

3.3 Elution

a. Zutabea banatzailetik atera eta helburu diren zelulak biltzeko tutu egokia jarri.
b. 5 mL buffer jarri zutabeari. Pistoia zutabean jarri eta barruraino sakatu magnetikoki markatutako zelulak erauzteko Hau da CD16+ monzitoen frakzioa.

3.4 Zelulen kontaketa

a. Zeulak bufferrean birsuspenditu 15 mL-etaraino (tutuaren gaitasun maximoraino).
b. Eppendorf batean bersuspentsioaren 10 µL eta Trypan Blueren beste 10 µL jarri.
c. Bertsuspensioaren 50 uL-ri 450 uL buffer gehitu zitometroan zenbatzeko.

4. CD14+ monozitoen isolaketa

2.4.2.1. CD14+ monozitoen isolaketa (MACS) atalean azaldua.

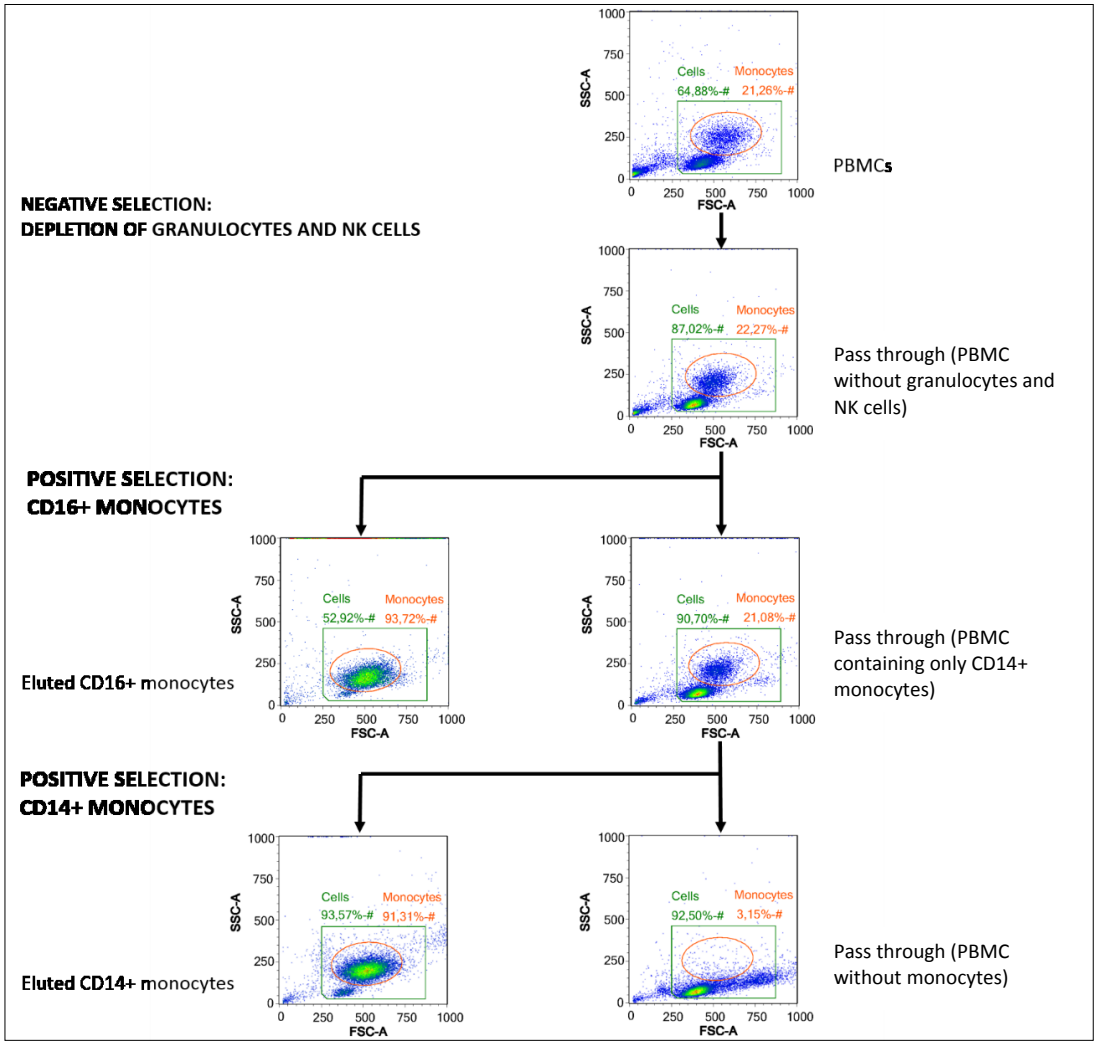

Figure 4.20. Zelula populazioen fluxuzko zitometria analisia isolaketan. "Cells" karratu berdea, zelula kopurua neurtzeko erabili zen, hondakinak neurtu gabe (grafikoaren beheko ezkerreko izkina). Elipse gorria, 'Monocyte', monocyte bat behatzekoerabili zen. Monocyte horren tamaina-aldea (FSC) eta konplexutasuna (SSC) neurtzen ziren. FSCk eta SSCk PBMCren eta gainerako PBMCen artean duten aldea ezaguna da, haien erabilera argitzeko adibide klasikoa izateraino*: (FlowJo, 2022)*

4.4.2.3. Monozito azpipopulazioen isolaketa (MACS eta FACS)

Monozito azpopulazio bakoitzaren ezaugarriak ulertzeko, beharrezkoa zen hiru populazioak banatzea eta horrek FACS teknikaren erabiliera beharrezkoa egiten zuen gainazlaeko errezeptoreen intentsiteren arabera banatzeko (2.17. Irudia).

Hala ere, lehen aipatu bezala, tarteko eta ez-klasikoak diren monozitoek monozito populazio osoaren %5 inguru sosatzen dute, eta monozitoek hasierako PBMCen %10-15, beraz euren portzentaia PMBCn %0,5 ingurukoa da. Esperimentuerako beharrezko zelula koporua lortzeko FACS banaketa erraldoai beharko litzateke, denbora (eta ondorioz, dirua, FACS banatzailearen erabilarengatik) asko eskatuko lukeena eta zelulen ongizatea eragin zezakeena.

Hasierako lagin txikiagoa izatzeko, laginaren monozitoak aberastea erabaki genuen, euren hautaketa negatiboa eginez MACS Pan Monocyte Isolation kit (#130-096-537; Miltenyi Biotec) erabilita.

Aberastutako markatu gabeko monozitoei fluoreszentzia markaketa egin zitzaien Miltenyi Biotec enpresako CD14 (CD14-PE; 130-110-519) eta CD16 (CD16-FITC; 130-106-703) errezeptoreen kontrako antigorputzak erabiliz monozitoen azpipopulazioen banaketa FACSJazz (BD Biosciences) gailuan egiteko. Protokoloa hurrengoa da:

1. **Zelulen prestaketa**

    a. Zelulen kopurua zehaztu Neubauer-en ganbera eta zitometroaren bidez.
    b. Zentrifugatu 300×g 10 minutuz.
    c. Gaineko likidoa pipetarekin kendu.

2. **Monozitoak ez diren zelulen deplezioa**

2.1 Monoztioak ez diren zelulen markaketa magnetikoa

a. Zelula pikorra 450 uL bufferean bersuspenditu 5 x 10^8 zelulako.
b. Gehitu 150 uL FcR Blocking Reagent eta 150 uL of Biotinadun antigorputz koktela 5 x 10^8 zelulako.
c. Ongi nahastu eta 5 minutuz eduki 4−8 °C-tan.
d. Gehitu 450 uL buffer eta 150 uL Anti-Biotin Microbeads 1.5 x 10^8 zelulako.
e. Ongi nahastu eta 10 minutuz eduki 4−8 °C-tan.
f. Zelula pikorra 1000 uL bufferean bersuspenditu 1.5 x 10^8 zelulako.

2.1 Banaketa magnetikoa: monozitoak ez diren zelulen deplezioa

a. LS zutabea eremu magnetikoa eragiten duen banatzaile egokian jarri.
b. Zutabea prestatu 3 mL buffer pasaraziz.
c. Zelula nahasketa zutabean jarri.
d. Markatu gabeko zelulak gorde 15 mL Falcon batean.
e. Zurabea hiru aldiz garbitu 3mL buffearekin; zutabea hustu arte itxoin berriro betetzeko.
f. Pasatako guztia gorde.

2.3 Zelulen kontaketa

a. Zeulak bufferrean birsuspenditu 15 mL-etaraino (tutuaren gaitasun maximoraino).
b. Eppendorf batean bersuspentsioaren 10 µL eta Trypan Blueren beste 10 µL jarri.
c. Bertsuspensioaren 50 uL-ri 450 uL buffer gehitu zitometroan zenbatzeko.

3. **Aberatutako monozitoen fluoreszentzia markaketa**

a. Zelulak zentrifugatu 300G 10 minutuz inguru tenperaturan.
b. Zelulen pikorra bersuspenditu 345 uL markaketa bufferan.
c. Gehitu 8,8 uL CD16-FITC antigorputzaren eta 2,2 uL CD14-PE antigorputzarena buferraren 100 uLko.
d. Ongi nahastu eta 10 minutuz eduki 4−8 °C-tan.
e. Zelulak 15 mL Falcon batean garbitu 13 mL buffer gehituz.
f. Zelulak zentrifugatu 300G 10 minutuz inguru tenperaturan.
g. Zelula pikorra 1000 uL bufferean bersuspenditu 1.5 x 10^8 zelulako

4. **Fluoreszentziaz markatutako monozitoen isolaketa**
Monozito azpipopulazio markatuak FACSJazz (BD Biosciences) zitometro batean sailkatu ziren lehen deskribatutako gating estrategia erabiliz.

4.4.3. Zelulen kultiboa

Zelula guztiak American Type Culture Collection (ATCC) erakundaren gidalerroan arabera eta zelulen kultiborako praktika hoberak erabiliz kultibatu dira.

4.4.3.1. Cell lines

IL12A aldakien presentzia laborategian erabilgarri zeuden zelula lerro guztietan aztertu egin zen zegozkien kultibo medio egokia erabiliz (4.11. Taula). Medioa astean bi edo hiru aldiz berritu egin zen. Zelula itsaskorren bersuspentsio eta azpikultiborako, PBSarekin garbituak izan ziren seruma kentzeko eta matrize zelularra tripsina (#11581861, Thermo Fisher Scientific) erabiliz digeritu zen, digestiia seruma zeukan medio berria gehituz gelditu zen, zelulak kontatue ta zentrifugatuak izan ziren tripsina guztia kentzeko.

ZELULA LERROA	KULTIBO MEDIOA
A549	DMEM + 10% FBS + 1% PS + 2 mM Glutamina
DU145	DMEM + 10% FBS + 1% PS + 2 mM Glutamina
HEK	DMEM + 10% FBS + 1% PS + 2 mM Glutamina
HELA	DMEM + 10% FBS + 1% PS + 2 mM Glutamina
HT-29	DMEM + 10% FBS + 1% PS + 2 mM Glutamina
JURKAT	RPMI-1640 + 10% FBS + 1% PS
MCF7	DMEM + 10% FBS + 1% PS + 2 mM Glutamina
PC3	RPMI-1640 + 10% FBS + 1% PS
SH-S5Y5	DMEM + 10% FBS + 1% PS + 2 mM Glutamina
THP1	RPMI-1640 + 10% FBS + 1% PS + 2 mM Glutamina +10 mM HEPES + 50 uM Beta-mercaptoetanol
U937	RPMI-1640 + 10% FBS + 1% PS

Table 4.11. Erabilitako zelula lerroetarko kultibo medioa. DMEM: Dulbecco's Modified Eagle's Medium (#D5795, Sigma-Aldrich); FBS: Fetal Bovine Serum (#F9665-500ML, Sigma-Aldrich); PS: Penicillin-Streptavidin (#P4333-100ML, Sigma-Aldrich); RPMI: Roswell Park Memorial Institute medium (#R-0883-500, Sigma-Aldrich); HEPES: (4-(2-hydroxyethil)-1-piperazineethanesulfonic acid) (#H3537-100ML). L-Glutamina (#G7513-100ML, Sigma-Aldrich).

4.4.3.2. Zelula primarioak

Monozitoak izan dira erabilitako zelula primarioak eta monozitoengatik eratorritako zelula dendritikoak sortzeko kultibatu izan dira. Helburu horretarako monozitoak 1×10^6 zelula/mL dentsitatean kultibatu izan ziren 6 edo aipatutako egunez Mo-DC medium (DM) erabiliz, RPMI

1640 medioa, FBS, L-Glutamina, IL-4 eta GMCSF daraman komertzialki (#130-094-812, Miltenyi Biotec) erabilgarri dagoen monozitoengatik eratorritako zelula dendritikoetara kultibatzeko medioa. Hirugarren egunean medioa berritzen zen hasierako Mo-DC medium bolumen berdina gehituz.

Esperimentu batzuetan moDCak beste aditibo batuzekin ere hazi ziren, erabiliena, AM580 (100 nM; A8843, Sigma). Heldugabeko monozitoetaik eratorritako zelula dendritikoak heltzeko IFN-g (AF-300-02, Perotech) eta lipopolisakaridoa (LPS; L6143, Sigma) erabili ziren kultibora gehituz.

4.4.4. Zelulen transfekzioa

Azterketarako behar ziren geneak eta proteinak ezaugarritzeko, bi teknika erabili ziren: DNA plasmidikoa eta RNA (siRNA) interferente txikia. Plasmid DNA bektorea, gure proteina interesgarrien kodifikazioa jasotzen duena, aukera eman zigun estudio eredu ezberdinetan adierazteko. siRNA edo isiltzeko RNA, 20-25 oinarri bikoitzeko RNA molekula harilkatu bikoitzak dira, mRNA osagarriaren degradazioa eragiteko gai direnak, eta, ondorioz, proteinen kodifikazio faltak zelulan duen eragina behatu eta aztertzeko. Interesaren kodifikazio-transkripzioaren adierazpena isilaraziz, geneen elkarreraginean duen eragina uler dezakegu.

4.4.4.1. Plasmid DNA

Zelula atxikiak bektoreekin transfektatu ziren (4.12 taula) proteinak adierazteko esperimentuetarako. Erabilitako zelula lerroak HEK293 eta HeLa ziren. HEK293 zelulen kasuan, transfekzioarako konfluentzia egokia lortu arte (>% 60ko konfluentzia) kultibatu ziren. Ondoren, transfektatu egin ziren, eta transfekzioa eta 24 ordura finkatu egin ziren.

Bektorea	Katalogo zenbakia	Ekoizlea
EMPTY VECTOR (EV)	PS100001	Origene
IL17	RC218057	Origene
IL17SP+ IL22RA2v2	Lan honetan klonatua	
IL2	RC210013	
IL-2EX4	Lan honetan klonatua	
IL22RA2v1	Subcloned from RC219095 with Exon 4 addition	
IL22RA2v2	RC219095	Origene
IL22RA2v3	RC215420	Origene
GRP94 WT	Yair Argon-ek emandakoa	
GRP94 NTD		
GRP94 MD		
GRP94 CTD		
GRP94 DA		
GRP94 WT GFP		
GRP94 E82A GFP		

Table 4.12. Lan honetan transfekzioetan reabilitako bektoreak.

Prozesua MACSfectin Reagent (#130-098-411, Miltenyi Biotec) erabiliz egin zen ekoizlearen protokoloarei jarraituz:

1. **Erreaktiboen prestaketa**

Hasteko garrantzitsua da erabilko diren erreaktibo eta laginak prest izatea. Horretarako hainbat neurketa eta kalkulu egin behar dira.

a. Transfekzio erreaktiboa (ingeleraz, transfection reagent, TR; MACSfectin Reagent) desizoztu eta homogenizatu.
b. Bektorearen DNA plasmidikoaren konzentrazioa neurtu Nanodrop gailuan (Abs 260/280: ≥ 1,8).
c. Kalkulatu transfekzioarako beharrezkoa den DNA bolumena.

PLAKA TAMAINA	Putzuaren bolumena (µL)	Bektorea (Lehengo tutua)		Transfekzioa (Bigarren tutua)		Nahasketa
		DNA kantitatea (µg/w)	SFM bolumena µL/w)	MACSfectin Reagent bolumena (µL/w)	SFM bolumena (µL/w)	Transfekzio bolumena (µL/w)
6	2000	3	50-x	6	44	100
12	1000	2	50-x	4	46	100
24	500	1	100-x	2	48	200

Table 4.13 Zelula itsakorretan DNA transfekzioa egiteko beharrezko transfekzio erreaktibo eta bektore kantitateak. Plasmidoaren konzentrazioan oinarritua, beharrazko bolumena kalkulatzend a beahrrezkoa den DNA µg kantitatea lortzeko. Serumik gabeko medioa (ingeleraz, serum free medium, SFM) bolumena horren arabera erabiltzen da. MACSfectin Reagent datasheet-etik moldatua.

d. Kalkuluen arabera bi tutak prestatu bost minutu baino denbora gutxiagoan. Lehenik SFMa gehitu tutu bakoitzari, gero bektore plasmidoa lehenengo tutura eta gero transfekzio erreaktiboa bigarrenera.

2. **Erreaktiboen nahasketa eta inkubazioa**
   a. Gehitu lehengo tutua bigarren tutura.
   b. Kontuz bersuspsenditu 5 aldiz nahasteko.
   c. 20 minutuz inkubatu inguru tenperaturan.

3. **Zelulen transfekzioa**
   a. Hartu putzu bakoitzerako dagokion transfekzio bolumena.
   b. Gehitu transfekzio nahasketa tantaka transketatuko den putzu bakoitzera.
   c. Kontuz homoneizatu putuzak.

4. **Transfektatutako zelulak inkubatu**

4.4.4.2. siRNA

Literatua zientifikoa eta merkatua aztertu genituen monozito eta monozitoetatik eratorritako zelula dendritikoen isiltzeko erreaktibo egokien bila. Lipocalyx GmbH enpresako Viromer produktuak hautagai egokiak zirela ikusi zen suspentsioan (berriki isolatutako monozitoak) eta itsatsita (kultibatutako monozito eta monozitoetatik eratorriako zelula dendritkoak) dauden zelulen isiltzerako. Viromerek lau produktu desberdin ditue kolore izenez (urdina, berdia, gorria eta horia) izendatuta bain horietako bi baino ez daude siRNA *in vitro* transfektatzeko optimizatuta: Viromer Blue (VB-01LB) eta Viromer Green (VG-01LB). 4.1.3 Silencing of *IL22RA2* in moDCs atalean azaldu bezala biak frogatu egin ziren. Protokolo orokorra hau izan zen:

1. Erreaktiboen prestatketa

Transfekzioaren kasuan bezala, neurketa eta kalkulu bazuk beharrezkoak dira.

1.1 siRNAren prestatketa, 1 TUTUA

a. siRNA diluitu hornitutako baferrean (urdin edo berderako espezifikoa) 11 uM-era suspenditutatko zeluletarako edo 2.75 uM itsatisatko zelulentzat.
b. 100 nMeko lagin bakoitzarentzako 5 µL prestatu.

1.1 Viromerraren prestateketa, 2 TUTUA

a. Jarri 100 nMeko lagin bakoitzeko 0,5 uL ko Viromer tanta bat tutu berri baten horman.
b. Berehala 45 uL buffer gehitu 100nM lagin bakoitzeko eta 3-5 segunduz vortexean jarri.
c. Beti gehitu buffera Viromerrari, ez alderantziz

2. Erreaktiboen nahasketa eta inkubazioa

a. 2 tututik Viromer soluzioko 45 uL jarri 5 uL siRNA dauzakn 1 Tutuko soluziora 100nM lagin bakoitzeko
b. Kontuz nahastu eta 15 mintuz inkubatu inguru tenperaturan.

3. Zelulen transfekzioa

100 nM eko putzu bakoitzeko erraktiboen nahasketaren 50 UL gehitu.

4. Isildutako zelulak inkubatu

4.5. Antigorputzetan oinarritutako teknika molekularrak

Antigorputzetan oinarritutako teknika molekularrek intereseko proteinak hainbat modutan detektatzeko aukera ematen dute. Ikerketa honetan bost teknika ezberdin erabili dira: immunoblottinga, afinitate purifikazioa, interaktomaren analisia, mikroskopia konfokala eta entzimari lotutako entsegu immunosorbentea (ingeleraz enzyme-linked immunosorbent assay (ELISA)). Immunoblottingak lagin batean dagoen proteina detektatzeko eta kuantifikatzeko aukera ematen digu, bere tamainaren arabera. Afinitate purifikazioak lagin konplexu eta diluitu batetik intereseko proteina isolatu eta kontzentratzeko aukera ematen du, gerora analisi hobea egiteko. Interaktomaren analisia interesaren proteinarekin elkarreragiten duten proteinak ulertzeko erabiltzen da eta zelularen barruan duen rol biologikoa ulertzen laguntzen digu. Mikroskopia konfokala erabiliz, posible da intereseko proteinak aurkitzea eta kolokalizatzea zelula-egituretan, eta, aldi berean, azterketa-zelulen morfologiari erreparatzea. Azkenik, ELISA laginean proteina objektibo baten kantitate oso txikiak detektatzeko eta kuantifikatzeko diseinatutako assay bat da (pg/mL-eraino).

4.5.1. Immunoblottinga (Western Blot)

Western blot deritzona biologia molekularraren oinarrizko tekniketako bat da eta proteinen detekzioarako urrezko patroia da. Prozesua lau pauso nagusitan banatu daiteke (4.21 Figure):

0. **Laginaren prestaketa**

Lehenik, garrantzitsua da lagina ongi prestatzea. Zelulen kasuan hurrengo pausuak jarraitu behar dira:

a. **Bersuspentsioa:** lagina prozesatze aldera zelulek suspentsioan egon behar dute, zelula itsaskorren kasuan PBS bufferan eta Eppendorf tutu batean.
b. **Zentrifugazioa;** 350G 10 minutuz inguru tenperaturan.
c. **Garbiketa:** zelula hondarrak eta beste partikulak kentzeko garbiketa egiten da laginari PBS mL bat gehituz eta zentrifugatuz (350 G 10 minutu inguru tenperaturan) hiru aldiz osotara.
d. **Lisia:** zelulak puskatu behar dira lagineko proteinak aske bersuspendituta egon daitezke. Horretarako lisi bufferak reabiltzen dira. Lan honetan RIPA eta Triton X-100 detergenteetan oinarritutako erabili izan dira (4.14. Taula). Laginak 20uL lisi bufferrean bersuspenditutak izan ziren eta 30 minutuz inkubatu ziren izotzean.
e. **Zentrifugazioa:** abiadurarik handienera 10 minutuz 4ºC-tan.
f. Fase likido a gorde eta pikorra bota.

Zelula lisatuen kantitate, eluitatuko frakzioen edo kultibo medioen bolumen berdina kargatu izan da western blot-ean. .

RIPA Buffer	Triton X-100 BUFFER
150 mM NaCl	300 mM NaCl
50 mM HEPES pH 7.4	50 mM NaH2PO4 pH8
0.5% sodium Deoxycholate	1% Triton X-100.
0.1% SDS	
Benzonase (1 U/mL) add just before use	

Table 4.14. Erabilitako lisi bufferen formula.

1. **Banaketa**

Proteinen ezaugarri elektrikoak erabilita, laginak konzentrazio desberdineko (%10 edo %12) akrilamida geletan kargazten dira, eta goikaldean karga ngatiboa jarriz eta behekaldean negatiboa, eremu elektrikoa sortzen da (20mA/minigel). Proteinak SDS-Page gelean zehar eueren, taimanaren arabera mugitzen dira, tamaina ezaguneko proteina eskailera (ingeleraz, ladder) erabiliz tamainaren araberako banaketa egiteko.

2. **Transferentzia**

Behin gelak banaketa burutu denean. Antigorputzak atxikitzek egokia den mintz batera transferitzen dria. Gure kasuan PVDF mintzak (IPVH00010, Millipore). Transferentzia hau ere gradiante elektriko bidez burutzen da. Gelari karkasa kendu eta mintz baten gainean jarri behar da. Tras-Blot ® Turbo Transfer System (# 1704150; Bio-Rad) erabiliz gure kasuan.

3. **Tindaketa**

a. **Blokeoa:** edozein antigorputz erabili aurretik garrantzitsua da tindaketa inespezifikoa blokeatzea, horretarako mintzak %2 kaseinan blokeatu ziren gauan zehar 4ºC-etan.
b. **Antigorputz primarioa:** antigorputz primario bakoitzaren (4.15. Taula) inkubazioa gauean zehar egiten da 4ºC-etan.
c. **Garbiketa:** antigorputz primario gehiegizkoa, proteinari lotu ez dena, mintzetik kendu behar da eta horretarako 10 minutuko 3 garbiketa egin ziren Tris-buffered saline, 0,1% Tween 20 (TBST) bufferrean
d. **Antigorputz sekundarioa:** t antigorputz primariak detektatuako proteina ikusi ahal izateko bigarren antigorputz bat erabiltzen da peroxidasa bati (ingeleraz, Horseradish peroxidase, HRP) lotuta dagoena (4.16. Taula) ordu batez inguru tenperaturan.
e. **Garbiketa:** gehiegizko antigorputza, 10 minutuko 3 garbiketa TBST bufferrean.
f. **Sustratuaren gehitzea:** HRP gai da seinale detektagarria emateko sustratu egokiaren bidez, kasu honetan, Bio Rad enpresako sustratu txemiluminiszentea (# 1705061).

4. **Bistaratzea**

Bistaratzea eta neurketa ChemiDoc Imaging System (Biorad) gailuaren bidez burutu zen.

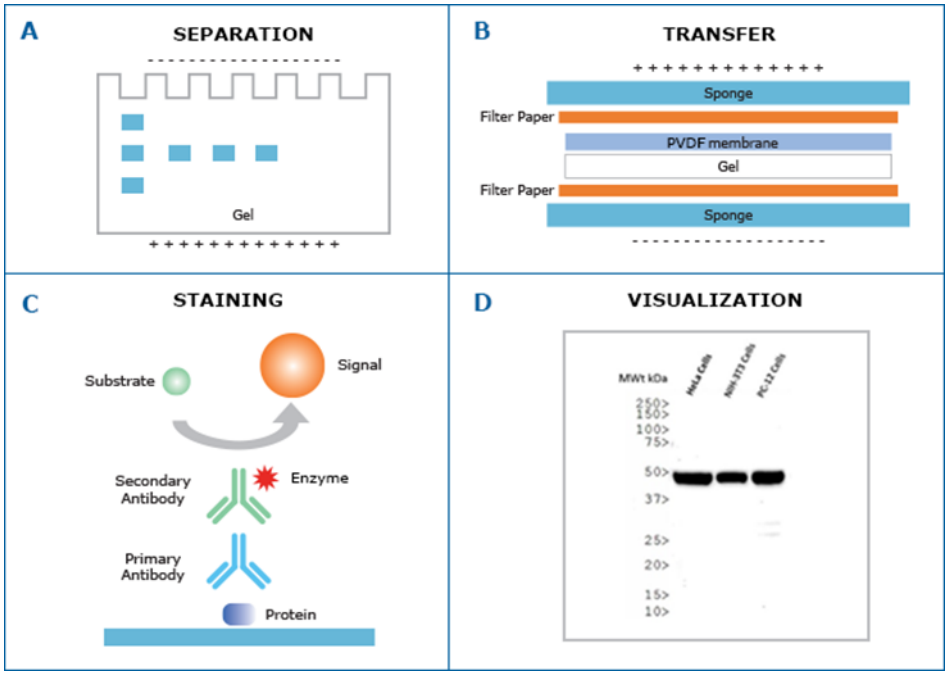

Figure 4.21. Wester blot teknikaren fase desberdinen irudikapena. A: banaketa; B: transferentzia; C: tindaketa; D: bistaratzea. *Iturria:* https://slideplayer.es/slide/16617467/

Xedea	Espeziea	Klonalitatea	Konjugatua	Diluzioa	Katologo zenbakia	Ekoizlea
Actin	Rb	Poliklonala		1 100an	A2066	Sigma-Aldrich
CNX	Rb	Poliklonala		1 1000an	ADI-SPA-860	Enzo
ERdj3	Rb	Poliklonala		1 1000an	15484-1-AP	Proteintech
FLAG	Rb	Poliklonala		1 1000an	20543-1-AP	Proteintech
GAPDH	Rb	Poliklonala		1 2000an	ABS16	Millipore
GRP170	Ms	Monoklonala		1 100an	10301	IBL
GRP78	G	Poliklonala		1 1000an	AF4846	R&D
GRP94	Rt	Monoklonala		1 1000an	ADI-SPA-850	Enzo
IL-22BP	G	Poliklonala		1 1000an	AF1087	R&D
IL-22BP	G	Poliklonala	Biotina	1 1000an	BAF1087	R&D
IL-22BP	Ms	Monoklonala		1 1000an	66190	Proteintech
KDEL	Ms	Monoklonala		1 1000an	ADI-SPA-827	Enzo

PPIB	Rb	Poliklonala		1 500ean	16045	Abcam
Tubulin	Ms	Monoklonala	HRP	1 1000an	A01490	GenScript

Table 4.15. WB antigorputz primarioak. G: goat, ahuntza; Ms, mouse, sagua; RB, rabbit, lapina; RT, rat, arratoia.

Xedea	Espeziea	Konjugatua	Diluzioa	Katalogo zenbakia	Ekoizlea
Ahuntza	Dk	HRP	1 1000an	705-035-003	Jackson
Sagua	Dk	HRP	1 1000an	715-035-150	Jackson
Lapina	Dk	HRP	1 1000an	711-035-152	Jackson
Arratoia	G	HRP	1 1000an	ABIN2703850	antibodies online

Table 4.16. WB antigorputz sekundarioak. Dk, donkey, astoa; G, goat, ahuntza.

4.5.2. Afintate bidezko purfikazioa

Afinitate bidezko purifikazioak soluzioan dagoen protein nahasketa batetik euretako bat isolatzean datzan matrize higiezin batera lotuta dagoen estekatzaile baten bidez. Orokorrean hiru pausu izaten ditu: laginaren inkubazioa, lotu gabeko laginaren garbiketa eta helburu den proteinaren eluzioa (disoziazioa eta berreskuratzea) buferraren baldintzak aldatuz.

Gure kasuan, antigorputzak erabili tenituen helburu genuen proteinaren estekatzaile bezala, eta horregatik inmunopurifikazioetaz dihardugu. Antigorputzak agorosa aleetara (erretxina) kobalenteki lotuta zeuden, protein purifikazioarako matrizerik hoberenetariko bat. Agarosa aleak nahiko handiak eta oso porotsuak dira proteinak inguruan, kanpotik eta barrutik mugitzea ahalbidetuz eta gainazale antigorputzez estalitat dute helburu den proteina lotzeko.

Lan honetan ikertutako proteina guztiak zeluletara transfektatu ziren etiketak zituztela. Kasu honetan etiketak peptido sekuentzia laburrak dira, zeinendako afinitate handiko antigorputzak eskuragarri dauden. Modu honetan proteinaren bereganatzea errezten da. Helburu izandako proteineik honak hiru etiketako bat zeukaten: FLAG (DYKDDDDK) c-Myc (EQKLISEEDL) edo S-tag (KETAAAKFERQHMDS), eta hurrengo erretxinetako bat erabili zen ekoizlearen argibideak jarraituz: anti-FLAG resin (GenScript, L00432), antic-Myc resin (Sigma, E6654) or S-protein agarose (Millipore, 69704).

Agarosa erretxina batera lotutako antigorputz espezifikoa erabiltzen duten inmunopurifikazioaei inmunoprezipitazioak (IP) deritze. Batzuetan helburu den proteinarekin interakzionatzen duten proteinak ikertu nahi dira. Helburua proteina bera baino berekin interakzionatzen duten proteinak direnean ko-inmunoprezipitazioa (ingeleraz, co-immunoprecipitation, co-IP) deritzo (4.22. Irudia).

Interakzionatzen dauden proteinak antzemateko beharrezkoa da proteienn arteko interakzioa mantentzea prozesuan zehar. Horrelako interakzioen indarrak handitzeko, crosslinker izeneko substantziak erabiltzen dira. Crosslinker hauek bi biomolekulen arteko talde funtzional batzuen artean lotura kobalenteak eratzea halbideten dute. Lan honetan dithiobis succinimidyl propionate (DSP) izenekoa erabili izan zen, amina taldeek erreakzionatzen duena, edo DMSO kontrol gisa. Crosslinkerra ezinbestekoa interaktoma ikerketetan.

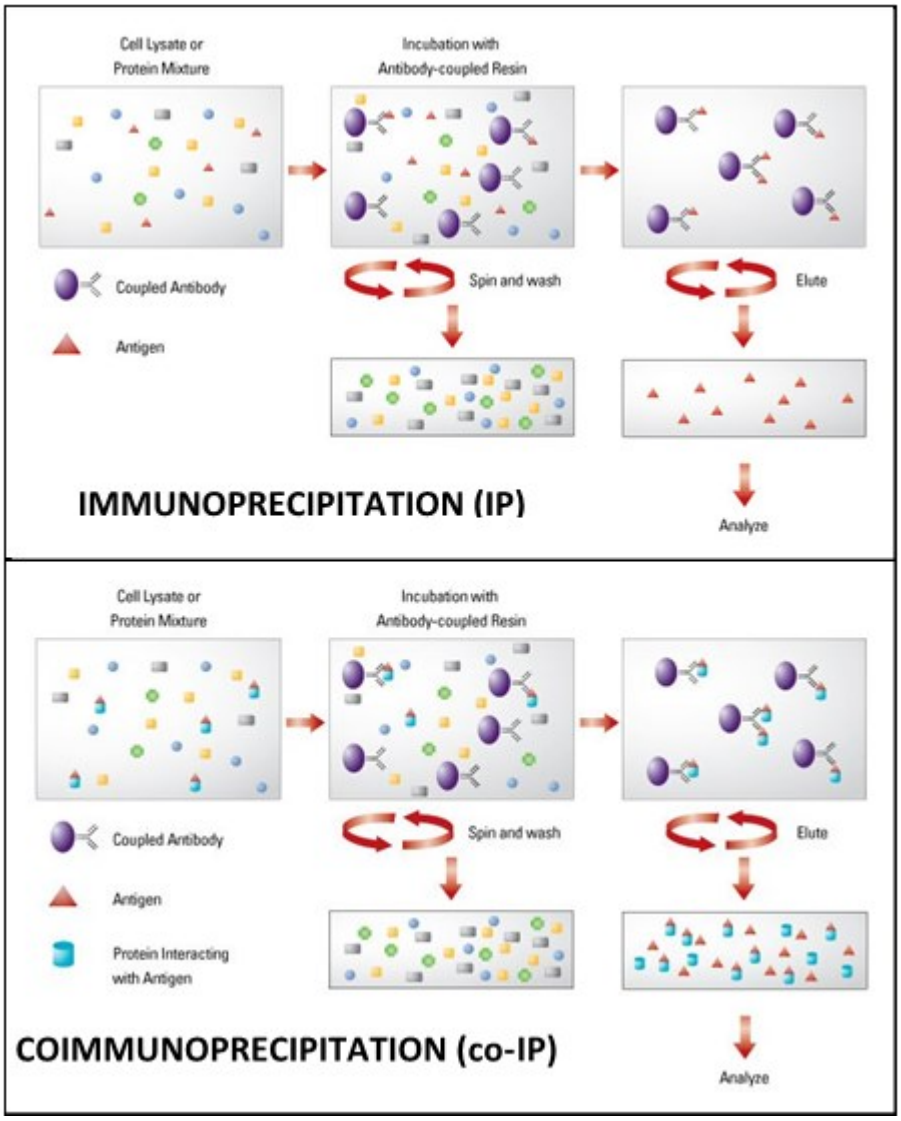

Figure 4.22. Imunoprezipitazioa eta koinmunoprezipitazioaren irudikapena. *Iturria:* (Thermo Fisher Scientific, 2022)

Hori egiteko protokoloa hurrengoa da:

1. **Zelulen kultiboa**

   HEK293 or Hela zeulak beharrizanen eta edukiontziaren araberako kopuruan hazi 24 orduz (37ºC, 5% CO_2, eta %95< hezetasunean) zelulen itsaste egokia bermatzeko.

2. **Transfekzioa**

   a. Zelulak %60-70eko konfluentiza transfektatu MACSfection reagent (130-098-412, Miltenyi Biotec) erabiliz.
   b. Inkubatu 20 orduz 37ºC eta 5% CO_2 –an.

3. **Biltzea eta garbitzea**

   a. Zelulak PBS hotzarekin 3 aldiz garbitu.

   b. Zelulak birsuspenditu 100µL PBSean / T75 flask bakoitzeko.

4. **Crosslinking (koinmunoprezipitazioentzat)**

   a. Gehitu DMSO edo DSP laginaren arabera:

   DMSO. 1 µL DMSO 100µL PBSko.
   DSP (hau momentuan prestatu behar da, stock soluzioa: 10mgDSP/mL-ko DMSOn disolbatuta). 1µL of DSP (stock soluziotik) 100µL PBSeko.

   b. 30 minutuz inkubatu inguru tenperatura (bost minuturo eskuarekin kontuz nahastu)
   c. **Erreakzioa gelditu** 1M TRIS-HCl pH7,5 bufferko 5 uL gehituz, amierako konzentrazioa 50 mM izateko. Vorexean kontuz nahastu eta inkubatu beste 15 minutuz inguru tenperaturan.
   d. Tutu bakoitza bitan banatuta. Lisia bi buffer desberdinetan egingo da.
   e. Zentrifugatu 300 g minutu bat, pikorra gorde ta likidoa bota.

5. **Lisis**

   a. Gehitu dagokion lisi buffera (RIPA edo Triton X-100 buferra) pikorraren tamainaren arabera.

   b. 30 minutuz inkubatu izotzean.

   c. Abiadura handienean zentrifugatu 15 minutuz eta gase likidoa bildu.

6. **Kuantifikazioa**

    a. **RIPA buferrean:** BCA assay delakoa proteina kuantifikazteko.

    b. **Triton X-100 buferra:** Bradford metodoa proteina kuantifikatzeko.

    c. Varioscan gailua erabili kuantifikatzeko.

7. **Afinitate bidezko purifikazioa**

7.1 Erretxinaren orekatzea eta laginaren inkubazioa

    a. Erretxina garbitu (20 µL tutuko) Equilibration bufer (50 mM Tris-HCl, 150 mM NaCl, pH 7.4) mililitro bat erabiliz. 4 aldiz osotara.

    b. Purifikazio bakoitza proteina kantitate berdina (aurreko puntuan kuantifikatua), orekatutako erretxinaren bolumen bera eta Equilibraton buferrarekin osatu behar da mililitro oso bat lortu arte.

    c. Noria batean inkubatu gau osoa 4ºC-tan.

7.2 Garbiketa

Zentriguatu 300×g 30 segunduz. Kontu handiz gaineko likidoa kendu eta TBS buffera gehitu 6 aldiz erretxina garbitzeko. Kendu gaineko likidorik ahalik eta gehiena baina erretxina ukitu gabe. Frakzio bakoitza gorde.

7.3 Eluzioa

a. Gehitu 45µL 0.1M glycine SDS-pH2 5 mintuz (30 segunduro nahastuz).
b. Zentrifugatu 300g minutuz batez.
c. Gorde gaineko likidoa erretxinarik hartu gabe (mikroskopioan ziurtatu).
d. Lortutako likideoa neutralizatu 5 µL 1M Tris-HCl, pH 8,5 gehituz.

4.5.3. Interactome analysis

Interaktoma analisia burutzeko, afinitatezko purifikazioa oraitxe azaldu bezala burutu zen eta eluzioa %10 precast SDS-PAGE gels (Bio-Rad, 4561034) gel batean jarri zen. Gel hauek zilarrarekin tindatu ziren erretilu garbi batean, mugimenduan eta beharrezko soluzioek gel osoa

estaliz ekoizlearen argibideei jarraituz (Thermo Fisher Scientific, 24612). Finkape, etanol eta gelditze soluzioak(2, 3 eta 10 pausoetan erabiliak) aurretiaz prestatu daitezke. Beste soluzioak momentuak prestatu behar dira. Hau egiteko protokoloa hurrengoa da:

1. **Garbiketa**
   Gel-a ur ultrapuruarekin garbitu 5 minutuz (x2).
2. **Finkaketa**
   Gel-a finkatu %30 etanol + %10 azido azetikoa duen soluzioan 15 minutuz. Soluzioa aldatu eta finkatu beste 15 minutuz.
3. **Garbiketa**
   a. Gel-a garbitu %10 etanoleko soluzioan 5 minutuz (x2).
   b. Gel-a ur ultrapuruarekin garbitu 5 minutuz (x2).
4. **Sentikortu**
   Gel-a Sensitizer Working Solution (1/500 Silver Stain Sensitizer in ultrapure water) soluzioan sartu mintu zehatz batez.
5. **Garbiketa**
   Gel-a ur ultrapuruarekin garbitu minutu batez (x2).
6. **Garbiketa azkarra**
   Gel-a ur ultrapuruarekin garbitu 20 segunduz (x2).
7. **Garapena**
   Gehitu Developer Working Solution (1/50 Silver Stain Enhancer in Silver Stain Developer) eta inkubatu proteina bandak agertu arte /2-3 minutu).
8. **Gelditu**
   Developer Working Solution gelditze soluzioarekin (%5 azido azetikoa) aldatu. Garbiketa azkarra egin, stop soluzioa berriro jarri eta 10 minutuz inkubatu.

Aukeratutako proteina bandak CICbioGuneko (Zamudio, Bizkaia) Féliz Elorzak zuzentzend duen Proteomikako plataformarekin laguntzarekin aztertu genituen. Eurek erabilitak prozedura hurrengoa izan zen.

Banda bakoitza tripsinarekin digeritua izan zen Sevchenko eta bere taldeak (Shevchenko et al., 1996) erabilitako protokoloa jarraituz. Lortutako peptidoak %0.1 azido formikoa

bersuspenditu ziren, Nano LC gailua erabiliz banataua eta elektroesprai masa espektrometria tandema erabiliz aztertu ziren.

Peptidoen banaketa SYNAPT G2-Si spectrometer (Waters, Milford, MA, USA) gailura konektatutako anoACQUITY UPLC sistemaren bidez burutu zen. Laginak elkarri konektutatuko bi zutabetatatik pasa ziren: Symmetry 300 C18 UPLC Trap column of 5, 180µm × 20mm (Waters, Milford, MA, USA) eta BEH130 C18 column of 1.7, 75µm × 200mm (Waters, Milford, MA, USA). Zutabea %3 azetonitriloa eta %0.1 azido formikoa zuen soluzioaren bidez orketu zen. Peptidoen eluzia 300 nL mintuuko abiadruan egin zen %3-50 acetonitrilozko gradiantea erabiliz 60 minutuz. Pepitodoen analisia SYNAPT G2-Si ESI Q-Mobility-TOF spectrometer (Waters, Milford, MA, USA) gailuan egin zen ion mobility chamber (T-Wave-IMS) gehigarria zerlamaraik.

Analisi guztiak elektroesprai inoizazioa modu positiboan erabiliz burutu ziren. Datuak bildu ostean masa zuzendu egin zen f [Glu1]-fibrinopeptide B ioi monosiotipikoa erabiliz. LC-MS data HDDA moduan bildu ze, ioien mugimendu banaketaren bidez seinalaren intentsitata handitzen duena. Peptidoen identitatea Mascot bilaketa tresnarekin (MatrixScience) egin zen Uniprot/Swissprot giza data basearekiko.

Bilaketa ezaugarriak horrela mugatu ziren: peptidoaren masa tolerantzia 10 ppm eta zatiena 0.2 Da. Zisteinen karbamidometilazioa aukeratu zen modifikazio modura eta metioninaren oxidazioa tripsinizatutako peptidoentzat. FDR < %1 behintzat zuten bi peptidoen bide identifikatu ziren proteinak azterketa gehiago eginez.

4.5.4. Immunofluoreszentziako mikroskopia

Immunofluoreszentiza mikroskopia etiketa fluoreszentea duten antigorputzen bidez helburu den proteina detektatu eta ikusaraztean datza. Inmunohistokimika edo inmunozitokimika (ingeleraz, immunocytochemistry, ICC) deitu daiteke ehun ebaketa edo zeluletan egiten den arabera. Gure lanean zelulak erabili ditugu eta horregatik erabilitako inmunofluoreszentziako mikroskopia ICC deitu dezakegu. Gure tindaketen helburua interesezko proteinen zeula barruko lokalizazioa ulrtzea zen eta horretarako magnifikazio handiak beharrezkoak dira. Irudiak Achucarro Basque Center for Neuroscienceko Leica TCS STED CW SP8 super-resolution mikroskopioan egin ziren.

Western blotean bezala, zelulak puskatu behar dira antigorputza proteinetara heldu dadin baina era berean euren morfologia eta arkitektura gorde nahi ditugu. Horretarako zelulek finkaketa jasatzen dute. Finkaketa lau helburu nagusi ditu inmunofluorezentzian: zeularen morfologia egonkortu eta mantentzeaz gain, lagina degradatu dezaketen entzimak inaktibatzen ditu, zurruntasuna ematen dio laginari prozesua jasateko eta mikrobioen kutsaduraz babesten du. Guk paraformaldeidoa (PFA) zeramaten soluzioak erabili ditugu finkaketarako crosslinking propietateak dituelako. Behin lagina finkatuta dagoenean, antigorputzak euren helburu diren proteinetara iritsi daitezke lagina permeabilizatuta. Orokorrean bi motatako erreaktiboak erabiltzen dira permabilizazioarako. Lehenengoa disolbatzaile organikoak, metanol eta azetona adibidez, proteinak koagulatzen dituzte eta finkaketa eta permeabilizazioa batera egin ditzazkete. Bigarren mota saponina, Triton X-100 eta Tween 20 bezalako detergenteak dira. Hauek mintzetako lipidoekin interakzionatzen dute zuloak eginez, eta bertatik antigorputzak eueren epitopoen bila sartu daitezke. Gure lanean Triton X-100 irabili izan da.

Finkaketa eta permeabilizazioa burutu ostean zelulak tindatzeko prest daude. Beste inmunotindaketetan bezala, pausu orokor batzuk jarraitzen ditu, elkartze ez-espezifikoen blokeoa, antigorputzen inkubazioa (kasu honetan konjugatu fluoreszentearekin) eta bistaratzea. Zelulen tindaketa kultibo plaken putzuen oinarrian jarritako estalkietan burutu ziren. Modu honetan ez zen harrezkoa itsatsitako zelualk mugitzea eta bertan finkatu egin ziren. Tindaketa estalkietan egiteak ere antigorputz bolumen txikiekin lan egitea ahalbidetzen du, gauza garrantzitsua IL-22BPren kasuan non 1 20ean diluzioa erabili zen. Orokorrean inmunofluoreszentzia protokoloa hurrengoa zen:

0. **Finkaketa**
   Zelulak %4% Paraformaldehyde (PFA) finkatu ziren 10 minutuz 4ºC-tan.

1. **Garbiketa**
   PFA garbitzeko, 5 minutuko 2 garbiketa inguru tenperaturan 1X PBS erabiliz.

2. **Permeabilizazioa eta blokeoa**
   Triton X-100 (permeabilizazioarako) eta %3 BSA (blokeatzeko) zeran buferra, hemendik aurrera mikroskopia buferra, erabili zen 30 minutuz inguru tenperaturan. Bi ezaugarri garrantzitsu hauek antigorputzen tindaketan mantendu eta hobetzeko, antigorputzan bufer honetan inkubatu ziren.

Erreaktiboa	Konzentrazioa	Kantitatea
PBS	1X	1000 ul
BSA	3%	0.03 g
X-100	2%	2 ul

Table 4.17. Microscopy buffer.

3. **Antigorputz primarioa**
   Antigorputzaren beharrezko diluzioa (4.18. Taula) microscopy bufferrean erabili zen ordu batez inguru tenperaturan arigitk babestua (ilunpean).

4. **Garbiketa** gehiegizko antigorputza, 10 minutuko 3 garbiketa PBS buferrean.
5. **Antigorputz sekundarioa**

Antigorputzaren beharrezko diluzioa (2.23. Taula) microscopy bufferrean erabili zen ordu batez inguru tenperaturan arigitk babestua (ilunpean).

6. **Nukeloaren tindaketa**

   4',5-diamidino-2-phenylindole (DAPI) izeneko tindatzailea fluoreszentea DNAri atxikitzen zaio nukleoaren bistaratzea ahalbidetuz.

   DAPI 1X PBSea dilutitta erabili zen 5 mintuz ilunean eta inguru tenperaturan.

7. **Garbiketa** gehiegizko antigorptuz eta DAPIa kentzeko, 10 minutuko 3 garbiketa PBS buferrean inunpean eta inguru tenperaturan.

8. **Montaketa**

   Behin tindaketa amaituta, montaketa medio (Fluoromount; 0100-01, Southern Biotech) tanta bat jarri zen mikrokopio porta batean eta bere gainean estalkia zulak portara begira. Gau pasa utzi zen ilunpean eta inguru tenperaturan.

Xedea	Espeziea	Klonalitatea	Konjugatua	Diluzioa	Katalogo zenbakia	Ekoizlea
ERp72	Rb	Poliklonala		1 500ean	ADI-SPS-720-F	Enzo
IL-22BP	G	Poliklonala		1 20ean	AF1087	R&D
IL-22BP	G	Poliklonala	Biotin	1 20ean	BAF1087	R&D
IL-22BP	Ms	Monoklonala		1 100ean	66190	Proteintech
TGOLN	Rb	Poliklonala		1 500ean	HPA012723	Atlas

Table 4.18. ICC antigorputz primarioak. G: goat, ahuntza; Ms, mouse, sagua; RB, rabbit, lapina.

Xedea	Espeziea	Konjugatua	Diluzioa	Katalogo zenbakia	Ekoizlea
Ahuntza	Dk	A647	1 500ean	705-605-147	Jackson
Streptavidin		A647	1 4000an	039S000-41	Tebu-bio
Lapina	Dk	A647	1 500ean	711-605-152	Jackson
DAPI			10 µg/mL	D9542	Sigma-Aldrich

Table 4.19. ICC antigorputz sekundarioak. DK, donkey, astoa.

4.5.5. ELISA

ELISA lagin likido batean proteina kantitae oso txikiak (pg/mL mailakoak) detektatzeko erabiltzen den teknika da. ELISA mota desberdinak daude, zuzena, zeharkakoa eta sandwicha.

ELISA zuzenean, helburu den antigenoa aurretiaz inmobilizatu behar da plaka batean eta gero entzima bat lotuta daraman antigorputza erabiltzen da berau detektatzeko. Antigorputzari lotutako entzimak substratu baten bidez ikusi eta neurtu daitekeen seinalean sortzen du. Zeharkako ELISAn, antigorputz primarioak ez darama entzimarik eta beharrezkoa da entzima daraman antigorputz sekundario bat erabiltzea primarioa detektatzeko.

Sandwich ELISA biengandik bereizten da antigenoa inmobilizatu beharrean antigorputza inmobilizatzen delako plakan, atzitze antigorputza. Gero lagina gehitzen da eta antigenoa atzitze antigorputzak inmobilizatzen du. Gero hautemate antigorputza erabiltzen da antigenoaren aurka. Antigorputz onek entzima edo biotina bezalako estekatzailea eraman dezake antigorputz sekundario batek detektatzeko. Gure kasuan sanwich ELISA baino ez ditu erabili, biotinari lotutako hautemate antigorputza erabiilz. Biotinadun antigorputza streptavidin lotuta duen HRPrekin lotzen da eta HRP entzimak burutzen du erreakzioa (4.23. Irudia).

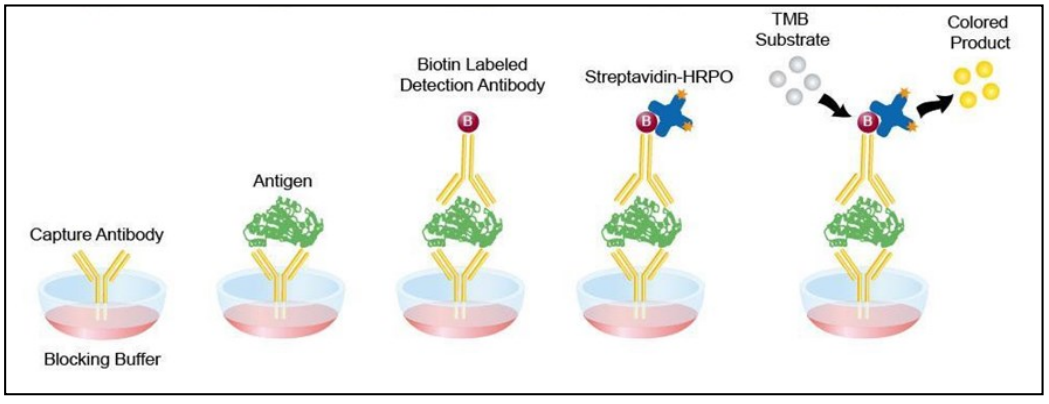

Figure 4.23. Sandwich ELISA biotinilatutako detekzio antigorputza erabiliz. Iturria: (Leinco, 2022)

Laginen kuantifikazioa, diluzio kurba baten lagunzarekin egiten da, ezaguna den konzentrazioko proteina berdinaren diluzio ezagunak (2.24. Irudia).

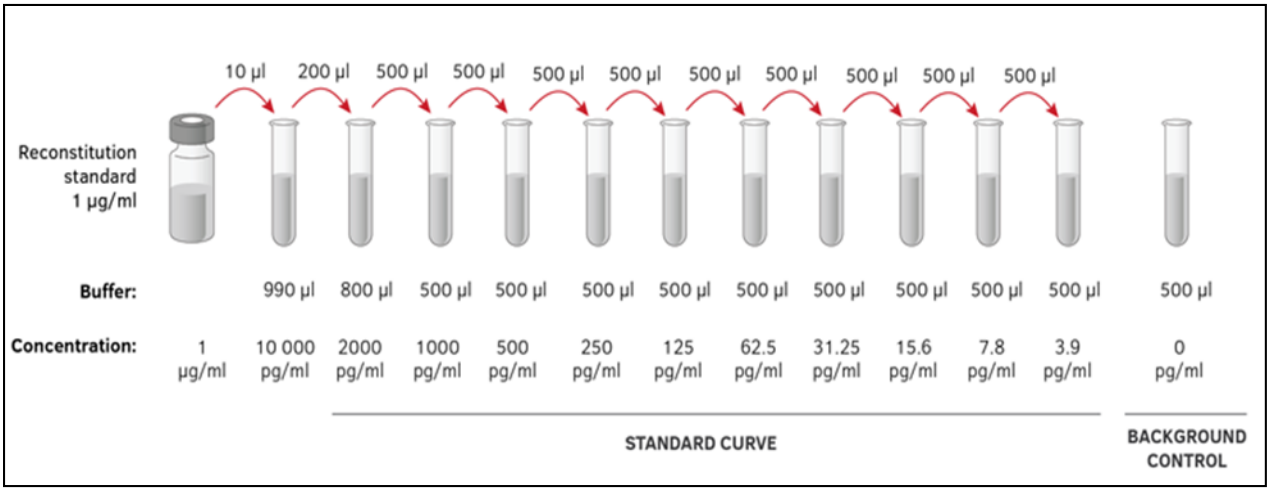

Figure 4.24. ELISA kuantifikatzeko diluzioen kurba. Iturria: (Mabtech, 2022)

4.5.5.1. In house designed IL-22BP ELISA

IL-22BP ELISA komertzilalekin detektatzeko arazoak zire leta, laborategain ELISA bat disenatu eta garatu zen. ELISA hau askotan frogatu egin zen emaitza onak lortuz eta lan honetan erabili zian da. Erabili ez zen elisa komertizal (ABIN841997; antibodies-online.com) bateko proteina ezaguna erabili zen, eta gero gurea ere ekoiztu genuen. Protokoloa ondoren azaltzen den moduan burutu zen, bufferen errezetak 4.20 Taulan daude:

1. **Lehenengo eguna: Plakan atzitze antigorputza jartzea (Plate coating)**
   a. Erabili baino lehenago, atzitze antigorputza (IL-22BP; AF1087, R&D) 0.5 µg/mL atzizte bufferean diluitu zen.
   b. Gehitu putzu bakoitzeko 50ul
   c. Estali eta gauean zehar inkubatu 4ºC-tan.
2. **Bigarren eguna: Blokeoa (Plate blocking)**
   a. Plaka inguru tenperaturan eduki, antigorputzaren soluzioa kendu eta hiru aldiz garbitu garbiketa buferrarekin, 200µL aldi bakoitzean.
   b. Gero, elkartze ez-espezifikoak blokatzeko, gehitu blokeo buferraren 200 ul.

c. Plaka zigilatu eta inkubatu gau osoan zehar 4ºC-tan edo 1 - 2 orduz inguru tenperaturan.

3. **Hirugarren eguna: lagina gehitzea, inkubatea eta irakurtzea**

3.1 Lagina gehitzea

a. Plaka ingur tenperatura edui eta blokeo soluzioa kendu.

b. Garbitu 3 aldiz garbiketa buferrarekin, 200 uL aldi bakoitzean.

c. Gehitu laginaren 50 µL (laginaren diluzioak kontutan hartu, diluzioak entsegu buferrean egin)

d. Plaka zigilatu eta inkubatu inguru tenperaturan 2 orduz.

e. Garbitu 6 aldiz garbiketa buferrarekin.

3.2 Hautemate antigorputza gehitzea

a. Hautemate antigorputza (IL-22BP; BAF1087, R&D) to 0.5 µg/mL entsegu bufereran diluitu.

b. Gehitu diluitutako antigorputzaren 50µL putzu bakoitzeko.

c. Plaka zigilatu eta inkubatu inguru tenperaturan Seal the plate and incubate at room temperature for 1 hour.

d. Garbitu 6 aldiz garbiketa buferrarekin.

3.3 Detekziorako Streptaividin-HRP gehitzea

a. Inbuatu 50µL Streptavidin-HRP entsegu buferrean 1:200 diluituta ordu bat.

b. Garbitu 6 aldiz garbiketa buferrean.

3.4 Koloretze erreaktiboa gehitzea (Garapena)

Add 45µL 1step ultra of TMB-ELISA to each well. Incubate at room temperature for 15-30 minutes.

3.5 Erreakzioa gelditzea

Gehitu 45µL azido sulfuriko (2M) erreakzioa gelditzeko.

3.6 Irakurketa

Absorbantzia 450nm-tan irakurri Varioskan gailuan.

Formula	pH	Bolumena	Erreaktiboa	Kantitatea
Atzitze buferra				
50mM Tris/HCl	pH 8.5	500 mL	Tris/HCl	3,0285 g
150 nM NaCl			NaCl	4,383 g
Garbiketa buferra				
50mM Tris/HCl	pH 7.4	300 mL	**Atzizte buferra**	299,85 mL
150mM NaCl				
0.05% Tween 20			Tween 20	150 uL
Blokeo buferra				
50mM Tris/HCl	pH 7.4	50 mL	**Atzizte buferra**	47,5 mL
150mM NaCl				
0.1% Casein			Casein 2%	2,5 mL
Entsegu buferra				
50mM Tris/Hcl	pH 7.4	25 mL	**Blokeo buferra**	24,9875 mL
150mM NaCl				
0.1% Casein				
0.05% Tween 20			Tween 20	12,5 uL

Table 4.20. Laborategian garatutako IL-22BP ELISA buferrak.

4.6. Analisi estatistikoa

Datuen analisi estatistikoa G GraphPad Prism version 9 (GraphPad Software, La Jolla, CA, USA) programarekin burutu zen. Datuak, batazbesteako ± batazbestekoaren errore estandararra (ingeleraz, standar error of the mean (SEM) bezala aurkeztu dira. Esanguratsutasun estatistikoarako $p < 0.05$ hartu da.

Taldeen arteko konparaketa egiteko Sutdent t-test erabili da bi talde zirenean eta ANOVA (ingeleraz analysis of variance; bariantzaren analisia) bi baino gehiago zirenean. Parekatutako t-test erabili da taldeak lagin beretik zetozenean, eta t-test independentea lagin desberdinak zirenean. ANOVAri dagokionez, bide bakarreko ANOVA (one way ANOVA, aldagai aske bakarra zegoenean) erabili da hiru talde desberdin batera aztertzeko, bide bikoitzeko ANOVA (two way ANOVA, bi aldagai aske daudenean) faktore desberdinen arteko interakzioa aztertzeko hiru talderen artean. Test ez parametrikoak erabili izan dira, test parametrikoak burutzeko baldintzak betetzen ez zirenean, Wilcoxon testa bi talde konparatzeko eta Krstal-Wallis testa hiru talde aztertzeko.

5. RESULTS

5.1. *IL22RA2* and IL-22BP

5.1.1. *IL22RA2* cell sources and expression levels characterization

At the beginning of this work, the cells sources and expression levels of *IL22RA2* were a matter of discussion. As stated by the authors of one the earliest high impact publications: “IL-22BP expression has been reported in different hematopoietic cells and also in intestinal epithelial cells. However, these studies (Witte et al., 2010; Xu et al., 2001) contradict each other.”(Huber et al., 2012).

In this context, the group of Régis Josien’s Lab published an article (Martin et al., 2014) that helped us to focus on the characterization of cells sources of *IL22RA2*. Their study was able to describe the expression of IL-22BP in the rat where “the highest levels were found in secondary lymphatic organs, i.e., spleen and mesenteric, axillary and cervical LNs [lymphoid nodes]” suggesting “a hematopoietic origin of IL-22BP sources”. A subset of steady state rat spleen and intestinal resident conventional DCs were found as the major sources of IL-22BP. This study was also able to report the expression of IL-22BP mRNA in human moDCs, which is strongly induced during monocyte differentiation and downregulated during moDCs maturation. They also found that retinoic acid receptor α agonist AM580, was able to boost *IL22RA2* expression when added to the differentiating moDCs culture. They were not able to detect all three variant on moDCs.

As explained in the introduction rodent *IL22RA2* gene lacks a long variant that appeared on primates through a retrotransposon forming an alternatively spliced extra exon. Therefore, our main interest was the characterization of *IL22RA2* in human cells sources to understand the biological significance in the context of MS. For that purpose, we focused on the study of the

moDCs, and in order to better understand them, we explored the different monocytes subpopulations that could generate moDCs, and the closest cell line to monocytes, U937, in order to try to develop a model for *IL22RA2* expression without need for primary cells.

Due to the relevance of the retinoic acid receptor alpha agonist AM580 in this work, it is useful to give some insights about it before finishing this introduction. Retinoic acid (RA) is of great relevance for MS since RA and its agonists ameliorate MS course (Abtahi Froushani et al., 2014; Fragoso et al., 2014) and astrocyte-derived RA can regulate BBB function ameliorating MS (Mizee et al., 2014). RA and its agonists induce upregulation of IL-22 and proinflammatory cytokines down-regulation (Mielke et al., 2013) and RA signaling pathway can induce proinflammatory cytokine downregulation via SOCS3 (Correale & Farez, 2013). RA induced proinflammatory downregulation has also been linked to the generation of tolerogenic DCs (tolDCs;(Papenfuss et al., 2011)). RA or its agonist keeps DCs in a more immature stage and potentiates a regulatory function (Bhatt et al., 2014; Chau et al., 2013). Indeed, synergistically with IL-4, RA can induce regulatory DCs (Zhu et al., 2013). This evidence is worth to mention given that our DM contains GM-CSF and IL-4, and thus, this synergetic effect can take place.

5.1.1.1. moDCs express all 3 variants of *IL22RA2*

In order to properly characterize gene expression levels of *IL22RA2* variants in human cell sources, moDCs were used. moDCs offered us the possibility of obtaining primary cell cultures of immune cells from different donors in a scalable manner. For that purpose, we isolated monocytes from PBMCs using CD14 microbeads and thus are classical monocytes in a large majority (>95%). Primary monocytes were cultivated for 6 days in DM, which apart from essential components like serum and essential AAs contains GM-CSF and IL-4 to drive the differentiation process from monocytes to moDCs as explained in Materials and Methods, section 4.4.3.2., Primary cells.

We used AM580 RA agonist described by Martin et al. 2014, in order to both increase the expression of *IL22RA2* and see if there was any difference in the expression of the different variants. Therefore an experiment with three different donors in the same conditions, $CD14^+$ monocytes cultured with and without AM580 for 6 days, was performed.

To ensure the best possible detection of all 3 variants of *IL22RA2*, specific primers were designed for conventional and qPCR as shown in Materials and Methods, section 4.2.2, *IL22RA2* variants (Figure 4.2). These primers allowed us to detect all three variants by qPCR and in agarose gel after conventional PCR.

We first tested the amplification of all the variants at using primers FW *IL22RA2* and RV *IL22RA2* in a conventional PCR. The predicted sizes of the products for the different variants were: 653 bp for *IL22RA2v1*, 555 bp for *IL22RA2v2* and 385 bp for *IL22RA2v3*. We used samples of moDCs cultured for 6 days in DM in two conditions, with and without AM580. We were capable of detecting the largest two variants but not *IL22RA2v3* (Figure 5.1).

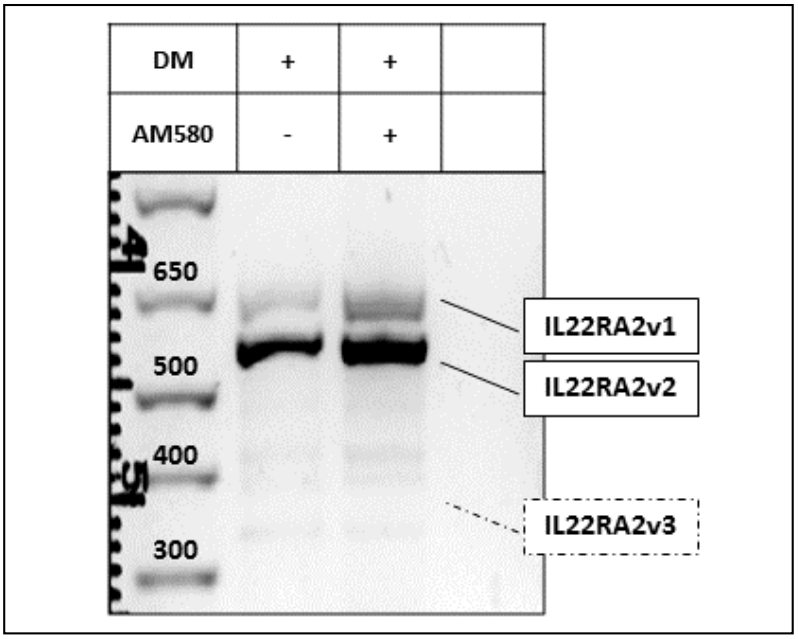

Figure 5.1. Agarose gel electrophoresis of all *IL22RA2* variants. PCR products generated by primers FW *IL22RA2* and RV *IL22RA2*.The empty lane is the negative control. Figure representative of three different experiments.

The absence of *IL22RA2v3* in the PCR did not mean necessarily that the variant was not expressed, since it was not possible to discard a level of expression that is at least several times lower than that of the other two. To discard or confirm this, two different PCR reactions were performed using *IL22RA2v2* plasmid expression vector as a control. In the first of them *IL22RA2v2* would be amplified, and then, the vector would be a positive control. In the second, *IL22RA2v2* would not be amplified and thus the vector would be a negative control.

The first of these two PCRs was performed using FW 2&3q, primer that cannot amplify *IL22RA2v1*, and primer RV*IL22RA2*. The predicted product sizes were: 399 bp for *IL22RA2v2* and 230 bp for *IL22RA2v3*. *IL22RA2v2* was detected in *IL22RA2v2* positive control and in both culture conditions, with a larger amount of PCR product obtained from moDCs of day 6 culture with AM580. Increasing the contrast of the gel image, we were able to detect a clear faint band

corresponding to *IL22RA2v3* in AM580 treated moDCs, showing that it was expressed at lower level than *IL22RA2v2* (Figure 5.2).

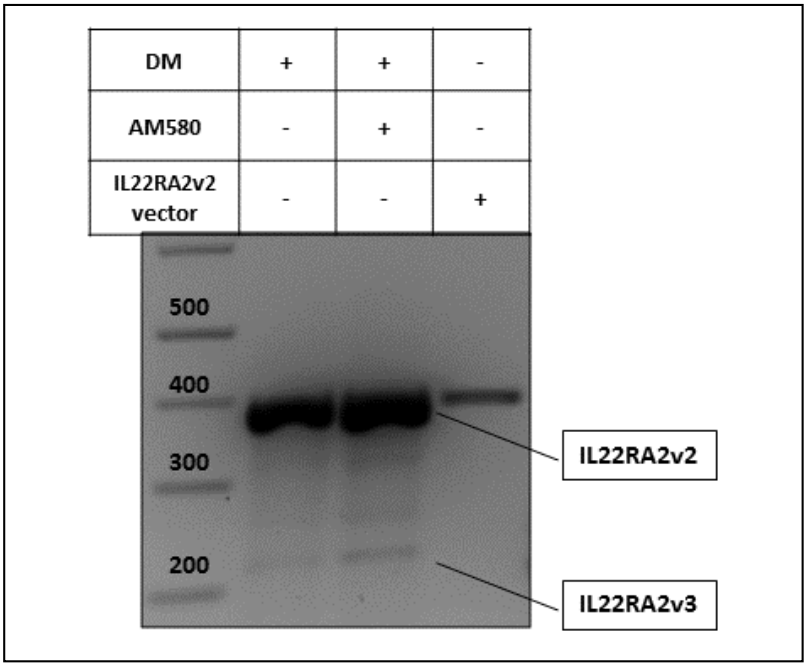

Figure 5.2. Agarose gel electrophoresis of *IL22RA2v2* and *IL22RA2v3*. PCR products generated by primers FW 2&3q and RV. Figure representative of three different experiments.

The second PCR design performed to confirm *IL22RA2v3* presence in the samples and was done using the *IL22RA2v3* specific primers designed for qPCR, FW2&3q and RV3q. The expected product size was 200 bp. The previously tested conditions were used and the lack of amplification of *IL22RA2v2* vector confirmed their specificity. In line with the previous PCR, *IL22RA2v3* expression was confirmed, being it higher in AM580-treated moDCs (Figure 5.3).

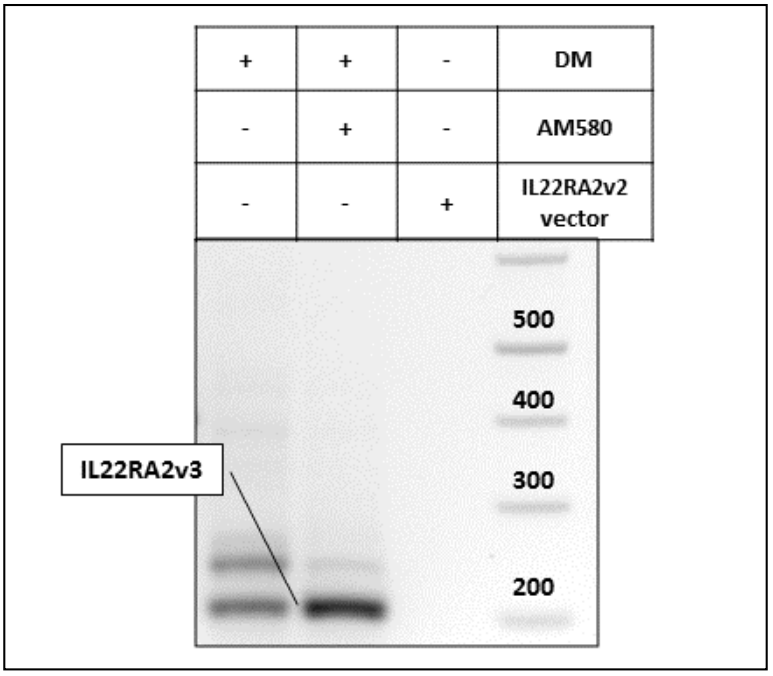

Figure 5.3. Agarose gel electrophoresis of *IL22RA2v3*. Products generated by primers FW 2&3q and RV *IL22RA2*. Figure representative of three different experiments.

The results shown on the agarose gels substantiated the expression of the three variants of *IL22RA2* on moDCs. The most prominent expression was the one of the canonical variant *IL22RA2v2*, that is homologous to rodent *IL22RA2*, but there was also an important expression of *IL22RA2v1*. The level of expression of *IL22RA2v3* was much lower, and it could be observed an increase of *IL22RA2* expression in cells treated with AM580 in the three variants.

Finally, the expression analysis off the variants was simultaneously carried out using variant-specific primers by RT-qPCR. Results confirmed that AM580 strongly induced the expression levels of each one of the splicing variants (Figure 5.4). The expression levels of *IL22RA2v1* and *IL22RA2v3* looked more similar than their previous detection on agarose gel electrophoresis (Figures 5.1-5.3). The reason for it is that primer efficiency can be different in qPCR, a much more sensitive technique where only a specific variant is been amplified, compared to previously performed conventional PCRs with simultaneous amplification of different variants.

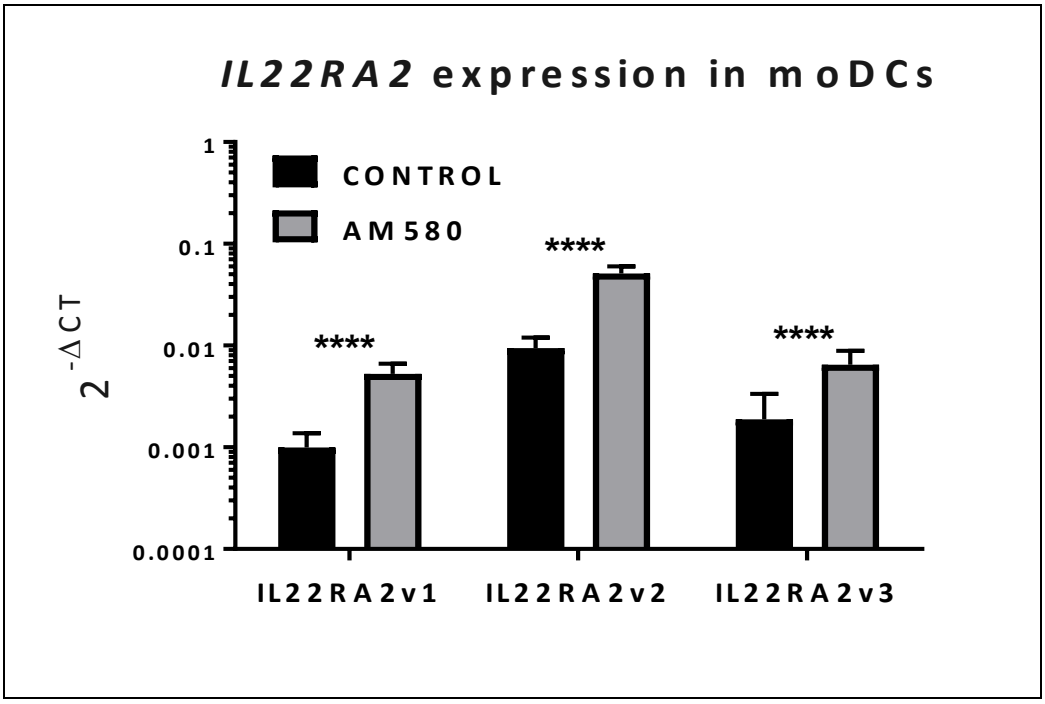

Figure 5.4. Gene expression of *IL22RA2* variants in moDCs. moDC of 6 days in culture analyzed by RT-qPCR using the variant-specific primers. Mean ± standard error of the mean (SEM) relative to the housekeeping gene GAPDH. **** p <0.0001 by 2way ANOVA.

Altogether, the results showed the expression of the three *IL22RA2* variants in moDCs cultured for 6 days, and the boosting effect of AM580 on *IL22RA2* was confirmed for the three variants, seemingly to a similar degree for all of them.

5.1.1.2. *IL22RA2* is upregulated during moDCs differentiation and downregulated by their maturation

In order to analyze *IL22RA2* expression during the monocyte to moDCs differentiation process and maturation of moDCs, a 3-donor time course experiment was performed. $CD14^+$ monocytes were isolated and cultured as previously described for 6 days and then treated with 1 µg/mL of LPS for 6 or 24 hours (LPS, matured moDCs) or left untreated (Control, immature moDCs). The time points for the time course were freshly isolated monocytes (day 0), differentiating monocytes (day 2, 4 and 6), and moDCs of 6 days (after 6 or 24 hours with or

without LPS). The results, consistent with those previously reported (Martin et al., 2014) showed an increase of *IL22RA2* expression during differentiation and a large downregulation induced by LPS at 24 hours post stimulation compared to control (Figure 5.5).

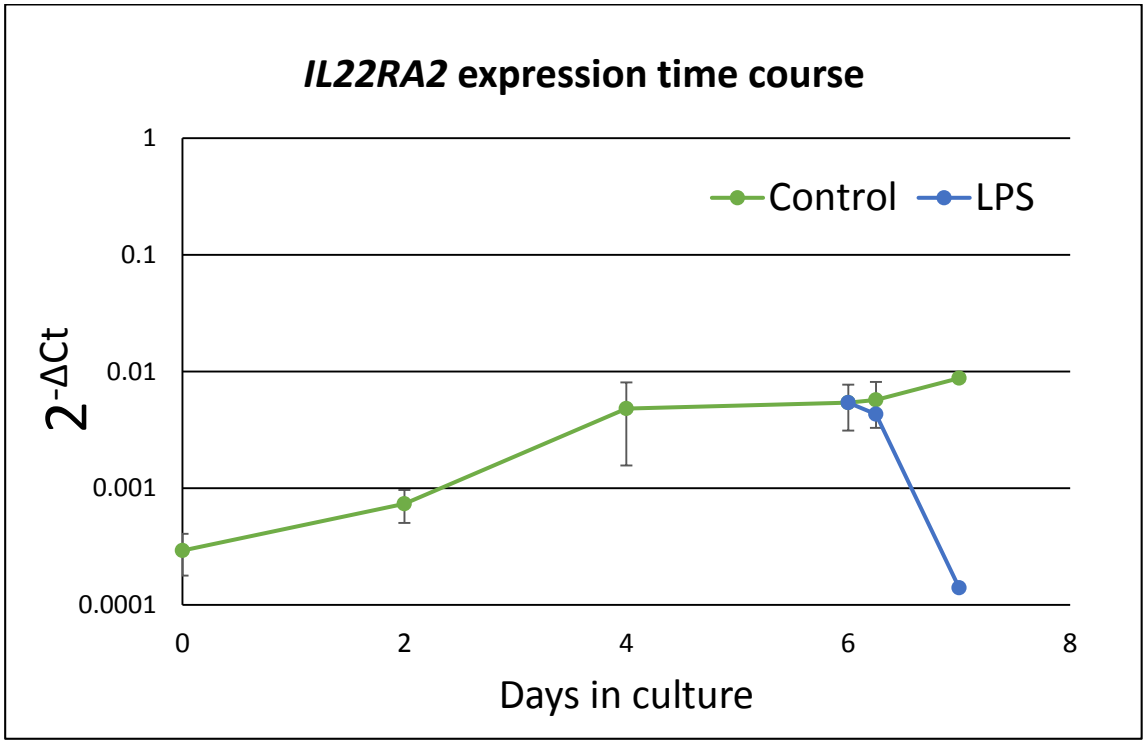

Figure 5.5. Gene expression of *IL22RA2*.in monocytes and moDCs. Time course analyzed by RT-qPCR. Mean ± SEM relative to the housekeeping gene ACTB. Control: untreated moDCs; LPS: 1 µg / mL treated moDCs.

We also tested the amplification of the different variants in the time course samples confirming that all variants, *IL22RA2v1* (v1), *IL22RA2v2* (v2) and *IL22RA2v3* (v3), followed similar expression patterns (Figure 5.6).

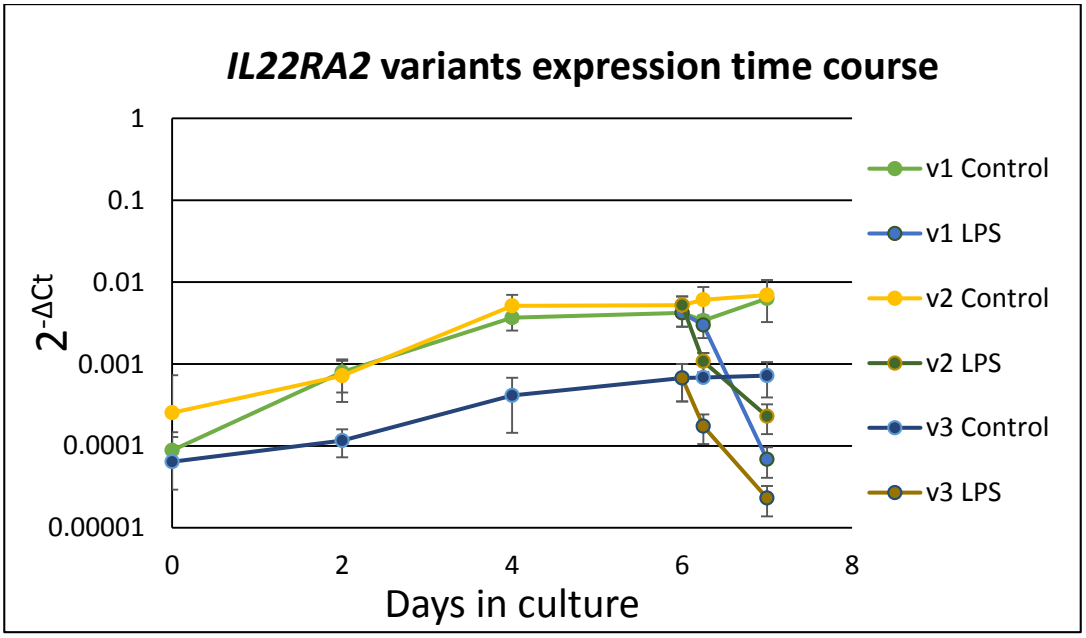

Figure 5.6. Gene expression of *IL22RA2* variants in monocytes and moDCs. Time course analyzed by RT-qPCR. Mean ± SEM relative to the housekeeping gene ACTB. Control: untreated moDCs; LPS: 1 µg / mL treated moDCs; moDCs; v1: *IL22RA2v1*; v2: *IL22RA2v2*; v3: *IL22RA2v3*.

We were interested to understand to what extent other cytokines produced by moDCs follow similar or contrasting expression profiles. For that purpose, we focused on previously reported cytokines like the IL-22 related IL10 cytokine family and interferons (Wolk et al., 2008a) and the well-studied IL12 family cytokines (Hayes et al., 1995; Seventer et al., 2002; Sun et al., 2015). Expression of the following cytokines was tested in the time course samples: IL4, IL10 family (*IL10. IL19*, *IL20. IL22*, *IL24*, and *IL26*), IL12 family (*IL12A*, *IL12B*, and *IL23A*) and interferon type I (interferon β, *IFNB*).

We did not detect expression of IL4, *IL20. IL22*, *IL24*, and *IL26* (data not shown). The results for the other cytokines have been divided into the time course (monocytes and moDCs of 2, 4 and 6 days; Figure 5.7) and LPS stimulation (with the expression been compared to samples not treated with LPS; Figure 5.8). In both cases, the time course and the LPS stimulation, *IL22RA2* showed a unique expression pattern.

Regarding the time course (Figure 5.7), results showed that, apart from *IL22RA2*, no other of the studied cytokines is upregulated during the moDCs differentiation process; if anything, minor increases in expression of *IL12A*, *IL12B* and *IFNB* were seen. There was also a minor decrease in *IL19* levels.

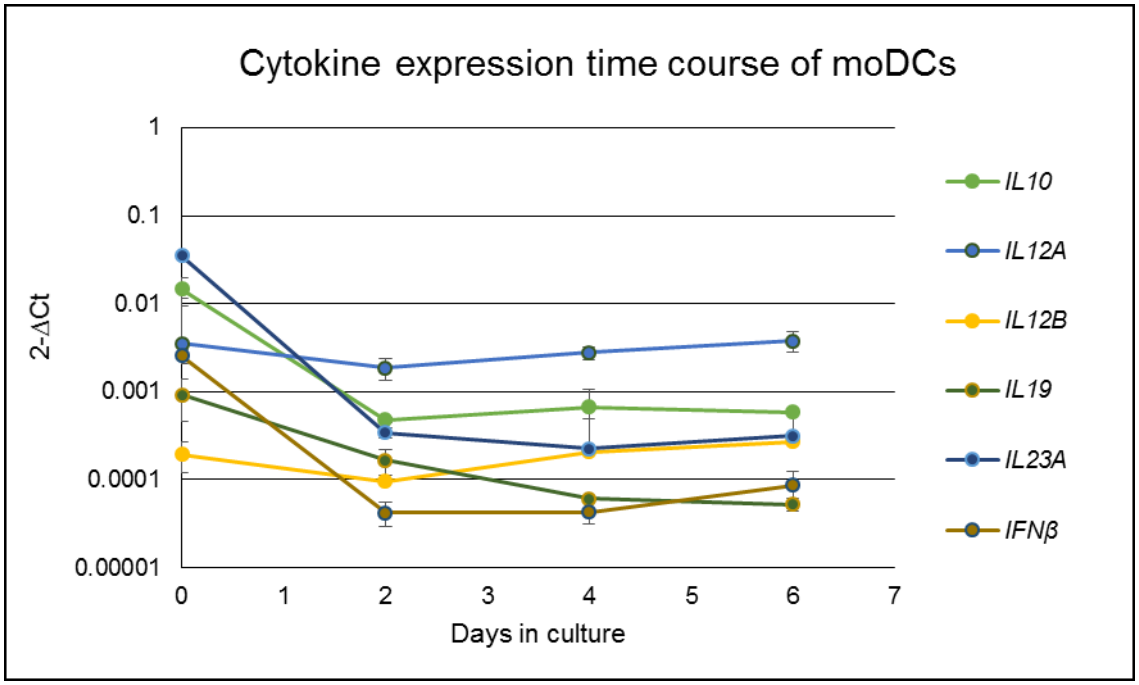

Figure 5.7. Gene expression of different cytokines in monocytes and moDCs. Time course analyzed by RT-qPCR. Mean ± SEM relative to the housekeeping gene ACTB.

In the case of LPS stimulation (Figure 5.8), there was an upregulation of cytokines after 6 hours, very strong in the case of *IL12B* (140-fold increase), strong for *IL23A*, *IL19* and *IL10* (10-20-fold) and moderate for *IL12A* and *IFNB* (three-fold) while a 3-fold decrease was observed for *IL22RA2*. After 24 hours with LPS, the cytokine expression levels were back to basal level except for *IL22RA2* that showed a strong 35-fold downregulation compared to the control.

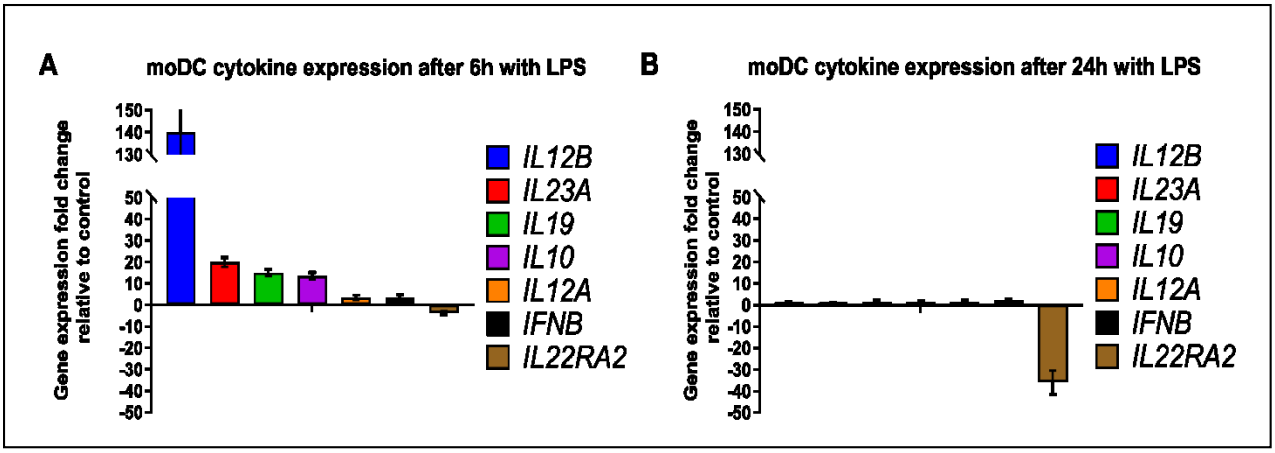

Figure 5.8. Gene expression fold change of different cytokines of moDCs. Gene expression fold change of moDCs stimulated with LPS (1 µg/mL) for 6 (A) or 24 (B) hours r to same time point untreated moDCs. Mean ± SEM relative to the housekeeping gene ACTB.

Altogether, the results demonstrated that *IL22RA2* is a cytokine whose expression increases during the differentiation process from monocytes to moDCs, and *IL22RA2* is downregulated by LPS. This feature makes it unique among all the other tested cytokines that do not show increase during differentiation but are upregulated by LPS.

5.1.1.3. U937 cell line as a model for *IL22RA2* expression

U937 is a human hematopoietic cell line derived from a patient with generalized histiocytic lymphoma by Nilsson and Sundström (Sundström & Nilsson, 1976) and since then used for terminal monocyte differentiation with a wide range of active compounds. U937 use in the context of *IL22RA2* was reported in the early stages of *IL22RA2* characterization (Wei et al., 2003).

To assess if U937 cells are capable of upregulate *IL22RA2* in primary monocyte culture conditions compared with cells growing in the regular medium we designed a time course experiment. To be able to compare with the time course of moDCs, apart from *IL22RA2*, an extensive analysis of *IL4*, IL10 family (*IL10. IL19*, *IL20. IL22*, *IL24*, and *IL26*), IL12 family (*IL12A*,

IL12B, and *IL23A*) and interferon type I (interferon β, *IFNB*) cytokines was done. In this case, there was again no detection of IL4, *IL20. IL22*, *IL24* and *IL26* (data not shown).

The results (Figure 5.9) confirmed that *IL22RA2* expression was increased in U937 cells cultured in DM in the same way to that seen on moDCs. The *IL10* cytokine family members detected, *IL10* and *IL19,* showed similar levels of expression along the time course.

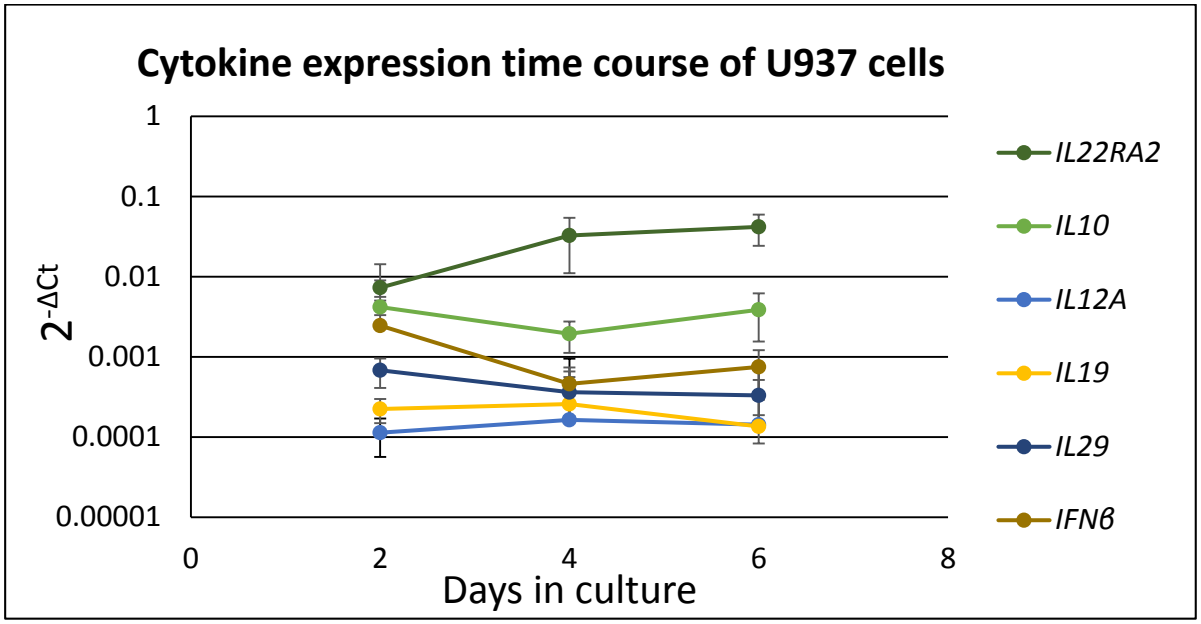

Figure 5.9. Gene expression of different cytokines in U937 cells. Time couse of U937 cells cultured in DM and analyzed by RT-qPCR. Mean ± SEM relative to the housekeeping gene ACTB.

However, there were some differences. Regarding IL12 cytokine family, no increase in *IL12A* was observed, and *IL12B* and *IL23A* were not detected. There were also differences in *IFNB* that showed a minor decreasing trend.

The analysis of the variants showed that *IL22RA2v1* expression relative to *IL22RA2v2* was lower in U937 (Figure 5.10) than on moDCs (Figure 5.6). While *IL22RA2v1* expression is comparable to the *IL22RA2v2* on moDCs, with a ratio of *IL22RA2v2/IL22RA2v1* lower than five, in the case of U937 the ratio is higher than fifty (Table 4.1).

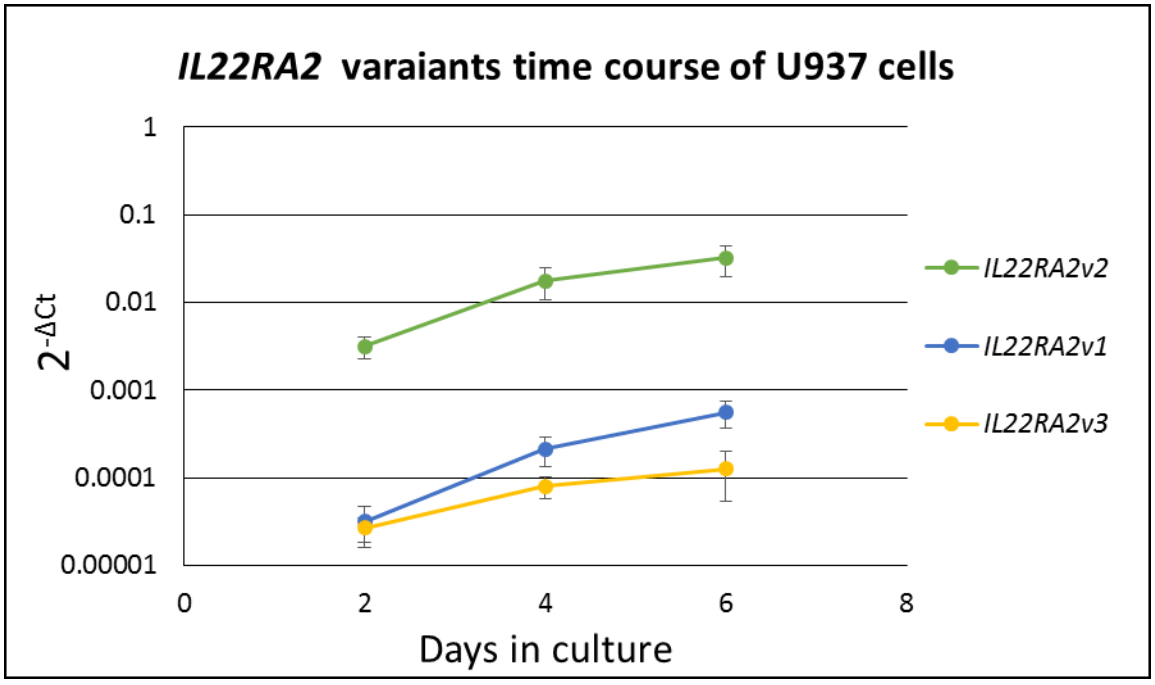

Figure 5.10. Gene expression of *IL22RA2* variants in U937 cells. Time couse of U937 cells cultured in DM and analyzed by RT-qPCR. Mean ± SEM relative to the housekeeping gene ACTB.

Taken together the results consistently confirmed the *IL22RA2* upregulation in U937 cells cultured in DM, and similar expression levels of IL10 cytokine family both in U937 cells and on moDCs. However, the differences between U937 cells and moDCs in IL12 family cytokines and IFNβ showed the limits of the model as summarized in Table 5.1.

The effect of LPS in U937 cells cultured for 6 days DM was studied at four different time points: 1, 3, 6 and 12 hours after LPS addition (Figure 5.11). LPS upregulated cytokines from the IL10 family, i.-e. *IL19*, and IFN*β*, while IL12 cytokine family members tended to remain relatively unaltered (*IL12A*), or declined (*IL12B*, *IL23A*). Despite these major changes, the downregulation of *IL22RA2* was clearly observed.

Gene	U937 cells	moDCs
IL22RA2	↑↑	↑↑
IL22RA2v2/IL22RAv1	>50	<5
IL10	≈	≈
IL19	↓	↓
IL12A	≈	↑
IL12B	×	↑
IL23A	×	≈
IFNB	↓	↑
IL4	×	×
IL20	×	×
IL22	×	×
IL24	×	×
IL26	×	×

Table 5.1. Compilation of cytokine expression trend in U937 cells vs moDCs. All were cultured in DM for 6 days. ↑↑: strong upregulation; ↑: upregulation; ≈: no variation; ↓: downregulation; ×: no detection.

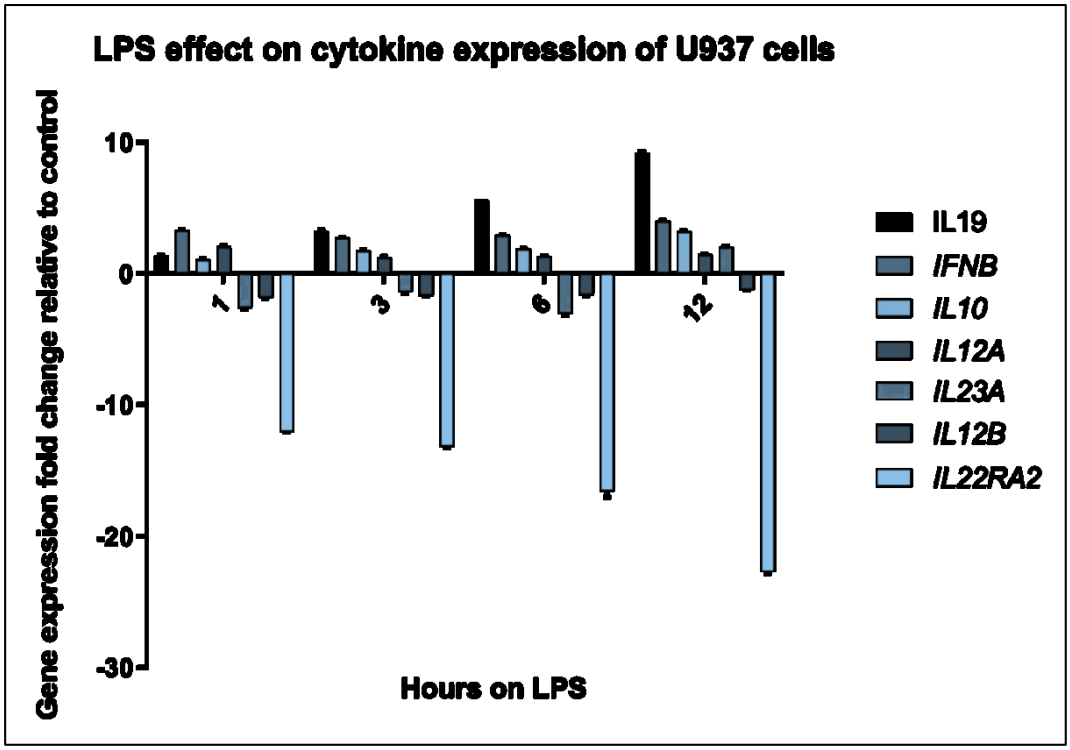

Figure 5.11. Gene expression fold change expression of different cytokines in U937 cells. Gene expression fold change of U937 cultured in DM and stimulated with LPS (1 µg/mL) relative to untreated DM cultured U937 cells. Mean ± SEM relative to the housekeeping gene.

The results showed considerable differences of U937 cells compared to moDCs. First, the range of cytokines that were upregulated was much narrower in U937 than in moDCs. U937 cells did not show the strong increases of IL12 family cytokines observed in IL12B (140-fold) and IL23A (20-fold) in moDCs after 6 hours with LPS. Regarding the IL10 cytokine response, over ten-fold increases were observed in IL19 (15-fold) and IL10 (13.5-fold) in moDCs after 6 hours, while in U937 cells the highest upregulation was a 9-fold increase in *IL19* after 12 hours with LPS. Regarding *IL22RA2*, the downregulation after 6 hour in LPS was stronger in U937 (16-fold decrease) versus moDCs (3.7-fold decrease). A complete comparison between U937 cells and moDCs cytokine expression in response to LPS at 6 hours is shown in Table 5.2.

Gene	U937 cells	moDCs
IL12B	-1.6	140
IL23A	-3	20
IL19	5.6	15
IL10	1.9	13.5
IL12A	1.3	3.4
IFNB	2.9	3.2
IL22RA2	-16	-3.7
IL4	ND	ND
IL20	ND	ND
IL22	ND	ND
IL24	ND	ND
IL26	ND	ND

Table 5.2. Compilation of gene expression fold change in U937 cells and moDCs. All cells were cultured in DM for 6 day and stimulated with LPS for 6 hours. Gene expression fold change relative to untreated equivalent cells. ND: not detected.

5.1.1.4. Monocyte subpopulations express different *IL22RA2* and IL-22BP levels

In order characterize the actual source of IL-22BP in the context of MS we set out to analyze in detail the expression of *IL22RA2* in the different monocyte subpopulations. As explained in Materials and Methods, classical monocytes ($CD14^{++}CD16^{-}$) account for around 90% of the total number of monocytes but various studies point to the relevance of the minority populations (intermediate ($CD14^{++}CD16^{+}$) and non-classical ($CD14^{+}CD16^{+}$)) in different autoimmune diseases like asthma (Moniuszko et al., 2009), inflammatory bowel diseases (Koch et al., 2010), rheumatoid arthritis (Rossol et al., 2012), sarcoidosis (Okamoto et al., 2003) and Sjögren's syndrome (Wildenberg et al., 2009).

At the time of this study, only two groups had published works about the relevance of monocyte subpopulations in MS, one led by La Flamme (Malaghan Institute, New Zeeland) and another by Ralf Linker (Erlangen University, Germany). La Flamme's team highlighted the relevance of $CD16^{+}$ monocyte subset in inflammatory response during MS (Chuluundorj et al., 2014). They also found that a well-known MS treatment, glatiramer acetate (La Mantia et al., 2010), induced a significant expansion of $CD16^{+}$ monocytes (both intermediate and non-classical) compared to healthy control subjects or untreated MS patients, and that the monocyte activation state more closely resembled those of healthy controls (Chuluundorj et al., 2017). Linker's work (Waschbisch et al., 2016), showed a reduced number of $CD16^{+}$ monocyte in the circulating blood of untreated RRMS patients, their presence in CSF and their ability to facilitate $CD4^{+}$ T cell migration (even with the limitation of not discriminating between intermediate ($CD14^{+}CD16^{+}$) and non-classical ($CD14^{-}CD16^{+}$)). Altogether, evidence highlighted the relevance of the minority monocyte populations in MS, with a distinctive monocyte population pattern in MS patients and changes of the monocyte profile under MS treatment.

Analysis of *IL22RA2* expression in moDCs showed that monocytes have a very low level of expression but only a very small fraction of purified monocytes prior to cultivation stained positively for IL-22BP in our immunofluorescence staining (Figure 5.12).

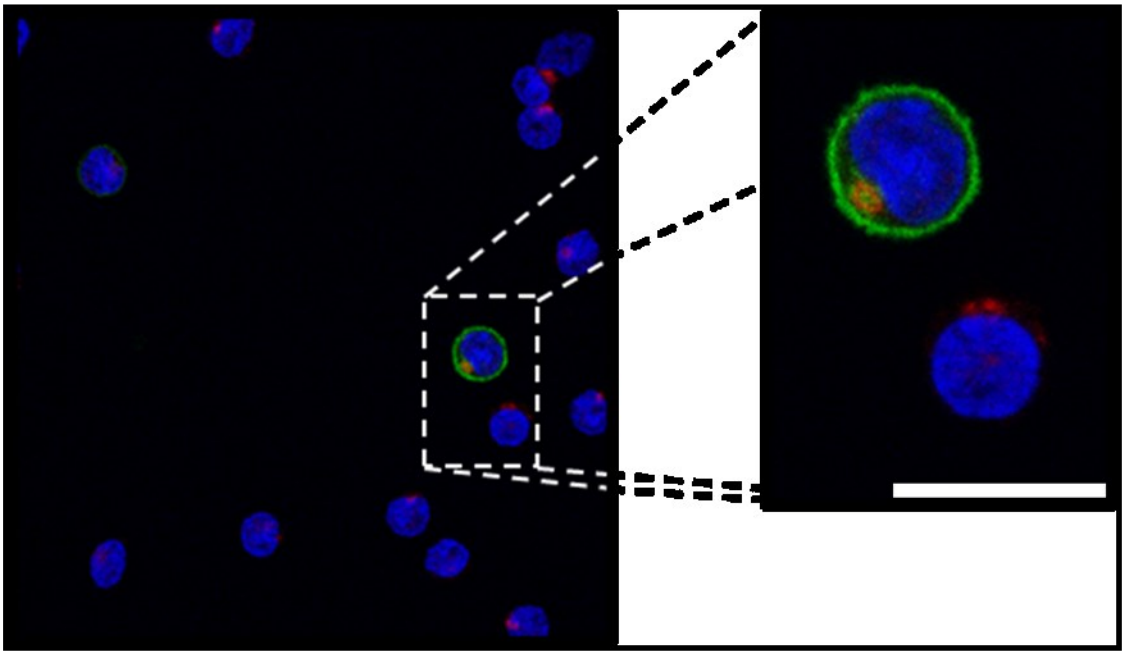

Figure 5.12. CD14$^+$ monocytes stained with DAPI (blue), trans-GOLGI (red) and IL-22BP (green). Scale bar: 10 µm.

This made us think about the possibility of differential *IL22RA2* expression in the different monocyte subsets since the low number of CD16$^+$ subsets could explain both the low level of *IL22RA2* expression in monocytes and the positive staining for few of them in microscopy. On one hand, in a pan-monocyte RNA extraction, results will predominantly reflect the low *IL22RA2* levels of the classical monocytes that make up the majority around 90%) of the total monocyte count. On the other hand, if CD16$^+$ monocytes have higher levels of *IL22RA2* expression than CD14$^+$, it would be expected to have a low number of positive cells in the staining. Therefore, we decided to analyzed *IL22RA2* expression levels of minority monocyte subpopulations.

Following Linker's group methodology (Waschbisch et al., 2016) we sorted and cultured $CD16^+$ and $CD16^-$ monocyte subsets (see Materials and Methods for further detail) for an initial test. Getting suitable numbers of each small subpopulation (intermediate and non-classical) required larger PMBC sample (they are the 5% of the monocytes, while monocytes are 5-15% of the PMBCs; on the whole, minority monocyte populations made less than 0.005% of the initial PBMCs number); thus, pooling both minor $CD16^+$ monocyte subsets, allowed us to test our hypothesis with a smaller initial blood sample and easier isolation procedure avoiding FACS.

An explorative one replicate time course with three stages was performed: freshly isolated monocytes, moDCs (after 7 days of differentiation) and matured moDCs (with IFNγ o/n and LPS for 24h). The idea was to assess the effect of monocyte differentiation to moDCs and the effect of maturation on moDCs. The $CD14^+CD16^-$ monocytes, would serve as a control, where low *IL22RA2* expression will be expected in freshly isolated monocytes that would significantly increase during differentiation to day 7, and dramatically decrease after application of maturation stimuli. moDCs differentiation and maturation status was addressed by flow cytometry (Table 5.3) using MoDC inspector moDC inspector containing antibodies against CD14, CD209 and CD83. The inspector stained CD16-CD14+ moDCs, showed that in both conditions above of 90% of the cells were the characteristic CD14 (monocyte marker) negative and CD209 (moDCs marker) positive. Regarding maturation status of the cells, it was addressed by suing CD83-APC as a marker. In the immature condition 92.20% of the CD14-CD209+ cells were CD83 negative, while in the matured condition 93.88% of the moDCs were CD83 positive. Altogether, the flow cytometry demonstrated the proper differentiation and maturation of the CD16-CD14+ monocytes. In the case of CD16+ moDCs, we observed none CD14 and lower CD209 staining than CD16-CD14+ moDCs in line with been previously reported CD209 expression in different monocyte subpopulation moDCs, where is lower in intermediate moDCs and almost absent in non-classical moDCs (Boyette et al., 2017). However, they responded to the maturation stimuli.

The *IL22RA2* expression in different stages showed a preliminary difference between the two populations (Figure 5.13). Based on these preliminary findings, our research continued in identifying the CD16^{+} monocyte subpopulation (intermediate, non-classical or both) that expressed higher levels of *IL22RA2*.

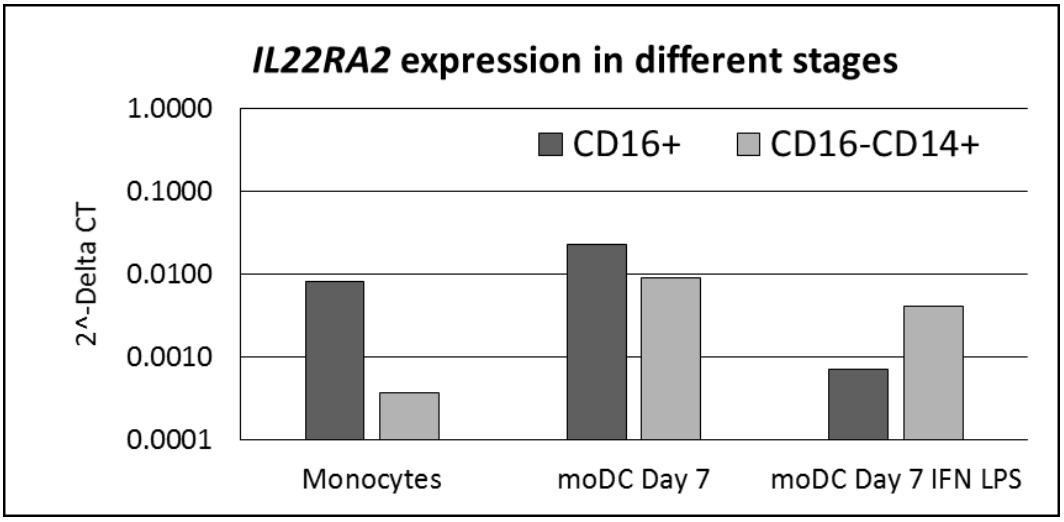

Figure 5.13. Gene expression of *IL22RA2* in the preliminary experiment. Results showed higher levels *IL22RA2* expression in freshly isolated CD16+ monocytes. After 7 days of culture (moDCs Day 7), *IL22RA2* was upregulated in both moDCs populations, and even the expression level of *IL22RA2* was higher, the difference between them was much smaller than between freshly isolated monocytes. Matured CD16^{+} moDCs, in the same line that matured CD16^{-}CD14^{+} moDC, showed decreased the *IL22RA2* expression level compared to unstimulated cells. In the case of CD16+ monocytes, the downregulation of *IL22RA2* was stronger with the levels of expression of matured moDCs below the levels of freshly isolated monocytes.

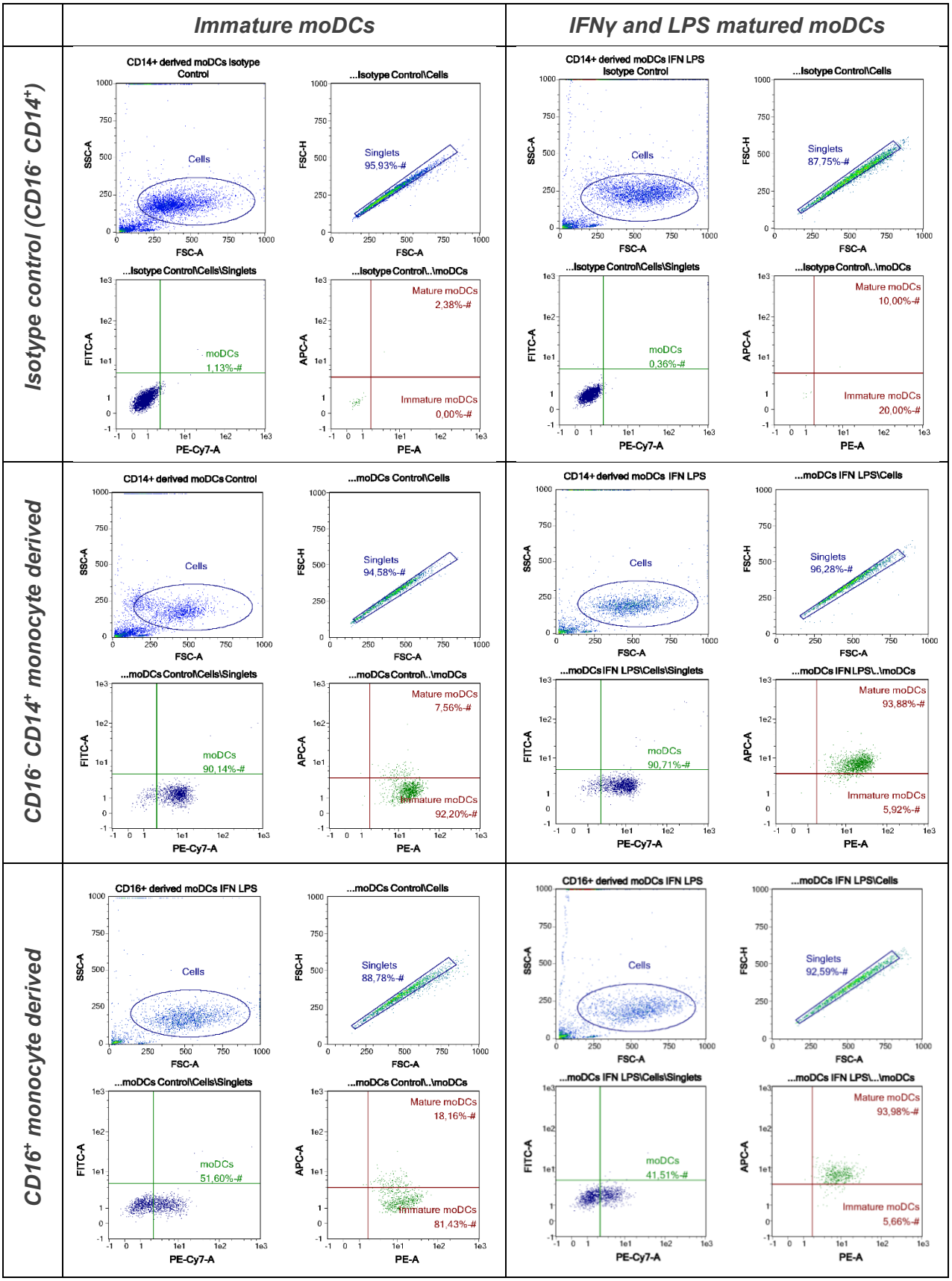
Immature moDCs
IFNγ and LPS matured moDCs
Isotype control (CD16- CD14+)
CD16- CD14+ monocyte derived
CD16+ monocyte derived
CD14+ derived moDCs Isotype Control
...Isotype Control\Cells
Cells
Singlets 95,93%-#
...Isotype Control\Cells\Singlets
moDCs 1,13%-#
...Isotype Control\..\moDCs
Mature moDCs 2,38%-#
Immature moDCs 0,00%-#
CD14+ derived moDCs IFN LPS Isotype Control
Singlets 87,75%-#
moDCs 0,36%-#
Mature moDCs 10,00%-#
Immature moDCs 20,00%-#
CD14+ derived moDCs Control
...moDCs Control\Cells
Singlets 94,58%-#
...moDCs Control\Cells\Singlets
moDCs 90,14%-#
...moDCs Control\..\moDCs
Mature moDCs 7,56%-#
Immature moDCs 92,20%-#
CD14+ derived moDCs IFN LPS
...moDCs IFN LPS\Cells
Singlets 96,28%-#
...moDCs IFN LPS\Cells\Singlets
moDCs 90,71%-#
...moDCs IFN LPS\..\moDCs
Mature moDCs 93,88%-#
Immature moDCs 5,92%-#
CD16+ derived moDCs IFN LPS
Singlets 88,78%-#
...moDCs Control\Cells\Singlets
moDCs 51,60%-#
Mature moDCs 18,16%-#
Immature moDCs 81,43%-#
Singlets 92,59%-#
moDCs 41,51%-#
Mature moDCs 93,98%-#
Immature moDCs 5,66%-#
SSC-A
FSC-A
FSC-H
FITC-A
APC-A
PE-Cy7-A
PE-A

Table 5.3. Flow cytometry analysis of moDCs of a preliminary experiment. Flow cytometry of moDCs by moDC inspector containing antibodies: CD14-FITC, CD209-PE and CD83-APC. moDCs are $CD14^{-}CD209^{+}CD83^{-}$, and once they mature, they become $CD14^{-}CD209^{+}CD83^{+}$. Due to the cell number limitations of CD16+ moDCs, the isotopic control was performed in the more abundant $CD16^{-}$CD14+ moDCs both in the immature, and, IFNγ and LPS matured conditions

Expression of *IL22RA2* in monocyte subpopulations was addressed following the methodology explained in Materials and Methods, section 4.4.2.3, Isolation of monocyte subpopulations (MACS and FACS). The sorted monocyte subpopulations were used for different purposes. The majority of the monocytes were used gene expression analysis experiments, and the remaining monocytes were used for immunocytochemistry.

It is important to remember how relatively rare intermediate ($CD14^{++}CD16^{+}$) and non-classical ($CD14^{+}CD16^{+}$) monocytes are. While classical monocytes ($CD14^{++}CD16^{-}$) account for more than 90% of the monocytes, the minority populations are around or below 5% each. That meant that we needed a starting sample of at least 400 M PBMCs from buffy coat of one donor, as described hereafter. Since monocytes are about 10% of PBMCs, after pan monocyte isolation, we obtained about 40 M monocytes. Those 40 M monocyte needed to be stained with fluorescently marked anti-CD16 and anti-CD14 mAb, and then, sorted in the flow cytometer in a process that could take up to 8 hours, to purify between 1 to 2 M intermediate or non-classical monocytes (5% of the total monocytes). Our sorter, FACSJazz (BD Biosciences), could only sort two populations at the time, which implied discarding more than 34 M classical monocytes while sorting the minority intermediate and non-classical populations in each experiment. Moreover, freshly isolated monocytes are mainly constituted of nucleus and they have low RNA, which required a minimum of 1 M cells to have enough RNA to perform gene expression analysis.

In this experiment, we analyzed *IL22RA2v1* and *v2* using variant-specific primers as well as global *IL22RA2* mRNA levels by BC primers. The qPCR analysis showed (Figure 5.14) that intermediate ($CD14^{++}CD16^{+}$) monocytes produced significantly higher *IL22RA2* levels than the

classical and non-classical monocytes. Non-classical monocytes *IL22RA2* expression levels were lower than those in the intermediate ones that also produced higher levels than the classical monocytes. Regarding the variants expression, all three monocyte types expressed similar ratios of *IL22RA2v1* vs. *IL22RA2v2* mRNA, with *IL22RA2v2* 5 to 10 times higher expression than *IL22RA2v1*. That was in line with our previous results (sections 5.1.1.1, and 5.1.1.2) where the ratios of the variants are similar even if the expression levels are different depending on the condition.

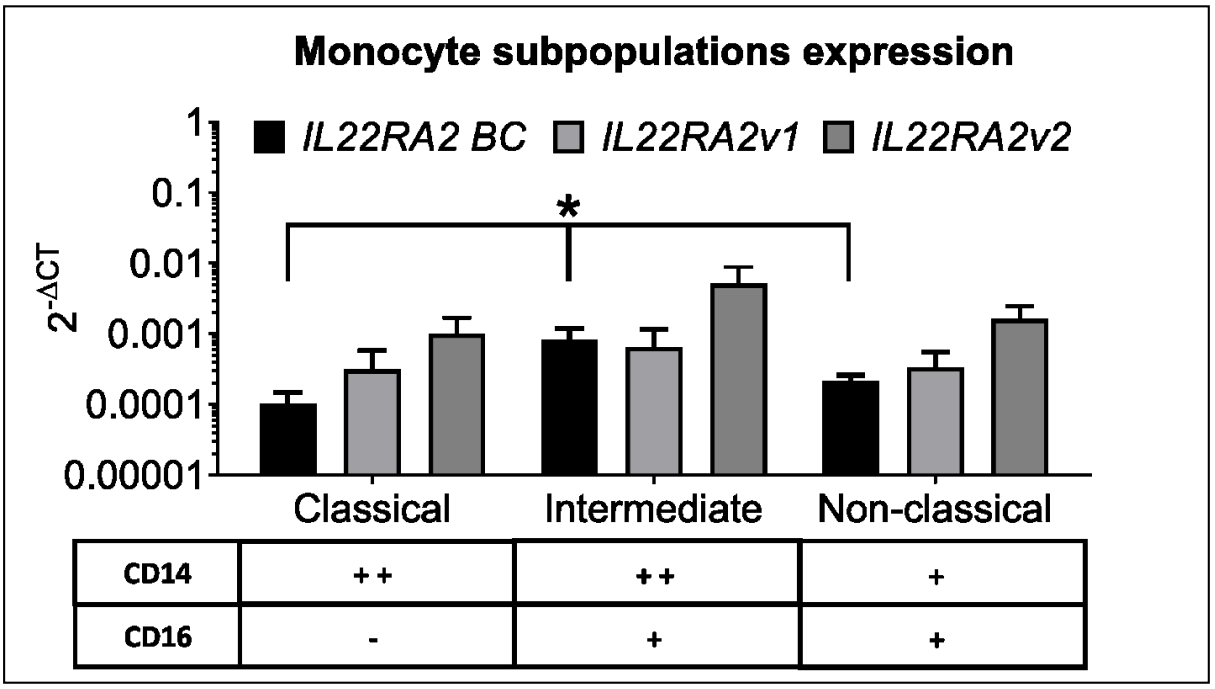

Figure 5.14. Gene expression of *IL22RA2* in monocyte subpopulations. *IL22RA2* gene's expression was addressed for all the variants (*IL22RA2* BC) or for specific variants (*IL22RA2v1* and *IL22RA2v2*). Bottom table describes CD14 and CD16 expression in each monocyte population. Mean ± SEM relative to the housekeeping gene GAPDH. *p < 0.05, Kruskal-Wallis test for comparison of differences in *IL22RA2* BC mRNA levels.

Monocytes of each subpopulations were also stained for IL-22BP using immunocytochemistry. As seen in Figure 5.12, monocytes have small cytoplasm; however, we were able to discriminate IL-22BP positive monocytes by immunofluorescence microscopy. The results of the quantification of the positive cells in more than 100 monocyte of each subpopulation

in three biological replicates confirmed gene expression data. Intermediate monocytes showed the highest IL-22BP positivity, followed by non-classical and with classical monocytes clearly below (Figure 5.14). Altogether, we demonstrated that monocyte subpopulations show different *IL22RA2* and IL-22BP levels.

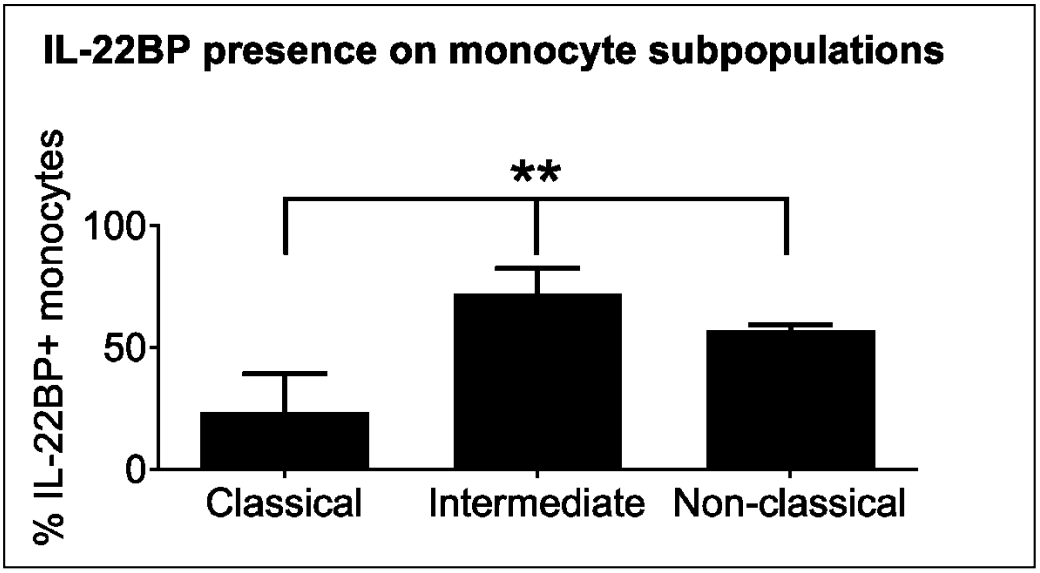

Figure 5.15. Percentage of IL-22BP positive cells of monocyte subpopulations. Different monocyte subpopulations were staining with anti-IL-22BP for confocal microscopy. Mean ± SEM. **p < 0.005, by one-way ANOVA.

5.1.1.5. Different monocyte subpopulations derived moDCs express similar *IL22RA2* levels

The first experiment comparing $CD16^+$ and $CD16^-CD14^+$ moDCs, raised the question to see if different monocyte subpopulations moDCs would show different *IL22RA2* expression levels. The intrinsic difficulty for getting large numbers of different subpopulations of monocytes described in the previous section, made it important to carefully design and perform the experiments. The starting number of cells for moDCs culture was between 0.4 to 1 M cells, but thanks to the differentiation effect on the cells, which results in the increase in cytoplasm, size and RNA content of the cells, it was possible to extract RNA from a lower number of cells. The

monocyte culture was performed as described, culturing the cells in DM for 6 days, adding fresh medium in day 3 of culture. The generated moDCs were analyzed by flow cytometry to assess their characteristics (Table 5.4). Non-classical derived moDCs showed extensive cell death in line with a previous report (Boyette et al., 2017), with no staining by moDC inspector antibodies and therefore hey were excluded from further analysis.

The analysis of the *IL22RA2* expression in monocyte subpopulation derived DCs (Figure 5.16), showed that the discrete difference earlier found between $CD16^+$ and $CD16^-CD14^+$ moDCs (Figure 5.13) disappeared when repeating the experiment with additional biological replicates (three in this case). The similarity in total *IL22RA2*, and variants *IL22RA2v1* and IL22RAv2 expression levels, between classical and intermediate moDCs, suggests that under the same culture conditions, i.e. in the presence of GM-CSF and IL-4, expression of the *IL22RA2* gene is regulated identically. This is distinct from the apparently discrete *IL22RA2* expression regulation mechanisms yielding very different mRNA levels as observed in the original monocyte subsets (Figure 5.14).

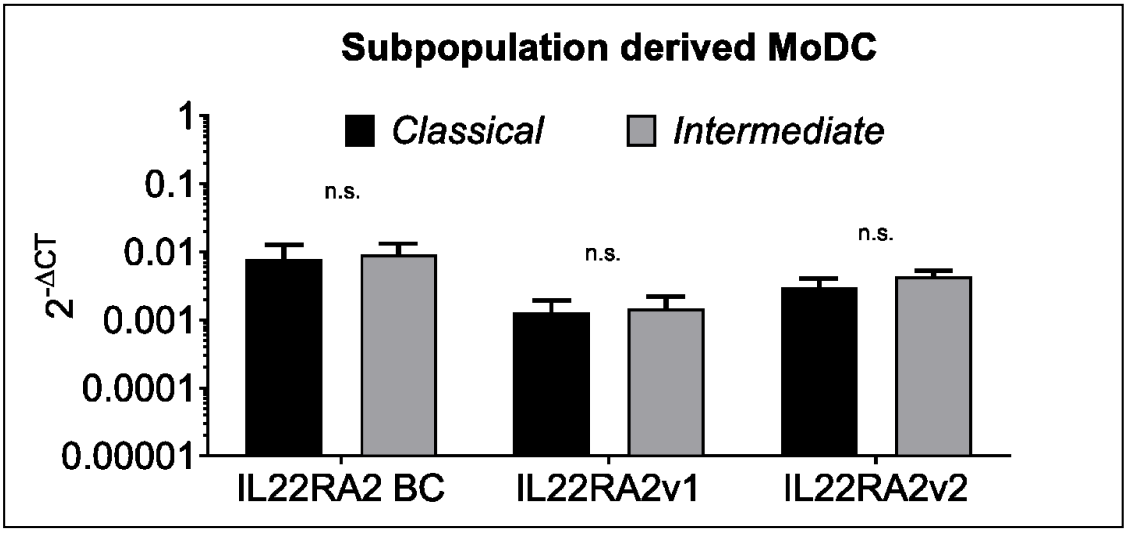

Figure 5.16. Gene expression of *IL22RA2* in monocytes subpopulations derived moDCs. Gene expression of overall and variant-specific *IL22RA2* in classical and intermediate monocytes differentiated to moDCs. Mean ± SEM relative to the housekeeping gene GAPDH, n.s., non-significant by t-test.

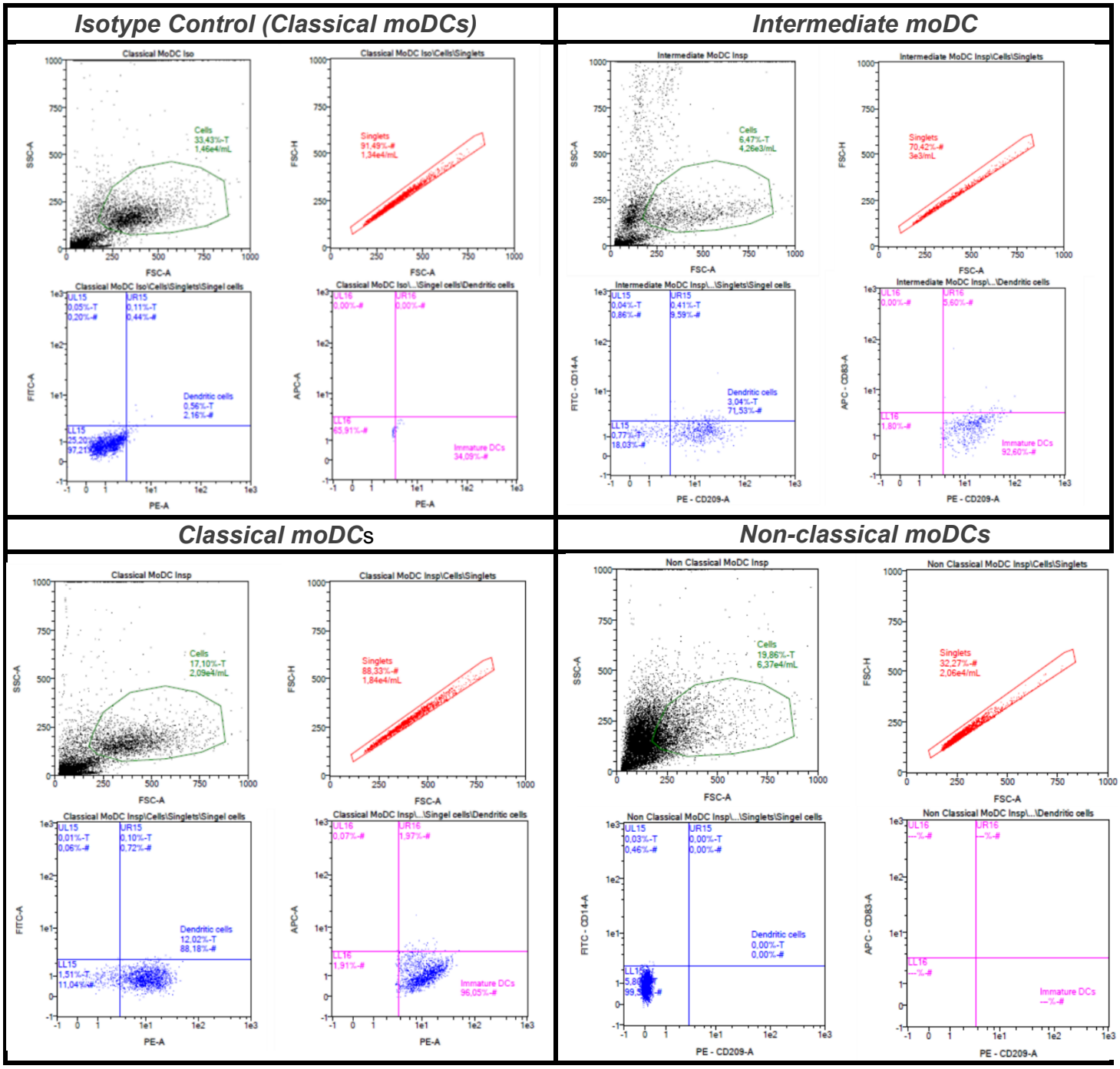

Table 5.4. Flow cytometry analysis of monocyte subpopulations derived moDCs. Flow cytometry of moDCs by moDC inspector containing antibodies: CD14-FITC, CD209-PE and CD83-APC. moDCs are $CD14^{-}CD209^{+}CD83^{-}$, and once they mature, they become $CD14^{-}CD209^{+}CD83^{+}$. Due to the cell number limitations, the isotype control was performed in the more abundant classical moDCs. 90% of the cells were the characteristic immature moDCs for classical and intermediate moDCs. Non-classical derived moDCs showed extensive cell death in line with a previous report (Boyette et al., 2017), with no staining by moDCs inspector antibodies and therefore hey were excluded from further analysis.

5.1.2. IL-22BP secretion

In order to understand *IL22RA2* expression and IL-22BP secretion by monocytes during the differentiation process to moDCs, and the impact of maturation stimuli on them, an experiment with large number of cells set. Monocytes from two different donors (n=2) were isolated by magnetic separation using $CD14^+$ microbeads and different time points were addressed:

- Day 0. freshly isolated monocytes.
- Day 2, 4 and 6 of culture monocytes in DM.
- Day 5 moDCs overnight primed with IFNγ (500 pg/mL) and stimulated with LPS on day 6 with LPS (200 ng/mL) for 12, 24 and 48 hours, or left unstimulated.
- Day 10 of culture in DM.

Cells at all the stages were checked by flow cytometry using moDC inspector. Differentiation of monocytes after 2, 4, 6 and 10 days of culture in DM confirmed the expected $CD14^-CD209^+$ profile with the isotype control guaranteeing the specificity of the staining (Table 5.5). Regarding the maturation state ($CD83^+$ cells) of the moDCs, results show that the spontaneous maturation is below 2% during the differentiation, until day 6, when cells are fully differentiated, and the levels are lower than 8%. From there we can observe that there is an increase in day 10 when the observed spontaneous maturation is around 33% (Table 5.5.). Regarding the maturation time points and their time equivalent controls (Table 5.6), there was a clear maturation induction ($CD83^+$ cells), with the mature moDCs under 16% in the untreated moDCs and over 80% in the IFN_Y and LPS treated cells (summarized in Figure 5.17). After ensuring the phenotypical expression of surface markers, and before analyzing their IL-22BP content, the *IL22RA2* expression was address by qPCR to ensure the previously observed expression levels of *IL22RA2*. The expected upregulation during differentiation and downregulation after treatment was observed (Figure 5.18).

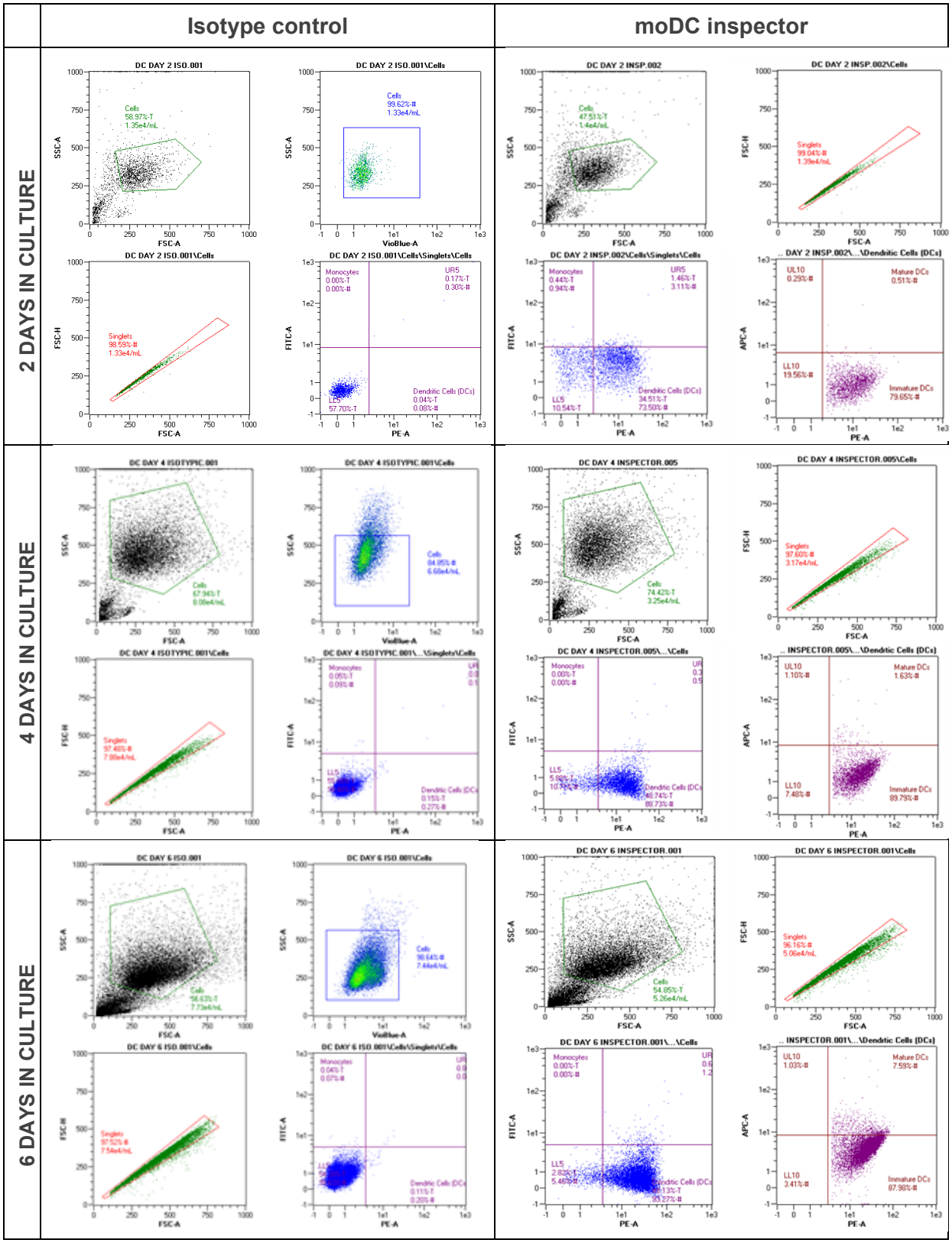
Isotype control
moDC inspector
2 DAYS IN CULTURE
4 DAYS IN CULTURE
6 DAYS IN CULTURE
DC DAY 2 ISO.001
DC DAY 2 ISO.001\Cells
DC DAY 2 ISO.001\Cells\Singlets\Cells
DC DAY 2 INSP.002
DC DAY 2 INSP.002\Cells
DC DAY 2 INSP.002\Cells\Singlets\Cells
DC DAY 4 ISOTYPIC.001
DC DAY 4 ISOTYPIC.001\Cells
DC DAY 4 INSPECTOR.005
DC DAY 4 INSPECTOR.005\Cells
DC DAY 6 ISO.001
DC DAY 6 ISO.001\Cells
DC DAY 6 INSPECTOR.001
DC DAY 6 INSPECTOR.001\Cells
SSC-A
FSC-A
FSC-H
VioBlue-A
FITC-A
PE-A
APC-A

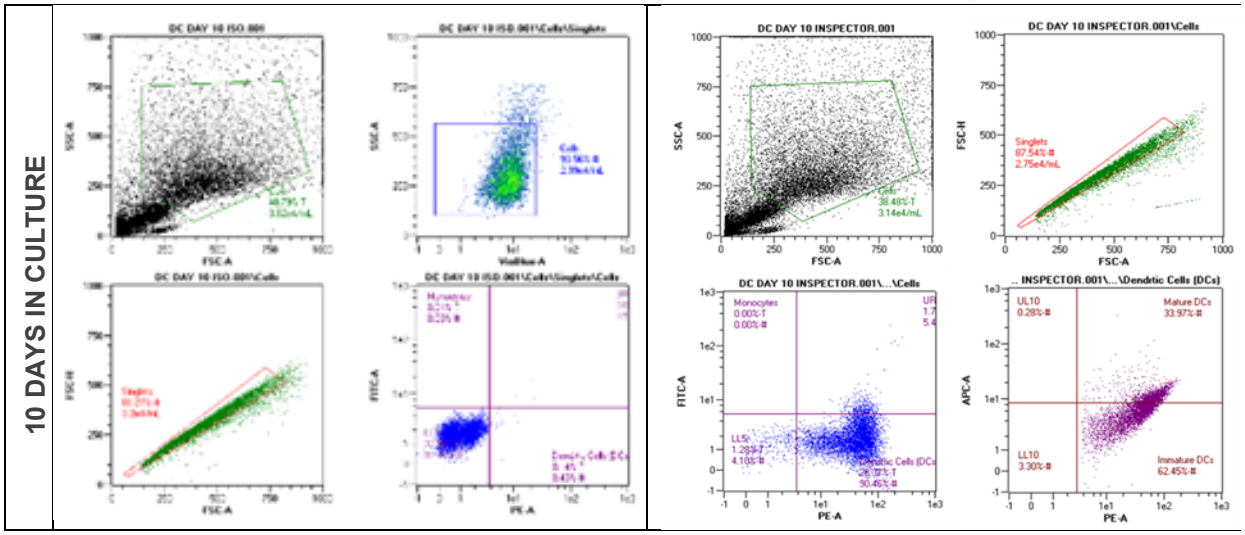

Table 5.5. Flow cytometry analysis of the moDCs time course. Flow cytometry of moDCs by moDC inspector containing antibodies: CD14-FITC, CD209-PE and CD83-APC. moDCs are $CD14^{-}CD209^{+}CD83^{-}$ and once they mature, they become $CD14^{-}CD209^{+}CD83^{+}$. Isotype control on all the samples.

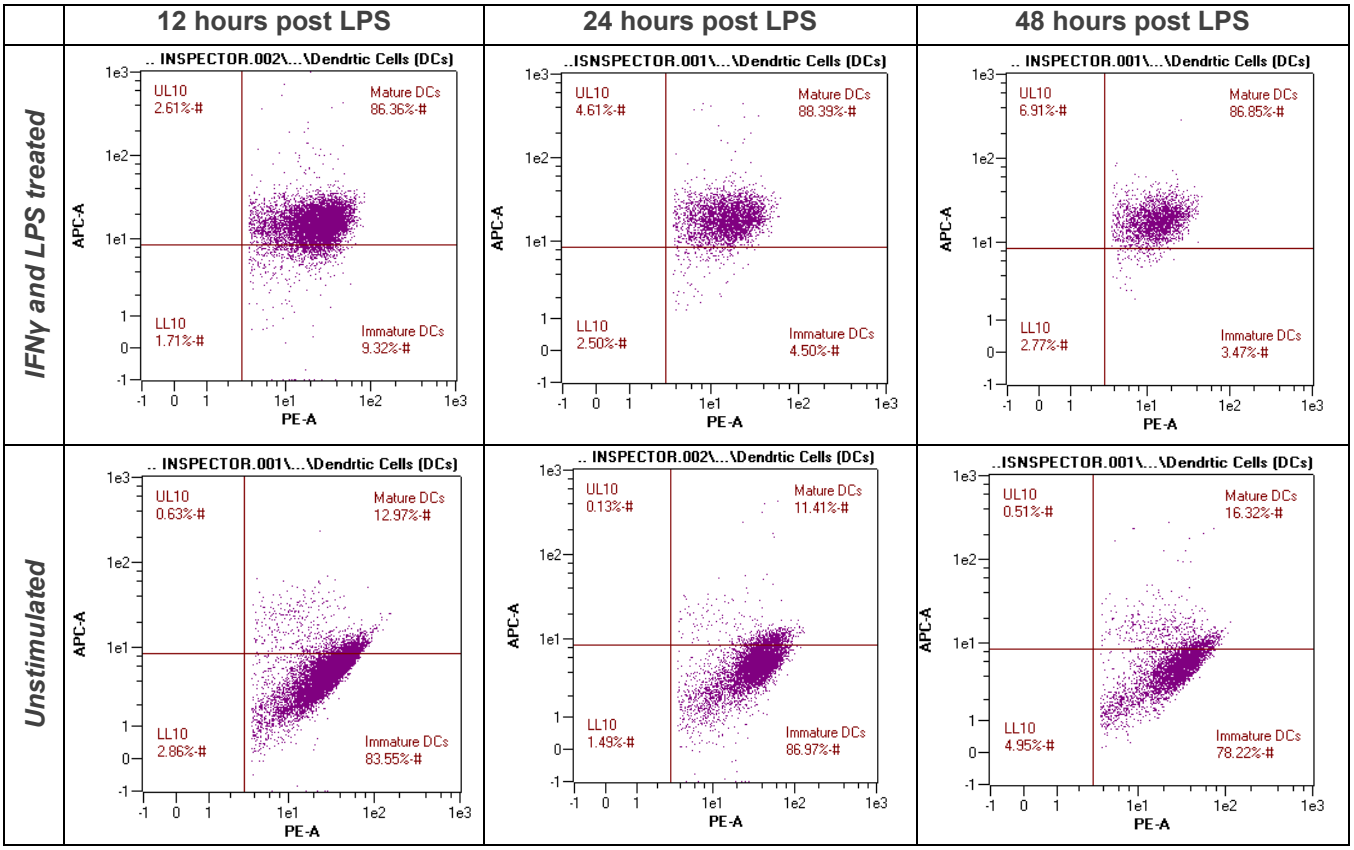

Table 5.6. Flow cytometry analysis of the maturation status of moDCs. Flow cytometry of moDCs by moDC inspector; for simplification purposes isotype control, and full gating strategy is not shown but was the same of Table 5.5. matured moDCs are $CD14^{-}CD209^{+}CD83^{+}$..The average of the maturation of the

moDCs ($CD14^{-}CD209^{+}CD83^{+}$) of the two experiments in the different time points is represented in Figure 5.17, and it shows that control cells did not mature (even if there was a slowly increasing self-maturation over time) while cells stimulated with IFN_{γ} and LPS showed strong maturation ($CD209^{+}CD83^{+}$).

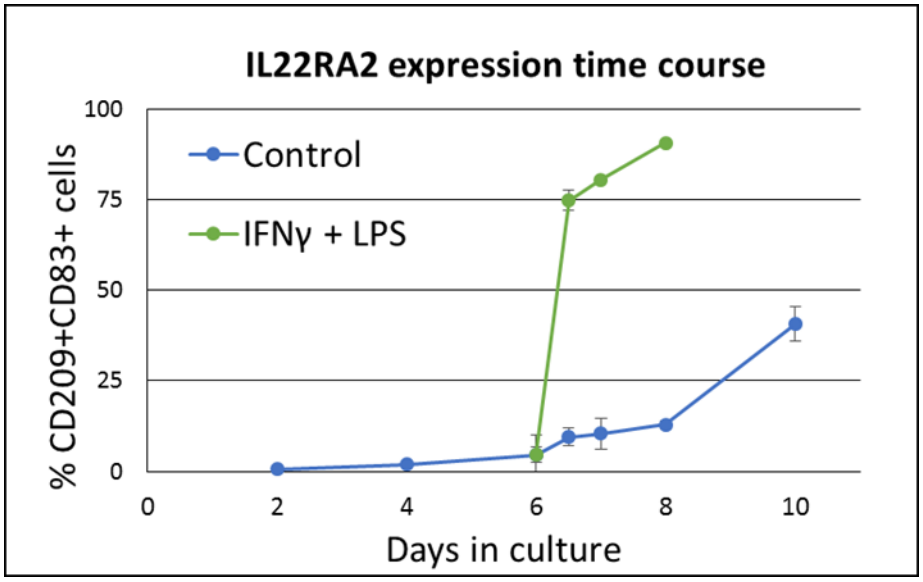

Figure 5.17. Percentage of mature moDCs measured by flow cytometry. Control: untreated moDCs; IFNγ + LPS: moDCs with overnight priming with IFNγ (500 pg/mL) and then treated with LPS (200 ng/mL) for 12, 24 and 48 hours.

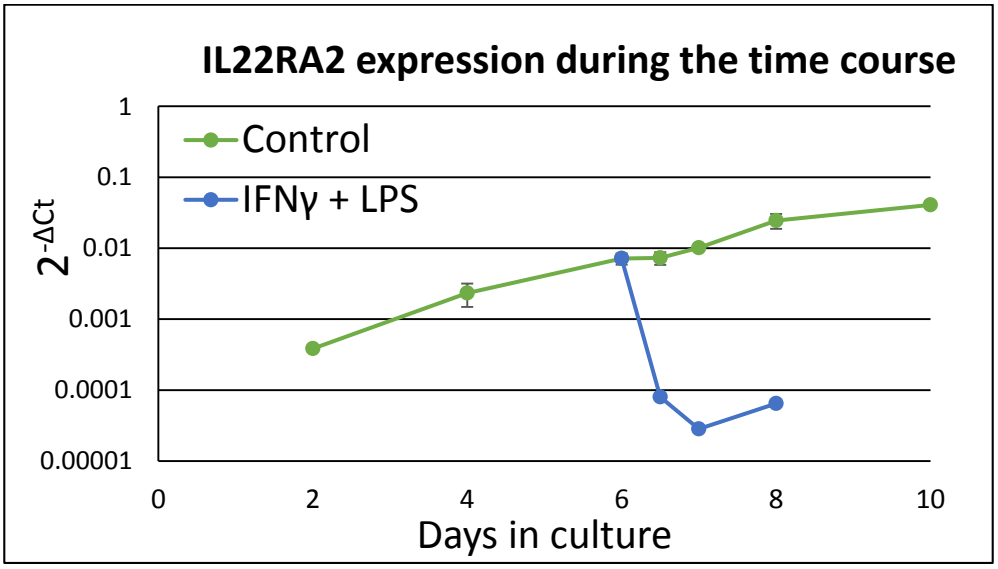

Figure 5.18. Gene expression of *IL22RA2* during the time course. moDC time course analyzed by RT-qPCR. Mean ± SEM relative to the housekeeping gene ACTB. Control: untreated moDCs; IFNγ + LPS: moDCs with overnight priming with IFNγ (500 pg/mL) and then treated with LPS (200 ng/mL) for 12, 24 and 48 hours.

Once the moDC markers and *IL22RA2* expression were established, cell lysates and the medium of the samples were analyzed by WB and ELISA respectively to detect IL-22BP. Immunoblotting with the monoclonal antibody against IL-22BP showed its absence in the cells lysates monocytes and an increase during differentiation (Figure 5.20) that remained stable over the duration of the experiment. The ELISA assay showed that, even there is a considerable *IL22RA2* mRNA upregulation, there is only a modest reflection of IL-22BP level increase in the culture medium (Figure 5.21). The lack of difference in IL-22BP levels with regard to the maturation time points, where there was low expression of *IL22RA2*, suggests that IL-22BP has stability for 48 hours. Taken together, the results open the possibility for complex regulation mechanisms in posttranscriptional level, at the point of translation, folding or secretion of the protein governing its secretion and degradation. Neither the WB nor the ELISA analysis were able to resolved the individual IL-22BP isoforms, and therefore, we used recombinant expression vectors transfected into HEK293 cells to gain more insight into the mechanisms governing the secretion of IL-22BPi1, 2 and 3 isoforms.

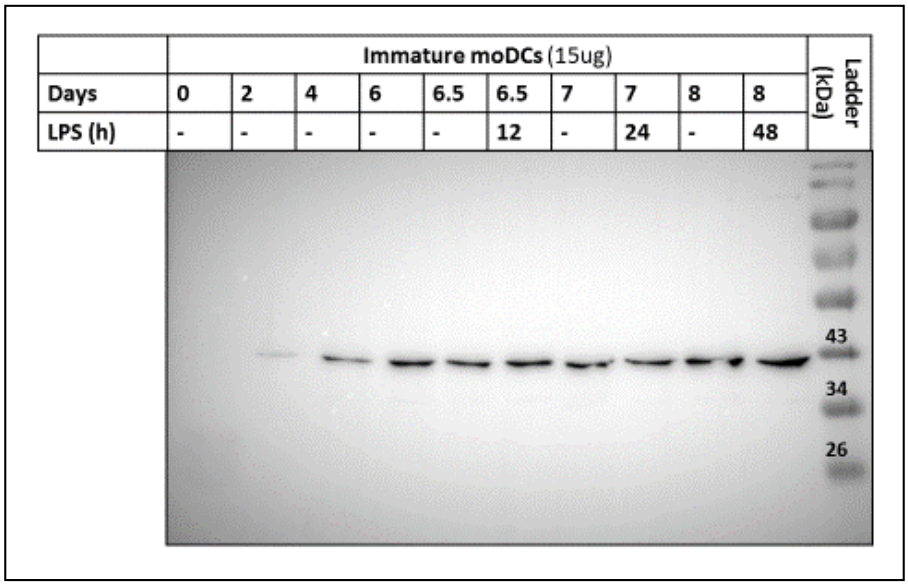

Figure 5.19. IL-22BP immunoblotting on moDC cell lysates. WB analysis with mous mAb against IL-22BP in all the analyzed time points of the moDC time course. As it can be observed IL-22BP is intracellularly accumulated during the time course and remains present even in cells treated with LPS.

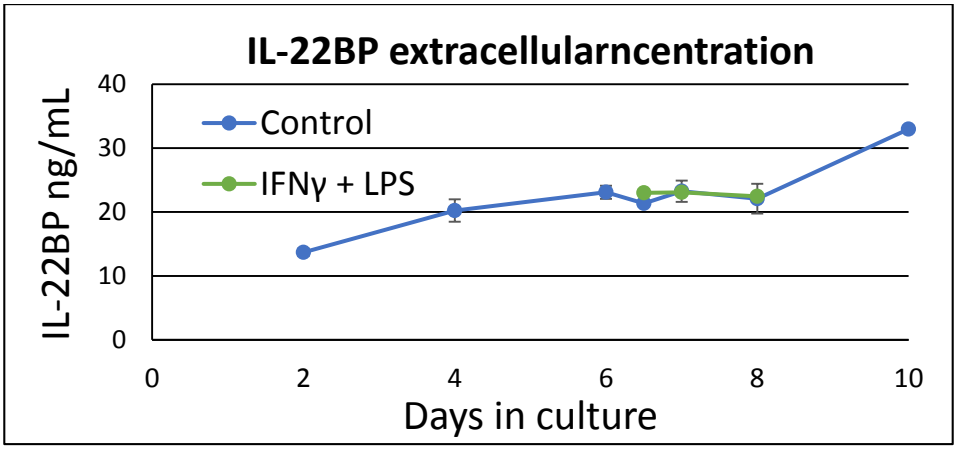

Figure 5.20. IL-22BP concentration in moDC medium. In-house designed ELISA measurement on the medium of the moDCs' time course points. Mean ± SEM. Control: untreated moDCs; IFNγ + LPS: moDCs primed with IFNγ and then treated with LPS for the 12, 24 and 48 hours.

5.1.2.1. IL-22BP isoforms secretion

5.1.2.1.1. IL-22BPi1 is poorly secreted and it is retained in the ER

For the understanding of production, storage and secretion of IL-22BP isoforms (IL-22BPi1 (BPi1), IL-22BPi2 (BPi2), and IL-22BPi3 (BPi3)), C-terminally Myc and FLAG-tagged expression plasmids were individually transfected into HEK293 cells. In order to find the subcellular location of the isoforms, immunofluorescence microscopy experiments were performed using ER and Golgi apparatus proteins as markers.

The ER is the site of synthesis of proteins destined for the cell surface or secretion (Otero et al., 2010). We used a specific antibody for staining ERp72 protein as ER marker. In line with that, in order to stain the Golgi apparatus, we selected and antibody against trans-Golgi apparatus protein, TGLON2. We cultured HEK293 cells, transfected independently with each isoform and fixed them 24 hour after the transfection. Cells were stained against IL-22BP with a goat biotinylated polyclonal antibody linked to an Alexa 488 fluorescent protein (A488) conjugated

streptavidin (in green).The markers, ER or Golgi, were detected by an anti-Rabbit secondary antibody conjugated with Alexa 647 fluorescent protein (A647).

The results of the co-staining of the different IL-22BP isoforms and ERp72 (Figure 5.21) showed that IL-22BPi1 formed a perinuclear diffuse granular staining pattern highly colocalizing with the ER marker while IL-22BPi2 and IL-22BPi3 showed a majority of the staining accumulated in densely stained deposits in one side of the nucleus, and only less intense signal with the diffuse pattern. In line with them, the co-staining of IL-22BP and TGLON2 (Golgi marker; Figure 5.22) showed the same IL-22BP staining than previously observed, but in this case, the BPi2 and BPi3 accumulation points that colocalized with TGOLN2 while the diffuse pattern of BPi1 was not. These data suggested that BPi2 and BPi3 were efficiently exported from ER to the Golgi apparatus but BPi1 was predominantly retained within the ER.

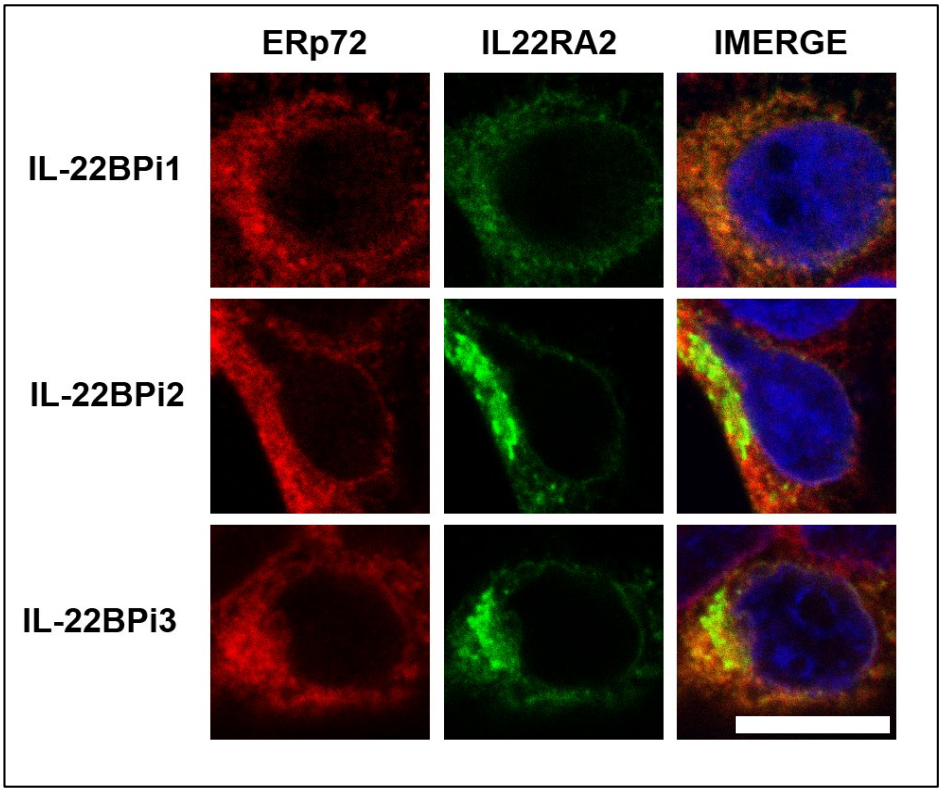

Figure 5.21. HEK293 cells transfected with IL-22BP isoforms stained with A488 (green), the ER marker ERp72 in A647 (red) and counterstained with DAPI. Figure representative of three different experiments. Scale bar: 10 μm. Figure representative of three different experiments.

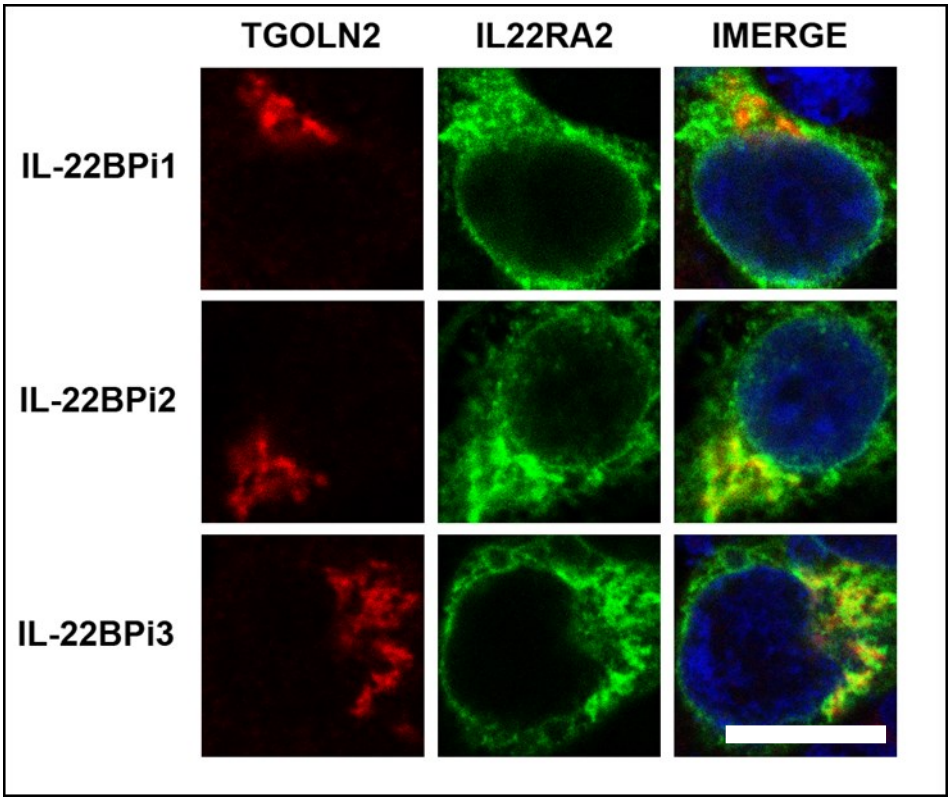

Figure 5.22. HEK293 cells transfected with IL-22BP isoforms stained with A488 (green), the Golgi apparatus marker TGOLN2 in A647 (red) and counterstained with DAPI. Figure representative of three different experiments. Scale bar: 10 μm. Figure representative of three different experiments.

Further experiments (Gómez-Fernández et al., 2018) were performed that confirm the microscopy observations. In those experiments, using transfected 293HEK cells, intracellular concentration of the individual isoforms was assessed by WB and the corresponding secreted protein levels by ELISA. The results showed detection of intracellular levels of IL-22BP1, but not of the other two isoforms. Regarding the secretion of the isoforms, high levels of IL-22BPi2 secretion were measured while those of BPi1 and BPi3 were much lower. An explanation for the IL-22BPi3 low secreted levels may have been a lower stability over time; however, other possibilities cannot be discarded.

5.1.2.1.2. Exon 4 of IL-22BPi1 is sufficient to retain an otherwise secreted cytokine in the ER

The only difference between IL-22BPi2, that is properly secreted, and the poorly secreted IL-22BPi1, is the presence of an extra 32-AA stretch code by an alternatively spliced exon 4. In order to determine that the presence of the exon was the cause of poor secretion, we cloned the sequence of exon 4 into IL-2, which is an efficiently secreted protein, as explained in Materials and Methods, section 4.3.2. (Insertion of *IL22RA2* exon4 into other cytokines expression vectors) exon4 was inserted in *XbaI* restriction site maintaining the original reading frame.

The first experiment consisted of comparing the newly generated IL-2 $^{+}$ Exon 4 (IL-2EX4) protein with the original IL-2. Comparison was performed in the intracellular levels (cell Lysate, CL), the culture medium (CM) and the culture medium concentrated by acetone precipitation (AP) by Western Blot using an anti-FLAG antibody. The results (Figure 5.23) showed that, as expected, IL-2 was secreted: little detection intracellularly in the CL, detection extracellularly in the CM, and strong increase after concentration of the medium by AP. On the contrary, IL-2EX4 was no detected in the CM, nor in the more concentrated AP, discarding its secretion while it was strongly detected in the CL. Taken together exon 4 sequence is sufficient to retain intracellularly an otherwise secreted IL-2.

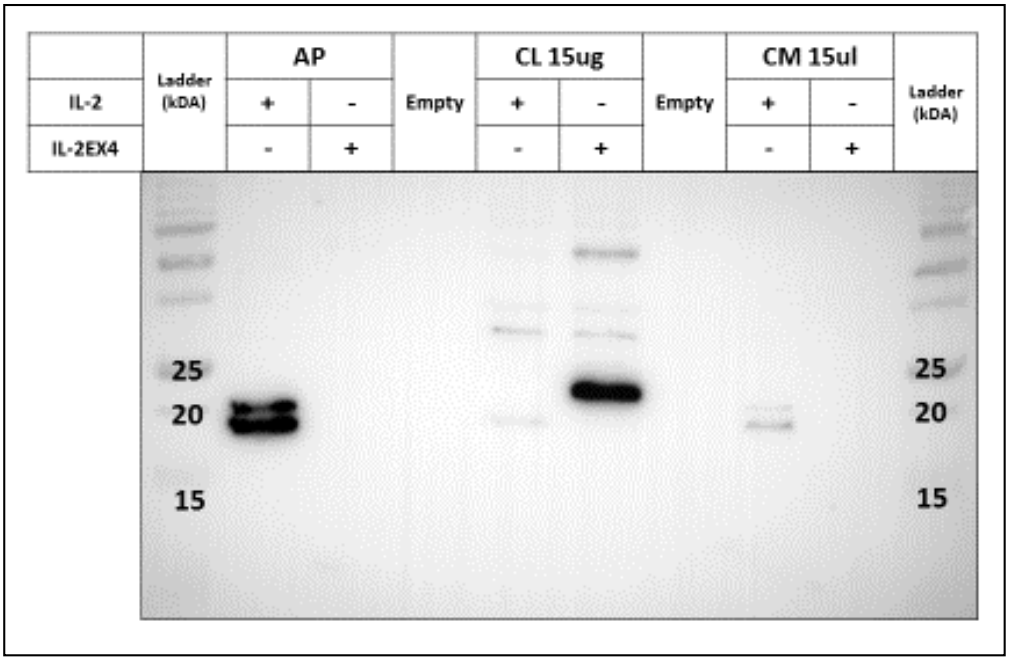

Figure 5.23. Immunoblot comparing IL-2 and IL-2EX4 using anti-FLAG antibody. IL-2 is the detected band below 20 kDa weight (corresponding with the 16 kDa plus weight the tags present in the expression vector: Myc (1,2 kDa) and FLAG (1 kDa)). IL-2EX4 is, due to the addition of the exon 4 sequence, detected between 20 and 25 kDa. Figure representative of three different experiments.

5.1.2.1.3. IL-22BP SP replacement with the one of IL-17 increases intracellular and secreted IL-22BP levels

The interest for the SP of IL-22BP came both from the observed low levels of secretion when we compared with other cytokines (Gómez-Fernández et al., 2018) and from a SNP identified in our lab (Vandenbroeck, 2012). The identified SNP was an infrequent functional variant in exon 2 of *IL22RA2* (rs28385692) that substitutes the Leucine AA for a Proline at position 16 of the protein, in the SP. The association between this SNP and MS was validated among different cohorts and the logistic regression analysis showed that associations of rs28385692 and the main *IL22RA2* GWAS SNP, rs17066096, with MS might be statistically independent (Gómez-Fernández et al., 2020).

An in silico analysis using digital tools like Phobius, suggested that the Pro16 variant renders import of the precursor IL-22BP isoforms into the ER less efficiently. To experimentally verify the effect of this variant on the secretion of the coded protein, site-directed mutagenesis to change Leu16 to Pro in the SP of the three wild-type IL-22BP isoforms cloned in expression vectors was performed. HEK293 cells were individually transfected, and both intracellular and secreted levels of IL-22BPi1, IL-22BPi2 and IL-22BPi3 were measured by ELISA. Compared to Leu16, Pro16 strongly decreased the secreted levels of each isoform (Gómez-Fernández et al., 2020).

To understand of the effect of the native SP of IL-22BPi2 in its secretion, the SP was replaced by the one of IL-17 as described in Materials and Methods, section 4.3.1 (*IL22RA2* with IL-17A SP in pCMV6-Entry vector). IL-17 is an efficiently secreted protein that was compared with native IL-22BPi2 and IL-22BPi2 with IL-17 SP (IL-17SP_IL-22BPi2). The SP replacement resulted in much higher levels of both intracellular and secreted IL-22BPi2 measured by WB (Figure 5.24). The results suggested that the IL-22BP SP is less efficient than that of IL-17 and may affect overall IL-22BP biogenesis. In line with that, there is growing evidence indicating that SP sequences contain information that specifies the choice of targeting pathway, the efficiency of translocation, the timing of cleavage and even post-cleavage functions (Hegde & Bernstein, 2006).

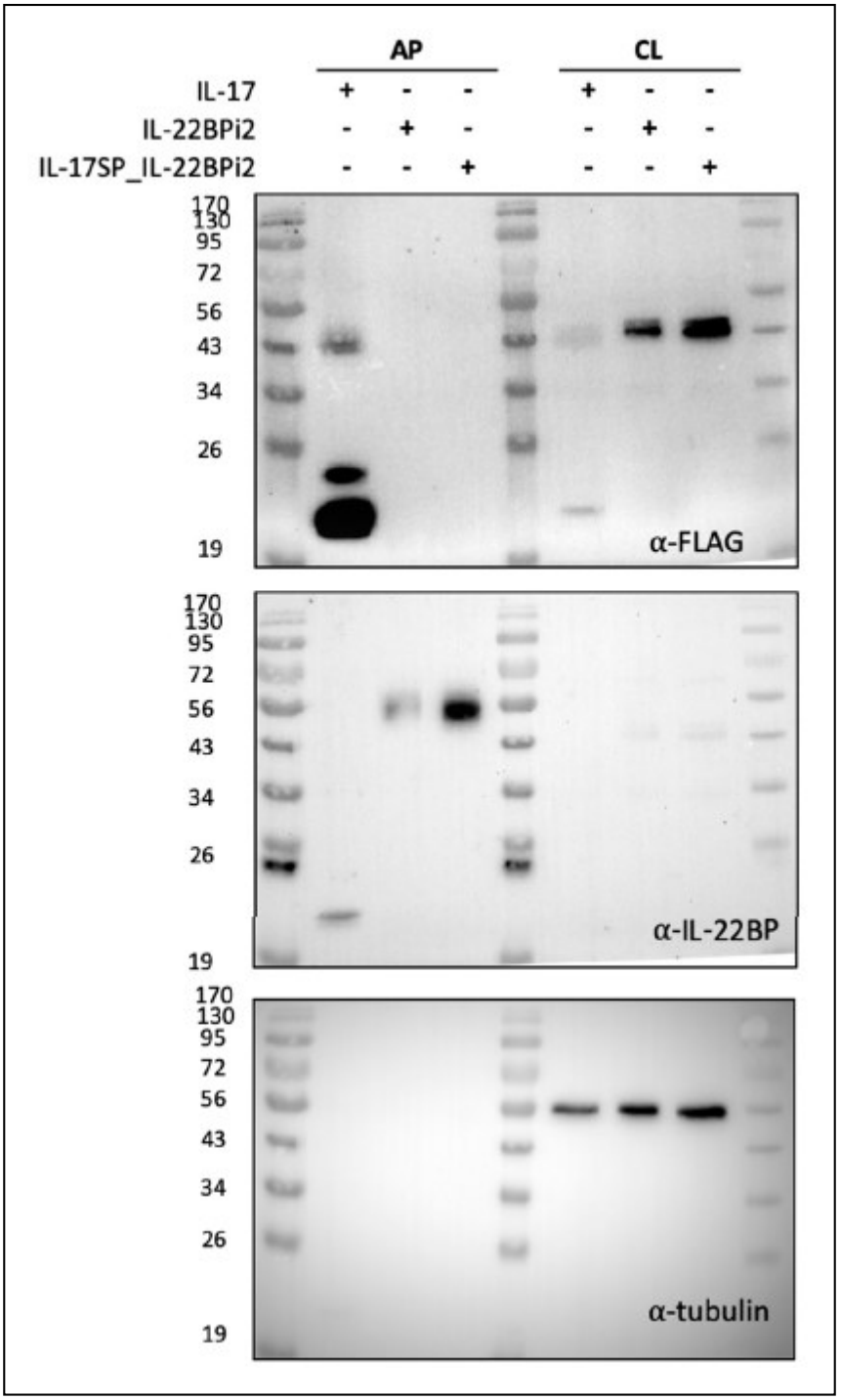

Figure 5.24. Immunobloting of IL-17SP_IL-22BPi2 construct. HEK293 cells were transfected for 24 hours with either IL-17, IL-22BPi2 or IL-17SP_IL-22BPi2. Intracellular content was analyzed in the CL and the secretion was measured using the medium was concentrated by AP. IL-17 has a 17 kDa weight but is detected above 19 kDa because of the Myc and FLAG tags. IL-22BPi2 has a 48 kDa weight but when secreted increases to 56 kDa due to complex N-glycosylation. Anti-FLAG antibody was able to detect the

three expression vectors intracellularly because all of them had the FLAG tag. As seen in the Figure, IL-17 was much more strongly detected in the AP than in the CL due to its high secretion efficiency. IL-22BPi2 containing expression vectors were only detected intracellularly, due N-glycosylation masking FLAG epitope, and therefore, anti-IL-22BPi2 mAb detecting the native conformation of the protein was able to detect the secreted forms of IL-22BP. As seen in the Figure, IL-17SP_IL-22BPi2 construct showed increased detection both intra- and extracellularly showing that. Anti-Tubulin was used as a loading control, to ensure that the protein amount of the cell lysates was equivalent. Figure representative of three different experiments.

5.1.2.1.4. Co-transfection of IL-22BPi2 with IL-22BPi1 or IL-2EX4 does not induce IL-22BPi2 secretion

Previous results provided evidence that IL-22BPi1 and IL-22BPi2 are client proteins and interact with identical domains of, GRP78 and GRP94 (two ER resident proteins that assist the conformational folding or unfolding of proteins, generally referred as chaperones), but IL-22BPi1 binds more strongly to them and it is accumulated intracellularly inside ER, as seen by immunofluorescence co-localization with ERp72. It was tested whether the expression of IL-22BPi1 activated the unfolded protein response (UPR), a transcriptional program to maintain ER homeostasis (Hetz, 2012), that is activated in response to accumulation of misfolded proteins in the ER. Experiments in HEK293 cells showed that IL-22BPi1 and IL-2EX4, but no IL-22BPi2, BPi3 or IL-2, induced expression of typical UPR genes including *GRP78*, *GRP94* and *ERp44* (Gómez-Fernández et al., 2018). Cell lysates revealed that protein levels of GRP78 and GRP94 were also increased in cells only transfected with IL-22BPi1 or IL-2EX4 after 24h and the UPR activation was confirmed by enhance splicing of XBP1 in the cells (Gómez-Fernández et al., 2018).

Given the observation that ectopic expression of GRP78 enhances secretion of both IL-22BPi2 and BPi1 (Gómez-Fernández et al., 2018) we analyzed whether co-transfection of IL-22BPi2 with IL-22BPi1 or IL-2EX4, may enhance secretion of IL-22BPi2 secondary to UPR induction of GRP78 by IL-22BPi1 or IL-2EX4. Different ratios of co-expression of IL-22BPi2 with

BPi1 or IL-2EX4 were analyzed in an experiment with two biological replicates. Transfection was done using a total quantity of 1 µg of vector, so we used EV to keep always the same total quantity in all the conditions. We used two transfection controls: one with the protein of study (IL-2, IL-2EX4 or BPi1) without BPi2, the negative control, and another with the maximum amount of BPi2 without the protein of study. Among the samples used at different concentrations, IL-2 worked also as control since it did not was not expected alter IL-22BPi2 secretion (Gómez-Fernández et al., 2018). IL-2EX4 was used to see if the exon alone was sufficient to induce any difference on IL-22BPi2 secretion, and IL-22BP1, been the naturally co-expressed protein was the protein of more interest (Table 5.7).

Quantity (µg)	Negative control	Positive control	Dilution			
			"1/1"	"1/5"	"1/15"	"1/50"
EV	0.5	0.5	0	0.4	0.47	0.49
IL-22BPi2	0	0.5	0.5	0.5	0.5	0.5
IL-2 / IL-2EX4 / IL-22BPi1	0.5	0	0.5	0.1	0.03	0.01
TOTAL	1	1	1	1	1	1

Table 5.7. Plasmid quantity for cotransfection experiment. EV = empty vector.

The ELISA analysis results (Figure 5.25) showed that all three co-transfected vectors with IL-22BPi2 worked similarly. In the negative control (cotransfection with EV instead of IL-22BPi2) there was no detection of IL-22BP on the samples of IL-2 and IL-2EX4 and only very low amount for IL-22BPi1. The positive control showed high levels in all three cases and 1:1 transfection ratio reduced secretion of IL-22BPi2 measure in ELISA, while at smaller ration approached those see in the natural produced cells at best a non-significant trend toward enhanced secretion of immunoreactive protein was observed. Altogether, we did not found any indication that the co-transfection of IL-22BPi2 with IL-22BPi1 or IL-2EX4 induces IL-22BPi2 secretion.

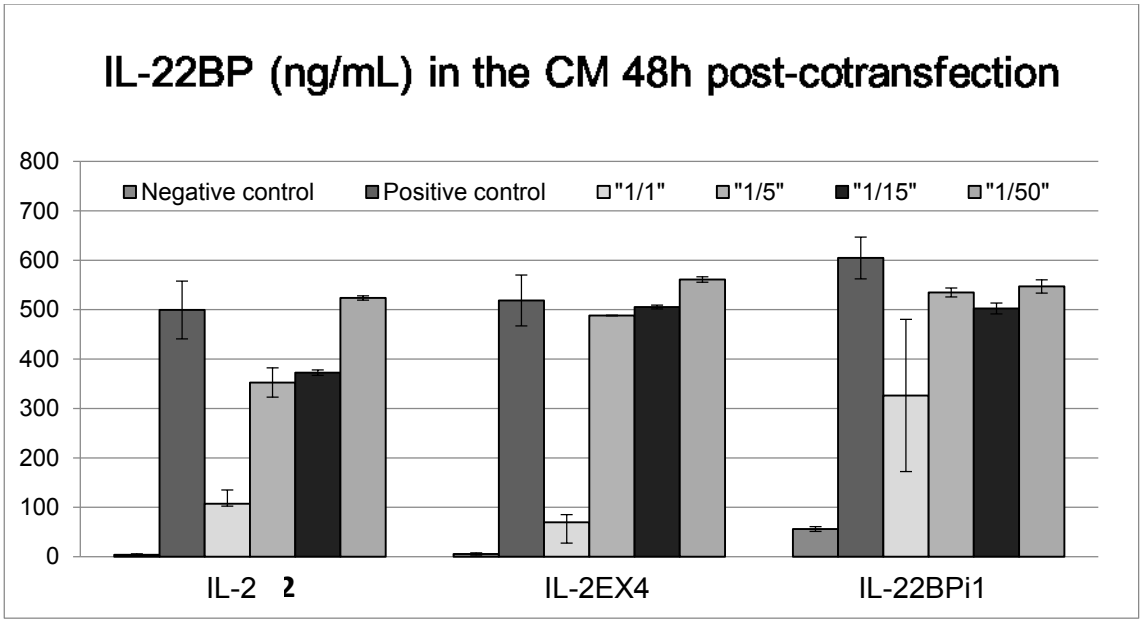

Figure 5.25. IL-22BP secretion on the cotransfection experiment. IL-22BP concentration (ng/mL) in the cell culture medium was measured by the in-house designed ELISA. Contransfection conditions are summarized in Table 5.7. Any contransfection condition was higher than the positive control, a similar trend was observed with IL-2, IL-2EX4 and IL-22BPi1 discardin any sequence especific effect. Mean ± SEM (n=2).

5.1.2.2. GRP78

5.1.2.2.1. GRP78 is the main interacting ER element of Exon 4

In order to identify the proteinaceous factors that may be responsible for the intracellular retention of IL-22BP1 and IL-2EX4, we analyzed the interactome of IL-2EX4, and the one of IL-2 as control, in HEK293 cell by liquid chromatography-mass spectrometry (LC MS/MS). For doing so, HEK293 cells were transfected with IL-2 or IL-2EX4 expression vectors. The cell lysates of the IL-2 or IL-2EX4 transfected cells were immnoprecipitated using FLAG resin. To obtain the best condition for IP, two different lysis buffers (based on Triton X-100 or RIPA) with and without crosslinking agent (DSP) were tested.

To ensure that both transfection and IP worked properly a WB was performed (Figure 5.26). A CL of the IL-2EX4 transfected cells lysed with Triton X-100 containing lysis buffer (right line of the ladder) was used as positive control for the IP elution (E) products. The positive controls signal was much lower because it have not been concentrated during a purification process. Even IL-2 was detected among all the conditions, IL-2EX4 was much higher, a result that was expected given that IL-2 is efficiently secreted and therefore it has a lower intracellular concentration to start with. All together, the WB showed that that the samples have been properly transfected and immnoprecipitated regardless of the lysis buffer and DSP.

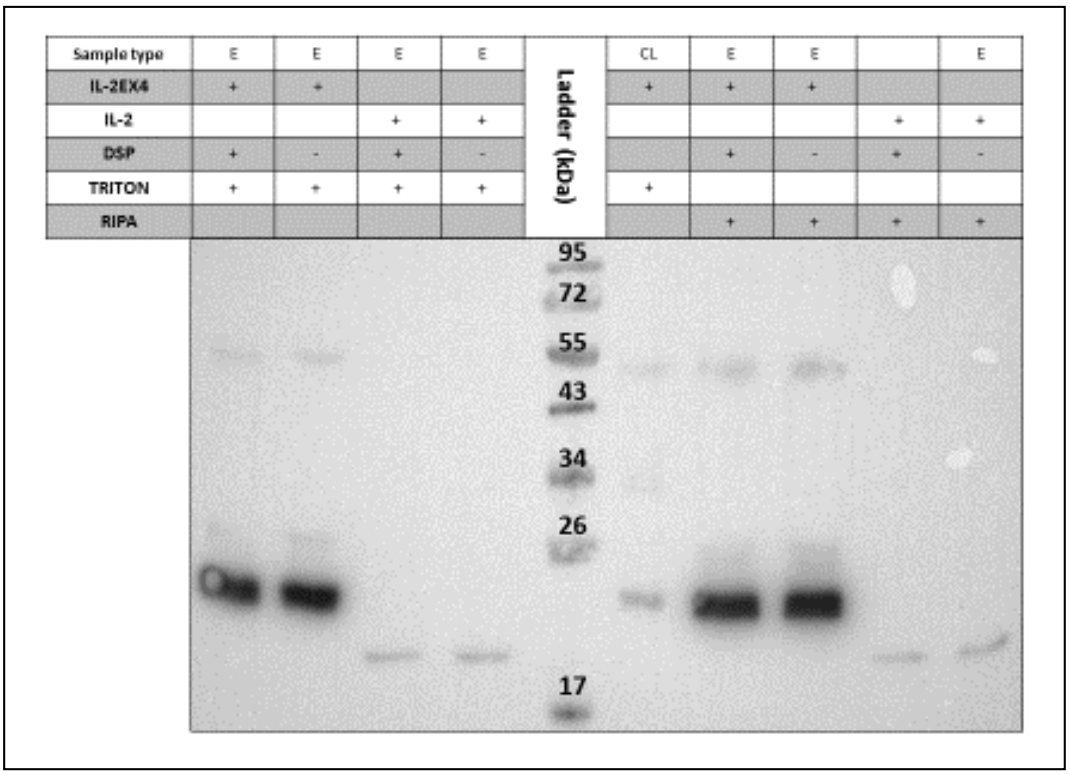

Figure 5.26. Immunoblot of IL-2 and IL-2EX4 co-IP. Detection was performed using anti-FLAG antibody, as explained in Figure 5.23 IL-2 is the detected at 20 kDa weight and-2EX4 little higher, between 20 and 25 kDa. Samples were loaded grouped by lysis buffer. The positive control (IL-2EX4 transfected CL in Triton X-100) is in the right line of the ladder. IL-2 detection is lower due to a lower starting intracellular quantity. Both lysis buffers (Triton X.100 and RIPA) performed similarly. E: eluted product of co-IP; CL: cell Lysate; IL-2EX4: transfection with homonymous vector; IL-2: transfection with the homonymous vector; DPS: cross-linking agent; Triton: Triton X—100-based lysis buffer; RIPA: RIPA based lysis buffer. Figure representative of three different experiments.

Once it was assured that the transfection and purification worked properly a silver staining was performed to detect the interacting proteins (Figure 4.47). The silver stained gel showed more clear results with Triton X-100 buffer (lanes 1 to 4) than with RIPA buffer (lanes 5 to 8). Among Triton X-100 buffer lysed cells; there was a clear band just above 72 kDa, specific of IL-2EX4 transfected conditions, regardless of DSP (lane 1 and 3 vs. lane 2 and 4). The purification and analysis of that band by LC MS/MS revealed that it corresponded to GRP78 (Table 4.5).

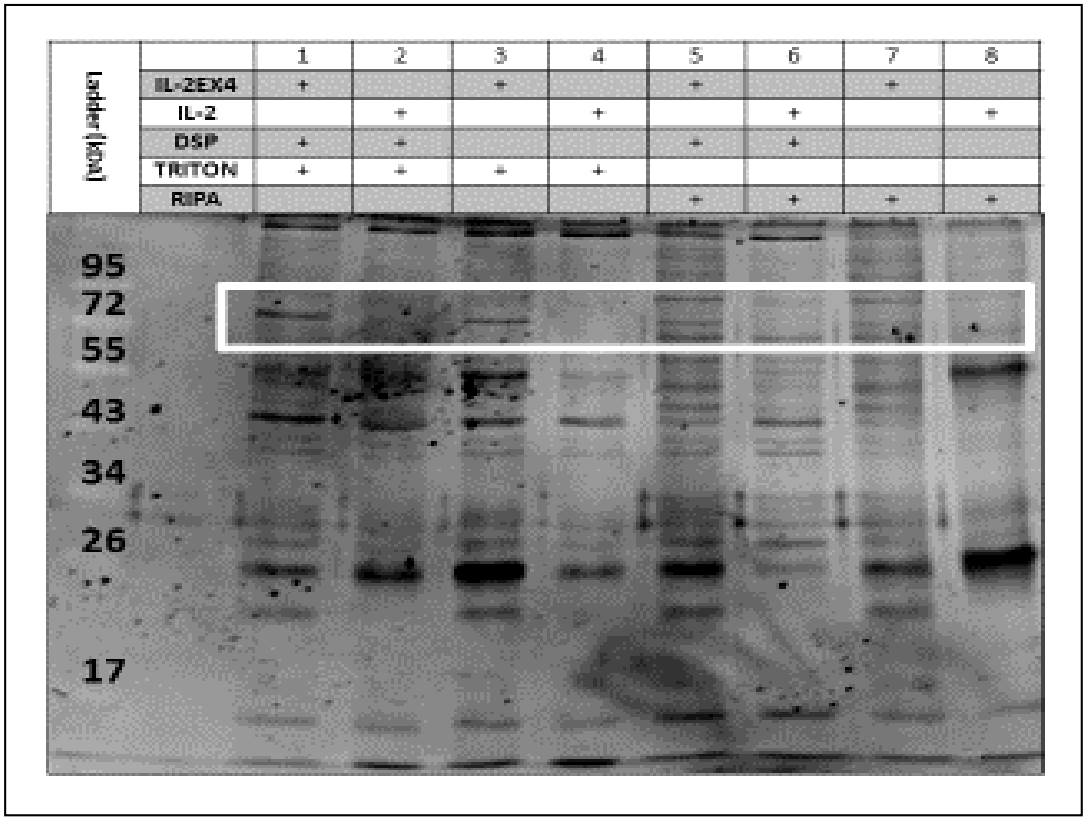

Figure 5.27. Silver staining results of IP. The white rectangle shows the selected bands at around 72kDa specific for IL-2EX4 transfections.

Accession	Description	Score	Coverage	Proteins	Unique Peptides	Peptides	#PSMs	#AAs	MW [kDa]
P11021	78 kDa glucose-regulated protein OS=Homo sapiens GN=HSPA5 PE=1 SV=2 - [GRP78_HUMAN]	915.99	39.30	395	19	21	21	654	72.3

Table 5.8. Highest-ranking score of the silver stained band characterization by LC MS/MS.

5.1.2.2.2. IL-22BPi1 and IL-22BPi2 bind to the SBD of GRP78

GRP78 is an ER luminal HSP70-type chaperone that binds newly synthesized proteins during translocation into the ER (Otero et al., 2010), and contains two functional domains, a nucleotide-binding domain (NBD) that binds ATP, and a SBD that binds to incompletely folded client proteins (Figure 5.28).

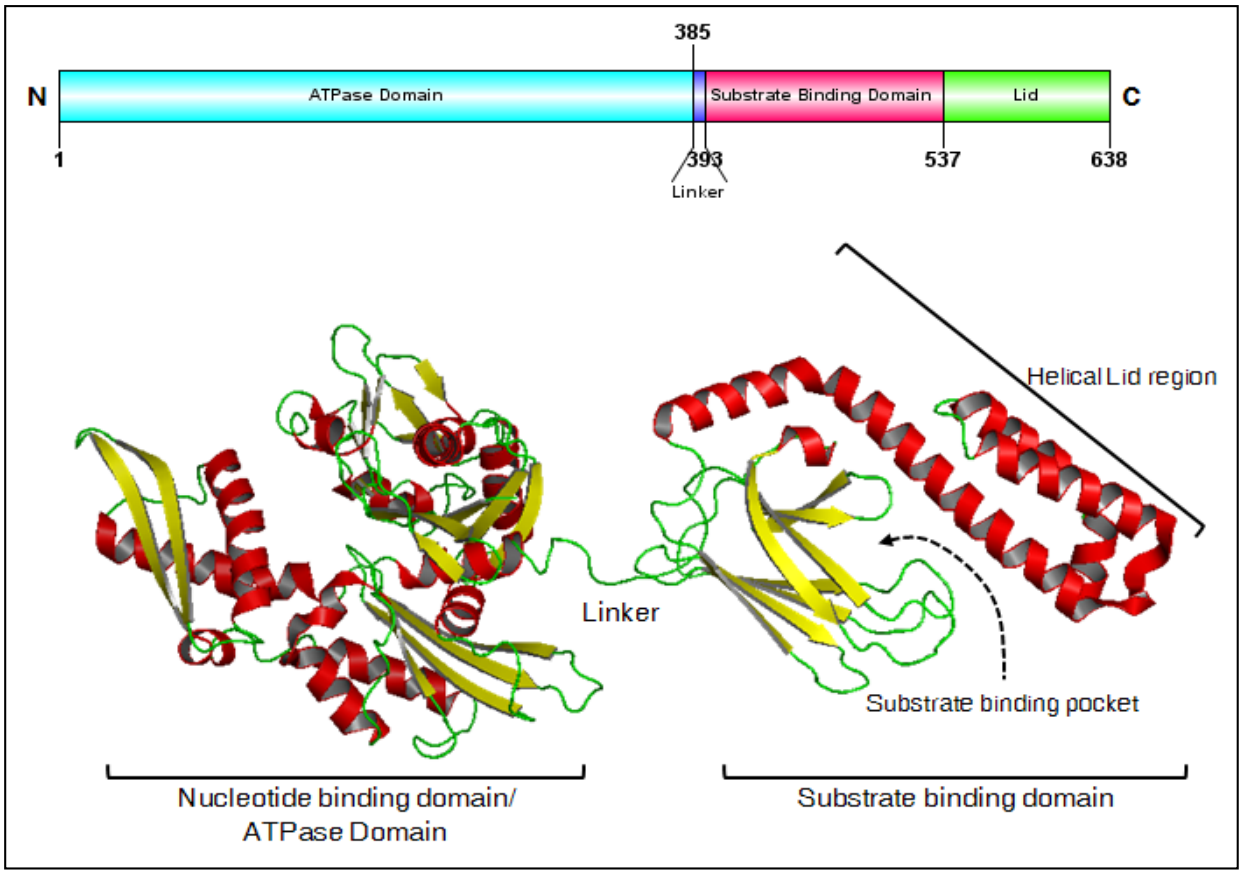

Figure 5.28. Structure and domain organization of Hsp70 family chaperones. Source: (R. et al., 2012)

A member of a family of cytotoxins described in Shiga toxigenic Escherichia coli (Paton et al., 2004), subtilase cytotoxine (SubAB), is able to cleave GRP78 (72kDa) into 44-kDa and 28-kDa fragments. The cleavage occurs in the exposed hinge that connects the ATPase domain with the protein-biding domain. The cleavage is specific to GRP78 since purified human Hsp70 and Hsc70 (two members of the Hsp70 family that are the closest homologues of GRP78, and are

identical at 7 of 11 amino-acid positions flanking the cleavage site) are not cleaved by SubAB *in vitro* (Paton et al., 2006).

In line with that, a more recent research study in B cells (Hu et al., 2009) confirmed that the two cleaved fragments corresponded to the N-terminal NBD (-44kDa) and the C-terminal SBD (-28Kda). They observed that GRP78 cleavage by SubAB was never complete. Newly synthesized GRP78 was nearly completely susceptible to cleavage, whereas the cleaved fraction of GRP78 measured at steady state never exceeded 75%. They reported that SubAB cleavage of GRP78 did not lead to a general block of the secretory pathway and that SubAB cleaved GRP78 SBD changes in absence of its regulatory NBD, and this induced locked-in association of the SBD with newly synthesized Ig light chains. Regarding detection, anti-KDEL antibody was able to detect both intact GRP78 and C-terminal SBD fragment, but no N-terminal NBD fragment, which was described as a less stable (Hu et al., 2009). They ability of SubAB to activate all three axes of the UPR signaling pathways (PERK, IRE1 and ATF6 signaling pathways) in mouse macrophages was reported with the ability to inhibit LPS-induced inflammatory response both in vitro and in vivo (Harama et al., 2009). In an study performed in rat cells (Yamazaki et al., 2009), among the three major branches of the UPR, the ATF6 pathway, but not others, was shown to be responsible for activation of the Akt-NF-kB signaling.

In order to find out whether the presence of the extra sequence in IL-22BPi1 influenced the site of GRP78 with which it interacts, we conceive series of experiments using SubAB and mutant SubAB (m-SubAB; unable to cleavage GRP78) provided by James Paton. First, we performed a preliminary time course experiment using of two concentrations (10 or 100 ng/mL) in HEK293 cells. While 10 ng/mL was not enough (Figure 5.29), 3 hours incubation with 100 ng/mL of SubAB was able to induce high cleavage of GRP78 (Figure 5.30). Thereafter, we treated cells with 100 ng/mL SubAB or m-SubAB for 3 hours in all the following experiments.

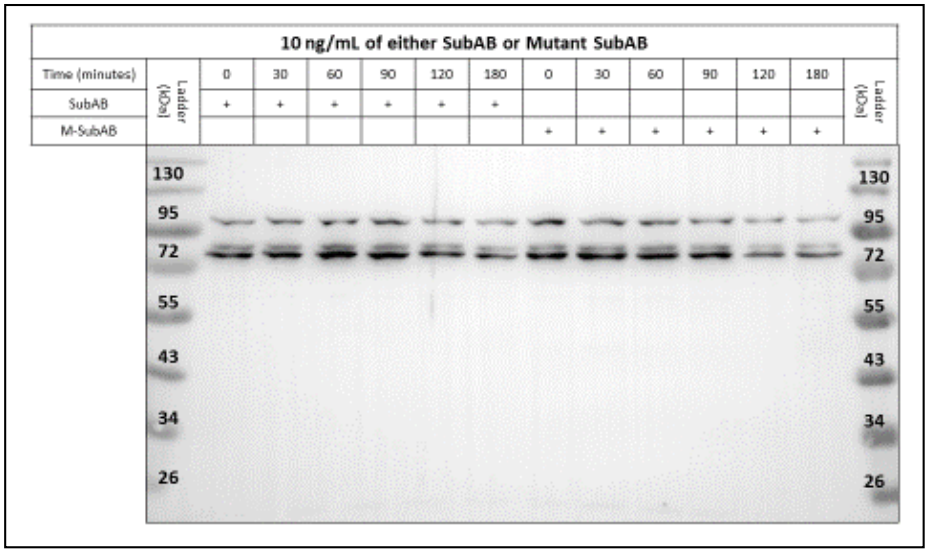

Figure 5.29. SubAB and m-SubAB time course at 10 ng/mL concentration. Immunoblot of the time course of cell lysates of HEK293 cells treated with 10 ng/mL of SubAB or m-SubAB using anti-KDEL antibody. From the anti-KDEL staining it was expected the detection of the uncleaved GRP78 at 78kDa, and that of the C-terminal SBD of the cleaved GRP78 at 28 kDa. While uncleaved GRP78 is detected between 72 and 95 kDa in all the samples, there was no cleavage detection at any time point of the time course of 10 ng /mL concentration of SubAB.

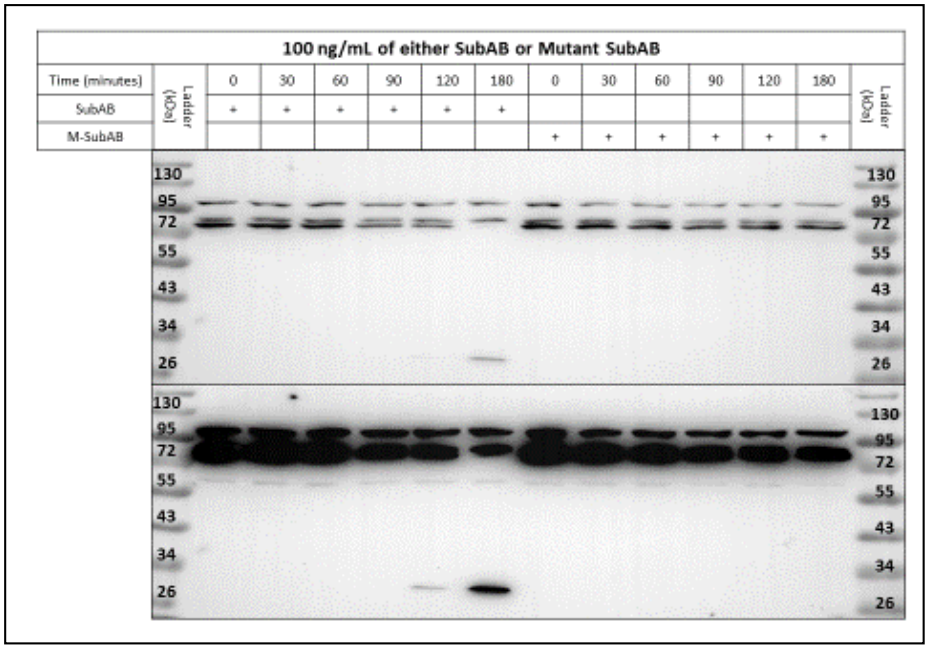

Figure 5.30. SubAB and m-SubAB time course at 100 ng/mL concentration. Immunoblot of the time course of cell lysates of HEK293 cells treated with 100 ng/mL of SubAB or m-SubAB using anti-KDEL antibody. From the anti-KDEL staining it was expected the detection of the uncleaved GRP78 at 78kDa,

and that of the C-terminal SBD of the cleaved GRP78 at 28 kDa. Both images correspond to the same immunoblot, the image below has increased exposure to undercover C-terminal SBD detection. In this case, 100 ng /mL concentration of SubAB was able after 120 minutes to show the cleaved C-terminal SBD, with a notorious reduction of the uncleaved signal at 180 post incubation with SubAB.

Next, we tested the effect of SubAB in all three IL-22BP isoforms and IL-2EX4. For doing so, we designed experiments consisting in co-IPs with and without crosslinking (DSP), using CL as a positive transfection controls in the blots. The relevance of the crosslinking is that it can increase the strength of the detection of the partner proteins.

The first set of experiments was performed on samples without crosslinking. HEK293 cells were transfected with different transfection vectors containing IL-2, IL-2EX4, IL-22BPi1 and IL-22BPi2. The intracellular content of the cells was analyzed in the CL and purified by IP FLAG resin (all the transfected proteins had this tag) to find the interacting partners of the transfected proteins and compare the differences between them.

In each replicated of the experiment, one gel was loaded with cells transfected with IL-22BPi1 and BPi2 and tested with anti-KDEL (Figure 5.31) and anti-FLAG (Figure 5.32) antibodies; another gel was loaded with cells transfected with IL-2EX4 and EV and also tested with anti-KEDL (Figure 5.33) and anti-FLAG (Figure 5.34) antibodies. The CL results showed that the procedure (transfection, SubAB incubation and IP) worked. Regarding the transfection there was a proper detection with FLAG of the transfected protein sequences; the effect of SubAB incubation was confirmed by GRP78 cleavage; and finally the IP showed an increase in the concentrations of the FLAG purified proteins.

Results showed that IL-22BPi1 have bigger intracellular concentration than IL-22BPi2 (Figure 5.32). Regarding the purification, the purification with FLAG showed a strong co-IP of GRP78 (78 kDa band, Figure 5.31) or the cleaved C-terminal SBD domain (28kDa band, Figure 5.31) than IL-22BPi2. GRP78 was present on IL-22BPi2 cell lysates but only a small fraction was

purified along with IL-22BPi2 showing that the interaction is not as strong as in the case of IL-22BPi1. In the case of IL-2EX4 and IL-2 transfected cells, the difference was even more notable. There was no detection of intracellular IL-2 in the CL of IL-2 transfected cells, nor there any purification of it (Figure 5.34). However, there was SubAB effect detectable in the GRP78 staining of the CLs (Figure 5.33). IL-2EX4 transfected cells, in line with what was observed in IL-22BPi1 transfected cells, showed a strong intracellular staining of the transfected proteins and a strong increase in the detection of GRP78, cleaved and uncleaved. The result showed that GRP78 interacts strongly with the exon 4 of IL-22BPi1 present in the sequence of IL-2 of the transfection vector IL-2EX4. However, it is necessary to mention that there was a technical issue, with an unspecific signal detected at 28kDa in all immunoblots revealed with anti-KDEL in all the IPs with m-SubAB that should not have it (Figure 5.31 and 5.33). In order to avoid it we started using affinity-purified Polyclonal Goat antibody for GRP78 (AF4846, R&D Systems). We decided to perform the experiment in crosslinking conditions to strength the interaction of the transfected protein partners, and to analyze IL-22BPi3.

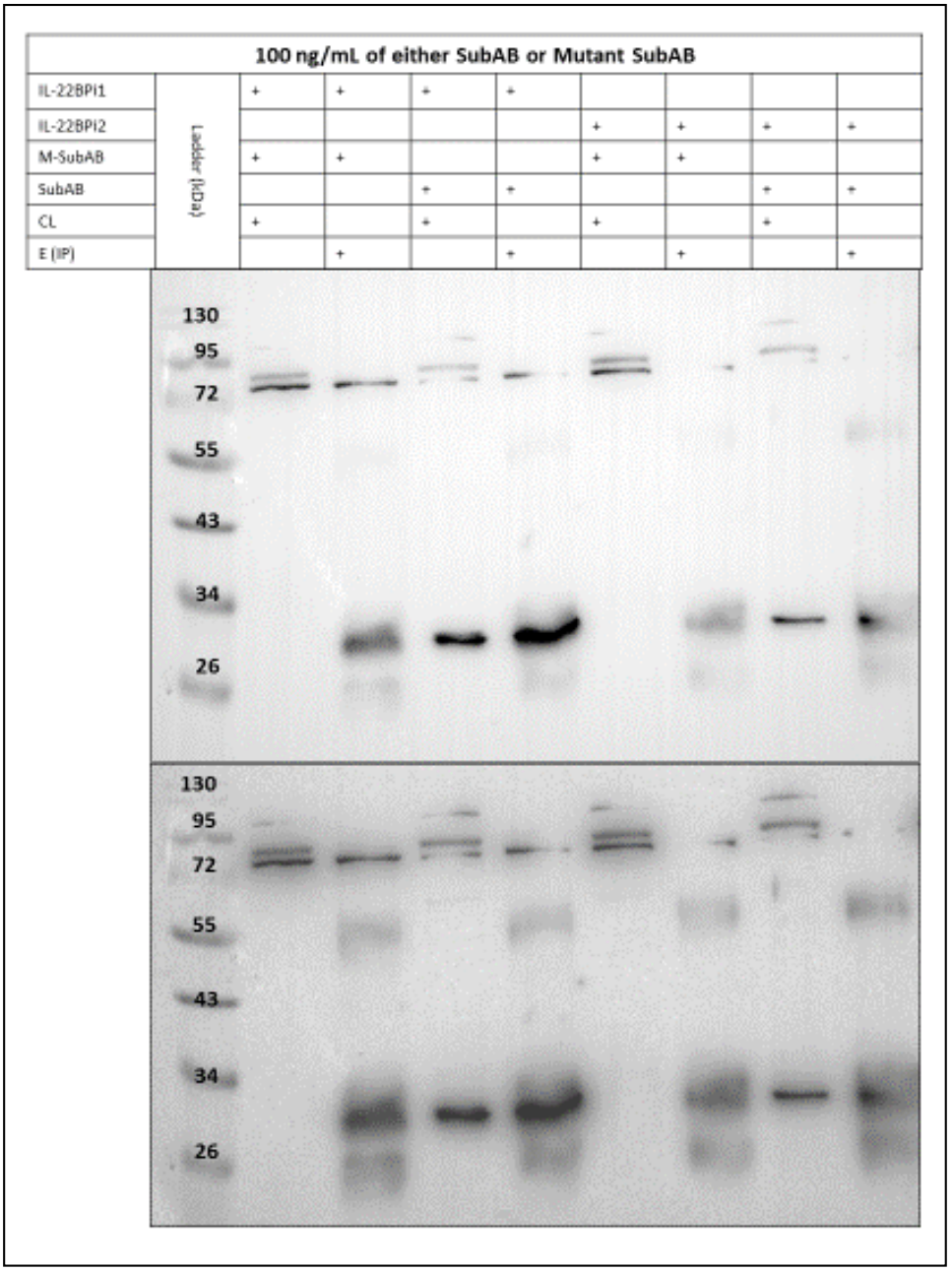

Figure 5.31. SubAB effect on IL-22BPi1 and IL-22BPi2 cells in ER proteins. Immunoblot of cell lysates (CL) and IP elutions (E IP) of IL-22BPi1 and BPi2 transfected HEK293 cells treated with 100 ng/mL of SubAB or m-SubAB using anti-KDEL antibody. From the anti-KDEL staining it was expected the detection of the uncleaved GRP78 at 78kDa, and that of the C-terminal SBD of the cleaved GRP78 at 28 kDa. Both images correspond to the same immunoblot; the image below has increased exposure to undercover faint detection. Figure representative of three different experiments.

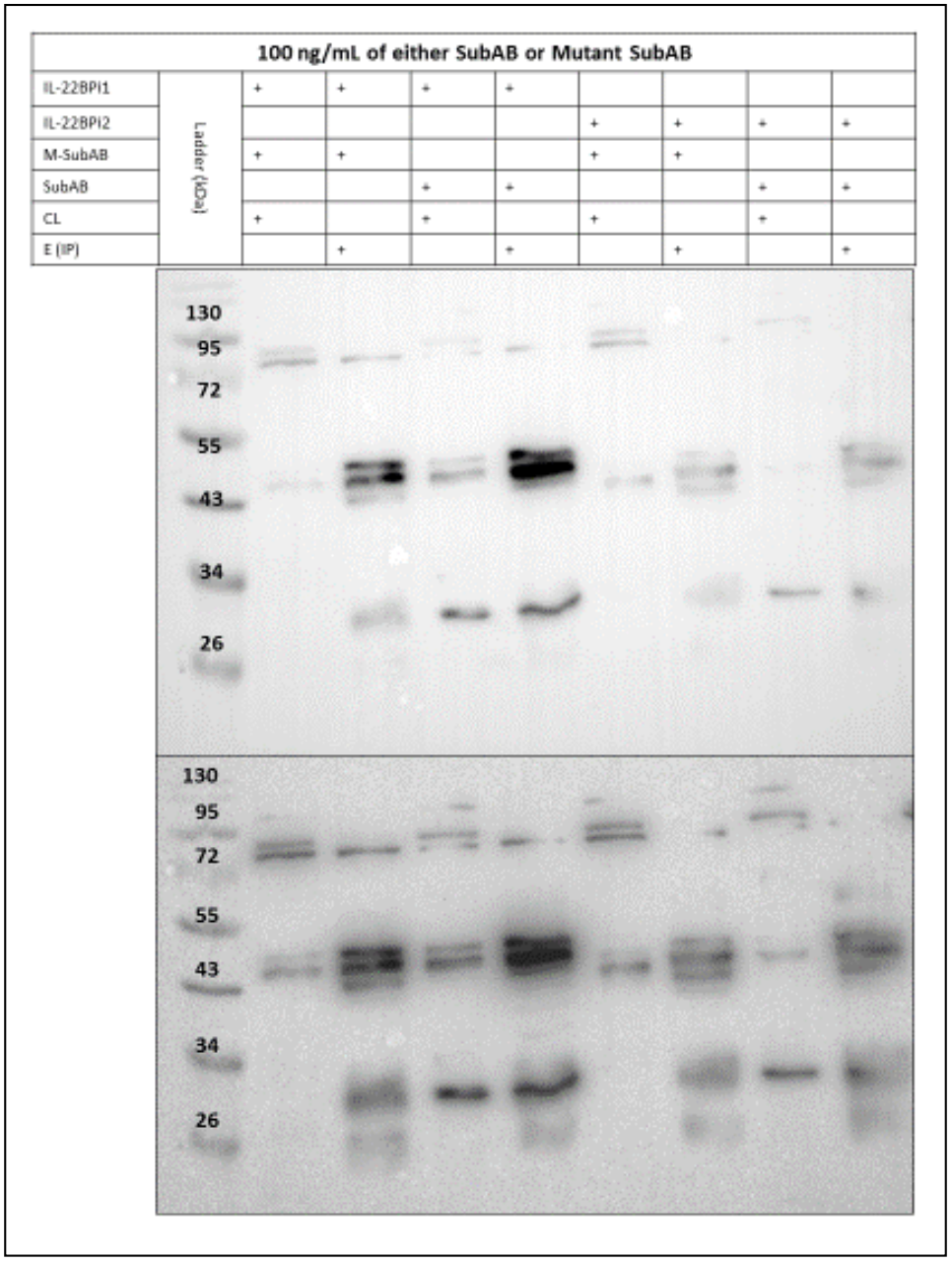

Figure 5.32. SubAB effect on IL-22BPi1 and IL-22BPi2 transfected cells in expressed proteins. Immunoblot of cell lysates (CL) and IP elutions (E IP) of IL-22BPi1 and BPi2 transfected HEK293 cells treated with 100 ng/mL of SubAB or m-SubAB using anti-FLAG antibody. From the anti-FLAG staining, it was expected the detection of IL-22BPi2 at around 48 kDa weight and that of the IL-22BPi1 3-4 kDa above of it due the extra 32 AA coded in the exon 4. Both images correspond to the same immunoblot; the image below has increased exposure to undercover faint detection. Trace of the previous staining of anti-FLAG (Figure 5.31) remains. Figure representative of three different experiments.

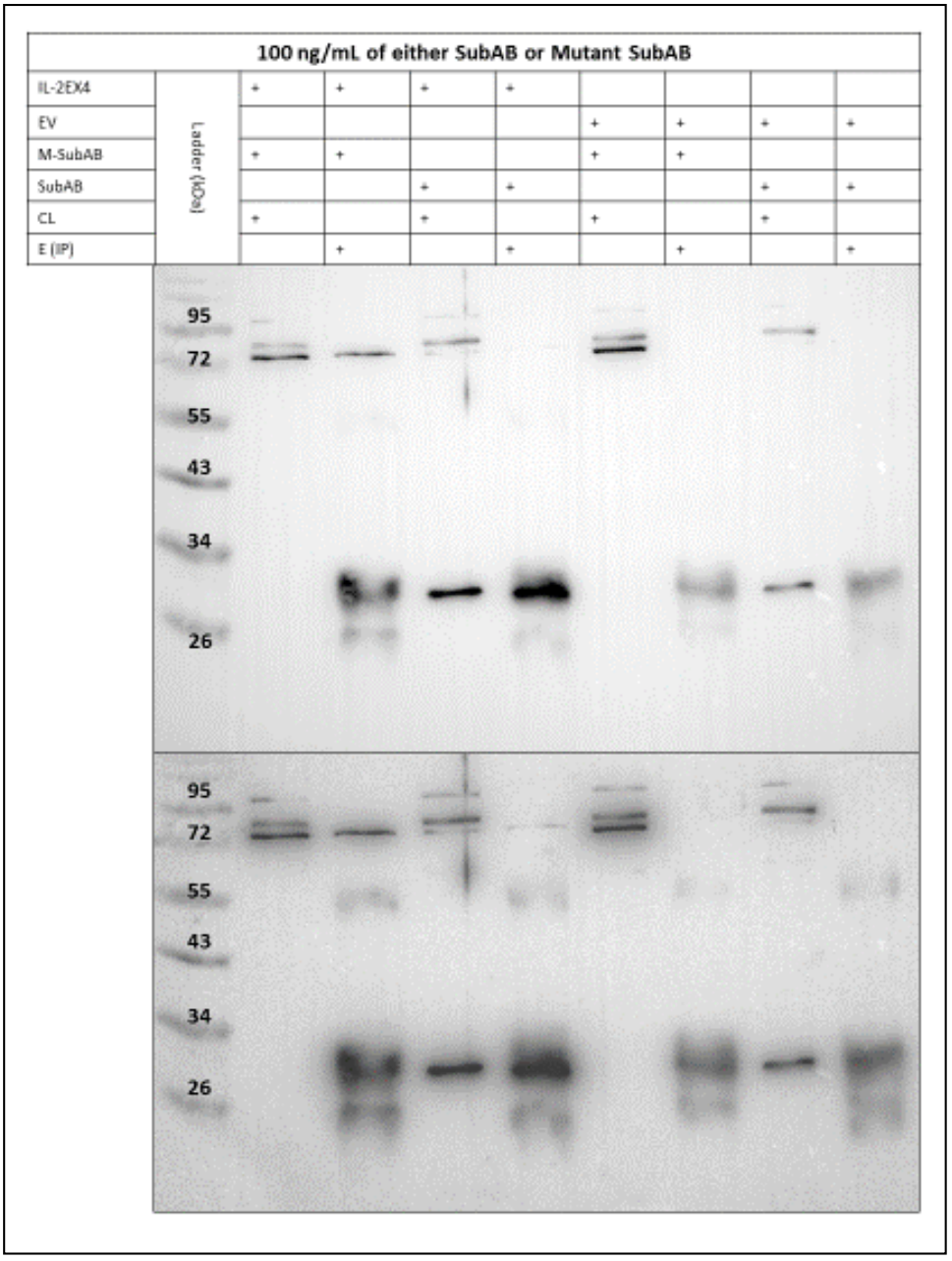

Figure 5.33. SubAB effect on IL-2 and IL-2EX4 transfected cells in ER proteins. Immunoblot of cell lysates (CL) and IP elutions (E IP) of IL-2 and IL-2EX4 transfected HEK293 cells treated with 100 ng/mL of SubAB or m-SubAB using anti-KDEL antibody. From the anti-KDEL staining it was expected the detection of the uncleaved GRP78 at 78kDa, and that of the C-terminal SBD of the cleaved GRP78 at 28 kDa. Both images correspond to the same immunoblot; the image below has increased exposure to undercover faint detection. Figure representative of three different experiments.

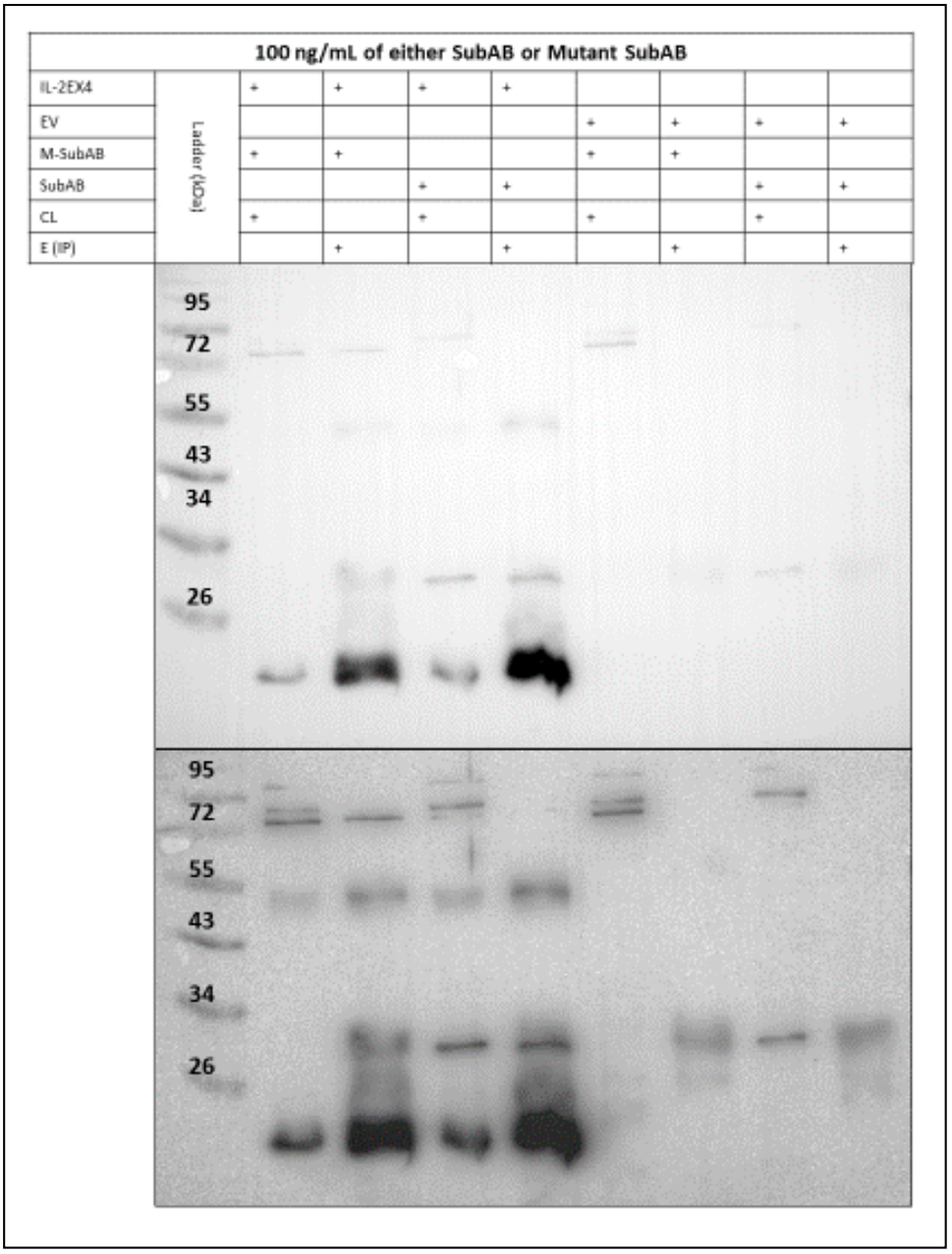

Figure 5.34. SubAB effect on IL-2 and IL-2EX4 transfected cells in expressed proteins. Immunoblot of cell lysates (CL) and IP elutions (E IP) of IL-22BPi1 and BPi2 transfected HEK293 cells treated with 100 ng/mL of SubAB or m-SubAB using anti-FLAG antibody. From the anti-FLAG staining it was expected the detection of IL-2 at around 19 kDa weight and that of the IL-2EX4 3-4 kDa above of it due the extra 32 AA coded in the exon 4. Both images correspond to the same immunoblot, the image below has increased exposure to undercover C-terminal SBD detection. Trace of the previous staining of anti-FLAG (Figure 5.32) remains. Figure representative of three different experiments.

In the crosslinking experiments, that included IL-22BPi3, the procedure was similar to the previous set of experiments with the difference of the addition of DSP before the lysis of the cells (see Materials and methods section 4.5.2. (Affinity purification)). In this way, HEK293 cells were transfected with different transfection vectors containing IL-2, IL-2EX4, IL-22BPi1 and IL-22BPi2. The intracellular content of the cells was analyzed in the CL and purified by IP FLAG resin (all the transfected proteins had this tag) to find the interacting partners of the transfected proteins and compare the differences between them. Samples were loaded in two different ways to better analyze the experiment.

Samples were loaded first based on their SubAB or m-SubAB treatment, allowing all the transfected proteins in the same gel. The different effect of SubAB and m-SubAB on GRP78 was clear; only the immunoblot of the cells treated with SubAB (Figure 5.37) showed the 28 kDa band corresponding to the cleaved C-terminal SBD of GRP78 along with the uncleaved GRP78 band of 78 kDa, while in the gel of the samples treated with m-SubAB the 28 kDa band was absent (Figure 5.35). Regarding the transfections, it was possible to detect with anti-FLAG antibody each of the transfected proteins (Figure 5.36 and 5.38) and therefore confirm a proper transfection of all the samples. The quantitative differences among the detected signal on the different transfected proteins reflect the differences in the intracellular accumulation and the secretory ability of each one of them. Non-secreted proteins such us IL-22BPi1 and IL-2EX4 have higher concentration than that of the secreted IL-22BPi2 and the one of the easily secreted IL-22BPi3 which is only detected after purification (16 kDa; Figure 4.56 and 4.58). The initial quantity of intracellular protein also conditions the quantity of IP protein and corresponding co-IP GRP78 in any form.

Results confirmed the interaction of IL-22BPi1 and IL2EX4 with GRP78, that was clearly purified with them (Figure 5.35) and specifically with the C-terminal SBD of the cleaved GRP78 (Figure 5.37). Increased exposure of the immunoblots allowed us to detect, in a lower extent,

interaction between IL-22BPi2 and uncleaved (Figure 5.35) and cleaved (Figure 5.37) GRP78. IL-22BPi3 did not show co-IP of uncleaved (Figure 5.35) or cleaved (Figure 5.37) GRP78, results in line with interactome of IL-22BP isoforms performed in the lab (Gómez-Fernández et al., 2018).

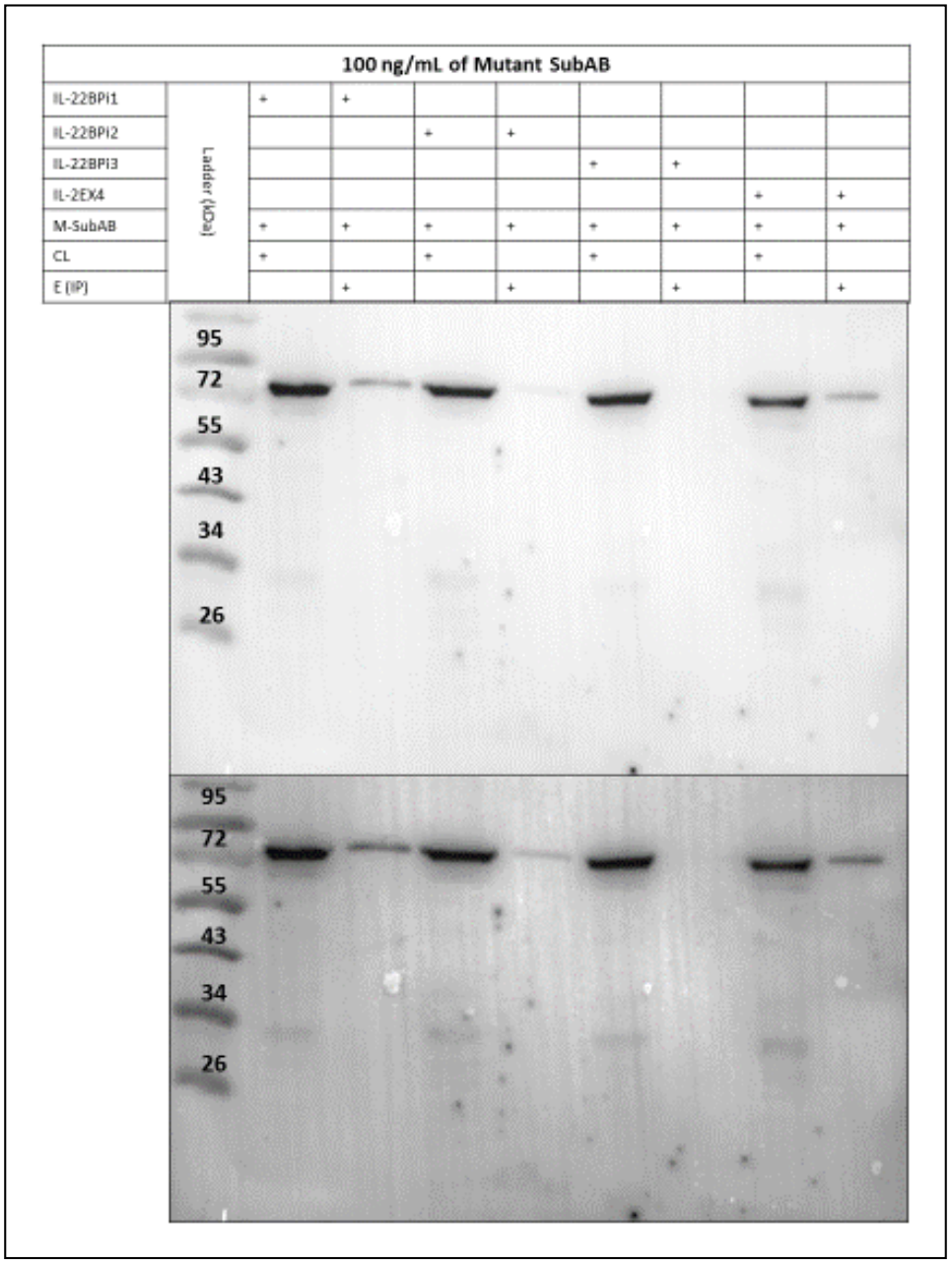

Figure 5.35. Co-IP immunoblot results of m-SubAB treated cells GRP78 staining. Immunoblot of cell lysates (CL) and IP elutions (E IP) of transfected HEK293 cells treated with 100 ng/mL of m-SubAB using anti-GRP78 antibody. From the anti-GRP78 staining it was expected the detection of the uncleaved GRP78

at 78kDa, and that of the C-terminal SBD of the cleaved GRP78 at 28 kDa. Both images correspond to the same immunoblot; the image below has increased exposure to undercover faint detection.

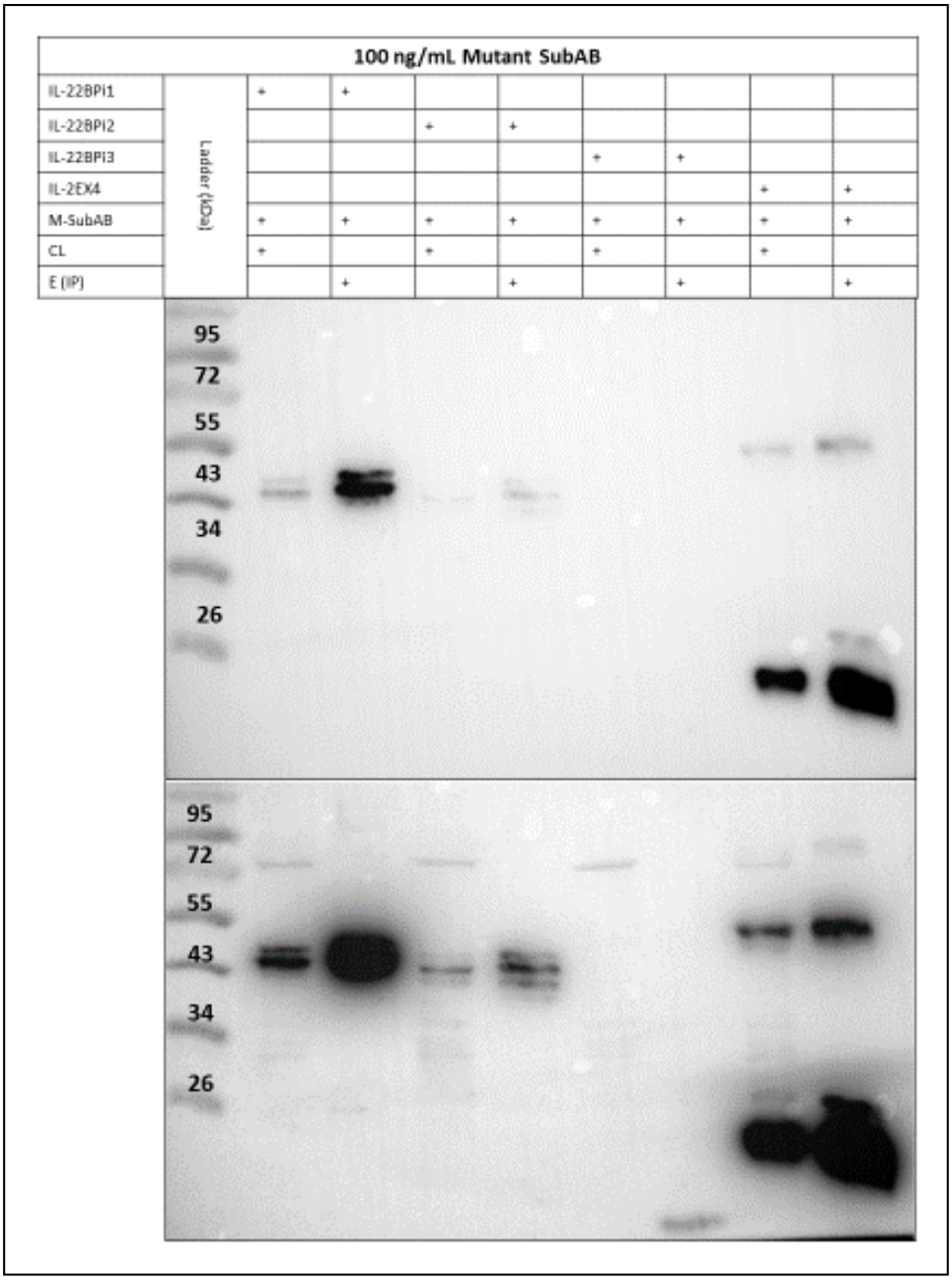

Figure 5.36. Co-IP immunoblot results of m-SubAB treated cells FLAG staining. Immunoblot of cell lysates (CL) and IP elutions (E IP) of transfected HEK293 cells treated with 100 ng/mL of m-SubAB using anti-FLAG antibody. From the anti-FLAG staining, it was expected the detection of IL-22BPi2 at around 48 kDa weight, that of the IL-22BPi1 3-4 kDa above, IL-22BPi3 at 16 kDa and IL-2EX4 at 23 kDa. Both images correspond to the same immunoblot; the image below has increased exposure to undercover faint detection. Figure representative of three different experiments.

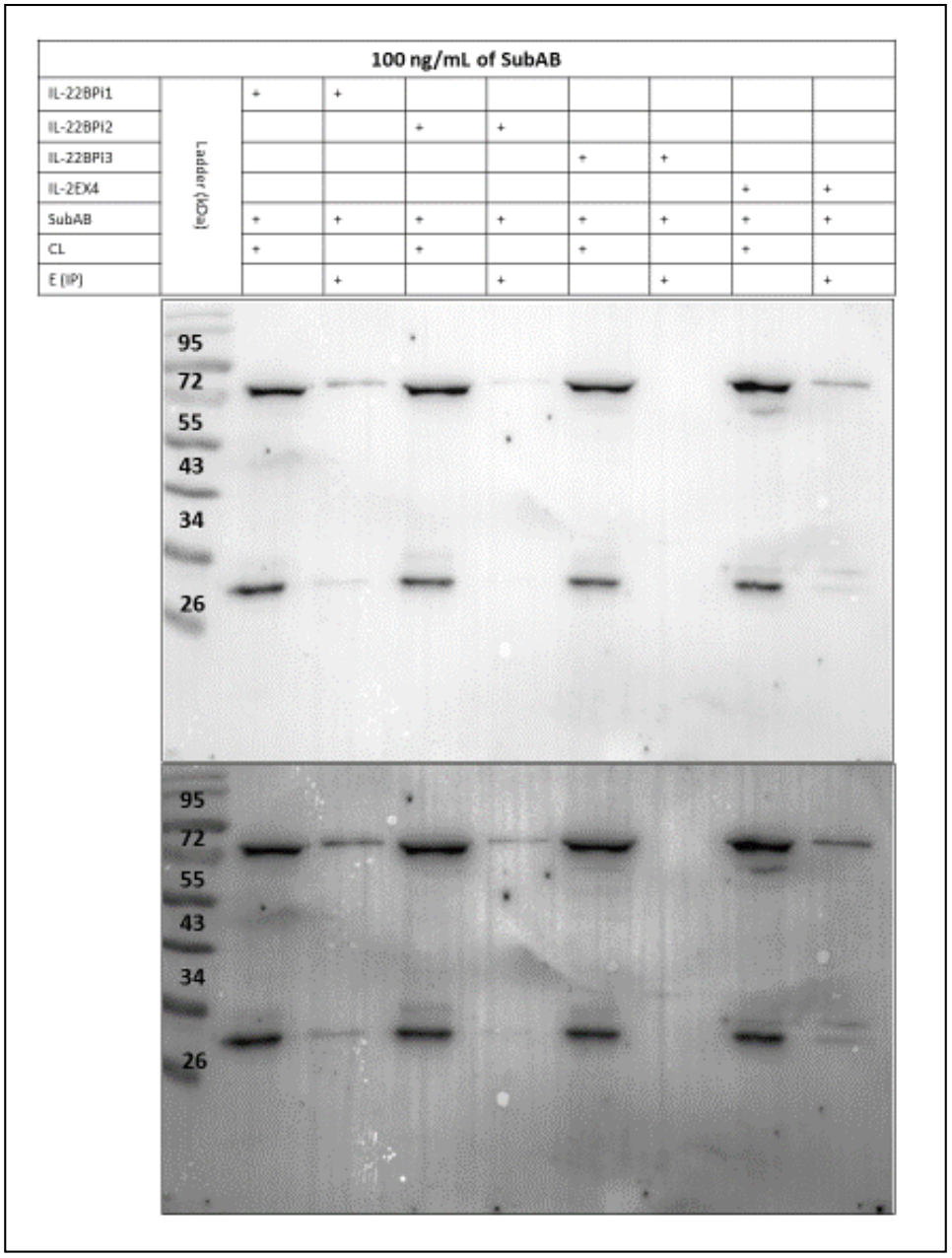

Figure 5.37. Co-IP immunoblot results of SubAB treated cells GRP78 staining. Immunoblot of cell lysates (CL) and IP elutions (E IP) of transfected HEK293 cells treated with 100 ng/mL of SubAB using anti-GRP78 antibody. From the anti-GRP78 staining it was expected the detection of the uncleaved GRP78 at 78kDa, and that of the C-terminal SBD of the cleaved GRP78 at 28 kDa. Both images correspond to the same immunoblot; the image below has increased exposure to undercover faint detection. Figure representative of three different experiments.

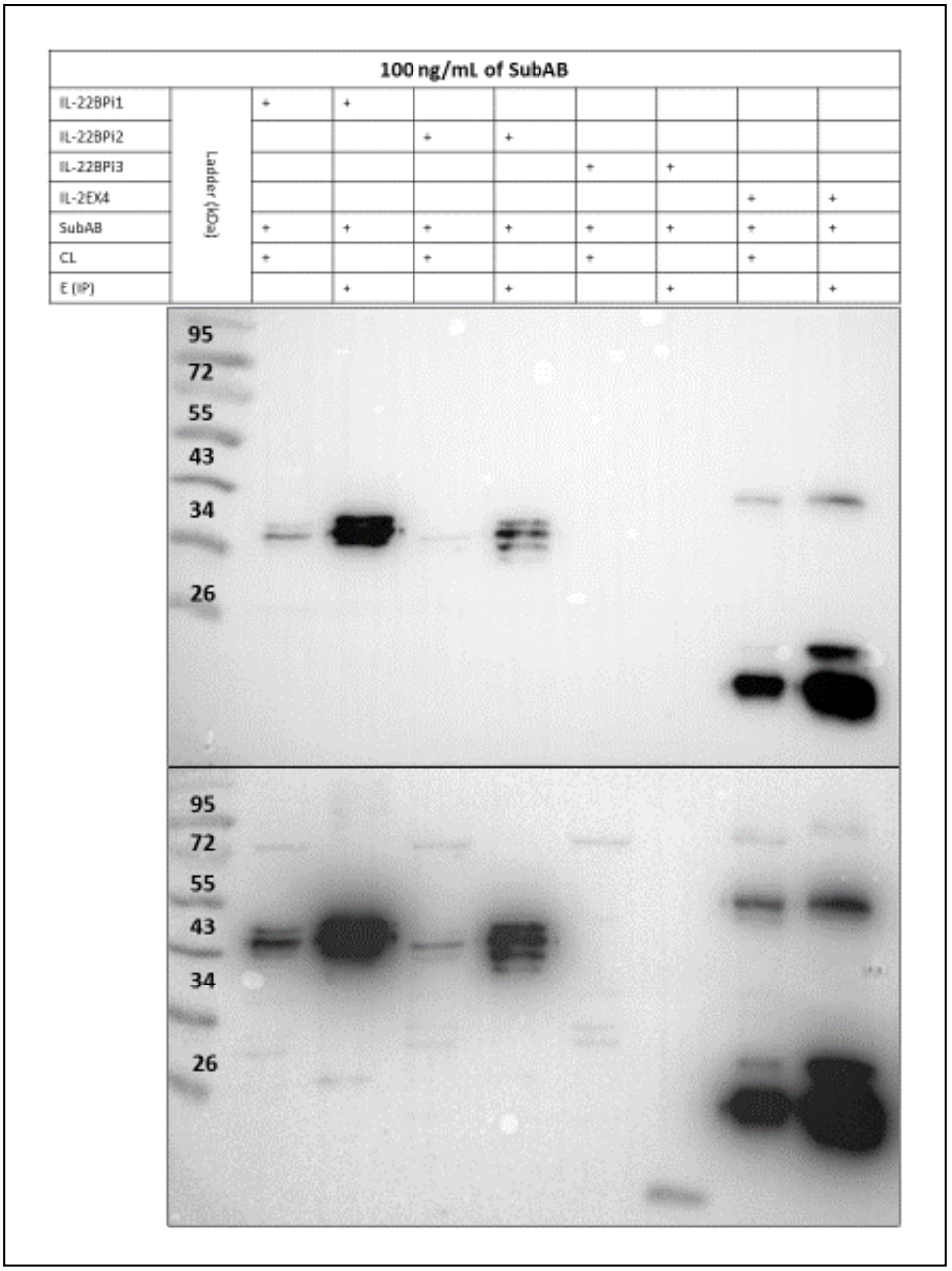

Figure 5.38. Co-IP immunoblot results of SubAB treated cells FLAG staining. Immunoblot of cell lysates (CL) and IP elutions (E IP) of transfected HEK293 cells treated with 100 ng/mL of SubAB using anti-FLAG antibody. From the anti-FLAG staining, it was expected the detection of IL-22BPi2 at around 48 kDa weight, that of the IL-22BPi1 3-4 kDa above, IL-22BPi3 at 16 kDa and IL-2EX4 at 23 kDa. Both images correspond to the same immunoblot; the image below has increased exposure to undercover faint detection. Figure representative of three different experiments.

In order to have a clearer image to appreciate the difference of the SubAB and m-SubAB, and the co-IP of each isoform, we decided to run samples of each isoform in individual gels. Among the isoforms, IL-22BPi1 (Figure 5.39) showed the strongest co-IP of GRP78 SBD domain, the IL-22BPi2 (Figure 5.40) was lower, and in very contrasted image of IL-22BPi3 (Figure 5.41) no GRP78 signal at all was detected in the co-IP fraction, but IL-22BPi3 was clearly detected after the purification. Finally, IL-2EX4 (Figure 5.42), in line with IL-22BPi1, showed a very strong GRP78 signal.

In a set of experiments the three IL-22BP isoforms were co-transfected with wild-type (wt) GRP78 or a mutant form of GRP78, in which substitution of Thr-37 with Gly (T37G) inhibits ATPase activity and blocks ATP-mediated release of cargo from GRP78 (Gaut & Hendershot, 1993). Wt but not GRP78T37G significantly increased secreted levels of IL-22BPi1 and IL-22BPi2, while it did not affect secretion of IL-22BPi3. This was mirrored by a tendency toward increased intracellular levels of IL-22BP isoforms in the presence of wtGRP78 (Gómez-Fernández et al., 2018). Thus, the binding of IL-22BPi1 and IL-22BPi2 to the SBD of GRP78 as well as their enhanced secretion upon overexpression with wt but not ATPase-deficient GRP78 suggests that both isoforms are natural client proteins of GRP78.

It is important to realize that GRP78 recognizes a "degenerate" peptide sequence enriched for aromatic and aliphatic AAs, such sequences are (very) widespread among cargo proteins. Thus, while the exon-4 may contain new GRP78 recognition sequences, the main determinant for a protein to interact with GRP78, as deduced from many studies, may be the availability of these sequences in the unfolded form or folding intermediate. Thus, even if exon-4 would not bind GRP78, its destabilizing effect on folding of IL22BPi1 may expose peptides within the IL22BPi2-part of the molecule for enhanced binding to GRP78. That is why we cannot make a conclusion on whether yes or no exon-4 interacts with GRP78. Similar for IL-2. Similarly, IL-22BPi3 may contain GRP78 binding sites but as it folds fast, it will not interact with GRP78.

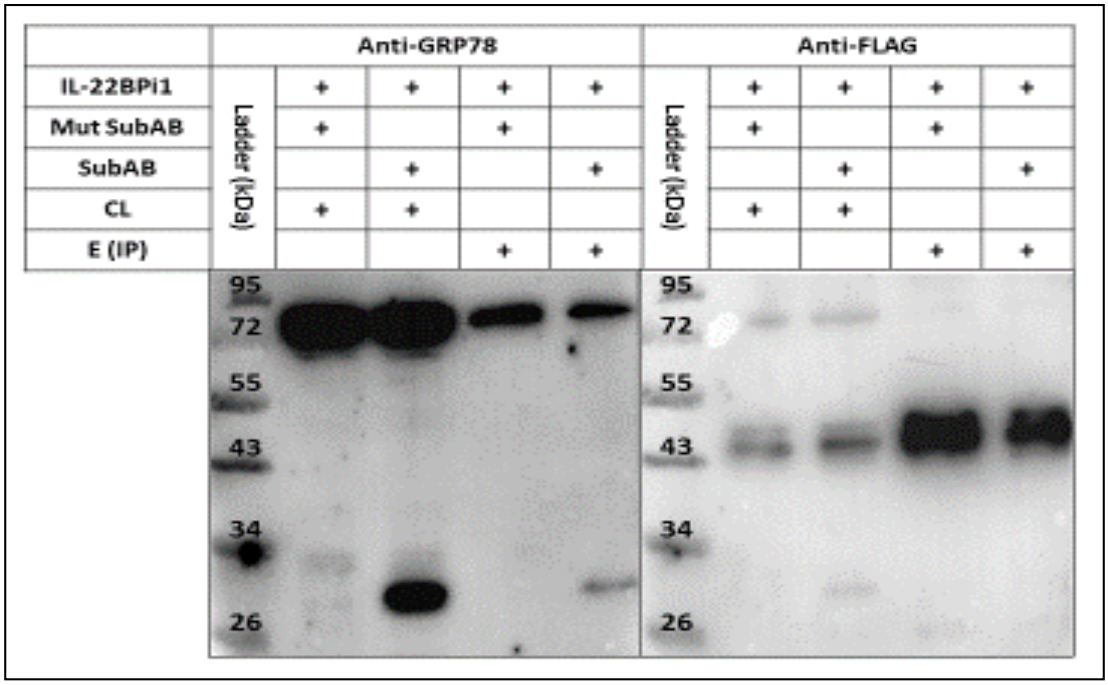

Figure 5.39. Co-IP immunoblot results of IL-22BPi1 transfected cells. Immunoblot of CL and E(IP) of transfected cells treated with 100 ng/mL of SubAB or m-SubAB with anti-GRP78 and anti-FLAG antibodies.

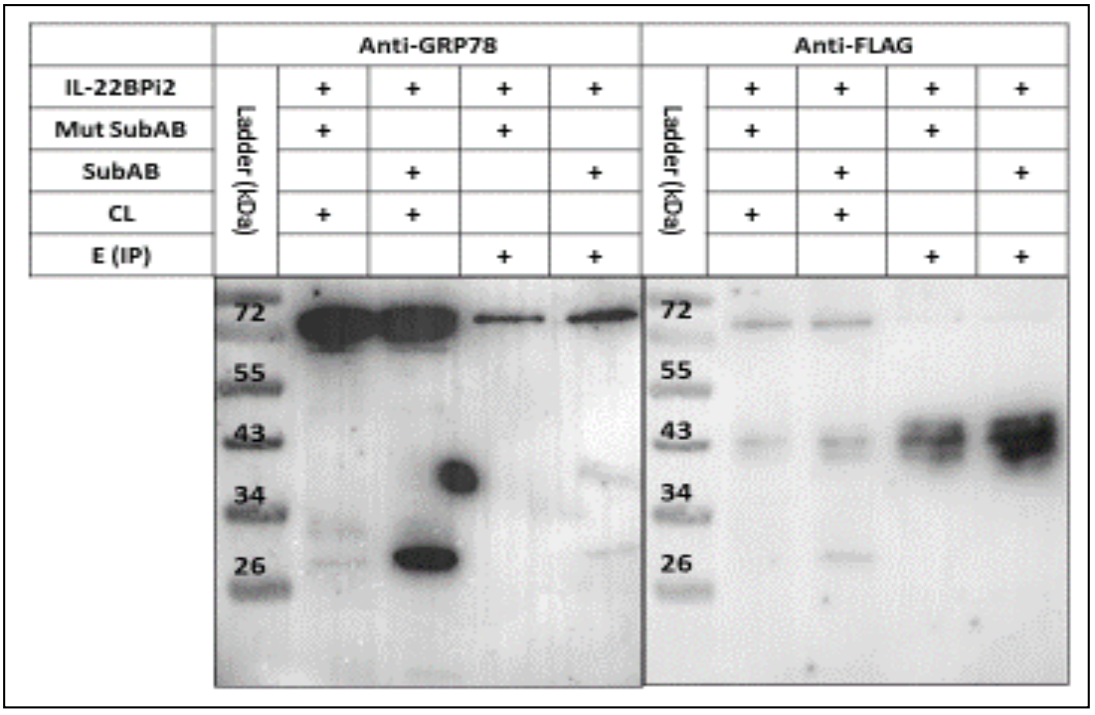

Figure 5.40. Co-IP immunoblot results of IL-22BPi2 transfected cells. Immunoblot of CL and E(IP) of transfected cells treated with 100 ng/mL of SubAB or m-SubAB with anti-GRP78 and anti-FLAG antibodies.

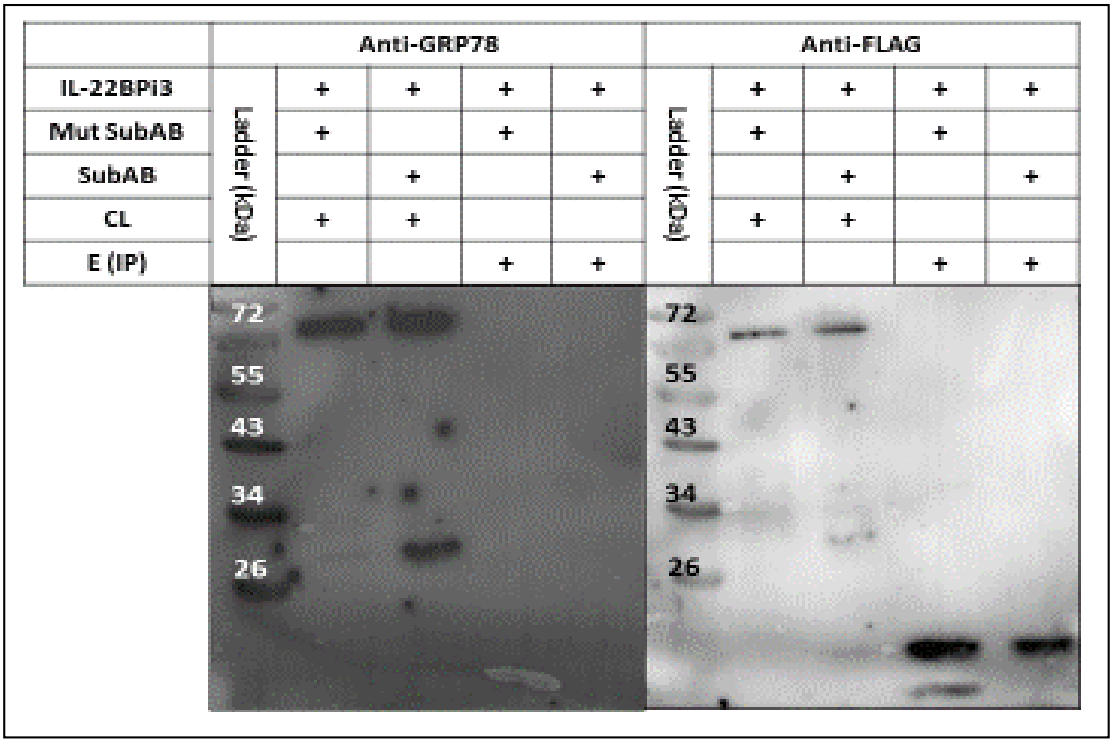

Figure 5.41. Co-IP immunoblot results of IL-22BPi3 transfected cells. Immunoblot of CL and E-IP of transfected cells treated with 100 ng/mL of SubAB or m-SubAB with anti-GRP78 and anti-FLAG antibodies.

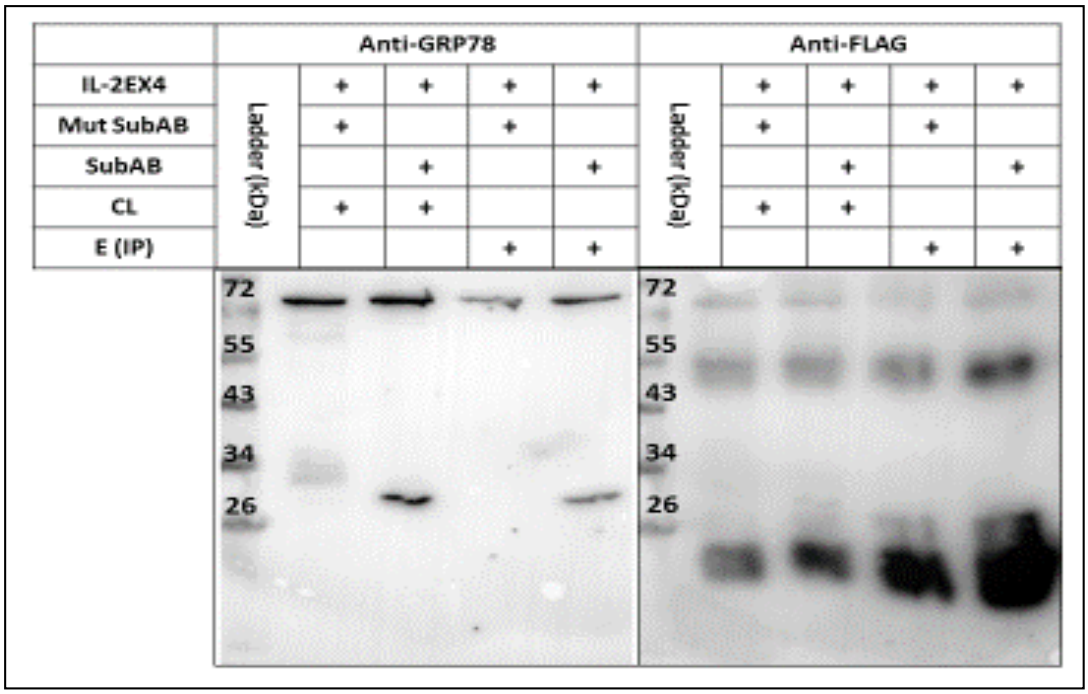

Figure 5.42. Co-IP immunoblot results of IL-2EX4 transfected cells. Immunoblot of CL and E-IP of transfected cells treated with 100 ng/mL of SubAB or m-SubAB with anti-GRP78 and anti-FLAG antibodies.

5.1.2.3. GRP94

5.1.2.3.1. IL-22BPi1 and IL-22BPI2 interact with the C-terminal half of the Middle Domain of GRP94

Interactomes of the IL-22BPi1 and BPi2 isoforms revealed three more partners than GRP78, those were calnexin, GRP94, and GRP170 (Gómez-Fernández et al., 2018). WB and co-IP experiments performed in the lab revealed that GRP94 amount was clearly higher in IL-2EX4 co-transfected cells than IL-22BPi1, IL-22BPi2 was borderline detectable and was not detected at all in IL-22BPi3. However, in a reverse co-IP with S-tagged GRP94, only IL-22BPi1 was found (Gómez-Fernández et al., 2018).

GRP94, like GRP78 is an ER luminal chaperone, but unlike GRP78, it has a highly selective client base of proteins, including specific Toll-like receptors and integrins, which apart from exhibiting disulfide-bonds share no further apparent structural features among them (Marzec et al., 2012; Wu et al., 2012a). It consists in three major domains: N-terminal domain (NTD) of 25 kDa that contains the ATP-binding site, a middle domain (MD) of 40 kDa containing substrate or client binding domain, an a C-terminal domain (CTD) which contains a cofactor recognition and an alternative ATP-biding sites (Prodromou & Pearl, 2003) as represented in Figure 5.43.

To identify the region(s) in GRP94 responsible for interacting with IL-22BPi1 or IL-22BPi2, we probed interaction of both isoforms with a series of GRP94 truncation and deletion mutants (Figure 5.44). The selection of constructs was based on well-defined GRP94 regions (Marzec et al., 2012) that constitute the modular fold of GRP94, and was previously used to investigate the interaction site of GRP94 with OS-9 (Dersh et al., 2014). They were provided by the Yair Argon from the University of Pennsylvania, the senior author of the mentioned paper (Dersh et al., 2014).

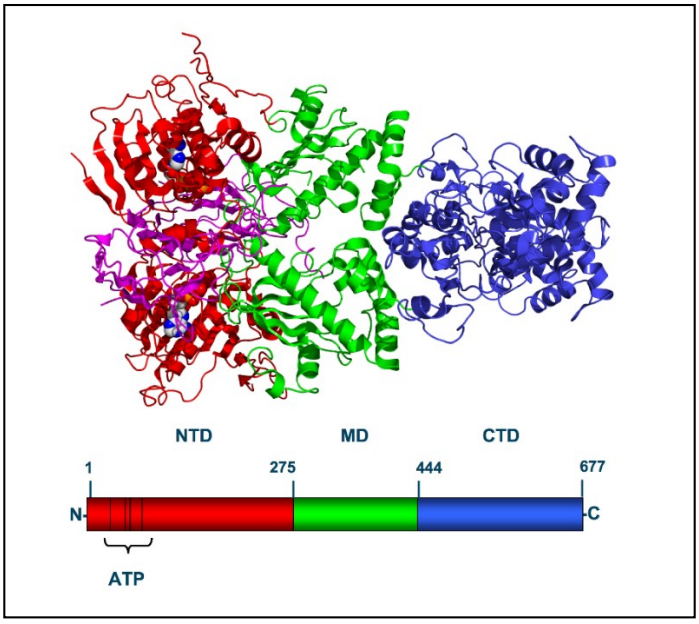

Figure 5.43. Structure and domain organization of Hsp90 family chaperones. NTD= N-terminal domain (red), MD = middle domain (green), CTD = C-terminal domain (blue). *Source: https://www.wikiwand.com/en/Hsp90.*

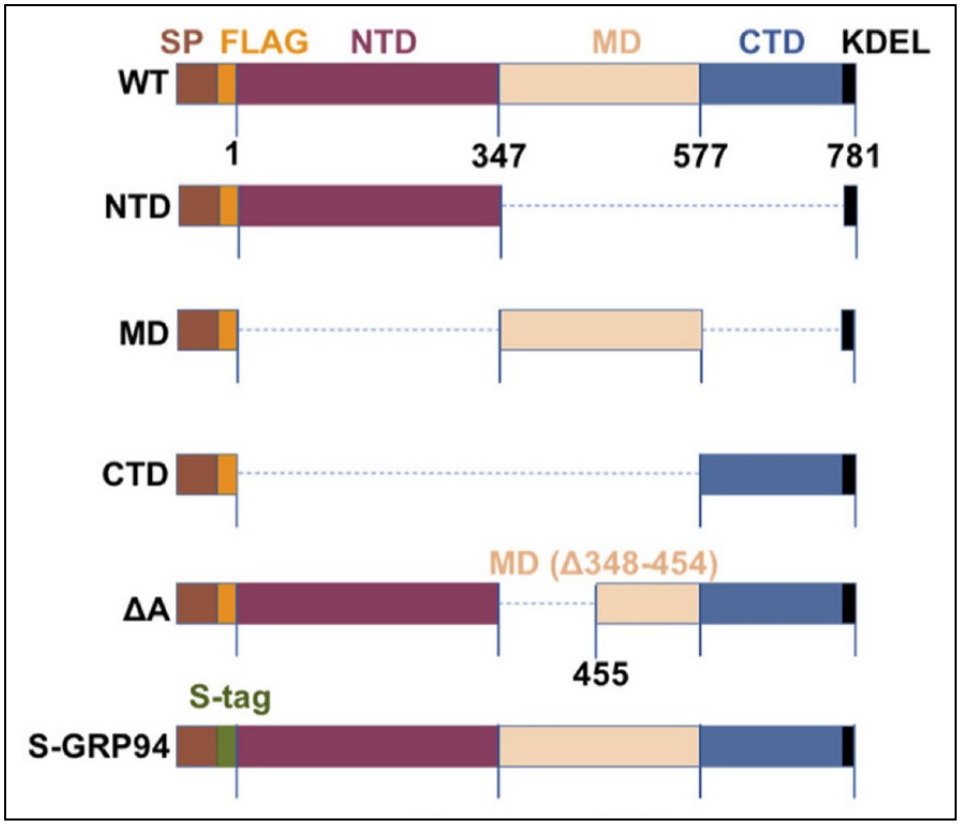

Figure 5.44. Structure and domain of employed GRP94 will type and mutant vectors. *Source: (Gómez-Fernández et al., 2018).*

The impact on secretion of IL-22BPi1 and BPi2 co-transfected with GRP94 mutants was addressed by the in house made IL-22BP ELISA. We performed two biological replicates that was complemented by another one done by other member of the lab. HEK293 cells were transfected with one of the GRP94 mutants and either IL-22BPi1 or IL-22BPi2. The cells medium was analyzed in the in-house made IL-22BP ELISA. The results showed levels of secretion of IL-22BPi1 (Figure 5.45A) ten times lower than the ones of IL-22BPi2 (Figure 5.45B). However, it was possible to observe the same trends in both, a strong decrease of IL-22BP isoforms in MD and ΔA GRP94 mutants (Figure 4.45C), and a stronger decrease with CTD in the case of IL-22BPi1.

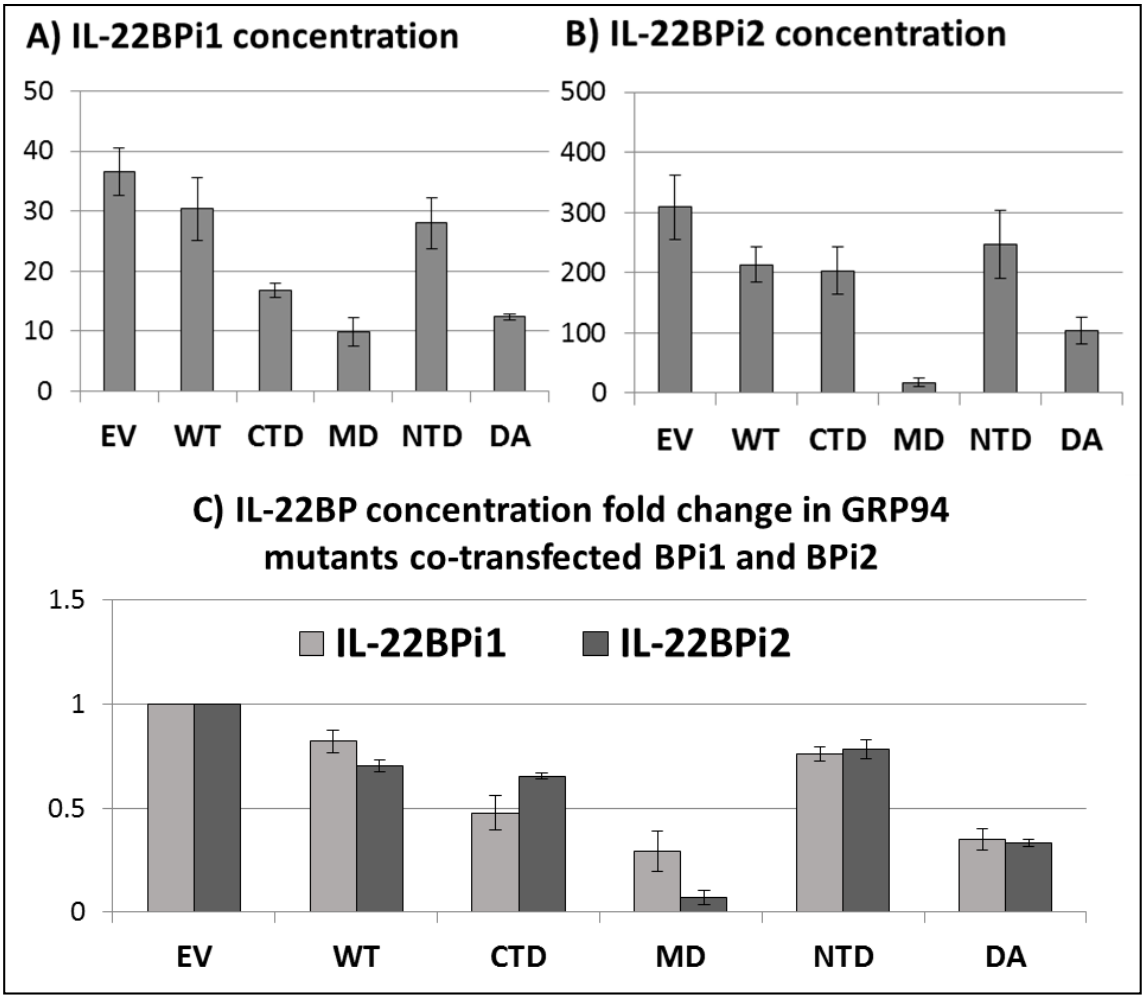

Figure 5.45. ELISA results of GRP94 mutants contransfection. IL-22BP isoforms concentration (ng/mL) in the medium of the different GRP94 mutants co-transfected with IL-22BPi1 (A) or IL-22BPi2 (B) measured by the in house designed ELISA. Concentration fold change of IL-22BP in IL-22BPi1 and IL-22BPi1 transfected cells cotransfected with GRP94 mutants compared to EV. Mean ± SEM (n=2). For the structure of the mutants, see Figure 5.44.

The results complemented by a third replicate (Figure 4.68), showed that co-expression of either GRP94 MD or ΔA GRP94 mutants with IL-22BPi1 or BPi2 isoforms significantly decreased their secretion, suggesting that interaction of these IL-22BP isoforms with these GRP94 mutants sequesters them from the productive folding/secretory pathway. Meanwhile the NTD mutant did not affect secretion and CTD mutant appeared to decrease secretion of IL-22BPi1 but not that of IL-22BPi2.

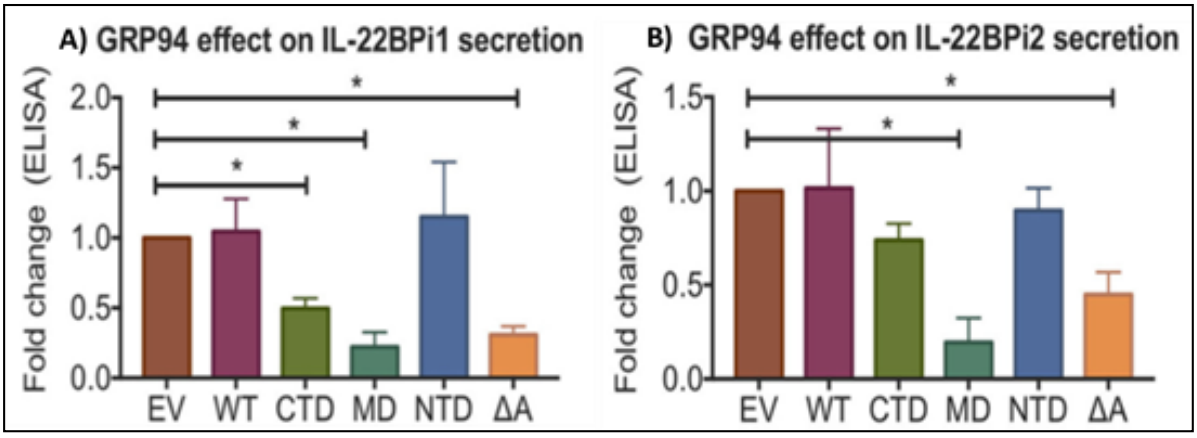

Figure 5.46. IL-22BP concentration fold change difference per IL-22BP isoform. IL-22BP isoforms concentration (ng/mL) in the medium of the different GRP94 mutants co-transfected with IL-22BPi1 (A) or IL-22BPi2 (B) measured by the in house designed ELISA. Mean + SEM; *p < 0.05 by paired t-test.

In line those results, co-transfections showed that MD and ΔA GRP94 mutants, and not CTD and NTD GRP94 mutants, interacted strongly with IL-22BPi1 and IL-22BPi2 (Gómez-Fernández et al., 2018). Altogether, the middle subdomain of GRP94 shared by MD and ΔA GRP94 (AAs 455-577) emerges as critical region for binding both IL-22BPi1 and IL-22BPi2. This client-binding site differs from that used by the ERAD component OS-9 (AAs 356–456 of the MD (Dersh et al., 2014)) or by GRP94 client proteins such as TLRs and integrins (AAs 635–656 of the CTD (Wu et al., 2012a)). Apart from the described plasmids we were also provided with two GFP-tagged GRP94 vectors (Figure 5.47), a wt GRP94 (WT-GFP) and another with a mutation on E82A making it ATPase negative GRP94 (E82A-GFP), previously used by Yair Argon team (Marzec et al., 2016).

Given their GFP-tag, we were able to analyze the co-expression of the two vectors with IL-22BP isoforms and IL-2EX4 by immunofluorescence. Results of WT-GFP (Figure 5.48) and E82A-GFP (Figure 5.49) showed a pronounced co-localization of either GRP94 form with IL-22BP1 and IL-2EX4 as well as with the reticular portion of IL-22BPi2 located outside the Golgi apparatus, but not with IL-22BPi3. Further experiment checked the impact of the co-transfections

of the two vectors with IL-22BP isoforms, revealing that when compared to WT-GFP, E82A-GFP significantly reduced secretion levels of IL-22BPi1 and IL-22BPi2, but not the ones IL-22BPi3 (Gómez-Fernández et al., 2018). Together, these experiments provide evidence that GRP94 interacts with both the former isoforms, and that the secretion of both isoforms is proportional to intact GRP94 activity.

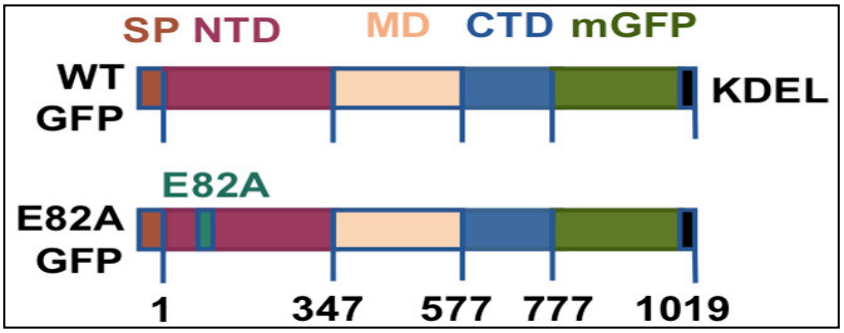

Figure 5.47. Structure and domains of GFP-tagged GRP94 vectors. *Source: (Gómez-Fernández et al., 2018)*.

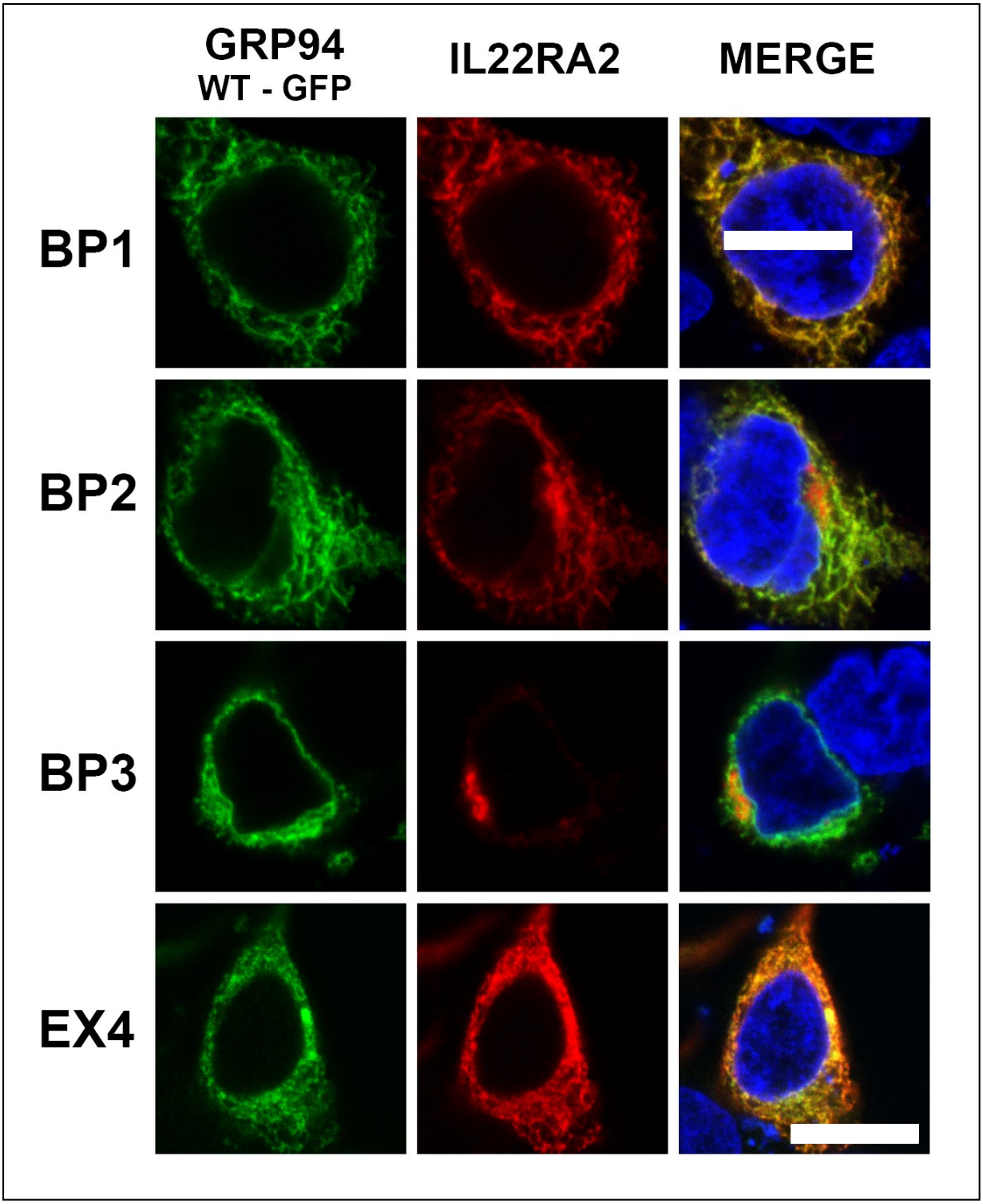

Figure 5.48. Cotransfection of GRP94WT-GFP vector with IL-22BP isoforms or IL-2EX4. Confocal microscopy Images of HEK293 cells co-transfected with GRP94 WT-GFP vector (green) and IL-22BP isoforms or IL-2EX4 stained with A647 (red) and counterstained with DAPI (blue). Scale bar: 10 μm. Figure representative of three different experiments.

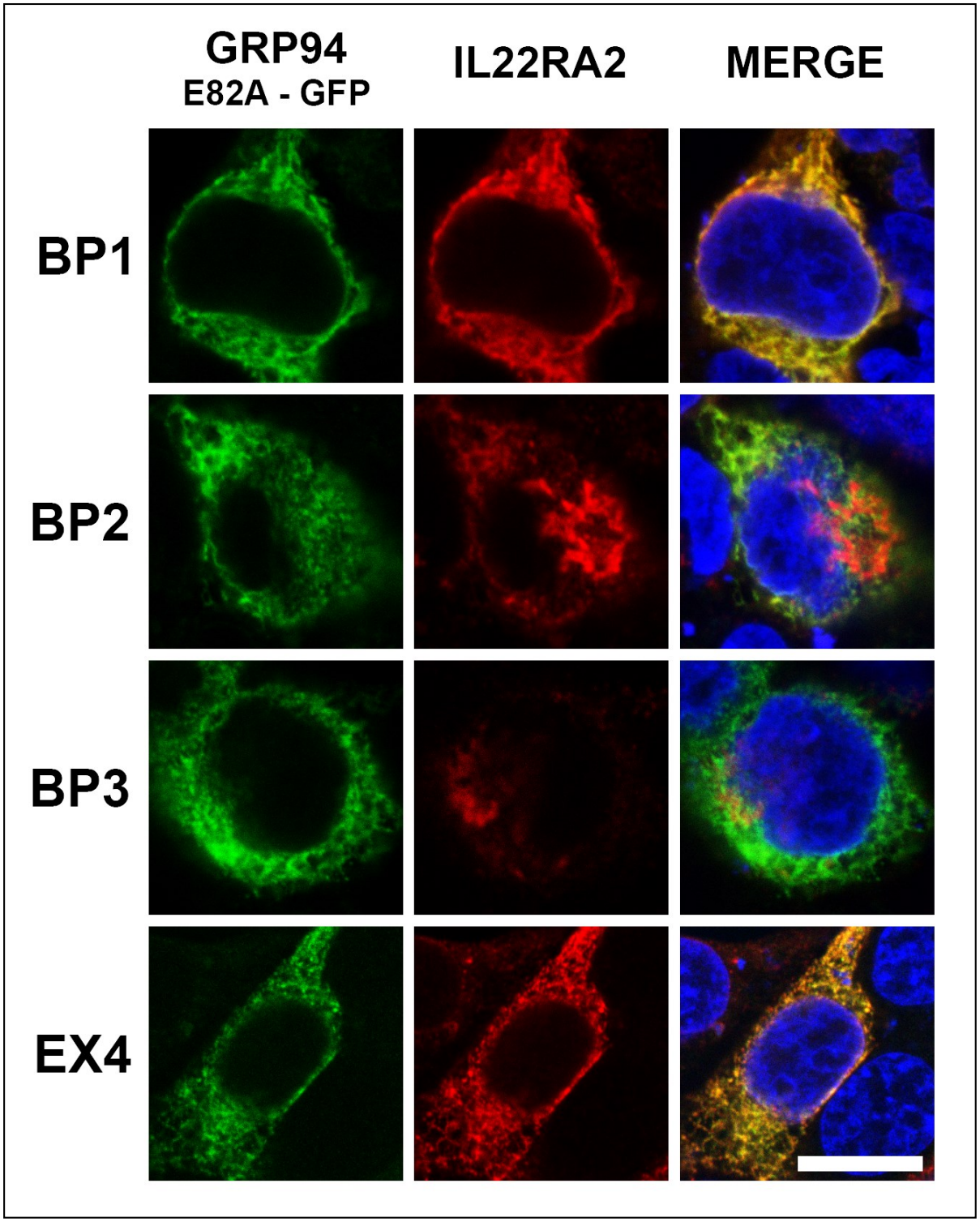

Figure 5.49. Cotransfection of GRP94E82A-GFP vector with IL-22BP isoforms or IL-2EX4. Confocal microscopy Images of HEK293 cells co-transfected with GRP94 WT-GFP vector (green) and IL-22BP isoforms or IL-2EX4 stained with A647 (red) and counterstained with DAPI (blue). Scale bar: 10 μm. Figure representative of three different experiments.

5.1.2.3.2. Pharmacological targeting of GRP94 and PPIB induces secretion of IL-22BPi1

In order to have a deeper understanding of the mechanisms governing IL-22BP secretion, and given the effects of GRP94 showed in the previous section, 5.1.2.3.1. (IL-22BPi1 and IL-22BPI2 interact with the C-terminal half of the Middle Domain of GRP94), different ER-resident chaperones presence was analyzed in moDCs. Using samples from the experiment described in section 5.1.2 (IL-22BP secretion), the presence of different chaperones was tested by immunoblotting. The presence of GRP94, an important interactor of IL-22BP in cell line models, was clearly detected in both immature and matured moDCs (Figure 4.72).

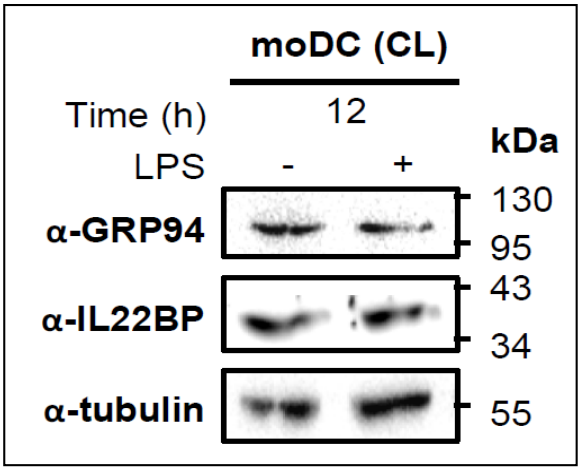

Figure 5.50. GRP94 detection in moDCs. Immunoblot of CL of 6 days CD14+ moDCs unstimulated or mature with IFNγ + LPS using anti-GRP94, anti-IL-22BP and anti-tubulin (loading control) antibodies.

Cyclophilins, a group of proteins that have peptidyl-porolyl cis-trans isomerase (PPI) activity and bind to immunosuppressive drug cyclosporine A (CsA, (P. Wang & Heitman, 2005)) were also studied. They are upregulated during the differentiation of CD14+ monocyte to moDCs (Naour et al., 2001) and play a role in regulating cytokine secretion (Dawar et al., 2017). By immunoblotting it was possible to detect the presence of cyclophilins A (PPIA), B (PPIB) and C (PPIB) on moDCs by an anti-PPIC antibody (Figure 5.51) that detects all three cyclophilins (Stocki

et al., 2014). Cyclophilin A is cytosolic so it was out of our ER-resident chaperone range, but cyclophilin B associates with other ER-resident proteins, such as GRP94, GRP78, and calreticulin (Jansen et al., 2012; Meunier et al., 2002; Zhang & Herscovitz, 2003). The enzymatic activity of PPIB is also been related to ER-associated degradation (ERAD) and ER redox homeostasis (Bernasconi et al., 2010; J. Kim et al., 2008; Stocki et al., 2014).

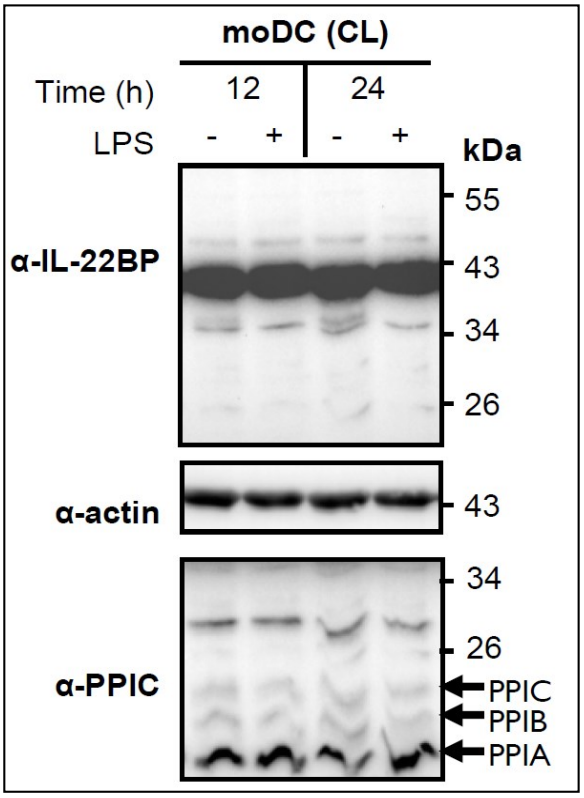

Figure 5.51. Cyclophilin detection in moDCs. Immunoblot of CL of 6 days CD14+ moDCs unstimulated or mature with IFNγ + LPS using anti-GRP94, anti-IL-22BP and anti-actin (loading control) antibodies.

Given that GRP94 and Cyclophilin B are co-expressed with IL-22BP on moDCs, we studied if secretion of the IL-22BP isoforms could be modulated by pharmacological targeting of GRP94 and cyclophilin B; either by means of geldanamycin, that binds to the ADP/ATP pocket shared by HSP90 paralogs like GRP94, or by CsA, which causes depletion of ER cyclophilin B levels through secretion.

Results showed that geldanamycin and its analogs did not influence secretion of IL-22BPi2 or IL-22BPi3, but significantly enhanced intracellular and secreted levels of IL-22BPi1. The secreted protein was heterogeneously glycosylated, with both high-mannose and complex-type glycoforms present. In addition, cyclosporine A augmented the secretion of IL-22BPi1 and reduced that of IL-22BPi2 and IL-22BPi3. Altogether, these results indicated that the ATPase activity of GRP94 and cyclophilin B are instrumental in ER sequestration and degradation of IL-22BPi1, and that blocking these factors mobilizes IL-22BPi1 toward the secretory route (Gómez-Fernández et al., 2019).

5.1.3. *IL22RA2* silencing in moDCs

5.1.3.1. *IL22RA2* silencing effectively silences IL22RA2v1 and IL22RA2v2

As mentioned in the materials and methods, section 4.4.4.2 (siRNA), Viromer products from Lipocalyx GmbH were used for silencing. Viromer offers four different products named with colors (blue, green red and yellow) but only two of them are optimized for *in vitro* transfection of siRNA: Viromer Blue (VB-01LB) and Viromer Green (VG-01LB). Both have been described for silencing on moDCs (Hadadi et al., 2016; Paijo et al., 2016). Considering the relevance of AM580 addition from the beginning of the differentiation for *IL22RA2* expression, we thought to induce the silencing at the beginning of the moDCs culture. Following Paijo et al, we decided to carry on monocyte silencing after the isolation, when monocytes would be attached to the well instead of in suspension. However many conditions remained open such as the necessary siRNA and cell concentrations. In order to optimize to obtain the best protocol for silencing, a large preliminary experiment with 18 conditions was designed with the two types of Viromer, two cell concentrations, two siRNA concentrations, and the corresponding control siRNAs (a non-silencing (NS) siRNA) and non-silenced controls (Table 5.9). Cells were in cultured for a total of 3 days in DM. As mentioned, one day after isolation, when monocytes were already attached to the surface of the wells, the silencing was performed. 48h later cells were harvested and RNA extracted to generate the cDNA that was run in a qPCR to assess the expression levels of *IL22RA2*.

# conditions	Viromer	Cell concentration (M/mL)	[RA2 siRNA] in nM		[NS siRNA] in nM	
			50	100	50	100
2	Blue	0.5	+	-	+	-
2	Blue	0.5	-	+	-	+
2	Blue	1	+	-	+	-
2	Blue	1	-	+	-	+
2	Green	0.5	+	-	+	-
2	Green	0.5	-	+	-	+
2	Green	1	+	-	+	-
2	Green	1	-	+	-	+
1	-	0.5				
1	-	1				
18	Total					

Table 5.9. *IL22RA2* silencing setting conditions in moDCs. [RA2 siRNA]: concentration of *IL22RA2* siRNA; [siRNA NS]: concentration of non-silencing siRNA; nM: nanomolar.

The experiment gave us valuable information (Figure 5.52). First, the non-silenced controls, the regularly cultured moDCs, and the NS siRNA silenced controls, showed similar levels of *IL22RA2* expression excluding the interference of the technique with its expression. However, cells silenced with *IL22RA2* siRNA using Viromer Blue reagent did not decrease *IL22RA2* expression either. In the case of Viromer Green, a clear silencing effect was influenced by cell and siRNA concentration. The lower the cell concentration, the better the silencing; and the higher the siRNA concentration, the better the silencing too. Therefore, we set Viromer Green with a siRNA concentration of 100 nM, as the best conditions for *IL22RA2* silencing, while a lower cell concentration was also more effective. The results grouped by type of Viromer used (Figure 5.53) give a more clear view of the results, with Viromer Green at 100 nM siRNA achieving over 85% reduction of *IL22RA2* mRNA levels.

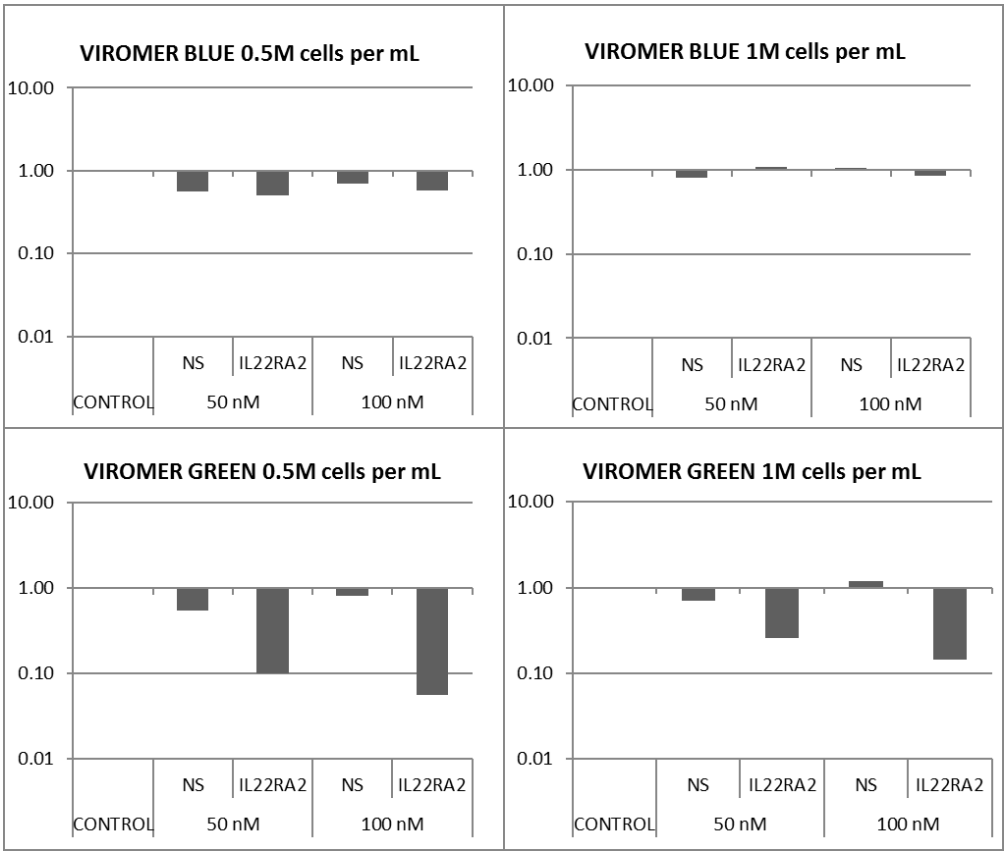

Figure 5.52. *IL22RA2* silencing in different conditions. Gene expression was assested by RT-qPCR and the gene expression fold change of 3 days cultured CD14+ moDCs treated with control (NS) or *IL22RA2* (RA2) siRNAin different conditions. Units represent gene expression fold change relative to non-silenced control.

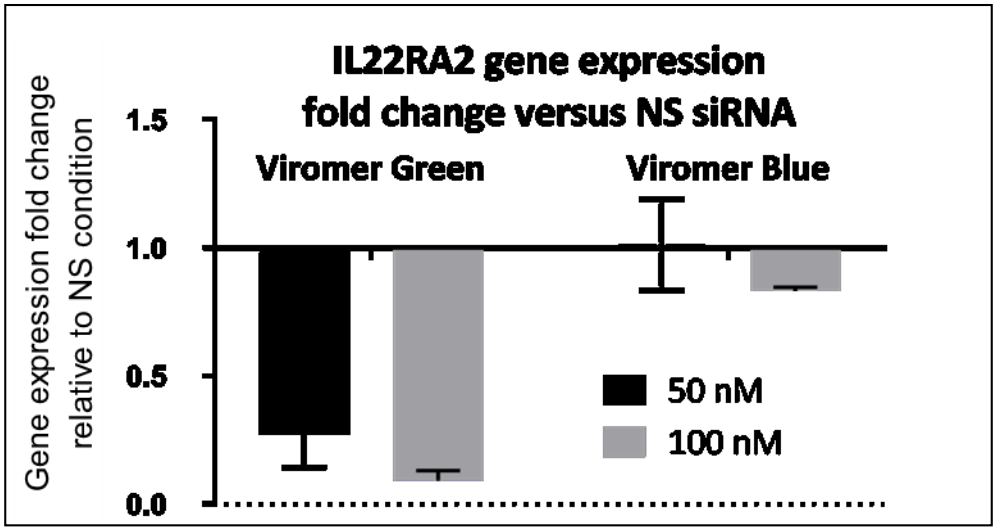

Figure 5.53. *IL22RA2* silencing in different concentrations. Gene expression fold change of moDCs treated with *IL22RA2* (RA2) siRNA with different Viromer type compared to non-silencing (NS) condition.

Given that that *IL22RA2* silencing was achieved in above described preliminary experiment, the silencing of the variants was addressed in a triplicate experiment in the best silencing condition. The ON-TARGET plus SMART pool human *IL22RA2* siRNA, as described in Materials and Methods, section 4.4.4.2 (siRNA), has four different siRNA that bind to the common sequence of *IL22RA2* gene, however we need to test if there could be any efficiency difference among the silencing of each variant. For that, qPCR analysis was performed in 3 days moDCs treated with *IL22RA2* siRNA assisted by Viromer Green using all variants amplifying *IL22RA2* BC primers and the in house designed *IL22RA2v1* and *IL22RA2v2* specific primers. The results (Figure 5.54) showed that the silencing worked on both isoforms equally, with the small difference been attributable to different primers affinity more than to isoform specific difference on silencing of the variants.

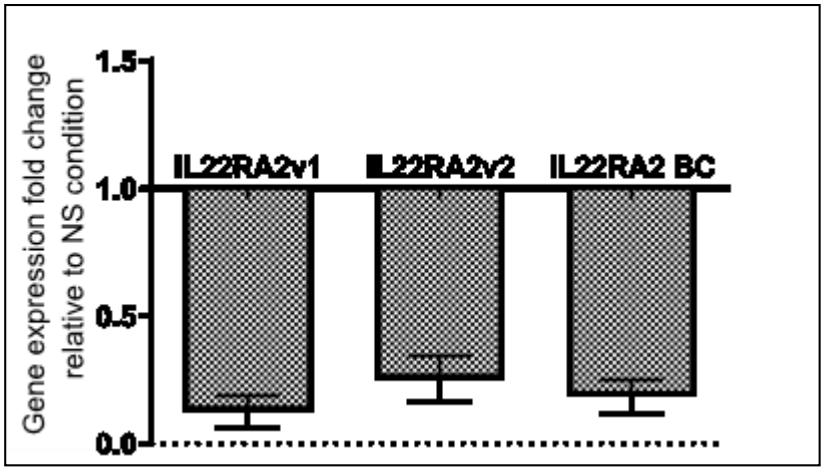

Figure 5.54. *IL22RA2* variant silencing. Gene expression fold change of 3 days cultured CD14+ moDCs treated with *IL22RA2* assisted by Viromer Green compared to non-silenced control CD14+ moDCs. Mean ± SEM (n=3).

5.1.3.2. *IL22RA2* silencing reduces *GRP78* and *ERP44* on moDCs

Even if we got important information regarding the type of Viromer, and the siRNA concentration that was better for *IL22RA2* silencing in all variants, we only tested on time point for silencing and we harvested the cells earlier than usual. In order to establish the best conditions for getting immature moDCs with the best *IL22RA2* silencing we considered different procedures. We knew that the *IL22RA2* expression increases during the differentiation process and that achieving good silencing levels might require more than one intervention. Based on our AM580 experience, where culturing cells with it from the beginning increases more the *IL22RA2* expression, we thought that the earlier we intervene the better results we would get also in the opposite direction. Viromer Green was designed to work on suspensions cells so we thought of silencing freshly isolated monocytes that were still in suspension. We designed four different silencing strategies (Table 5.10). Two approaches were made silencing in freshly isolated monocytes in day 0 only (A), or with a re-silencing in day 3 (B), being both harvested in day 6. Unsure of the ability of the silencing of the suspension monocytes we designed two strategies where the silencing was done in attached monocytes, like in the previous experiment. One of

them (C) have the silencing on day 1, re-silenced on day 4 and harvested on day 7. The last one (D) was the latest to be silenced, on day 2 of culture, with the idea that at the beginning of the differentiation process there is little *IL22RA2* expression, and therefore a bit later intervention may be able to hold the effect during the differentiation process until day 6. We decided to set the experiment to get information about both *IL22RA2* gene expression and IL-22BP levels. For that, at the harvesting point, we divided the cells of each condition, to get RNA and cell lysate.

	DAYS OF CULTURE							
CONDITION	**0**	**1**	**2**	**3**	**4**	**5**	**6**	**7**
A	S						Harvest	
B	S			S			Harvest	
C		S			S			Harvest
D			S				Harvest	

Table 5.10. *IL22RA2* silencing schemes. S: silencing.

Regarding the *IL22RA2,* gene expression, that was addressed by qPCR, two of the conditions, A and B, showed a marked reduction when comparing NS to RA2 of about 40-fold change (Figure 5.55). Those conditions were also the ones showing the highest expression in NS control. In the conditions C and D, the *IL22RA2* silenced sample showed just slightly higher *IL22RA2* expression than A and B conditions, but the NS expression level was clearly lower and that made the reduction fold change about a bit more of half of the mentioned two first conditions.

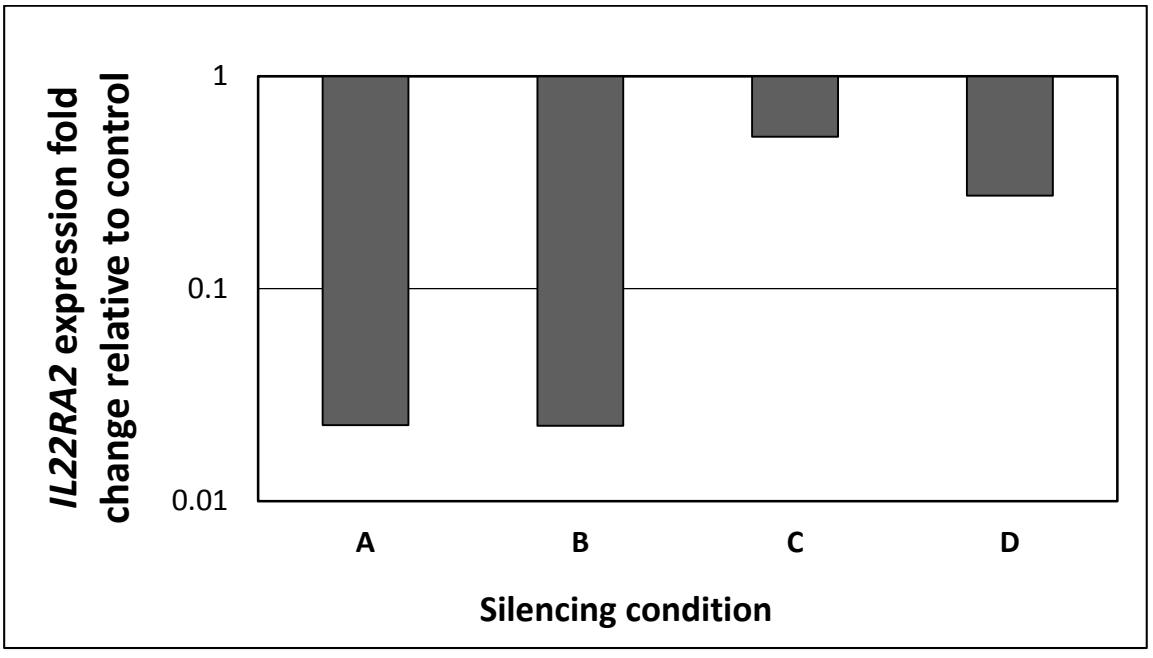

Figure 5.55. *IL22RA2* expression fold change of silenced vs control moDCs.

Regarding the IL-22BP protein levels, they were addressed by the in house made IL-22BP ELISA (Figure 5.56). The relations observed on gene expression did not completely repeat at the protein level. Condition B, showed a four times reduction of the protein levels, and the highest protein concentration on the NS sample. Condition A had a more modest effect, reducing half of the protein level when compare to NS. Finally, conditions C and D, that showed a moderate gene expression, also showed a moderate protein level reduction of around 35%.

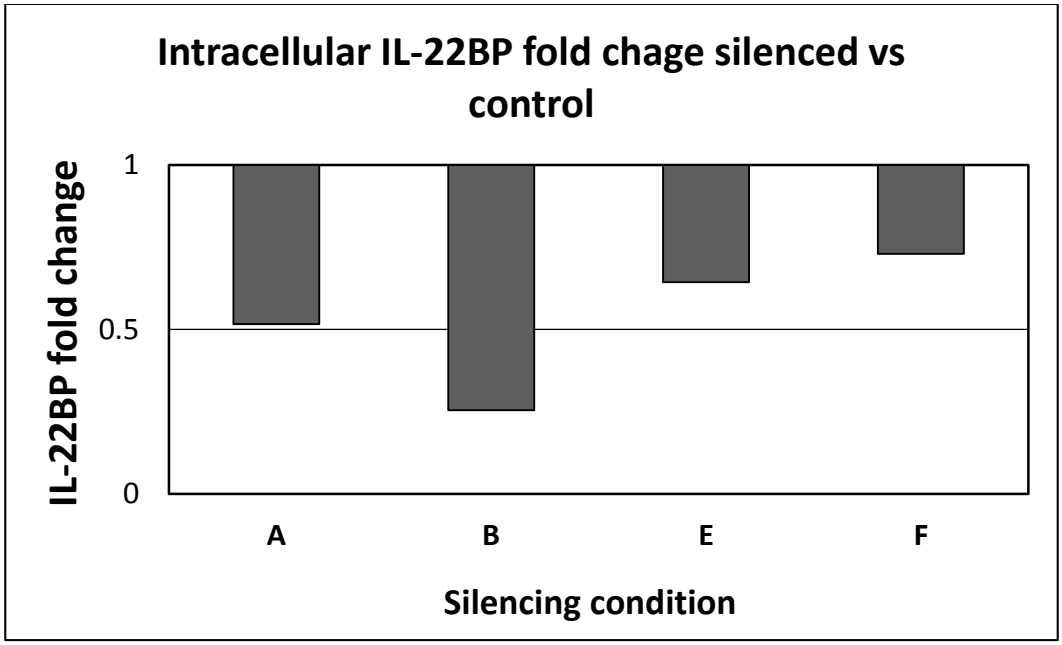

Figure 5.56. IL-22BP concentration fold change of silenced vs control moDCs.

Taken together the results gave a clear way to go. Conditions C and D reduced both mRNA and protein concentration, but only showed a moderate effect. Conditions A and B, were the best performing conditions, and had different features in common. In both there was a silencing in freshly isolated monocytes that were in suspension, showing the Viromer Green ability to silence them and the relevance of doing the silencing at the very beginning of the cell culture. The two conditions were also harvested on day 6 of culture. However, condition B, outperformed condition A on reducing protein expression by two-fold, likely, because it has a second silencing on day 3 that condition A did not have. Due to this results condition B, consisting on a strategy of

generating moDCs for six days with siRNA silencing of *IL22RA2* in freshly isolated monocytes (day 0) and right after the medium change on day 3, was chosen for future experiments.

With a proper moDC silencing scheme set in place (Table 5.11), we were able to investigate the indication of a relationship between *IL22RA2* expression and GRP78 suggested by the Results, section 5.1.2.2 (GRP78), performing a large experiment. Considering the ability of AM580 to boost the expression of *IL22RA2*, with no isoform discrimination, we consider using it also in order to see if the increased *IL22RA2* expression may increase the difference with the silenced counterpart.

DAYS OF CULTURE							
0	**1**	**2**	**3**	**4**	**5**	**6**	**7**
SI			SI			Harvest	

Table 5.11. *IL22RA2* silencing scheme. It was used for 6-day CD14+ moDCs experiment with and without AM580. SI = silencing induced days; Harvest = day of harvest.

Following the silencing scheme, the monocytes of each of the donors were divided on 8 different wells, with duplicates the four conditions used, with or without *IL22RA2* silencing, and with or without AM580 (Table 5.12). The experiment have duplicates of each condition to check two different time points: day 3 and day 6 of culture.

		NS Control	NS AM580	RA2 Control	RA2 AM580
Silencing	**NS**	+	+	-	-
	IL22RA2	-	-	+	+
Culture additive	**None**	+	-	+	-
	AM580	-	+	-	+

Table 5.12. *IL22RA2* silencing culture conditions. NS Control: non-silenced untreated moDCs; NS AM580: non-silenced AM580 treated moDCs; RA2 Control: *IL22RA2* silenced untreated moDCs; RA2 AM580: *IL22RA2* silenced AM580 treated moDCs.

Apart from *IL22RA2* and GRP78 genes, other genes whose expression was upregulated in HEK293 cells transfected with IL-22BPi1 or Il-2EX4 (Gómez-Fernández et al., 2018) were

studied. In accordance with them, *GRP78* and *ERP44* were the genes that showed a significant decrease on *IL22RA2* silenced samples (Figure 5.57). While the effect on *GRP78*, the strongest IL-22BPi1 interacting partner, showed a significant reduction both in control and AM580 treated moDCs, the effect on *ERP44* was only significant in AM580. The *IL22RA2* inducing properties of AM580 explain why the silencing effect is more accentuated in AM580 treated samples when comparing to the control. Altogether, we showed that *IL22RA2* expression level in immature moDCs influences *GRP78* expression level and confirmed the observations made in HEK293 cells.

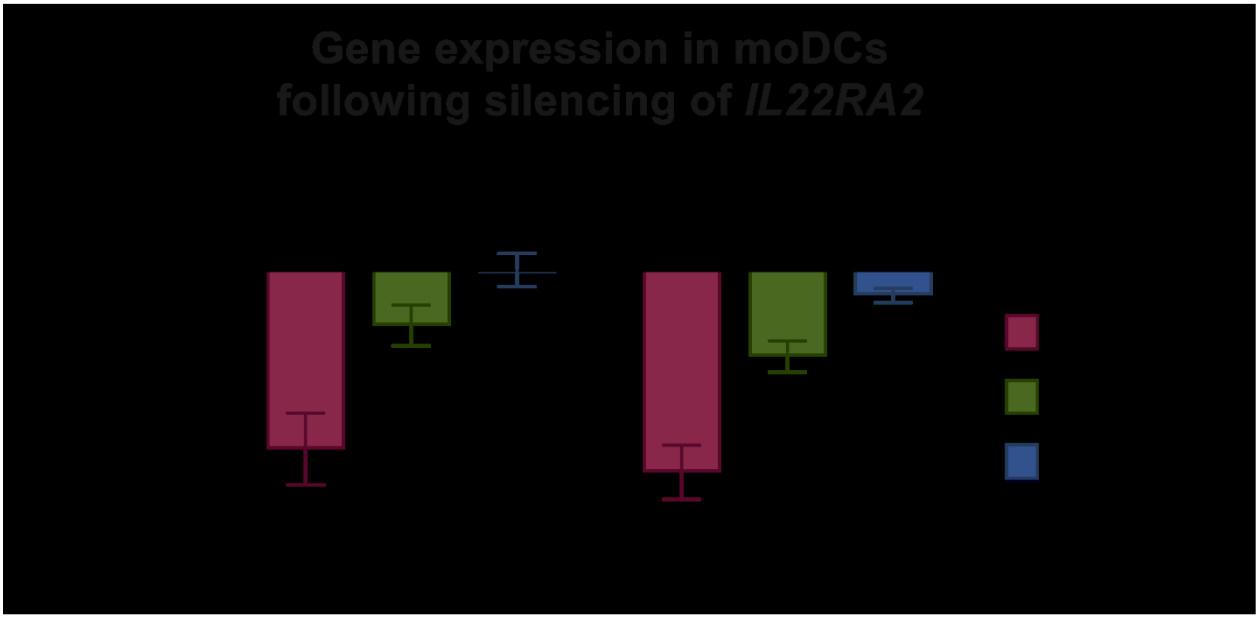

Figure 5.57. *IL22RA2* silencing effect on 6-day moDCs. CD14+ monocytes were cultured in DM in the absence or presence of AM580 starting on day 0 up to the day o harvest, and silenced as expressed in Table 5.10 Gene expression levels of *IL22RA2*, *GRP78*, and *ERp44* were measured over 6 (control) and 5 (AM580) independent samples by RT-qPCR. Bars represent average of gene expression fold change (Mean ± SEM) relative to non-silencing control based on the housekeeping gene *HPRT1*. *p < 0.03 by Wilcoxon test (n=3).

5.2. *IL12A*

5.2.1. *IL12A* variants characterization in different cell lines and moDCs

Due to the lack of information on *IL12A* variants, its study was performed using variants discriminating primers described in section 4.2.3. (*IL12A* variants). Three different PCRs were performed for this goal and canonical *IL12A* vector was used as a positive control. Based on previous research supporting a possible role of *IL12A* on cancer (Kubin et al., 1994; Roszak et al., 2012; Sattler et al., 2000; Shi et al., 2016; Yue et al., 2016) we tested the all the available cancer cell lines in the lab. Apart from them moDCs were also tested being a perfect primary cell candidate since both DCs and moDCs produce IL-12 and IL-35 when stimulated with a maturation stimuli like IFNγ and LPS (Dixon et al., 2015; Ebner et al., 2001). The use of IFNγ and LPS as an stimuli, apart from moDCs, also made sense in rest of the cell lines since all nucleated cells respond to IFNγ (Castro et al., 2018) and tumor cells express TLR4 (J. Li et al., 2017) which is responsible for LPS response. For understanding purposes, the structure of the content and figures goes PCR by PCR and follows the sequence: first, information of primers and amplicons; second, results of moDCs and HEK293 and U937; and last, results of cell lines (including HEK293 and U937).

The first of the PCR was able to generate variants specific amplicons for variants 201, 203, 205 and 206 (Figure 5.58). The results of both, different samples of moDCs (Figure 5.59) and the different cell lines (Figure 5.60) were the same. Unsurprisingly, the only observable amplified product had 313 bp size, corresponding to the expected size for the canonical variant, *IL12A-201*; but as shown in Figure 5.54, another variant, *IL12A-206*, characterized by an small retained intron between exon 4 and 5, also give the same amplification product and therefore the its expression could not be excluded.

None of the two other possible bands was detected. One smaller, of 199 bp, corresponding with *IL12A-205*, which lacks one of the canonical variant exons. The other one bigger, of 638 bp, corresponding with variant *IL12A-203*, which retains three of the introns of the canonical variant. With these results, we considered that the level of the expression of the variants 203 and 205 was if not absent at least several order of magnitude smaller than the combined expression of variants 201 and 204. This was the only of the three PCR that could detect *IL12A-205*, one of the two variants that lack one of the exons present on the canonical variant.

Primer pair for the amplification of variants *201, 203, 205*, and *206*

For the recognition of the variants *201, 203, 205* and *206*, primers FW1 and RV1 were used. As represented below, the amplified sequence starts in exon 1 and go until exon 4.

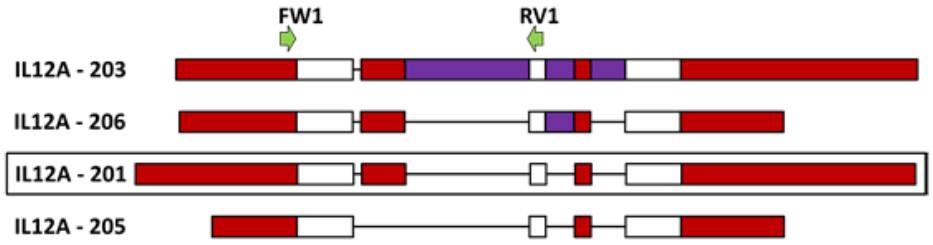

	AMPLICON
IL12A_203	638 bp
IL12A_206	313 bp
IL12A_201	313 bp
IL12A_205	199 bp

	Sequence (5'->3')
Forward primer	GCTCAGCATGTGTCCAG
Reverse primer	GGTCTCTCTGGAATTTAGGC

	Template strand	Length	Tm	GC%	Self-complementarity	Self-3' complementarity
Forward primer	Plus	17	55.18	58.82	5.00	1.00
Reverse primer	Minus	20	55.23	50.00	4.00	2.00

Figure 5.58. Information on primers and their amplified products of the IL12 variants PCR1.

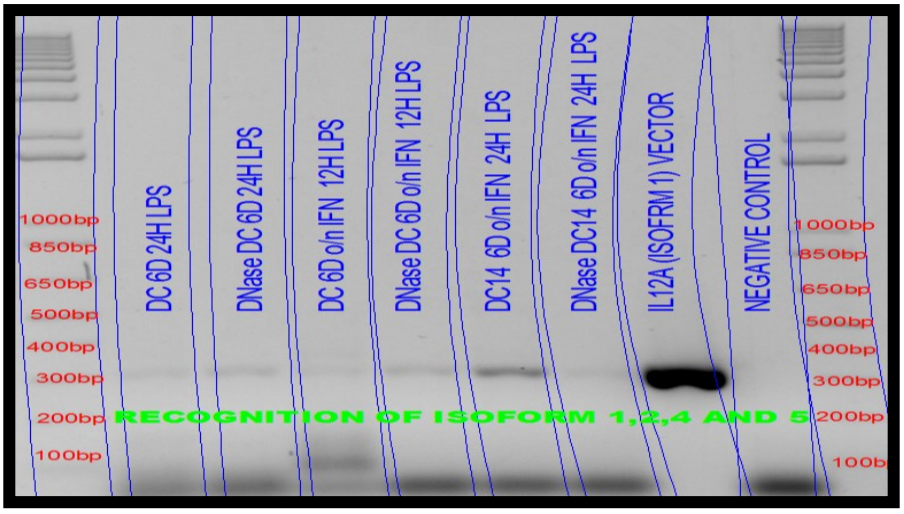

Figure 5.59. PCR1 results in moDCs. Figure representative of three different experiments.

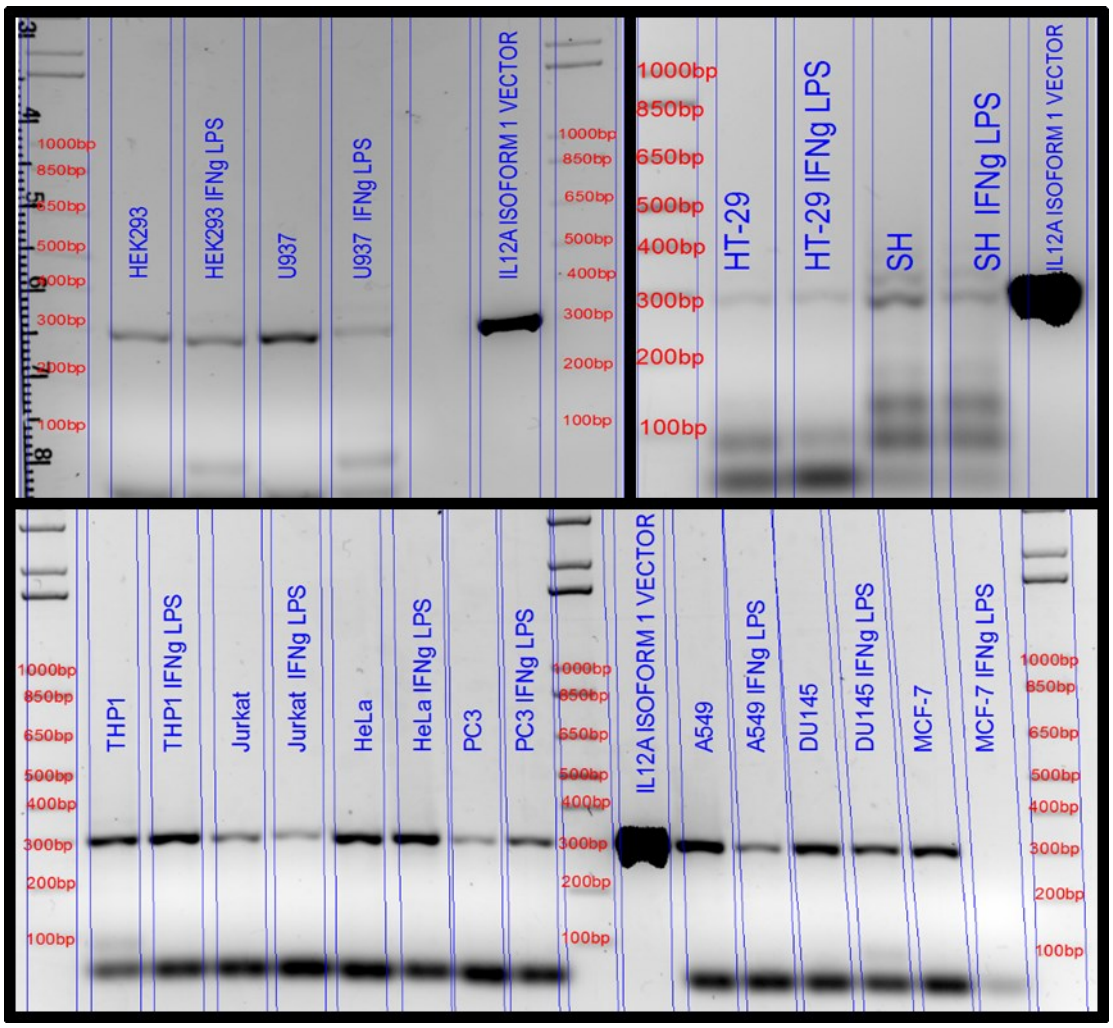

Figure 5.60. PCR1 results in cell lines. Figure representative of three different experiments.

The possibility of the presence of the canonical variant overshadowing the other variants was considered and was one of the reasons for the design of the PCR 1.1. The PCR 1.1, as explained in Figure 5.61, was able to amplify the exon retained in variants *203* and *206*. The results of the PCR1.1 brought an interesting observation, consistent with the results of the PCR1: the expression of variant *206* was observed both on moDCs (Figure 5.62) and in cell lines (Figure 5.63), while expression of variant *203* remained not detectable. The detection of the variant *206* raised the question about the level of expression in comparison with the canonical variant because it was clear that both variants were contributing to the amplified product detected on the PCR1.

Primer pair for the amplification of variants *203* and *206*

For the recognition of the variants 3 and 6, primers FW1 and RV1.1 were used. As represented below, the amplified sequence starts in exon 1 and go until retained intron 4.

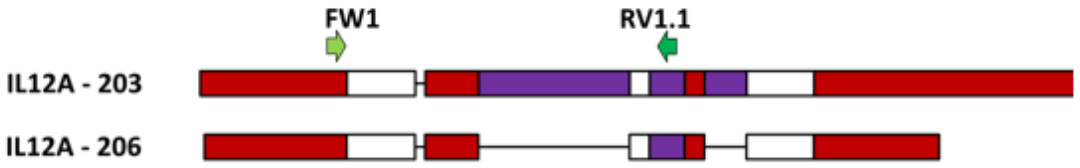

	AMPLICON
IL12A_003	712 bp
IL12A_006	387 bp

	Sequence (5'->3')
Forward primer	GCTCAGCATGTGTCCAG
Reverse primer	TAATCAGACATCAGTGATATGAAT

	Template strand	**Length**	**Tm**	**GC%**	**Self-complementarity**	**Self-3' complementarity**
Forward primer	Plus	17	55.18	58.82	5.00	1.00
Reverse primer	Minus	24	53.40	29.17	7.00	4.00

Figure 5.61. Information on primers and their amplified products of the IL12 variants PCR 1.1.

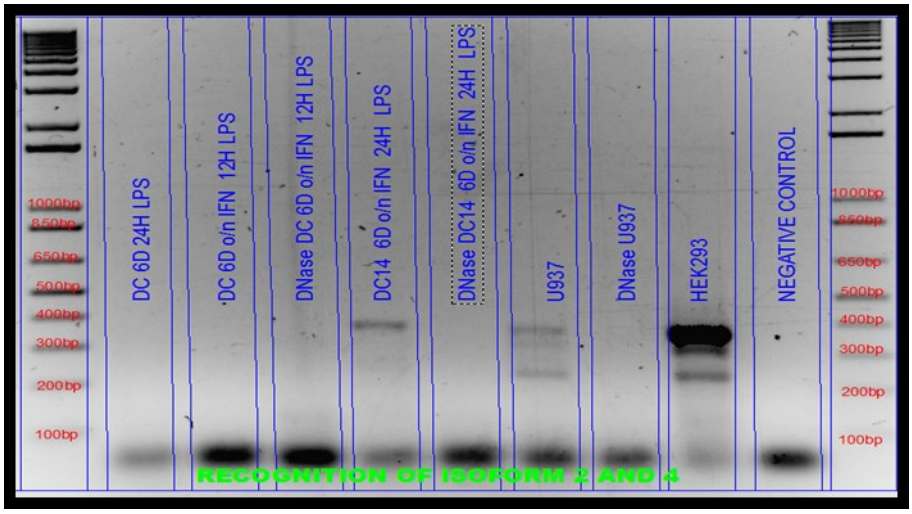

Figure 5.62. PCR1.1. results in moDCs and U937 and HEK293 cell lines. Figure representative of three different experiments.

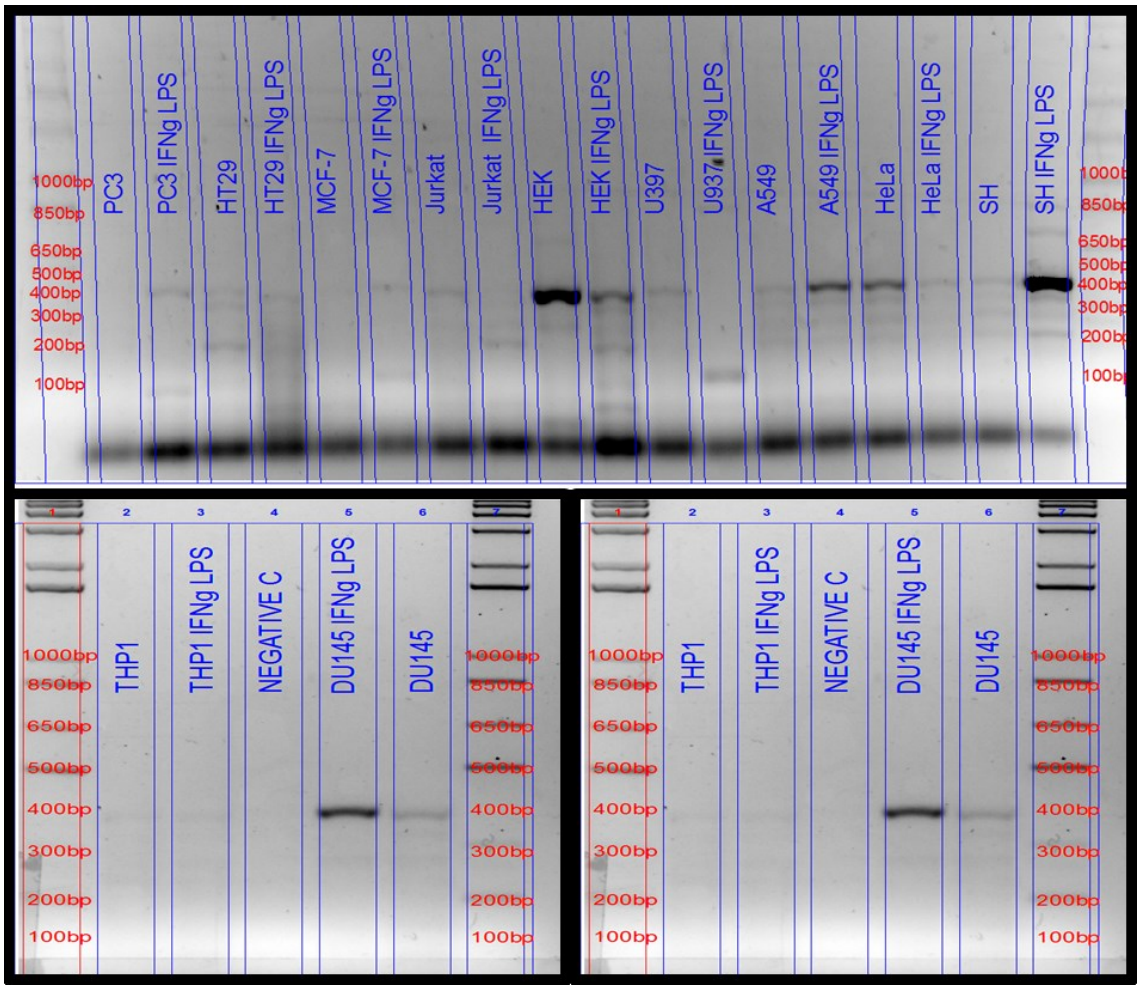

Figure 5.63. PCR1.1 results in cell lines. Figure representative of three different experiments.

For the purpose of undercover *IL12-201* and *IL12-206* differences it was designed a third PCR, PCR2 (Figure 5.64). This PCR was the only of the three able to amplify *IL12A-202*, a variant that lacks one of the exons of the canonical *IL12A*. As explained in Figure 5.62, this PCR has also the ability to amplify genomic DNA.

Primer pair for the amplification of variants *201*, *202*, *203*, and *206*

For the recognition of the variants *201*, *202*, *203* and *206*, primers FW2 and RV2 were used. As represented below, the amplified sequence starts in exon 3 and go until exon 6.

	AMPLICON
IL12A_203	659 bp
IL12A_206	243 bp
IL12A_201	168 bp
IL12A_202	126 bp

	Sequence (5'->3')
Forward primer	ACAAAAGATAAAACCAGCACAGTG
Reverse primer	GTCTTCATAAATACTACTAAGGCACA

	Template strand	Length	Tm	GC%	Self-complementarity	Self-3' complementarity
Forward primer	Plus	24	58.41	37.50	5.00	5.00
Reverse primer	Minus	26	56.83	34.62	6.00	3.00

Figure 5.64. Information on primers and their amplified products of the IL12 variants PCR 2.

The PCR 2 clearly confirmed the previous results: the canonical variant, *IL12-201*, is the most expressed variant and only one of the other variants, *IL12-206*, could be detected in significant amount even when compared with it both on moDCs (Figure 5.65) and cell lines (Figure 5.66).Regarding the rest of the variants, no detection of variant *IL12A-202* or *IL12A-205* was achieved on the PCRs. The variant *203* was not the detected in the previous two PCRs, and the fine band present in PCR2, could be as explained by genomic DNA, therefore we conclude that in the context of the studied samples, its expression extremely low or absent. As initially explained these primer pairs were not able to amplify *IL12A-204*.

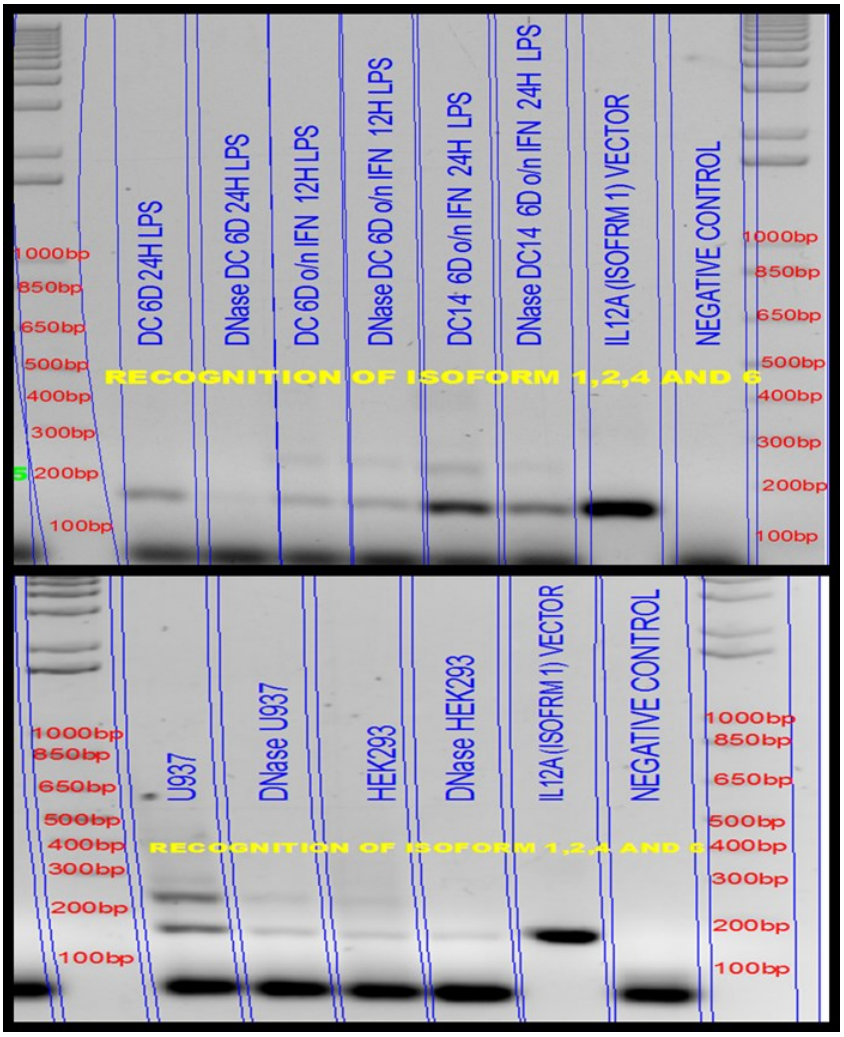

Figure 5.65. PCR2 results in moDCs and U937 and HEK293 cells. Figure representative of three different experiments.

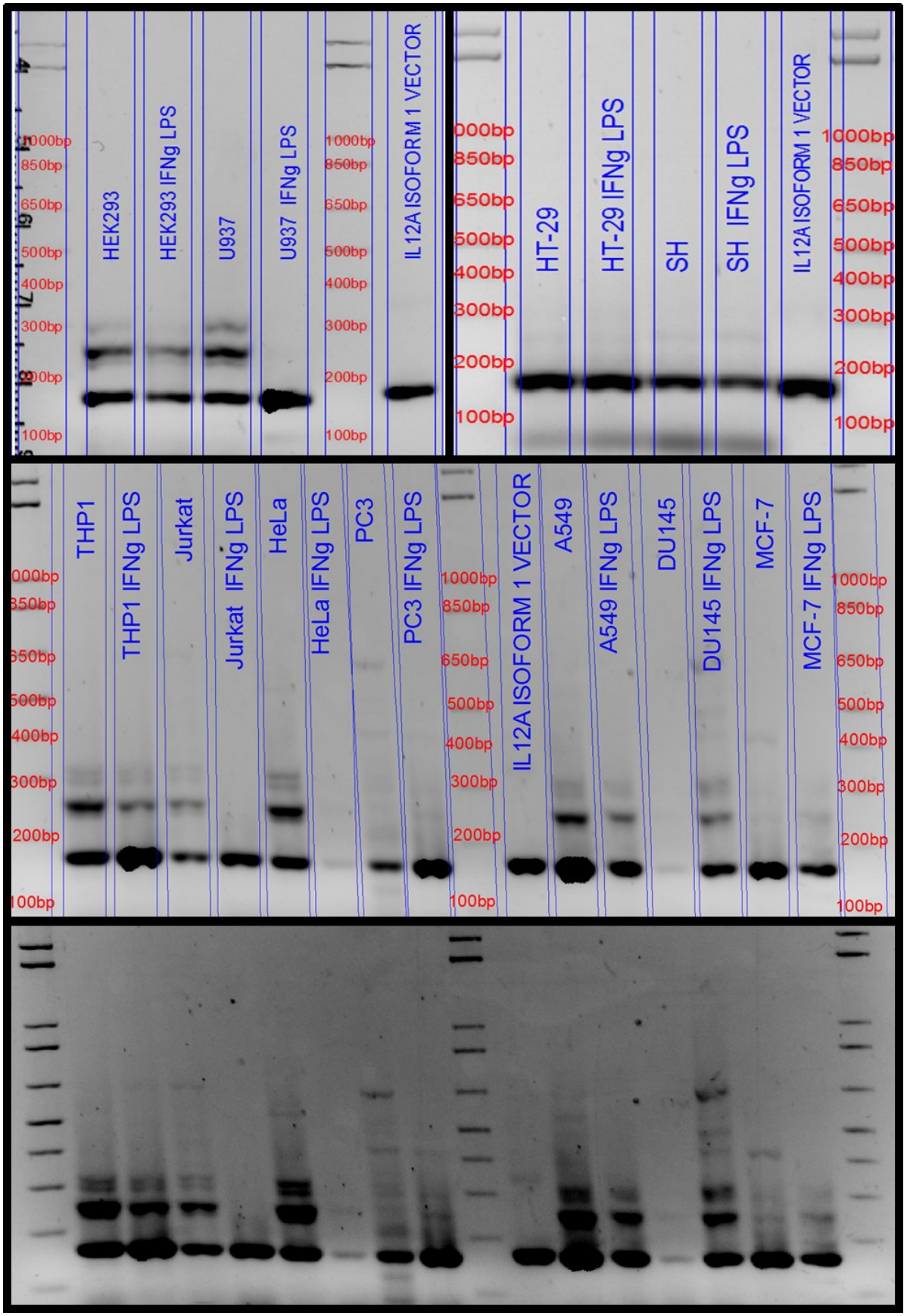
HEK293
HEK293 IFNg LPS
U937
U937 IFNg LPS
IL12A ISOFORM 1 VECTOR
HT-29
HT-29 IFNg LPS
SH
SH IFNg LPS
IL12A ISOFORM 1 VECTOR
THP1
THP1 IFNg LPS
Jurkat
Jurkat IFNg LPS
HeLa
HeLa IFNg LPS
PC3
PC3 IFNg LPS
IL12A ISOFORM 1 VECTOR
A549
A549 IFNg LPS
DU145
DU145 IFNg LPS
MCF-7
MCF-7 IFNg LPS
1000bp
850bp
650bp
500bp
400bp
300bp
200bp
100bp

Figure 5.66. PCR2 results in different cell lines. In the central image, a band corresponding 650 bp is the expected size for *IL12A-203*. In the lower image, increasing the contrast is more clearly seen. However, in this PCR the amplification of the genomic sequence of *IL12A* and *IL12-A203* is the same since the variant retains all the introns in the amplified sequence, and some genomic DNA contamination cannot be excluded. The lack of the *IL12A-203* in the first PCR, that do not amplify genomic DNA, supports absence of the variant. Figure representative of three different experiments.

The presence of the IL12-006 variant along with the canonical *IL12-201*, but no of the other variants, was true for both moDCs and cell lines. Among the cell lines there is a large diversity, among them cell lines their selves, their *IL12A-203* expression and the effect on the expression of stimulating with IFN$_\gamma$ and LPS. On the table 5.13, there are summarized the main results obtained regarding the variant *IL12-206*. IFN$_\gamma$ and LPS have an effect on *IL12A* expression in almost all the cell lines, but with different behavior depending on the cell line. Both decreasing and increasing of *IL12-206* expression were observed. Some cell lines showed contradictory results, like A549, with an increase of the variant in the presence of IFN$_\gamma$ and LPS in PCR1.1 and a decrease in PCR2, or the detection in one of the PCRs was little problematic such as in DU145, HT-29, PC3 or SH. While in HT-29 was difficult to see any difference, PC3 and SH cell lines showed a clear increase in PCR1.1. A confirmed increase on *IL12-206* level in both PCRs was observed for MCF7 cell line. The rest of cell lines with the same pattern in both PCRs were showing a decreasing trend.

In our effort to understand *IL12A-206,* we decided to analyze the IFN$_\gamma$ and LPS in the canonical *IL12A-201* to see if the trend was always the same or not. For that we analyzed the results of the PCR2, were we could observe the presence of the two variants at the same time, in the cell lines showing clear and consisted *IL12A-206* trend in the two PCR. As explained before, the main trend was to decrease except for MCF7 cell line, but the results of *IL12A-001* where different. While half of the candidates showed an increase of the canonical variant upon stimulation with IFN$_\gamma$ and LPS, the other half showed a decrease. We saw that the cell lines with

an increase in the canonical variant after IFN$_\gamma$ and LPS were immune system derived cells while the epithelial cell showed a decrease (Table 5.14).

CELL LINE	PCR 1.1		PCR 2	
	Unstimulated	Stimulated with IFN LPS	Unstimulated	Stimulated with IFN LPS
A549	✓	✓✓	✓✓	✓
DU145	✓✓	✓	✓	✓
HEK	✓✓	✓	✓✓	✓
HELA	✓	✓↓	✓✓	×
HT-29	✓	✓	~✓	~✓
JURKAT	✓	×	✓	×
MCF7	×	✓	×	✓
PC3	×	✓	×	~✓
SH	✓	✓✓	~✓	~✓
THP1	~✓	~✓	✓✓	✓
U937	✓	×	✓✓	×

Table 5.13. Presence level of *IL12A-206* in cell line samples. ✓: detection of the presence; ✓✓: strong detection; ✓↓: detection of the presence that is lower than the detection in the other condition; ×: no detection; ~✓: limited or unclear detection.

With the obtained results, it was clear that the *IL12A-206* expression is detectable along many cell lines and needs to be addressed for the understanding of the *IL12A* gene. It also significant that in immune derived cell lines is regulated, with a decrease when IL-12 that needs the canonical *IL12A-201*, that also increases. If *IL12A-206* is also a premature messenger RNA that allows the cells to have a storage pool of almost ready canonical mRNA that in the event of activation is rapidly spliced, or if the non-canonical variant can compete for translation and eventually association with IL12p40 or EBI3 to form IL-12 or IL-35 remains as an open question.

Sample	*IL12A-201*		*IL12A-206*		Tissue	Cell type	Culture
	Detection	Effect	Detection	Effect			
THP1	✓	Increase	✓	Decrease	Peripheral blood	Monocyte	Suspension
+ IFNγ LPS	✓		✓				
JURKAT	✓	Increase	✓	Decrease	Peripheral blood	T lymphocyte	Suspension
+ IFNγ LPS	✓						
U937	✓	Increase	✓	Decrease	Pleural effusion	Lymphocyte	Suspension
+ IFNγ LPS	✓						
HELA	✓	Decrease	✓	Decrease	Cervix	Epithelial	Adherent
IFNγ LPS	✓						
HEK	✓	Decrease	✓	Decrease	Embryonic kidney	Epithelial	Adherent
+ IFNγ LPS	✓		✓				
MCF7	✓	Decrease		Increase	Mammary gland	Epithelial	Adherent
IFNγ LPS	✓		✓				

Table 5.14. Effect of IFNγ and LPS on *IL12A* variants *201* and *206* in cell lines based on their origin.

.

6. DISCUSSION

This work may be considered as one of the myriad of the studies that have been conducted to understand the genetic background of different diseases. The comprehension of the genetic background of the disease has been one of the most powerful tools for unveiling of the mechanisms of many diseases. According to prestigious database Online Mendelian Inheritance in Man (OMIM, 2022) there are up to 7,200 genetically affected disease phenotypes including single-gene disorders, somatic cell genetic diseases and susceptibilities to cancer and complex diseases. More than 4,600 genes with phenotype-causing mutation have been identified, the large majority, around 4,300 of them, linked to single gene disorders and traits, and in some cases, linked to susceptibility to complex diseases as well.

MS is one of those complex diseases, and the genetic factors are the major contributors to individual differences in MS susceptibility, and the role of genetic variants may be the key to understanding its pathogenesis (He et al., 2021). As explained in the sections 2.1.6 and 2.2.1 of the introduction, GWAS have been performed to identify the genomic risk loci of MS. The results of GWAS studies have sometimes provided insight into disease biology, for example a GWAS implicated the IL-12/IL-23 pathway in Crohn's diseases supported the clinical trials for drugs targeting the IL-22/IL-23 pathway (Uffelmann et al., 2021). Both *IL22RA2* and *IL12A* have been identified as a genomic risk loci of MS (IMSGC, 2019b) and therefore their detailed functional study was a needed contribution for better understanding of their role in MS. The *IL22RA2* coded IL-22BP protein exerts its functions through the blocking of IL-22 and therefore, the roles of both *IL22* and *IL22RA2* genes and their respective proteins IL-22 and IL-22BP are covered in this discussion although their roles are not yet clearly understood since protective and deleterious effects have been described in different cells and conditions.

In this context, our findings about *IL22RA2* expression and IL-22BP secretion highlight the particularities of this soluble receptor of IL-22. With the purpose of making the discussion of the mentioned results in an organized and clear way, different sections have been made. The three

initial sections give a general perspective of the current knowledge in the matter that serves as a basis for the detailed discussion of the results in the last sections. The first block containing the general perspective starts with a section about IL-22, since the IL-22BP effects are the results of its blocking, in animal models of autoimmunity diseases affecting the CNS. The next section describes the current knowledge obtained in animal models regarding IL-22BP. The last section of the block summarized the information about the role of IL-22 and IL-22BP in MS patients. After giving a general view of the field of study, the discussion of the results are structured in three sections parallel to the structure of the results themselves. In this way, the results relative to *IL22RA2* expression presented in section 5.1.1 of the results are discussed in the section 6.4 of the discussion; the ones relative to secretion of IL-22BP (of the homonym section 5.1.2. of the results) go after; and finally the relatives to *IL12A* are discussed in the closing section 6.6.

6.1. IL-22 effects in animal models

Together with IL-17, IL-22 seems to compromise the BBB integrity, enabling lymphocyte ingress into the CNS, which raises the possibility that this cytokine may contribute to MS severity (Kebir et al., 2007). A study in Lewis rats showed that expression of IL-22 is increased during the acute phase of EAE and decreased in its recovery phase (Almolda et al., 2011). Studies regarding IL-22BP in EAE support a role for IL-22BP during priming the periphery rather than during the effector phase or the response in the CNS (Lindahl et al., 2019). A protective function of IL-22BP may happen in murine glioma where IL-22 enhances symptoms, while diminishing expression levels, either with IL-22 KO mice or IL-22 neutralizing antibody demonstrated protective effect on glioma development (Liu et al., 2017).

In contrast, other CNS autoimmune diseases models, like experimental autoimmune uveitis, that targets the neural retina and related tissues (Agarwal et al., 2012) and in Theiler's

virus-induced demyelination, support a protective role of IL-22. In the experimental autoimmune uveitis model, the administration of IL-22 on day 4 and 8 after immunization results in milder disease (Ke et al., 2011), while the IL-22 KO exacerbates the pathology when compared to wild type (Mattapallil et al., 2019). In Theiler's virus induced demyelination in mice, epitope-specific $CD8^+$ T cells causing minimal cytotoxicity in the CNS expressed a higher level of IL-22 mRNA than highly cytotoxic $CD8^+$ T cells (Myoung et al., 2012).

This dual role of IL-22 has been reported in other diseases, i.e. in cardiovascular diseases. On the one hand, it plays a role in inhibiting inflammation and protecting the normal function of the heart in myocarditis, atherosclerosis and myocardial infarction. On the other hand, IL-22 participates aggravating disease progression in aortic dissection and myocardial hypertrophy (Che et al., 2020).

6.2. IL-22BP effects in animal models

The role of IL-22BP in disease is being elucidated, mainly through analysis of transgenic animals with the deletion of *il22* or *il22ra2* gene in different disease experimental models, were both beneficial and detrimental effects in disease on a context dependent manner have been reported.

The first report was in a colon cancer model of DSS-induced colitis, where *il22ra2* KO mice was associated with increased tumor burden, which was attributable to excessive IL-22 that showed during intestinal tissue damage, both protective (during the peak) and detrimental (during recovery) effects (Huber et al., 2012).

Pathogenic effects through blockage of protective IL-22 have been described in different models. In *ulcerative* colitis, a model of $CD4^+$ T cell transfer colitis, donor IL-22BP deficient $CD4^+$

T cells induced less epithelial damage indicating that IL-22BP aggravates colitis (Pelczar et al., 2016). In line with it, in respiratory diseases, *il22ra2* KO mice are more resistant to pneumococcal lung infection than wild type mice and that is correlated with increased IL-22 at the baseline as well as increase IL-22 in the lung after infection with pneumococcus (Trevejo-Nunez et al., 2019). *il22ra2* KO mice are also protected during influenza suggesting IL-22BP proinflammatory role that impair epithelial barrier function (Abood et al., 2019).

On the contrary, in the liver, during acute liver damage induced by two clinically relevant models the IL-22BP-deficient mice showed greater damage, finding that endogenous IL-22BP has protective effect (Kleinschmidt et al., 2017). IL-22BP-deficient mice also showed impaired antigen uptake by the Peyer's patches, a gut associated lymphoid tissue (Jinnohara et al., 2017). The most clear context where IL-22BP has demonstrated a protective effect is in experimental psoriasis models, where il22bp KO exacerbates skin inflammation in rats (Martin et al., 2017) and mice (Fukaya et al., 2018) and where results were pharmacologically confirmed by using an IL-22BP neutralizing antibody (Martin et al., 2017) or recombinant proteins (Fukaya et al., 2018).

Specifically regarding MS, different studies have been carried out in EAE model and all point towards a detrimental effect of *il22ra2.* Il22 deleted mice do not have altered clinical or histopathological presentation of EAE (Kreymborg et al., 2007), but *il22ra2* KO mice have less severe EAE, displaying reduced CNS inflammation and demyelination, with significant reduction in the relative proportion as well as the total cell number of inflammatory monocyte/macrophages (mouse counterpart to human classical monocytes) (Laaksonen et al., 2014). The *il22ra2* KO mice showed an overall less severe disease course as compared to wild-type littermates (Laaksonen et al., 2014), and the same was true for an inducible IL-22BP knockdown in rats (Lindahl et al., 2019). Further EAE experiments in mice, comparing *il22* or *il22ra2* genes heterozygous, individual or joint deletion, showed that heterozygous deletion of *il22ra2* was sufficient to achieve the

protective effect previously reported and that the protective effect of *il22ra2* was lost when *il22* was also deleted (Lindahl et al., 2019).

However, the detrimental effect of *il22ra2* observed in EAE might not perfectly mirror *IL22RA2* in humans with MS. In EAE models, neuroinflammation, subsequent paralysis and physical disability are induced by active immunization to identical genetic background mice, and lesions are predominantly found on the spinal cord (Rangachari & Kuchroo, 2013). Meanwhile, MS is strongly influenced by genetic polymorphisms, triggered by environmental factors, and has diverse clinical manifestations with lesions at both the brain parenchyma and spinal cord (Palle et al., 2017). The disparity between the EAE animal model and MS patients has been already shown in translational approaches with other cytokines (Table 6.1 and (Palle et al., 2017)). A good example is the case of interferons, both *Ifnb* and *Ifng* gene KO mice exhibit increase EAE severity, but while IFN-β is a first RRMS treatment, the intravenous infusion of IFN-γ exacerbates disease severity (Palle et al., 2017). The expected differences between the mouse model EAE and human MS for *il22ra2* and *IL22RA2* and may be even bigger. As explained in chapter 1.2.2 of the introduction, mice *IL22RA2* only codes for the counterpart of human *IL22RA2v2*, only presenting a protein equivalent to IL-22BPi2 (Wei et al., 2003; Weiss et al., 2004) and thus, there are clear limitations of the mouse model for the study of MS susceptibility *IL22RA2* gene. For this reason, it is so important to investigate human cells for a correct understanding of the gene, as has been carried out in this study.

GM-CSF	T cells	Elevated	*Gmcsf* KO mice completely resistant to EAE	Anti-GM-CSF mAb Otilimab approved for rheumatoid arthritis but not MS
			Ifnb KO mice increased EAE severity	First line treatment in RRMS
IFN-γ	T cells, NK cell, NKT cells	Elevated	*Ifng* KO mice increased EAE severity	Intravenous IFN-γ exacerbates disease severity
			Il1r1 KO mice resistant to EAE	
IL-10	T cells, macrophages, DCs, B cells	Reduced	*Il10* KO mice increased EAE severity	Not reported
			Il12a KO mice increased EAE severity	Anti-IL12/IL-23 p40 mAb Ustekinumab does not show efficacy in phase II trial
IL-17	T cells, NKT cells	Elevated	*Il17a* KO mice partially resistant to EAE	Anti-IL-17A mab Secukinumab reduces disease severity
			Il23r KO mice completely resistant to EAE	Anti-IL12/IL-23 p40 mAb Ustekinumab does not show efficacy in phase II trial
TNF-α	Macrophages	Elevated	*TNfrsf1a* KO mice partially resistant to EAE	Treatment with anti-TNF-α exacerbates disease severity

Table 6.1. Major cytokines contributing to the pathogenesis of MS and EAE. GM-CSF: granulocyte-macrophage colony-stimulating factor; IFN: interferon; IL: interleukin; TNF: tumor necrosis factor; DCs: DCs; pDCs: plasmacytoid DCs; NK: natural killer cells; NKT: nature killer T cells; RRMS: relapsing-remitting multiple sclerosis; mAb: monoclonal antibody. Bright orange background: strong disease improvement; Light green background: partial disease improvement; Red background: increased disease severity; Light red background: treatment inefficiency. *Source:* adapted from (Palle et al., 2017).

6.3. IL-22 and IL-22BP relevance in MS patients

The relevance of the role of IL-22 and IL-22BP in human disease has already been shown by some studies. For example in the Guillain-Barré Syndrome, an acute autoimmune-mediated

inflammatory demyelinating disease, CSF and plasma concentrations of IL-22 appear to correlate with severity of the disease (Li et al., 2012).

In MS, it has been reported that the level of IL-22 in the serum of MS patients with active disease was higher than in the serum of inactive and progressive MS patients and especially of healthy controls, while it was not detectable in the CSF of patients with active MS (Perriard et al., 2015; Xu et al., 2013). Regarding IL-22BP, a trend towards an increased secretion of IL-22BP in MS patients compares to healthy controls has been reported, and its detection in the CSF of 86% of active MS patients (Perriard et al., 2015). CSF level of IL-22BP correlates with magnetic resonance imaging lesion load in MS patients (Lindahl et al., 2019).

However, it is not known whether such elevations underline these disorders or, rather, represent a compensatory response of the host to limit inflammatory damage (Burmeister & Marriott, 2018). Therefore, the role of IL-22 in MS is still unclear. IL-22 is often described as a pleiotropic cytokine with a high degree of context dependency regarding its downstream effects (Sabat et al., 2014). The net inflammatory effects of IL-22 may be opposite between barrier surfaces and CNS (Lindahl et al., 2019). This double-edged role for IL-22 in viral infections has been described, where this cytokine promotes pathogen spread to the CNS, but also limits inflammatory damage within the brain once the BBB has been breached (Burmeister & Marriott, 2018). In line with this, the target for the combined IL-22/IL-22BP effect is not clear either. The IL-22 receptor, IL-22R1, expression has been documented in MS in barrier surfaces, such endothelial cells (Kebir et al., 2007), and the CNS, in astrocytes (Perriard et al., 2015) and oligodendrocytes (Lindahl et al., 2019). IL-22R1 expression in hematopoietic cells remains controversial. In fact, some groups have not reported any detection (Perriard et al., 2015; Wolk et al., 2004). Others have reported its presence in immune cells in disease, such us, T cells in EAE (Lindahl et al., 2019) or even myeloid cells in primary Sjögren's syndrome, a chronic systemic

autoimmune disease characterized by deregulated immune responses and a higher rate of non-Hodgkin lymphoma (Ciccia et al., 2015), opening the door for further studies in the matter.

Finally, the study of SNPs linked to MS in *IL22RA2* also reinforces the complex and dual role of this gene in MS. On the one hand, the main GWAS associated susceptibility variant in *IL22RA2* gene is rs17066096 (IMSGC et al., 2011, 2013) that has an intergenic location and misses functional effect in silico annotations (Gómez-Fernández et al., 2020). Patients carrying the risk genotype have higher *IL22RA2* expression in differentiated monocytes, but no increase in IL-22BP concentration in plasma or CSF was found (Lindahl et al., 2019). On the other hand, in our lab it was discovered another SNP in *IL22RA2*, rs28385692 (Vandenbroeck et al., 2012), a comparatively rare genetic variant in *IL22RA2* that is strongly (and likely independently of the primary GWAS signal) associated with MS that causes an AA change in the SP of IL-22BP (Gómez-Fernández et al., 2020). The study of all three isoforms of IL-22BP with and without the mutation in the SP, revealed a 50-60% reduction of secreted IL-22BP levels in all isoforms carrying the SP substitution comparing with the wild types in transfected HEK293 cells (Gómez-Fernández et al., 2020).

6.4. Relevance of the findings regarding the expression of *IL22RA2* gene

Taken together, current literature highlights the relevance of IL-22BP in the pathophysiology of MS and also the relevance of monocytes, the specific contribution of each subpopulation and their cytokine expression in MS, where the developmental sequence and the fate and plasticity of monocyte subpopulations are subjects of ongoing debate (Waschbisch et al., 2016). Our results contribute to better understand the complex and possibly dual role of IL-22BP in MS and give insights about the *IL22RA2* expression in natural producer cells.

Regarding the characterization of cell sources and expression levels of *IL22RA2*, we have achieved interesting results. First, in section 5.1.1.1 of the results, have we have confirmed that the human *IL22RA2* gene co-expresses three transcript variants in moDCs coding for three partially distinct proteins in agreement with other reports (Lim et al., 2016; Martin et al., 2014) and demonstrated that the expression ratio between variants is generally the same among different conditions.

We also found that *IL22RA2* is unique compared to a wide range of cytokines, namely IL4, IL10 family (*IL10*, *IL19*, *IL20. IL22*, *IL24*, and *IL26*), IL12 family (*IL12A*, *IL12B*, and *IL23A*) and interferon type I (interferon β, *IFNB*). In contrast with those cytokines, *IL22RA2* expression levels increase during moDC differentiation and down regulated by their maturation. This has been independently confirmed by recent studies (Lindahl et al., 2019).

We also tested U937 cells that exhibit many characteristics of the monocytes and are easy to use. A virtually unlimited number of relatively uniform cells can be prepared and thus, they have been used as the experimental model to elucidate mechanisms of monocyte and macrophage differentiation (Chanput et al., 2015). For instance, it has been an important model in the investigation of the mechanisms involved in monocyte-endothelium attachment (Liu et al., 2004). With regard to *IL22RA2* as shown in section 5.1.1.3 of results, U937 cells could model *IL22RA2* expression but showed a number of differences in the expression of other cytokines and were not able to show a strong characteristic maturation response of moDCs limiting their potential for the understanding of *IL22RA2* and IL22BP biology.

The recent advances in the implication of the different immune cells in MS also highlight the relevance of the findings presented in this work. Historically, autoreactive T cells have been the main cellular focus in pathogenesis of MS, as they can be detected in early lesions (Popescu & Lucchinetti, 2012), and autoreactive T cells directed against oligodendrocyte antigens can be

found in circulating $CD4^+$ T cells (Bielekova et al., 2004) and in lymph nodes of MS patients (van Zwam et al., 2009). Autoreactive clonally expanding B cells are also considered typical feature of MS (Prinz & Priller, 2017). However, growing evidence in EAE implies peripheral monocytes as a prominent cell type in early disease (Ajami et al., 2011) and the effector phase (Mildner et al., 2009), with monocyte participation in pro- and anti-inflammatory response in mice and humans (Waschbisch et al., 2016; Yamasaki et al., 2014).

In this context, the discovery of distinct *IL22RA2* levels according to monocyte subpopulation is very appealing since the three monocyte subsets, classical, intermediate and non-classical, express different antigen and cytokines and perform different functions (Wong et al., 2011, 2012) and are thought to be a result of a gradual maturation process (Patel et al., 2017; Tak et al., 2017). Similar subset exist in mouse (Table 6.2), but based on different markers (Ziegler-Heitbrock et al., 2010) and in different proportions (Yang et al., 2014), demonstrating again the limitations of animal models for the study of human chronic inflammatory and autoimmune diseases.

Human subsets	Surface markers	% of total monocytes	Mouse counterpart	Surface markers	% of total monocytes
Classical	$CD14^{++}CD16^-$	80-95	$Ly6C^{high}$ ($Ly6C^+$)	$CD11b^+CD15^+Ly6C^{high}$	40-45
Intermediate	$CD14^{++}CD16^+$	2-11	$Ly6C^{middle}$ ($Ly6C^+$)	$CD11b^+CD15^+Ly6C^{middle}$	5-32
Non-classical	$CD14^+CD16^{++}$	2-8	$Ly6C^{low}$ ($Ly6C^-$)	$CD11b^+CD15^+Ly6C^{low}$	26-50

Table 6.2. Human and mouse monocyte subpopulations by surface markers. CD: cluster of differentiation; Ly6C: lymphocyte antigen 6 complex. *Source:* adapted from (Yang et al., 2014).

Nonetheless, the impact of the minority populations (intermediate ($CD14^{++}CD16^+$) and non-classical ($CD14^+CD16^+$) has been reported in different chronic inflammatory and autoimmune diseases both in animal models and human patients. In a mouse model of arthritis, non-classical

monocytes are important as mediators of tissue destruction (Puchner et al., 2018) and their expansion was observed in Sjögren's syndrome (Wildenberg et al., 2009). In the case of coronary artery disease, there is a shift from classical to intermediate monocytes (Höpfner et al., 2019), and in psoriasis the absolute count of intermediate and non-classical monocytes was increased in patients (Kouris et al., 2014). In the case of severe asthmatic patients enhanced frequencies of intermediate but not non-classical monocytes on peripheral blood was observed and the inhaled glucocorticoid treatment modulate both populations differently (Moniuszko et al., 2009). Intermediate monocytes in peripheral blood are also boosted in active Crohn' disease, particularly in patients with high Crohn's disease activity index and colonic involvement (Koch et al., 2010), and in rheumatoid arthritis where they correlate with Th17 cells (Rossol et al., 2012).

Regarding monocyte subpopulations in MS, different studies have highlighted differences regarding in $CD16^{+}$ monocytes in MS patients compared to healthy controls (Chuluundorj et al., 2014; Gjelstrup et al., 2018; Waschbisch et al., 2016). In newly diagnosed (median disease duration of half year) treatment-naïve MS patients circulating $CD16^{+}$ monocyte percentage was reduced compared to healthy controls, especially in non-classical monocytes (Waschbisch et al., 2016). However, in untreated RRMS patients in a relapse stage the percentage of $CD16^{+}$ monocytes was increased (Chuluundorj et al., 2014) and also in MS treated patients (median, six to seven years) versus the controls (Waschbisch et al., 2016). Another study comparing RRMS patients and healthy controls also demonstrated an increment of $CD16^{+}$, and more specifically of non-classical monocytes (Gjelstrup et al., 2018), but there is a debate on the specific subpopulation expanded with a study linking the increase in total $CD16^{+}$ to intermediate monocytes ($CD14^{++}CD16^{+}$) (Chuluundorj et al., 2017). The apparent discrepancy is most likely due to the composition of the different patient cohorts, and reflects an important point of disease heterogeneity (Gjelstrup et al., 2018).

Glatiramer acetate, a well–known MS treatment (La Mantia et al., 2010), induced a significant expansion of $CD16^+$ monocytes (both intermediate and non-classical) compared to healthy control subjects or untreated MS patients, and the monocytes from healthy controls and glatiramer acetate-treated patients displayed a similar response to LPS activation, which was reduced compared to the untreated MS cohort (Chuluundorj et al., 2017).

Immune cells that enter CSF-filled spaces via the choroid plexus have been attributed a major role in the steady-state immune surveillance of the CNS, and it is within the subarachnoid spaces that autoreactive T cells encounter their cognate antigens presented to them by monocyte-derived meningeal or perivascular macrophages and DCs, and $CD16^+$ monocytes are enriched within the CSF, closely resembling the peripheral blood intermediate and non-classical monocyte subset (Waschbisch et al., 2016). Evidence suggests that $CD16^+$ monocytes promote $CD4^+$ T cell trafficking via the endothelial barrier, supporting the hypothesis of $CD16^+$ monocytes adhering to the brain micro vasculature and contributing to the breakdown of the blood-brain barrier (Waschbisch et al., 2016).

Overall, considering the emerging relevance of monocyte subsets implication on MS and the strong susceptibility association of the gene *IL22RA2* with it, the higher level of *IL22RA2* in intermediate and non-classical monocytes compared to classical monocytes deserves further interest. Results in the section 5.1.1.4 (Monocyte subpopulations express different *IL22RA2* and IL-22BP), show a significant increase among intermediate and non-classical monocytes when taken all the variants together. In line with the gene expression results, the percentage of cells positively stained with anti-IL-22BP showed a very significant increase among the $CD16^+$ monocyte subpopulations. In deed in both cases the pattern is similar, with the classical showing the lowest level, followed by the non-classical and the intermediates having the highest levels in terms of gene expression and protein staining. Taken together they may suggest that differential mechanisms involved in the regulation of *IL22RA2* expression exists as these subsets may harbor

therefore a specific transcription factor enhancing *IL22RA2* expression. Further identification of such factors may help to understand the role of *IL22RA2* in the intermediate subset in MS.

Finally, the disappearance of the differences on *IL22RA2* expression between classical and intermediate subpopulations monocytes derived moDCs indicates the relevance of the microenvironment in the expression of *IL22RA2*. The high concentrations of GM-CSF and IL-4 present in the culture medium for the differentiation of monocytes to moDCs seems to give rise to a uniform phenotype of cells with similar *IL22RA2* expression. Monocytes cultured with only GM-CSF are used to generate monocyte derived macrophages (Jaguin et al., 2013) and do not show *IL22RA2* expression (Lindahl et al., 2019). Monocytes cultured only with IL-4 have been reported to take moDC like characteristics (Roy et al., 2004) and showed and increased *IL22RA2* expression (Lindahl et al., 2019), but the highest *IL22RA2* is achieved by the synergic effect of GM-CSF and IL-4 (Lindahl et al., 2019). Therefore, there is a strong relation between the synergic effect of GM-CSF and IL-4 to both, generate consistent moDCs, and express *IL22RA2*. Altogether, we concluded that use of classical monocytes, or for technical reasons $CD14^+$ monocytes (from which more about 95% are classical monocytes and the remaining intermediate monocytes) are adequate model to study *IL22RA2* in moDCs.

Our study opens questions about the implications of the results in MS patients. There is already evidence about different expression levels of *IL22RA2* in healthy controls and MS patients, since *IL22RA2* expression was higher in classical monocytes and moDCs of MS patients than healthy controls (Perriard et al., 2015). In this sense, it would be interesting to analyze the individual variants of *IL22RA2* in MS patients that may help to understand the dual role attributed to IL-22BP. The study of the effects of 1,25-dihidroxy vitamin D3 on *IL22RA2* expression in healthy control and MS patients in vitro and in vivo would be also of interest, taking into account the reported beneficial effect of the vitamin D3 in MS (Sintzel et al., 2017). The analysis of the *IL22RA2* gene expression in monocyte subpopulations of MS patients, that already show

alteration on their numbers, represent as well an appealing focus for further investigations. Finally, recent evidence in mice reported *IL22RA2* detection in microglia, the CNS resident myeloid resident population (Lindahl et al., 2019). Despite of the difficulty of getting human microglia samples, it would be of great interest to understand the role of IL-22BP protein on microglia in the context of MS. The put in the words of the last report of the International Multiple Sclerosis Genetic Consortium: “we must now (i) resolve the implicated cell type and whether pathways shared with immune cells are having their MS susceptibility effect in the periphery or in the brain; and (ii) more deeply identify additional functional consequences that may be present in only a subset of cells, such as microglia or activated astrocytes, that are obscured in the cortical level profile” (IMSGC, 2019b).

6.5. Relevance of the findings regarding the secretion of IL-22BP protein

As explained in chapter 2.2.2 of the introduction, *IL22RA2* gene is capable of expressing three partially distinct protein isoforms that share an identical SP, and lack of intracellular and transmembrane domains, but differ in their binding capacity of IL-22. Protein isoform 2, IL-22BPi2, exhibits the highest affinity for IL-22, compared to the membrane-bound receptor IL-22R1 (de Moura et al., 2009; Jones et al., 2008; Wolk et al., 2007). In addition, the shorter isoform IL-22BPi3, is also capable of neutralizing IL-22 activity with a lower affinity than IL-22BPi2 (Jones et al., 2008; Lim et al., 2016).

We have demonstrated that the longest isoform, IL-22BPi1, is not capable of interacting with IL-22. As previously explained, IL-22BPi1 differs from IL-22BPi2 by the insertion of a 32-AA sequence that does not disrupt the reading frame, and hence, the intact primary sequence of IL-22BPi2 is in its entirety included in IL-22BPi1. The biological function of IL22BPi1 was not known.

The immunofluorescence study using confocal microscopy, which is presented in the section 5.1.2.1.1 of the results, revealed that IL-22BPi2 and IL-22BPi3, but not IL-22BPi1, were mainly visible as intensely staining deposits co-localizing with a trans-Golgi protein marker. The diffuse perinuclear staining pattern of IL-22BPi1, in contrast, resembled that of the luminal ER protein ERP72, suggesting that the extra sequence acts as a powerful ER retention signal limiting transit toward the Golgi apparatus. In agreement of these results, further experiments were unable to detect IL-22BPi1 in concentrated culture medium of transfected cells by western blot, even though we could discern small amounts of secreted protein by ELISA, in line with previous reports (Lim et al., 2016).

The insertion of the exon that is only present in IL-22BPi1 into the reading frame of IL-2 (IL-2EX4), an abundantly secreted cytokine, was sufficient to block its secretion. The subcloning of the alternatively spliced exon from IL-22BPi1 into IL-22BPi3 also arrested the latter's secretion (Lim et al., 2016). We set out to determine the factors that cause intracellular retention of IL-22BPi1. GRP78, a crucial luminal ER chaperone involved in translocation, folding and retrograde transport of newly synthesized proteins via direct interaction with the polypeptide backbone (Otero et al., 2010) was identified in the interactome analysis of the affinity-tagged IL-22BP isoforms purified from total cell lysates as main interacting partner of IL- 22BPi1, IL-22BP2, and IL-2EX4. These three proteins, but not IL-22BPi3, were found to interact with the substrate-binding domain (SBD) of GRP78 and thus, the extra exon sequence does not appear to change site of interaction with GRP78.

The experiments of this thesis related to the secretion of IL-22BP are part of a larger project that also involved the now Dr. Gómez-Fernández, whose experiments complement the ones presented here, and for which they were jointly published (Gómez-Fernández et al., 2018, 2019). From now on, when experiments carried out in our laboratory that are not part of the results

chapter are mentioned, they will refer to the experiments carried out by Dr. Gómez-Fernández in the aforementioned publications.

The in-house performed experiments co-transfecting IL-22BP with wtGRP78, but not the ATPase-negative T37G GRP78mutant (Gaut & Hendershot, 1993), significantly increased secretion of IL-22BPi1 and BPi2, but not that of BPi3, as measured in ELISA. Hence, both IL-22BPi1 and IL-22BPi2 appear to behave as bona fide secretory client proteins of GRP78. Similarly, interactomes analysis of IL-22BPi1 and IL-22BPi2 performed in the lab found also interactions with GRP94, calnexin and GRP170, and in western blot analysis, ERdj3 was also detected (Gómez-Fernández et al., 2018). Altogether suggesting a complex process for the folding of both IL-22BPi1 and IL-22BPi2.

The study of the interaction of IL-22BP isoforms with different GRP94 mutants revealed that the C-terminal half (AAs 455-577) of the middle domain of GRP94 is critical client binding region of both IL-22BPi1 and BPi2. This region differs from that identified for the GRP94 clients OS-9 or TLRs and integrins (Dersh et al., 2014; Wu et al., 2012b), but the implications remain to be clarified since the mechanistic information about GRP94 interaction with its client proteins is very limited. The ATPase-negative GRP94 MD and DA mutants showed strong interaction with both isoforms and when cotransfected with them, reduced IL-22BP isoforms secretion, indicative of competition with a productive “pro-secretion” role of GRP94 in IL-22BPi1 or IL-22BPi2 folding dependent on functionally intact GRP94.

Using confocal microscopy IL-22BPi1 and IL-2EX4 showed virtually perfect co-localization with GRP94, identifying this chaperone as crucially associated with their arrest of transit to Golgi. The relevance of the results obtained in cells lines by confocal microscopy was highlighted by other experiments in the lab, which detected GRP94 by immunoblotting in the IL-22BP natural

producers moDCs, and the enhancement of intracellular and secreted levels of IL-22BPi1 by pharmacological targeting of GRP94 cell lines (Gómez-Fernández et al., 2019).

Calnexin is part of the ER quality control system that acts to retain unfolded N-linked glycoproteins (Williams, 2006), compatible with mono-glycosylation of the high-mannose type N-glycans we identified on intracellular IL-22BP isoforms. GRP170, an HSP70-type chaperone, and ERdj3, a DnaJ-family GRP78 co-factor, recognize distinct sets of peptide sequences in unfolded proteins. Interestingly, while GRP78 and ERdj3 can interact with many diverse client peptide sequences, GRP170 was shown recently to interact specifically with rarer, aggregation-prone regions which, if continuously exposed, may trigger disposal of the protein by ERAD given the toxicity of protein aggregates to cell survival (Behnke et al., 2016). The potential link to ERAD was substantiated by the observation that both *IL22*-BPi1 and IL-22BPi2, but not IL-22BPi3, appear to be partially degraded by the proteasome. We also tested the capacity of IL-22BP isoforms to activate ER stress signaling via induction of UPR through accumulation of misfolded protein, pathway that has been previously described (Malhotra & Kaufman, 2007). Lab experiments transfecting HEK293 cells with IL-22BPi1 strongly upregulated expression of UPR genes resulting in increased GRP78 and GRP94 protein levels, suggesting that under these experimental conditions ERAD alone is insufficient to restore ER folding capacity has previously been shown (Molinari & Sitia, 2005). In contrast, IL-22BPi2 did not augment GRP78 and GRP94 protein levels indicating that it has a more balanced export from the ER through either secretion or ERAD may eliminate the need for UPR induction.

In order to understand if the link between IL-22BP and UPR was active in natural producer cells we decided to silence *IL22RA2* expression in moDCs. We designed an optimized protocol for *IL22RA2* silencing in moDCs, and we observed that the *GRP78* mRNA levels were also significantly reduced. The use of AM580, *IL22RA2* expression inductor, to increase the silencing versus control differences, showed an increase silencing in *GRP78*, and a significant reduction

on *ERp44*. Those results were in agreement with experiments carried out in the lab transfecting IL-22BPi1 and IL-2EX4 into HEK293 cells, which observed an up regulation of the both genes.

Take all the results together; we have shed some insight on the IL-22BPi1 protein's failure to fold and to be secreted. The general propensity of alternatively spliced exons to encode intrinsically disordered protein regions may contribute to the inability of IL-22BPi1 to fold (van der Lee et al., 2014). The addition of disordered regions to proteins via exonization processes may perhaps serve as a mechanism for this, and many of these areas are involved in protein-protein interactions (Buljan et al., 2010). Additionally, IL-22BPi2 has phenotypically evolved its sequence and structure for high-affinity binding to and neutralization of IL-22. This selection pressure is broken by IL-22BPi1's additional exon. We cannot rule out the potential that some advantageous interactions between IL-22BPi1 and as-yet unidentified partners within natural producer cells or in the extracellular environment may occur.

In line with that idea, our research reveals that one advantage of IL-22BPi1 and IL-22BPi2 co-expression may be their capacity to increase GRP78 and GRP94 levels through UPR induction. Increased secretion levels of IL-22BPi2 by moDCs may thus be a favorable selection characteristic, as both of these chaperones are essential for the folding of this protein. In order to study this, experiments using genome-editing methods like CRISPR, eliminating isoform-1 expression in moDCs should be conducted. Finally, in the absence of further research, constitutively higher levels of ER chaperones may prime immature moDCs' ERs for improved processing of secretory and membrane proteins like MHC receptors, integrins, and cytokines, which are immediately and massively expressed in response to TLR ligands or other maturation triggers (Wolk et al., 2008b).

6.6. The impact of the detection of *IL12A*-006

Regarding *IL12A* findings, the detectable levels of variant *IL12-206* open new possibilities regarding its function in the expression of the protein coded by *IL12A*. Further studies are needed in order to clarify the role of *IL12A* in MS and our results show that it would be necessary to address the implication of the splicing variants in both IL-12 and IL-35 in the course of the disease. Once again, animal model might not be able to explain clinical observations. Mice lacking *Il12a* are still susceptible to EAE (Becher et al., 2002; Gran et al., 2002) while mice lacking *Il12b* (Gran et al., 2002) or *Il23r* (Cua et al., 2003) are resistant to EAE and suggest that IL-23, and not IL-12, is the critical factor in the autoimmune inflammation. However, high levels of IL-12 are correlated with disease progression in human patients (Balashov et al., 1997; Comabella et al., 1998) and ustekinumab, a IL12/23 p40 neutralizing antibody, failed to show efficacy in in treating RRMS in phase II trial (Segal et al., 2008).

Similarly, the genetic studies have also showed that there are SNPs associated with MS in the *IL12A* gene but not in *IL12B* or *IL23A*. Although *IL23A* variants have been associated with psoriasis susceptibility (Tsoi et al., 2017), there is no evidence of any IL-23 related gene linked to MS (Buniello et al., 2019; IMSGC, 2019b). In the case of *IL12B*, there are two SNPs associated with MS, rs10866713 (IMSGC et al., 2011) and rs2546890 (IMSGC, 2019b; IMSGC et al., 2011), in the close vicinity of the gene but out of it. Taking into account *IL12A* gene's vicinity, there are five different SNPs associated with MS. Three of them, rs4680534 (De Jager et al., 2009), rs522127 (IMSGC et al., 2013) and rs1014486 (IMSGC, 2019b; IMSGC et al., 2013), are out of *IL12A* gene in the neighboring *IL12a antisense RNA 1* (*IL-12AS1*) gene. The other two SNPs are in the *IL12A* sequence, both in intragenic regions: rs10936182 (IMSGC, 2019b) in the intron between exon 2 and 3, and thus present in the *IL12A-203* splicing variant, and rs2243123 (IMSGC

et al., 2011) in the intron between exon 6 and 7. These last two SNPs are also present in *IL-12AS1* gene.

The *IL-12AS1* gene is long noncoding RNA (lncRNA) running in the opposite direction of *IL12A* gene that has been associated in GWAS analysis with different autoimmune diseases, such as Behcet's disease, celiac disease, biliary liver cirrhosis, systemic lupus erythematosus and systemic scleroderma (Buniello et al., 2019). The Ensembl.org database records up to 14 different splicing variants but with no or little evidence to support them (Yates et al., 2020). The specific function of this particular lncRNA has not been studied, but other lncRNAs in cytokines have been reported to be involved in the regulation of their neighboring coding genes such as AS-IL1α, lnc-IL7R, and IL-1β-eRNA (E. K. Robinson et al., 2020). In fact, certain lncRNAs have been shown to play a crucial role in the regulation of alternative splicing in response to several stimuli or during disease (Romero-Barrios et al., 2018).

In this way, mutations affecting *IL12A* or *IL12A-AS1* may have an effect on the splicing variants of *IL12A*. Even the canonical variant has been deeply studied there is little information about the rest of them, mostly coming from the analysis of human chromosome 3 (Muzny et al., 2006) and with low transcript support levels (Yates et al., 2020). Our results have been able to demonstrate the presence of the non-coding *IL12A-206* variant but no any other in different cells lines. Among the tested cell lines there were monocyte and lymphocyte derived cell lines, namely JURKAT, THP1 and U937, that showed a decrease of its detection and the upregulation of the canonical *IL12A-201* after stimulation with IFN$_\gamma$ and LPS. Epithelial cells that showed also the presence of *IL12A-206* but under IFN$_\gamma$ and LPS all *IL12A* variants decreased.

Emerging data suggest that non-coding variants often require specific context to exert their effect, and this has recently also been suggested for autoimmune disease risk gene, including MS (Alasoo et al., 2018; Shooshtari et al., 2017). While the possibility of the presence of *IL12-*

206 to be the last previous step to the definitive splicing of *IL12A* canonical variant remains, research developed in mice (Skrombolas et al., 2015) showed that transcript variant *IL12A-205* that has a retained intron 4 like *IL12A-206*, codes for a truncated protein that can inhibit the action of IL-12. The study of the similarities between human *IL12A* and mice *il12a*, gives power to this hypothesis.

A phylogenetic study of *IL12A* shows that is highly conserved within a large range of animal species (Cunningham et al., 2022). The human *IL12A* gene and *Il12a* gene of the mouse are orthologues with the maximum score based on two parameters. First, the gene order conservation score indicates how many of the four closest neighbors of a gene match between orthologous pairs. And secondly, by the whole genome alignment score that calculates the coverage of the alignment over the orthologue pair (Cunningham et al., 2022). The similarities of the exon structure between *IL12A* (Figure 6.1) and *il12a* (Figure 6.2) variants it is apparent, both in the case of canonical isoforms and between *IL12A-206* and *IL12A-205*.

AA sequence analysis also shows the similarities in the alignment between the canonical IL12 protein of human and mice (Figure 5.6 a). The theoretical AA sequence of mouse *IL12A-205* aligned with the canonical mouse IL-12 (Figure 5.6 b) and the one of the human *IL12A-206* and human IL-12 (Figure 5.6 c) show similarities as well.

In conclusion, the detection of the *IL12A-206* variant in different cell lines and moDCs rises the need for further investigation of the involvement of the transcript not only in MS but also in cancer and in other pathologies were IL-12 plays a role. In this context, taking into account the similarities with mouse Il-12i205, which is able to inhibit canonical mouse IL-12 *in vitro*, similar experiment with human IL-12 and IL-12i206 should be performed to confirm or discard the same effect in the human protein.

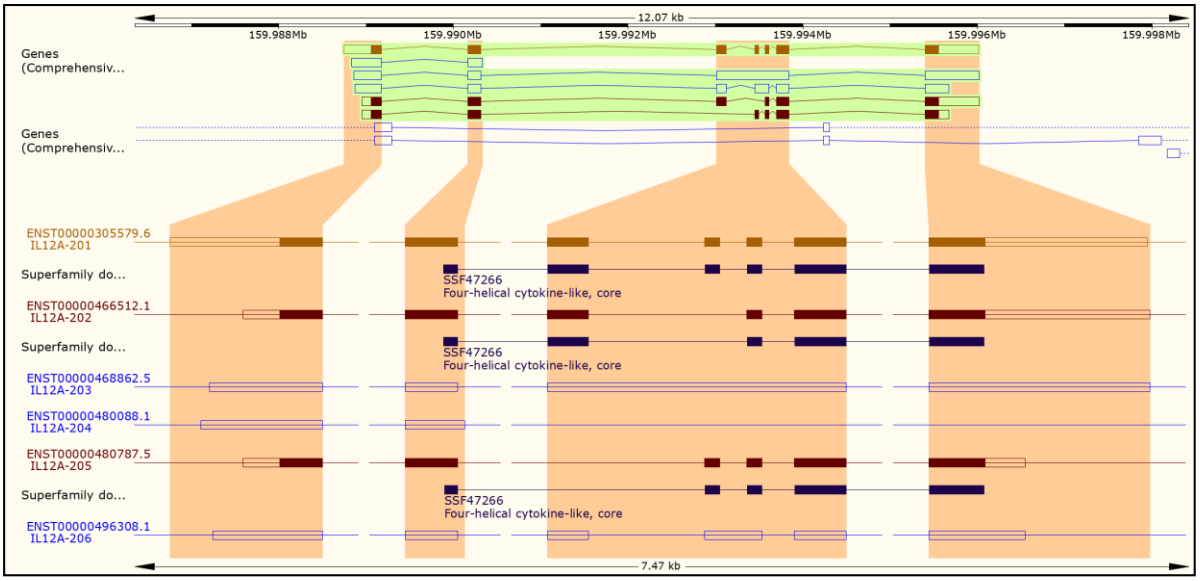

Figure 6.1. Transcript variants of human *IL12A* gene. In gold the canonical variant; red considered protein-coding variants; blue considered non-coding variants. *Source:* (Cunningham et al., 2022).

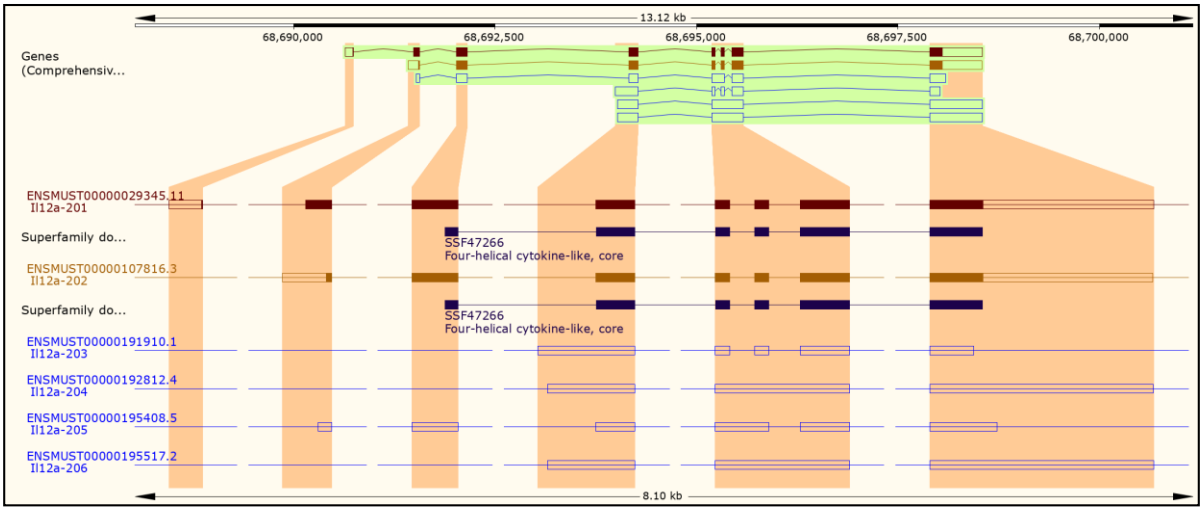

Figure 6.2. Transcript variants of mouse Il12a gene. In gold, the canonical variant, red considered protein-coding variants, blue considered non-coding variants. *Source: (Cunningham et al., 2022)*.

Figure 6.3. Clustal O (1.2.4) alignments of different *IL12A* and Il12a derived isoforms. Different exons shown by alternating letters color between black and blue. Symbols under the alignment representing fully conserved residue (asterisk, *), residue conservation between groups of strongly similar properties as below-roughly equivalent to scoring >0.5 in the Gonnet PAM 250 matrix (colon, :) or residues of weakly similar properties scoring 0-0.5 in the Gonnet PAM 250 matrix (period, .). a) Human and mouse canonical

IL-12 isoforms alignment. b) Mouse Il12a derived isoforms alignment. c) Human *IL12A* derived isoforms alignment. *Source: European Bioinformatics Institute.*

a) Canonical human IL12A isoform, IL12A-201, aligned with canonical mouse Il12a isoform, Il12a-202

```
IL12A-201       MWPPGSASQPPPSPAAATGLHPAARPVSLQCRLSMCPARSLLLVATLVLLDHLSLARNLP  60
I112a-202       ------------------------------MCQSRYLLFLATLALLNHLSLARVIP  26
                                               ** :* **::***.**:****** :*

IL12A-201       VATPDPGMFPCLHHSQNLLRAVSNMLQKARQTLEFYPCTSEEIDHEDITKDKTSTVEACL  120
I112a-202       VSGP----ARCLSQSRNLLKTTDDMVKTAREKLKHYSCTAEDIDHEDITRDQTSTLKTCL  82
                *: *       ** :*:***::..:*::.**:.*:.* **:*:*******:*:***:::**

IL12A-201       PLELTKNESCLNSRETSFITNGSCLASRKTSFMMALCLSSIYEDLKMYQVEFKTMNAKLL  180
I112a-202       PLELHKNESCLATRETSSTTRGSCLPPQKTSLMMTLCLGSIYEDLKMYQTEFQAINAALQ  142
                **** ****** :****  *.****  :***:**:***.**********.**:::** *

IL12A-201       MDPKRQIFLDQNMLAVIDELMQALNFNSETVPQKSSLEEPDFYKTKIKLCILLHAFRIRA  240
I112a-202       NHNHQQIILDKGMLVAIDELMQSLNHNGETLRQKPPVGEADPYRVKMKLCILLHAFSTRV  202
                 . ::**:**:.**..******:**.*.**: **  : * * *:.*:********* *.

IL12A-201       VTIDRVMSYLNAS      253
I112a-202       VTINRVMGYLSSA      215
                ***:***.**.::
```

b) Mouse truncated protein translated from mouse il12a 205 aligned with canonical mouse il12a

```
I112a-202    MCQSRYLLFLATLALLNHLSLARVIPVSGPARCLSQSRNLLKTTDDMVKTAREKLKHYSC   60
I112a-205    MCQSRYLLFLATLALLNHLSLARVIPVSGPARCLSQSRNLLKTTDDMVKTAREKLKHYSC   60
             ************************************************************

I112a-202    TAEDIDHEDITRDQTSTLKTCLPLELHKNESCLATRETSSTTRGSCLPPQKTSLMMTLCL   120
I112a-205    TAEDIDHEDITRDQTSTLKTCLPLELHKNESCLATRETSSTIVSKHSK---GSFPMTDS-   116
             ****************************************** ..      *: ** .

I112a-202    GSIYEDLKMYQTEFQAINAALQNHNHQQIILDKGMLVAIDELMQSLNHNGETLRQKPPVG   180
I112a-205    ------------------------------------------------------------   116

I112a-202    EADPYRVKMKLCILLHAFSTRVVTINRVMGYLSSA   215
I112a-205    ----------------------------------   116
```

c) Potentially truncated protein translated from of human IL12A-206 aligned with canonical human IL12A

```
IL12A-201       MWPPGSASQPPPSPAAATGLHPAARPVSLQCRLSMCPARSLLLVATLVLLDHLSLARNLP  60
IL12A-206       MWPPGSASQPPPSPAAATGLHPAARPVSLQCRLSMCPARSLLLVATLVLLDHLSLARNLP  60
                ************************************************************

IL12A-201       VATPDPGMFPCLHHSQNLLRAVSNMLQKARQTLEFYPCTSEEIDHEDITKDKTSTVEACL  120
IL12A-206       VATPDPGMFPCLHHSQNLLRAVSNMLQKARQTLEFYPCTSEEIDHEDITKDKTSTVEACL  120
                ************************************************************

IL12A-201       PLELTKNESCLNSRETSFITNGSCLASRKTSFMMALCLSSIYEDLKMYQVEFKTMNAKLL  180
IL12A-206       PLELTKNESCLNSRETSFITVSQKMKSFS----------LYDEFISLMSDY------FF  163
                ******************** .. : * .           :*:::     ::      ::

IL12A-201       MDPKRQIFLDQNMLAVIDELMQALNFNSETVPQKSSLEEPDFYKTKIKLCILLHAFRIRA  240
IL12A-206       L------------------------------------------------------------  164
                :

IL12A-201       VTIDRVMSYLNAS      253
IL12A-206       -------------      164
```

7. CONCLUSION

The results obtained in the present doctoral thesis suggest the next main conclusions:

1. ***IL22RA2* is a unique gene whose expression levels increase during differentiation and are down regulated by different maturation stimuli.**

In contrast with all the other cytokine genes studied in this work, the cytokines of the IL10 cytokine family (namely IL10, IL19, IL20, *IL22*, IL24 and IL26), IL12 family (*IL12A*, IL12B and IL23A) and interferon β), *IL22RA2* expression is upregulated during monocyte differentiation to moDCs and dramatically decreases in response to different maturation stimuli.

2. **moDCs express all three variants of *IL22RA2* and represent an important model to understand the human *IL22RA2* gene and the coded IL-22BP.**

In line with the results of other research group (Lim et al., 2016), we have shown that the three variants of *IL22RA2* are expressed in moDCs. Among them *IL22RA2v2* is the most expressed, followed by *IL22RA2v1*, and *IL22RA2v3* is the less abundant. When the levels of *IL22RA2* increase all variants do it proportionally, and therefore the ratio of expression seems to stable. Taking into account the consistent ability for the expression of *IL22RA2*, and in line with other reports (Lim et al., 2016; Martin et al., 2014, 2017), we consider moDCs an important model to study this gene.

4. ***IL22RA2* expression is differentially expressed in monocyte subpopulations, $CD14^{++}/CD16^{+}$ intermediate monocytes produced a higher level of *IL22RA2* mRNA than classical and non-classical monocytes.**

Circulating monocytes are crucial during inflammatory response (Ginhoux & Jung, 2014; Kapellos et al., 2019) and therefore it is important to understand the characteristics and differences in their subsets. Our work has shown that there is a difference in the expression of

IL22RA2 among the different subsets, and can play a role in the understanding of both the gene's and the specific monocytes' response in MS.

5. IL-22BP isoform 1 displays hallmarks of a poorly secreted, intracellularly retained protein with intrinsic capacity to trigger the unfolded protein response that strongly interacts with GRP78 and GRP94

The experiments conducted in this study have been able to properly establish the two folding proteins, GRP78 and GRP94, that have the closest relationship with IL-22BP folding and secretion and detail their specific sites of union. It has been demonstrated that they are able to retain IL-22BPi1 in the ER, and that GRP94 pharmacological targeting, can induce its secretion of protein. Taken together is give a developed mechanistic explanation for the IL-22BPi1 retention.

6. *IL12A* coded 206 variant is expressed in moDCs and different cells lines.

The detection of the *IL12-206* variant in different cells lines rises important questions for the understanding of *IL12A*. While still can simply be a precursor of the *IL12A* canonical variant; the results of the research in mice with the *IL12A-206* counterpart *IL12A-205* (Skrombolas et al., 2015), may indicate otherwise. Considering that similarities between the isoforms and the fact that the *IL12A-205* coded Il-12i205 protein is able to inhibit canonical mouse IL-12 in vitro, similar experiment should be conducted in human. If mice results were confirmed that would open new era in the understanding of one of the most important cytokines, *IL12A* and IL-12A.

Taken as a whole, the experiments developed during this thesis have been able described in detail of the expression of *IL22RA2* in different conditions, identifying the interesting relationship with vitamin D3, a well-established factor for MS, and also, describing for the first time the differences in its expression among distinct monocyte subsets. In addition to the contribution in

the understanding of *IL22RA2* gene, the proteins related to the folding and secretion of the coded proteins have been unequivocally described. On the other hand, the small side project of *IL12A* has been able to identify the presence of a variant not reported before. This finding may be key in the proper understanding of the gene regulation in not only MS but also any inflammatory process where *IL12A* is one of the master regulatory genes.

8. BIBLIOGRAFIA

Abood, R. N., McHugh, K. J., Rich, H. E., Ortiz, M. A., Tobin, J. M., Ramanan, K., Robinson, K. M., Bomberger, J. M., Kolls, J. K., Manni, M. L., Pociask, D. A., & Alcorn, J. F. (2019). IL-22-binding protein exacerbates influenza, bacterial super-infection. *Mucosal Immunology*, *12*(5), 1231–1243. https://doi.org/10.1038/s41385-019-0188-7

Abtahi Froushani, S. M., Delirezh, N., Hobbenaghi, R., & Mosayebi, G. (2014). Synergistic effects of atorvastatin and all-trans retinoic acid in ameliorating animal model of multiple sclerosis. *Immunological Investigations*, *43*(1), 54–68. https://doi.org/10.3109/08820139.2013.825269

Abualrous, E. T., Sticht, J., & Freund, C. (2021). Major histocompatibility complex (MHC) class I and class II proteins: Impact of polymorphism on antigen presentation. *Current Opinion in Immunology*, *70*, 95–104. https://doi.org/10.1016/j.coi.2021.04.009

Agarwal, R. K., Silver, P. B., & Caspi, R. R. (2012). Rodent Models of Experimental Autoimmune Uveitis. *Methods in Molecular Biology (Clifton, N.J.)*, *900*. https://doi.org/10.1007/978-1-60761-720-4_22

Ahlfors, H., Morrison, P. J., Duarte, J. H., Li, Y., Biro, J., Tolaini, M., Meglio, P. D., Potocnik, A. J., & Stockinger, B. (2014). IL-22 Fate Reporter Reveals Origin and Control of IL-22 Production in Homeostasis and Infection. *The Journal of Immunology*, *193*(9), 4602–4613. https://doi.org/10.4049/jimmunol.1401244

Ajami, B., Bennett, J. L., Krieger, C., McNagny, K. M., & Rossi, F. M. V. (2011). Infiltrating monocytes trigger EAE progression, but do not contribute to the resident microglia pool. *Nature Neuroscience*, *14*(9), 1142–1149. https://doi.org/10.1038/nn.2887

Alasoo, K., Rodrigues, J., Mukhopadhyay, S., Knights, A. J., Mann, A. L., Kundu, K., HIPSCI Consortium, Hale, C., Dougan, G., & Gaffney, D. J. (2018). Shared genetic effects on chromatin and gene expression indicate a role for enhancer priming in immune response. *Nature Genetics*, *50*(3), 424–431. https://doi.org/10.1038/s41588-018-0046-7

Almolda, B., Costa, M., Montoya, M., González, B., & Castellano, B. (2011). Increase in Th17 and T-reg lymphocytes and decrease of IL22 correlate with the recovery phase of acute EAE in rat. *PloS One*, *6*(11), e27473. https://doi.org/10.1371/journal.pone.0027473

Ascherio, A., Munger, K. L., & Simon, K. C. (2010). Vitamin D and multiple sclerosis. *The Lancet. Neurology*, *9*(6), 599–612. https://doi.org/10.1016/S1474-4422(10)70086-7

Badihian, S., Shaygannejad, V., Soleimani, P., Mirmosayyeb, O., Samee, Z., Manouchehri, N., & Esmaeil, N. (2018). Decreased serum levels of interleukin-35 among multiple sclerosis patients may be related to disease progression. *Journal of Biological Regulators and Homeostatic Agents*, *32*(5), 1249–1253.

Balashov, K. E., Smith, D. R., Khoury, S. J., Hafler, D. A., & Weiner, H. L. (1997). Increased interleukin 12 production in progressive multiple sclerosis: Induction by activated CD4+ T cells via CD40 ligand. *Proceedings of the National Academy of Sciences*, *94*(2), 599–603. https://doi.org/10.1073/pnas.94.2.599

Bastian, D., Wu, Y., Betts, B. C., & Yu, X.-Z. (2019). The IL-12 Cytokine and Receptor Family in Graft-vs.-Host Disease. *Frontiers in Immunology*, *10*. https://doi.org/10.3389/fimmu.2019.00988

Becher, B., Durell, B. G., & Noelle, R. J. (2002). Experimental autoimmune encephalitis and inflammation in the absence of interleukin-12. *The Journal of Clinical Investigation*, *110*(4), 493–497. https://doi.org/10.1172/JCI15751

Behnke, J., Mann, M. J., Scruggs, F.-L., Feige, M. J., & Hendershot, L. M. (2016). Members of the Hsp70 Family Recognize Distinct Types of Sequences to Execute ER Quality Control. *Molecular Cell*, *63*(5), 739–752. https://doi.org/10.1016/j.molcel.2016.07.012

Berg, M. G., Singh, L. N., Younis, I., Liu, Q., Pinto, A. M., Kaida, D., Zhang, Z., Cho, S., Sherrill-Mix, S., Wan, L., & Dreyfuss, G. (2012). U1 snRNP Determines mRNA Length and Regulates Isoform Expression. *Cell*, *150*(1), 53–64. https://doi.org/10.1016/J.CELL.2012.05.029

Bernasconi, R., Soldà, T., Galli, C., Pertel, T., Luban, J., & Molinari, M. (2010). Cyclosporine A-sensitive, cyclophilin B-dependent endoplasmic reticulum-associated degradation. *PloS One*, *5*(9). https://doi.org/10.1371/journal.pone.0013008

Bettini, M., Castellaw, A. H., Lennon, G. P., Burton, A. R., & Vignali, D. A. A. (2012). Prevention of autoimmune diabetes by ectopic pancreatic β-cell expression of interleukin-35. *Diabetes*, *61*(6), 1519–1526. https://doi.org/10.2337/db11-0784

Beyeen, A. D., Adzemovic, M. Z., Ockinger, J., Stridh, P., Becanovic, K., Laaksonen, H., Lassmann, H., Harris, R. A., Hillert, J., Alfredsson, L., Celius, E. G., Harbo, H. F., Kockum, I., Jagodic, M., & Olsson, T. (2010). IL-22RA2 associates with multiple sclerosis and macrophage effector mechanisms in experimental neuroinflammation. *Journal of Immunology (Baltimore, Md.: 1950)*, *185*(11), 6883–6890. https://doi.org/10.4049/jimmunol.1001392

Bezzini, D., Ulivelli, M., Gualdani, E., Razzanelli, M., Ferretti, F., Meucci, G., Francesconi, P., & Battaglia, M. A. (2020). Increasing prevalence of multiple sclerosis in Tuscany, Italy. *Neurological Sciences: Official Journal of the Italian Neurological Society and of the Italian Society of Clinical Neurophysiology*, *41*(2), 397–402. https://doi.org/10.1007/s10072-019-04090-0

Bhatt, S., Qin, J., Bennett, C., Qian, S., Fung, J. J., Hamilton, T. A., & Lu, L. (2014). All-trans retinoic acid induces arginase-1 and inducible nitric oxide synthase-producing dendritic cells with T cell inhibitory function. *Journal of Immunology (Baltimore, Md.: 1950)*, *192*(11), 5098–5108. https://doi.org/10.4049/jimmunol.1303073

Bielekova, B., Sung, M.-H., Kadom, N., Simon, R., McFarland, H., & Martin, R. (2004). Expansion and functional relevance of high-avidity myelin-specific CD4+ T cells in multiple sclerosis. *Journal of Immunology (Baltimore, Md.: 1950)*, *172*(6), 3893–3904. https://doi.org/10.4049/jimmunol.172.6.3893

Bjornevik, K., Cortese, M., Healy, B. C., Kuhle, J., Mina, M. J., Leng, Y., Elledge, S. J., Niebuhr, D. W., Scher, A. I., Munger, K. L., & Ascherio, A. (2022). Longitudinal analysis reveals high prevalence of Epstein-Barr virus associated with multiple sclerosis. *Science*, *375*(6578), 296–301. https://doi.org/10.1126/science.abj8222

Boudjadi, S., Chatterjee, B., Sun, W., Vemu, P., & Barr, F. G. (2018). The expression and function of PAX3 in development and disease. *Gene*, *666*, 145–157. https://doi.org/10.1016/j.gene.2018.04.087

Boutet, S. C., Cheung, T. H., Quach, N. L., Liu, L., Prescott, S. L., Edalati, A., Iori, K., & Rando, T. A. (2012). Alternative Polyadenylation Mediates MicroRNA Regulation of Muscle Stem Cell Function. *Cell Stem Cell*, *10*(3), 327–336. https://doi.org/10.1016/J.STEM.2012.01.017

Boyette, L. B., Macedo, C., Hadi, K., Elinoff, B. D., Walters, J. T., Ramaswami, B., Chalasani, G., Taboas, J. M., Lakkis, F. G., & Metes, D. M. (2017). Phenotype, function, and differentiation potential of human monocyte subsets. *PLOS ONE*, *12*(4), e0176460. https://doi.org/10.1371/journal.pone.0176460

Bramow, S., Frischer, J. M., Lassmann, H., Koch-Henriksen, N., Lucchinetti, C. F., Sørensen, P. S., & Laursen, H. (2010). Demyelination versus remyelination in progressive multiple sclerosis. *Brain: A Journal of Neurology*, *133*(10), 2983–2998. https://doi.org/10.1093/brain/awq250

Briggs, F. (2019). Unraveling susceptibility to multiple sclerosis. *Science*, *365*(6460), 1383–1384. https://doi.org/10.1126/science.aay1439

Bright, J. J., Musuro, B. F., Du, C., & Sriram, S. (1998). Expression of IL-12 in CNS and lymphoid organs of mice with experimental allergic encephalitis. *Journal of Neuroimmunology*, *82*(1), 22–30. Scopus. https://doi.org/10.1016/S0165-5728(97)00184-7

Brownell, B., & Hughes, J. T. (1962). The distribution of plaques in the cerebrum in multiple sclerosis. *Journal of Neurology, Neurosurgery, and Psychiatry*, *25*(4), 315–320.

Buckingham, M., & Relaix, F. (2015). PAX3 and PAX7 as upstream regulators of myogenesis. *Seminars in Cell & Developmental Biology*, *44*, 115–125. https://doi.org/10.1016/j.semcdb.2015.09.017

Buljan, M., Frankish, A., & Bateman, A. (2010). Quantifying the mechanisms of domain gain in animal proteins. *Genome Biology*, *11*(7), R74. https://doi.org/10.1186/gb-2010-11-7-r74

Buniello, A., MacArthur, J. A. L., Cerezo, M., Harris, L. W., Hayhurst, J., Malangone, C., McMahon, A., Morales, J., Mountjoy, E., Sollis, E., Suveges, D., Vrousgou, O., Whetzel, P. L., Amode, R., Guillen, J. A., Riat, H. S., Trevanion, S. J., Hall, P., Junkins, H., … Parkinson, H. (2019). The NHGRI-EBI GWAS Catalog of published genome-wide association studies, targeted arrays and summary statistics 2019. *Nucleic Acids Research*, *47*(D1), D1005–D1012. https://doi.org/10.1093/nar/gky1120

Burmeister, A. R., & Marriott, I. (2018). The Interleukin-10 Family of Cytokines and Their Role in the CNS. *Frontiers in Cellular Neuroscience*, *12*. https://doi.org/10.3389/fncel.2018.00458

Campbell, R. D., & Trowsdale, J. (1993). Map of the human MHC. *Immunology Today*, *14*(7), 349–352. https://doi.org/10.1016/0167-5699(93)90234-C

Castro, F., Cardoso, A. P., Gonçalves, R. M., Serre, K., & Oliveira, M. J. (2018). Interferon-Gamma at the Crossroads of Tumor Immune Surveillance or Evasion. *Frontiers in Immunology*, *9*. https://doi.org/10.3389/fimmu.2018.00847

Chanput, W., Peters, V., & Wichers, H. (2015). THP-1 and U937 Cells. In K. Verhoeckx, P. Cotter, I. López-Expósito, C. Kleiveland, T. Lea, A. Mackie, T. Requena, D. Swiatecka, & H. Wichers (Eds.), *The Impact of Food Bioactives on Health: In vitro and ex vivo models*. Springer. http://www.ncbi.nlm.nih.gov/books/NBK500159/

Charcot, J. (1868). Histologie de sclérose en plaques. *Gazzete Des Hópitaux Civils et Militaires*, *41*, 554, 557–558, 566.

Charoenngam, N., & Holick, M. F. (2020). Immunologic Effects of Vitamin D on Human Health and Disease. *Nutrients*, *12*(7), 2097. https://doi.org/10.3390/nu12072097

Chau, J., Moza, D., Hossain, N., Lee, J. K., Bienenstock, J., & Karimi, K. (2013). Increased production of IFN-γ by natural killer cells triggered with bone marrow-derived dendritic cells cultured in the presence of retinoic acid. *European Journal of Pharmacology*, *715*(1–3), 321–327. https://doi.org/10.1016/j.ejphar.2013.04.050

Che, Y., Su, Z., & Xia, L. (2020). Effects of IL-22 on cardiovascular diseases. *International Immunopharmacology*, *81*, 106277. https://doi.org/10.1016/j.intimp.2020.106277

Chehrehasa, F., Meedeniya, A. C. B., Dwyer, P., Abrahamsen, G., & Mackay-Sim, A. (2009). EdU, a new thymidine analogue for labelling proliferating cells in the nervous system. *Journal of Neuroscience Methods*, *177*(1), 122–130. https://doi.org/10.1016/j.jneumeth.2008.10.006

Cheung, T. H., & Rando, T. A. (2013). Molecular regulation of stem cell quiescence. *Nature Reviews. Molecular Cell Biology*, *14*(6), 329–340. https://doi.org/10.1038/nrm3591

Choi, J. K., Dambuza, I. M., He, C., Yu, C.-R., Uche, A. N., Mattapallil, M. J., Caspi, R. R., & Egwuagu, C. E. (2017). IL-12p35 Inhibits Neuroinflammation and Ameliorates Autoimmune Encephalomyelitis. *Frontiers in Immunology*, *8*, 1258. https://doi.org/10.3389/fimmu.2017.01258

Chuluundorj, D., Harding, S. A., Abernethy, D., & La Flamme, A. C. (2014). Expansion and preferential activation of the CD14(+)CD16(+) monocyte subset during multiple sclerosis. *Immunology and Cell Biology*, *92*(6), 509–517. https://doi.org/10.1038/icb.2014.15

Chuluundorj, D., Harding, S. A., Abernethy, D., & La Flamme, A. C. (2017). Glatiramer acetate treatment normalized the monocyte activation profile in MS patients to that of healthy controls. *Immunology and Cell Biology*, *95*(3), 297–305. https://doi.org/10.1038/icb.2016.99

Ciccia, F., Guggino, G., Rizzo, A., Bombardieri, M., Raimondo, S., Carubbi, F., Cannizzaro, A., Sireci, G., Dieli, F., Campisi, G., Giacomelli, R., Cipriani, P., De Leo, G., Alessandro, R., & Triolo, G. (2015). Interleukin (IL)-22 receptor 1 is over-expressed in primary Sjogren's

syndrome and Sjögren-associated non-Hodgkin lymphomas and is regulated by IL-18. *Clinical and Experimental Immunology*, *181*(2), 219–229. https://doi.org/10.1111/cei.12643

Collins, C. A., Olsen, I., Zammit, P. S., Heslop, L., Petrie, A., Partridge, T. A., & Morgan, J. E. (2005). Stem Cell Function, Self-Renewal, and Behavioral Heterogeneity of Cells from the Adult Muscle Satellite Cell Niche. *Cell*, *122*(2), 289–301. https://doi.org/10.1016/J.CELL.2005.05.010

Comabella, M., Balashov, K., Issazadeh, S., Smith, D., Weiner, H. L., & Khoury, S. J. (1998). Elevated interleukin-12 in progressive multiple sclerosis correlates with disease activity and is normalized by pulse cyclophosphamide therapy. *The Journal of Clinical Investigation*, *102*(4), 671–678. https://doi.org/10.1172/JCI3125

Correale, J., & Farez, M. F. (2013). Parasite infections in multiple sclerosis modulate immune responses through a retinoic acid-dependent pathway. *Journal of Immunology (Baltimore, Md. : 1950)*, *191*(7), 3827–3837. https://doi.org/10.4049/jimmunol.1301110

Correale, J., Marrodan, M., & Carnero Contentti, E. (2021). Interleukin-35 is a critical regulator of immunity during helminth infections associated with multiple sclerosis. *Immunology*, *164*(3), 569–586. https://doi.org/10.1111/imm.13389

Cua, D. J., Sherlock, J., Chen, Y., Murphy, C. A., Joyce, B., Seymour, B., Lucian, L., To, W., Kwan, S., Churakova, T., Zurawski, S., Wiekowski, M., Lira, S. A., Gorman, D., Kastelein, R. A., & Sedgwick, J. D. (2003). Interleukin-23 rather than interleukin-12 is the critical cytokine for autoimmune inflammation of the brain. *Nature*, *421*(6924), 744–748. https://doi.org/10.1038/nature01355

Cunningham, F., Achuthan, P., Akanni, W., Allen, J., Amode, M. R., Armean, I. M., Bennett, R., Bhai, J., Billis, K., Boddu, S., Cummins, C., Davidson, C., Dodiya, K. J., Gall, A., Girón, C. G., Gil, L., Grego, T., Haggerty, L., Haskell, E., … Flicek, P. (2019). Ensembl 2019. *Nucleic Acids Research*, *47*(D1), D745–D751. https://doi.org/10.1093/nar/gky1113

Cunningham, F., Allen, J. E., Allen, J., Alvarez-Jarreta, J., Amode, M. R., Armean, I. M., Austine-Orimoloye, O., Azov, A. G., Barnes, I., Bennett, R., Berry, A., Bhai, J., Bignell, A., Billis, K., Boddu, S., Brooks, L., Charkhchi, M., Cummins, C., Da Rin Fioretto, L., … Flicek, P. (2022). Ensembl 2022. *Nucleic Acids Research*, *50*(D1), D988–D995. https://doi.org/10.1093/nar/gkab1049

Dawar, F. U., Xiong, Y., Khattak, M. N. K., Li, J., Lin, L., & Mei, J. (2017). Potential role of cyclophilin A in regulating cytokine secretion. *Journal of Leukocyte Biology*, *102*(4), 989–992. https://doi.org/10.1189/jlb.3RU0317-090RR

De Jager, P. L., Jia, X., Wang, J., de Bakker, P. I. W., Ottoboni, L., Aggarwal, N. T., Piccio, L., Raychaudhuri, S., Tran, D., Aubin, C., Briskin, R., Romano, S., International MS Genetics Consortium, Baranzini, S. E., McCauley, J. L., Pericak-Vance, M. A., Haines, J. L., Gibson, R. A., Naeglin, Y., … Oksenberg, J. R. (2009). Meta-analysis of genome scans and replication identify CD6, IRF8 and TNFRSF1A as new multiple sclerosis susceptibility loci. *Nature Genetics*, *41*(7), 776–782. https://doi.org/10.1038/ng.401

de Morree, A., Klein, J. D. D., Gan, Q., Farup, J., Urtasun, A., Kanugovi, A., Bilen, B., van Velthoven, C. T. J., Quarta, M., & Rando, T. A. (2019). Alternative polyadenylation of Pax3 controls muscle stem cell fate and muscle function. *Science (New York, N.Y.)*, *366*(6466), 734–738. https://doi.org/10.1126/science.aax1694

de Moura, P. R., Watanabe, L., Bleicher, L., Colau, D., Dumoutier, L., Lemaire, M. M., Renauld, J. C., & Polikarpov, I. (2009). Crystal structure of a soluble decoy receptor IL-22BP bound to interleukin-22. *FEBS Letters*. https://doi.org/10.1016/j.febslet.2009.03.006

Degelman, M. L., & Herman, K. M. (2017). Smoking and multiple sclerosis: A systematic review and meta-analysis using the Bradford Hill criteria for causation. *Multiple Sclerosis and Related Disorders*, *17*, 207–216. https://doi.org/10.1016/j.msard.2017.07.020

Der Vartanian, A., Quétin, M., Michineau, S., Auradé, F., Hayashi, S., Dubois, C., Rocancourt, D., Drayton-Libotte, B., Szegedi, A., Buckingham, M., Conway, S. J., Gervais, M., & Relaix,

F. (2019). PAX3 Confers Functional Heterogeneity in Skeletal Muscle Stem Cell Responses to Environmental Stress. *Cell Stem Cell*, *24*(6), 958-973.e9. https://doi.org/10.1016/j.stem.2019.03.019

Dersh, D., Jones, S. M., Eletto, D., Christianson, J. C., & Argon, Y. (2014). OS-9 facilitates turnover of nonnative GRP94 marked by hyperglycosylation. *Molecular Biology of the Cell*, *25*(15), 2220–2234. https://doi.org/10.1091/mbc.E14-03-0805

Devergne, O., Birkenbach, M., & Kieff, E. (1997). Epstein-Barr virus-induced gene 3 and the p35 subunit of interleukin 12 form a novel heterodimeric hematopoietin. *Proceedings of the National Academy of Sciences of the United States of America*, *94*(22), 12041–12046. Scopus. https://doi.org/10.1073/pnas.94.22.12041

Devergne, O., Hummel, M., Koeppen, H., Beau, M. M. L., Nathanson, E. C., Kieff, E., & Birkenbach, M. (1996). A novel interleukin-12 p40-related protein induced by latent Epstein-Barr virus infection in B lymphocytes. *Journal of Virology*, *70*(2), 1143–1153.

Disanto, G., Pakpoor, J., Morahan, J. M., Hall, C., Meier, U. C., Giovannoni, G., & Ramagopalan, S. V. (2013). Epstein-Barr virus, latitude and multiple sclerosis. *Multiple Sclerosis (Houndmills, Basingstoke, England)*, *19*(3), 362–365. https://doi.org/10.1177/1352458512451942

Dixon, K. O., van der Kooij, S. W., Vignali, D. A. A., & van Kooten, C. (2015). Human tolerogenic dendritic cells produce IL-35 in the absence of other IL-12 family members. *European Journal of Immunology*, *45*(6), 1736–1747. https://doi.org/10.1002/eji.201445217

Dobson, R., & Giovannoni, G. (2019). Multiple sclerosis—A review. *European Journal of Neurology*, *26*(1), 27–40. https://doi.org/10.1111/ene.13819

Dubois, P. C. A., Trynka, G., Franke, L., Hunt, K. A., Romanos, J., Curtotti, A., Zhernakova, A., Heap, G. A. R., Ádány, R., Aromaa, A., Bardella, M. T., van den Berg, L. H., Bockett, N. A., de la Concha, E. G., Dema, B., Fehrmann, R. S. N., Fernández-Arquero, M., Fiatal, S., Grandone, E., … van Heel, D. A. (2010). Multiple common variants for celiac disease

influencing immune gene expression. *Nature Genetics*, *42*(4), 295–302. https://doi.org/10.1038/ng.543

Dumitru, A., Radu, B. M., Radu, M., & Cretoiu, S. M. (2018). Muscle Changes During Atrophy. *Advances in Experimental Medicine and Biology*, *1088*, 73–92. https://doi.org/10.1007/978-981-13-1435-3_4

Dumoutier, L., Lejeune, D., Colau, D., & Renauld, J. C. (2001). Cloning and characterization of IL-22 binding protein, a natural antagonist of IL-10-related T cell-derived inducible factor/IL-22. *Journal of Immunology (Baltimore, Md. : 1950)*, *166*(12), 7090–7095.

Dungan, L. S., McGuinness, N. C., Boon, L., Lynch, M. A., & Mills, K. H. G. (2014). Innate IFN-γ promotes development of experimental autoimmune encephalomyelitis: A role for NK cells and M1 macrophages. *European Journal of Immunology*, *44*(10), 2903–2917. https://doi.org/10.1002/eji.201444612

Ebner, S., Ratzinger, G., Krösbacher, B., Schmuth, M., Weiss, A., Reider, D., Kroczek, R. A., Herold, M., Heufler, C., Fritsch, P., & Romani, N. (2001). Production of IL-12 by human monocyte-derived dendritic cells is optimal when the stimulus is given at the onset of maturation, and is further enhanced by IL-4. *Journal of Immunology (Baltimore, Md.: 1950)*, *166*(1), 633–641. https://doi.org/10.4049/jimmunol.166.1.633

Edwards, S. L., Beesley, J., French, J. D., & Dunning, A. M. (2013). Beyond GWASs: Illuminating the dark road from association to function. *American Journal of Human Genetics*, *93*(5), 779–797. https://doi.org/10.1016/j.ajhg.2013.10.012

Electrospinning Company. (2022). *Myelination Assay*. Myelination Assay. https://www.electrospinning.co.uk/case-studies/myelination-assay/

El-Shabrawi, Y., Livir-Rallatos, C., Christen, W., Baltatzis, S., & Foster, C. S. (1998). High levels of interleukin-12 in the aqueous humor and vitreous of patients with uveitis. *Ophthalmology*, *105*(9), 1659–1663. Scopus. https://doi.org/10.1016/S0161-6420(98)99035-2

Eslami, M., Rafiei, A., Baghbanian, S. M., Fattahi, S., Yazdani, Z., Valadan, R., & Kardan, M. (2022). Serum levels and genetic variation of IL-35 are associated with multiple sclerosis: A population-based case-control study. *Immunologic Research*, *70*(1), 75–85. https://doi.org/10.1007/s12026-021-09246-9

Etemadifar, M., Nikanpour, Y., Neshatfar, A., Mansourian, M., & Fitzgerald, S. (2020). Incidence and prevalence of multiple sclerosis in persian gulf area: A systematic review and meta-analysis. *Multiple Sclerosis and Related Disorders*, *40*, 101959. https://doi.org/10.1016/j.msard.2020.101959

FlowJo. (2022). https://www.flowjo.com/learn/flowjo-university/flowjo/before-flowjo/58

Fragoso, Y. D., Stoney, P. N., & McCaffery, P. J. (2014). The evidence for a beneficial role of vitamin A in multiple sclerosis. *CNS Drugs*, *28*(4), 291–299. https://doi.org/10.1007/s40263-014-0148-4

Fukaya, T., Fukui, T., Uto, T., Takagi, H., Nasu, J., Miyanaga, N., Arimura, K., Nakamura, T., Koseki, H., Choijookhuu, N., Hishikawa, Y., & Sato, K. (2018). Pivotal Role of IL-22 Binding Protein in the Epithelial Autoregulation of Interleukin-22 Signaling in the Control of Skin Inflammation. *Frontiers in Immunology*, *9*. https://doi.org/10.3389/fimmu.2018.01418

Gaffen, S. L., Jain, R., Garg, A. V., & Cua, D. J. (2014). The IL-23–IL-17 immune axis: From mechanisms to therapeutic testing. *Nature Reviews Immunology*, *14*(9), 585–600. https://doi.org/10.1038/nri3707

Gao, Z., Nissen, J. C., Ji, K., & Tsirka, S. E. (2014). The experimental autoimmune encephalomyelitis disease course is modulated by nicotine and other cigarette smoke components. *PloS One*, *9*(9), e107979. https://doi.org/10.1371/journal.pone.0107979

Garbers, C., Hermanns, H. M., Schaper, F., Müller-Newen, G., Grötzinger, J., Rose-John, S., & Scheller, J. (2012). Plasticity and cross-talk of interleukin 6-type cytokines. *Cytokine & Growth Factor Reviews*, *23*(3), 85–97. https://doi.org/10.1016/j.cytogfr.2012.04.001

Gaut, J. R., & Hendershot, L. M. (1993). Mutations within the nucleotide binding site of immunoglobulin-binding protein inhibit ATPase activity and interfere with release of immunoglobulin heavy chain. *The Journal of Biological Chemistry*, *268*(10), 7248–7255.

GBD 2016 Multiple Sclerosis Collaborators. (2019). Global, regional, and national burden of multiple sclerosis 1990-2016: A systematic analysis for the Global Burden of Disease Study 2016. *The Lancet. Neurology*, *18*(3), 269–285. https://doi.org/10.1016/S1474-4422(18)30443-5

GBD 2017 Disease and Injury Incidence and Prevalence Collaborators. (2018). Global, regional, and national incidence, prevalence, and years lived with disability for 354 diseases and injuries for 195 countries and territories, 1990-2017: A systematic analysis for the Global Burden of Disease Study 2017. *Lancet (London, England)*, *392*(10159), 1789–1858. https://doi.org/10.1016/S0140-6736(18)32279-7

Giovannoni, G., Butzkueven, H., Dhib-Jalbut, S., Hobart, J., Kobelt, G., Pepper, G., Sormani, M. P., Thalheim, C., Traboulsee, A., & Vollmer, T. (2016). Brain health: Time matters in multiple sclerosis. *Multiple Sclerosis and Related Disorders*, *9 Suppl 1*, S5–S48. https://doi.org/10.1016/j.msard.2016.07.003

Gjelstrup, M. C., Stilund, M., Petersen, T., Møller, H. J., Petersen, E. L., & Christensen, T. (2018). Subsets of activated monocytes and markers of inflammation in incipient and progressed multiple sclerosis. *Immunology and Cell Biology*, *96*(2), 160–174. https://doi.org/10.1111/imcb.1025

Göbel, K., Ruck, T., & Meuth, S. G. (2018). Cytokine signaling in multiple sclerosis: Lost in translation. *Multiple Sclerosis Journal*, *24*(4), 432–439. https://doi.org/10.1177/1352458518763094

Goldberg, P. (1974). Multiple sclerosis: Vitamin D and calcium as environmental determinants of prevalence. *International Journal of Environmental Studies*, *6*(1), 19–27. https://doi.org/10.1080/00207237408709630

Gómez-Fernández, P., Lopez de Lapuente Portilla, A., Astobiza, I., Mena, J., Urtasun, A., Altmann, V., Matesanz, F., Otaegui, D., Urcelay, E., Antigüedad, A., Malhotra, S., Montalban, X., Castillo-Triviño, T., Espino-Paisán, L., Aktas, O., Buttmann, M., Chan, A., Fontaine, B., Gourraud, P.-A., … Vandenbroeck, K. (2020). The Rare IL22RA2 Signal Peptide Coding Variant rs28385692 Decreases Secretion of IL-22BP Isoform-1, -2 and -3 and Is Associated with Risk for Multiple Sclerosis. *Cells*, *9*(1). https://doi.org/10.3390/cells9010175

Gómez-Fernández, P., Urtasun, A., Astobiza, I., Mena, J., Alloza, I., & Vandenbroeck, K. (2019). Pharmacological Targeting of the ER-Resident Chaperones GRP94 or Cyclophilin B Induces Secretion of IL-22 Binding Protein Isoform-1 (IL-22BPi1). *International Journal of Molecular Sciences*, *20*(10). https://doi.org/10.3390/ijms20102440

Gómez-Fernández, P., Urtasun, A., Paton, A. W., Paton, J. C., Borrego, F., Dersh, D., Argon, Y., Alloza, I., & Vandenbroeck, K. (2018). Long Interleukin-22 Binding Protein Isoform-1 Is an Intracellular Activator of the Unfolded Protein Response. *Frontiers in Immunology*, *9*, 2934. https://doi.org/10.3389/fimmu.2018.02934

Gran, B., Zhang, G.-X., Yu, S., Li, J., Chen, X.-H., Ventura, E. S., Kamoun, M., & Rostami, A. (2002). IL-12p35-deficient mice are susceptible to experimental autoimmune encephalomyelitis: Evidence for redundancy in the IL-12 system in the induction of central nervous system autoimmune demyelination. *Journal of Immunology (Baltimore, Md.: 1950)*, *169*(12), 7104–7110. https://doi.org/10.4049/jimmunol.169.12.7104

Gu, X., Tian, T., Zhang, B., Liu, Y., Yuan, C., Shao, L., Guo, Y., & Fan, K. (2015). Elevated plasma interleukin-35 levels predict poor prognosis in patients with non-small cell lung cancer. *Tumour Biology: The Journal of the International Society for Oncodevelopmental Biology and Medicine*, *36*(4), 2651–2656. https://doi.org/10.1007/s13277-014-2887-8

Hadadi, E., Zhang, B., Baidžajevas, K., Yusof, N., Puan, K. J., Ong, S. M., Yeap, W. H., Rotzschke, O., Kiss-Toth, E., Wilson, H., & Wong, S. C. (2016). Differential IL-1β secretion

by monocyte subsets is regulated by Hsp27 through modulating mRNA stability. *Scientific Reports*, *6*, 39035. https://doi.org/10.1038/srep39035

Haji Abdolvahab, M., Mofrad, M. R. K., & Schellekens, H. (2016). Interferon Beta: From Molecular Level to Therapeutic Effects. *International Review of Cell and Molecular Biology*, *326*, 343–372. https://doi.org/10.1016/bs.ircmb.2016.06.001

Haller, S., Duval, A., Migliorini, R., Stevanin, M., Mack, V., & Acha-Orbea, H. (2017). Interleukin-35-Producing CD8α+ Dendritic Cells Acquire a Tolerogenic State and Regulate T Cell Function. *Frontiers in Immunology*, *8*. https://doi.org/10.3389/fimmu.2017.00098

Harama, D., Koyama, K., Mukai, M., Shimokawa, N., Miyata, M., Nakamura, Y., Ohnuma, Y., Ogawa, H., Matsuoka, S., Paton, A. W., Paton, J. C., Kitamura, M., & Nakao, A. (2009). A subcytotoxic dose of subtilase cytotoxin prevents lipopolysaccharide-induced inflammatory responses, depending on its capacity to induce the unfolded protein response. *Journal of Immunology (Baltimore, Md.: 1950)*, *183*(2), 1368–1374. https://doi.org/10.4049/jimmunol.0804066

Harirchian, M. H., Fatehi, F., Sarraf, P., Honarvar, N. M., & Bitarafan, S. (2018). Worldwide prevalence of familial multiple sclerosis: A systematic review and meta-analysis. *Multiple Sclerosis and Related Disorders*, *20*, 43–47. https://doi.org/10.1016/j.msard.2017.12.015

Hartung, D. M., Bourdette, D. N., Ahmed, S. M., & Whitham, R. H. (2015). The cost of multiple sclerosis drugs in the US and the pharmaceutical industry: Too big to fail? *Neurology*, *84*(21), 2185–2192. https://doi.org/10.1212/WNL.0000000000001608

Hayes, M. P., Wang, J., & Norcross, M. A. (1995). Regulation of interleukin-12 expression in human monocytes: Selective priming by interferon-gamma of lipopolysaccharide-inducible p35 and p40 genes. *Blood*, *86*(2), 646–650.

He, Y., Huang, L., Tang, Y., Yang, Z., & Han, Z. (2021). Genome-wide Identification and Analysis of Splicing QTLs in Multiple Sclerosis by RNA-Seq Data. *Frontiers in Genetics*, *12*, 769804. https://doi.org/10.3389/fgene.2021.769804

Hedström, A. K., Hillert, J., Olsson, T., & Alfredsson, L. (2013). Smoking and multiple sclerosis susceptibility. *European Journal of Epidemiology*, *28*(11), 867–874. https://doi.org/10.1007/s10654-013-9853-4

Hedström, A. K., Katsoulis, M., Hössjer, O., Bomfim, I. L., Oturai, A., Sondergaard, H. B., Sellebjerg, F., Ullum, H., Thørner, L. W., Gustavsen, M. W., Harbo, H. F., Obradovic, D., Gianfrancesco, M. A., Barcellos, L. F., Schaefer, C. A., Hillert, J., Kockum, I., Olsson, T., & Alfredsson, L. (2017). The interaction between smoking and HLA genes in multiple sclerosis: Replication and refinement. *European Journal of Epidemiology*, *32*(10), 909–919. https://doi.org/10.1007/s10654-017-0250-2

Hegde, R. S., & Bernstein, H. D. (2006). The surprising complexity of signal sequences. *Trends in Biochemical Sciences*, *31*(10), 563–571. https://doi.org/10.1016/j.tibs.2006.08.004

Hernandez, P., Gronke, K., & Diefenbach, A. (2018). A catch-22: Interleukin-22 and cancer. *European Journal of Immunology*, *48*(1), 15–31. https://doi.org/10.1002/eji.201747183

Hetz, C. (2012). The unfolded protein response: Controlling cell fate decisions under ER stress and beyond. *Nature Reviews. Molecular Cell Biology*, *13*(2), 89–102. https://doi.org/10.1038/nrm3270

Hollenbach, J. A., & Oksenberg, J. R. (2015). The Immunogenetics of Multiple Sclerosis: A Comprehensive Review. *Journal of Autoimmunity*, *64*, 13–25. https://doi.org/10.1016/j.jaut.2015.06.010

Höpfner, F., Jacob, M., Ulrich, C., Russ, M., Simm, A., Silber, R. E., Girndt, M., Noutsias, M., Werdan, K., & Schlitt, A. (2019). Subgroups of monocytes predict cardiovascular events in patients with coronary heart disease. The PHAMOS trial (Prospective Halle Monocytes Study). *Hellenic Journal of Cardiology: HJC = Hellenike Kardiologike Epitheorese*, *60*(5), 311–321. https://doi.org/10.1016/j.hjc.2019.04.012

Horton, R. M., Cai, Z., Ho, S. N., & Pease, L. R. (2013). Gene Splicing by Overlap Extension: Tailor-Made Genes Using the Polymerase Chain Reaction. *BioTechniques*, *54*(3), 129–133. https://doi.org/10.2144/000114017

Hu, C.-C. A., Dougan, S. K., Winter, S. V., Paton, A. W., Paton, J. C., & Ploegh, H. L. (2009). Subtilase cytotoxin cleaves newly synthesized BiP and blocks antibody secretion in B lymphocytes. *The Journal of Experimental Medicine*, *206*(11), 2429–2440. https://doi.org/10.1084/jem.20090782

Huber, S., Gagliani, N., Zenewicz, L. A., Huber, F. J., Bosurgi, L., Hu, B., Hedl, M., Zhang, W., O'Connor, W., Murphy, A. J., Valenzuela, D. M., Yancopoulos, G. D., Booth, C. J., Cho, J. H., Ouyang, W., Abraham, C., & Flavell, R. A. (2012). IL-22BP is regulated by the inflammasome and modulates tumorigenesis in the intestine. *Nature*, *491*(7423), 259–263. https://doi.org/10.1038/nature11535

IMSGC. (2019a). A systems biology approach uncovers cell-specific gene regulatory effects of genetic associations in multiple sclerosis. *Nature Communications*, *10*(1), 2236. https://doi.org/10.1038/s41467-019-09773-y

IMSGC. (2019b). Multiple sclerosis genomic map implicates peripheral immune cells and microglia in susceptibility. *Science (New York, N.Y.)*, *365*(6460). https://doi.org/10.1126/science.aav7188

IMSGC, Beecham, A. H., Patsopoulos, N. A., Xifara, D. K., Davis, M. F., Kemppinen, A., Cotsapas, C., Shah, T. S., Spencer, C., Booth, D., Goris, A., Oturai, A., Saarela, J., Fontaine, B., Hemmer, B., Martin, C., Zipp, F., D'Alfonso, S., Martinelli-Boneschi, F., … McCauley, J. L. (2013). Analysis of immune-related loci identifies 48 new susceptibility variants for multiple sclerosis. *Nature Genetics*, *45*(11), 1353–1360. https://doi.org/10.1038/ng.2770

IMSGC, Wellcome Trust Case Control Consortium 2, Sawcer, S., Hellenthal, G., Pirinen, M., Spencer, C. C. A., Patsopoulos, N. A., Moutsianas, L., Dilthey, A., Su, Z., Freeman, C.,

Hunt, S. E., Edkins, S., Gray, E., Booth, D. R., Potter, S. C., Goris, A., Band, G., Oturai, A. B., … Compston, A. (2011). Genetic risk and a primary role for cell-mediated immune mechanisms in multiple sclerosis. *Nature*, *476*(7359), 214–219. https://doi.org/10.1038/nature10251

Jackson, J. R., Kirby, T. J., Fry, C. S., Cooper, R. L., McCarthy, J. J., Peterson, C. A., & Dupont-Versteegden, E. E. (2015). Reduced voluntary running performance is associated with impaired coordination as a result of muscle satellite cell depletion in adult mice. *Skeletal Muscle*, *5*, 41. https://doi.org/10.1186/s13395-015-0065-3

Jafarzadeh, A., Jamali, M., Mahdavi, R., Ebrahimi, H. A., Hajghani, H., Khosravimashizi, A., Nemati, M., Najafipour, H., Sheikhi, A., Mohammadi, M. M., & Daneshvar, H. (2015). Circulating levels of interleukin-35 in patients with multiple sclerosis: Evaluation of the influences of FOXP3 gene polymorphism and treatment program. *Journal of Molecular Neuroscience: MN*, *55*(4), 891–897. https://doi.org/10.1007/s12031-014-0443-z

Jaguin, M., Houlbert, N., Fardel, O., & Lecureur, V. (2013). Polarization profiles of human M-CSF-generated macrophages and comparison of M1-markers in classically activated macrophages from GM-CSF and M-CSF origin. *Cellular Immunology*, *281*(1), 51–61. https://doi.org/10.1016/j.cellimm.2013.01.010

Jalah, R., Rosati, M., Ganneru, B., Pilkington, G. R., Valentin, A., Kulkarni, V., Bergamaschi, C., Chowdhury, B., Zhang, G.-M., Beach, R. K., Alicea, C., Broderick, K. E., Sardesai, N. Y., Pavlakis, G. N., & Felber, B. K. (2013). The p40 Subunit of Interleukin (IL)-12 Promotes Stabilization and Export of the p35 Subunit IMPLICATIONS FOR IMPROVED IL-12 CYTOKINE PRODUCTION. *Journal of Biological Chemistry*, *288*(9), 6763–6776. https://doi.org/10.1074/jbc.M112.436675

Jansen, G., Määttänen, P., Denisov, A. Y., Scarffe, L., Schade, B., Balghi, H., Dejgaard, K., Chen, L. Y., Muller, W. J., Gehring, K., & Thomas, D. Y. (2012). An Interaction Map of

Endoplasmic Reticulum Chaperones and Foldases. *Molecular & Cellular Proteomics*, *11*(9), 710–723. https://doi.org/10.1074/mcp.M111.016550

Jersild, C., Hansen, G., Svejgaard, A., Fog, T., Thomsen, M., & Dupont, B. (1973). HISTOCOMPATIBILITY DETERMINANTS IN MULTIPLE SCLEROSIS, WITH SPECIAL REFERENCE TO CLINICAL COURSE. *The Lancet*, *302*(7840), 1221–1225. https://doi.org/10.1016/S0140-6736(73)90970-7

Jersild, C., Svejgaard, A., & Fog, T. (1972). HL-A ANTIGENS AND MULTIPLE SCLEROSIS. *The Lancet*, *299*(7762), 1240–1241. https://doi.org/10.1016/S0140-6736(72)90962-2

Jia, L., & Wu, C. (2014). The biology and functions of Th22 cells. *Advances in Experimental Medicine and Biology*, *841*, 209–230. https://doi.org/10.1007/978-94-017-9487-9_8

Jinnohara, T., Kanaya, T., Hase, K., Sakakibara, S., Kato, T., Tachibana, N., Sasaki, T., Hashimoto, Y., Sato, T., Watarai, H., Kunisawa, J., Shibata, N., Williams, I. R., Kiyono, H., & Ohno, H. (2017). IL-22BP dictates characteristics of Peyer's patch follicle-associated epithelium for antigen uptake. *Journal of Experimental Medicine*. http://jem.rupress.org/content/early/2017/05/15/jem.20160770.long

Jones, B. C., Logsdon, N. J., & Walter, M. R. (2008). Structure of IL-22 bound to its high-affinity IL-22R1 chain. *Structure (London, England : 1993)*, *16*(9), 1333–1344. https://doi.org/10.1016/j.str.2008.06.005

Kaida, D., Berg, M. G., Younis, I., Kasim, M., Singh, L. N., Wan, L., & Dreyfuss, G. (2010). U1 snRNP protects pre-mRNAs from premature cleavage and polyadenylation. *Nature*, *468*(7324), 664–668. https://doi.org/10.1038/nature09479

Kamal, A., Hosny, M., Abd Elwahab, A., Shawki Kamal, Y., Shehata, H. S., & Hassan, A. (2021). FOXP3rs3761548 gene variant and interleukin-35 serum levels as biomarkers in patients with multiple sclerosis. *Revue Neurologique*, *177*(6), 647–654. https://doi.org/10.1016/j.neurol.2020.07.010

Ke, Y., Sun, D., Jiang, G., Kaplan, H. J., & Shao, H. (2011). IL-22-induced regulatory CD11b+ APCs suppress experimental autoimmune uveitis. *Journal of Immunology (Baltimore, Md.: 1950)*, *187*(5), 2130–2139. https://doi.org/10.4049/jimmunol.1100482

Kebir, H., Kreymborg, K., Ifergan, I., Dodelet-Devillers, A., Cayrol, R., Bernard, M., Giuliani, F., Arbour, N., Becher, B., & Prat, A. (2007). Human TH17 lymphocytes promote blood-brain barrier disruption and central nervous system inflammation. *Nature Medicine*, *13*(10), 1173–1175. https://doi.org/10.1038/nm1651

Keefe, A. C., Lawson, J. A., Flygare, S. D., Fox, Z. D., Colasanto, M. P., Mathew, S. J., Yandell, M., & Kardon, G. (2015). Muscle stem cells contribute to myofibres in sedentary adult mice. *Nature Communications*, *6*(1), 7087. https://doi.org/10.1038/ncomms8087

Kim, J., Choi, T. G., Ding, Y., Kim, Y., Ha, K. S., Lee, K. H., Kang, I., Ha, J., Kaufman, R. J., Lee, J., Choe, W., & Kim, S. S. (2008). Overexpressed cyclophilin B suppresses apoptosis associated with ROS and Ca2+ homeostasis after ER stress. *Journal of Cell Science*, *121*(Pt 21), 3636–3648. https://doi.org/10.1242/jcs.028654

Kim, Y. J., Kim, H. J., Lee, W. J., & Seong, J. K. (2020). A comparison of the metabolic effects of treadmill and wheel running exercise in mouse model. *Laboratory Animal Research*, *36*, 3. https://doi.org/10.1186/s42826-019-0035-8

Kinoshita, M., Obata, K., & Tanaka, M. (2015). Latitude has more significant impact on prevalence of multiple sclerosis than ultraviolet level or sunshine duration in Japanese population. *Neurological Sciences: Official Journal of the Italian Neurological Society and of the Italian Society of Clinical Neurophysiology*, *36*(7), 1147–1151. https://doi.org/10.1007/s10072-015-2150-0

Kleinschmidt, D., Giannou, A. D., McGee, H. M., Kempski, J., Steglich, B., Huber, F. J., Ernst, T. M., Shiri, A. M., Wegscheid, C., Tasika, E., Hübener, P., Huber, P., Bedke, T., Steffens, N., Agalioti, T., Fuchs, T., Noll, J., Lotter, H., Tiegs, G., … Huber, S. (2017). A Protective Function of IL-22BP in Ischemia Reperfusion and Acetaminophen-Induced Liver Injury.

Journal of Immunology (Baltimore, Md.: 1950), *199*(12), 4078–4090. https://doi.org/10.4049/jimmunol.1700587

Kobayashi, K. S., & van den Elsen, P. J. (2012). NLRC5: A key regulator of MHC class I-dependent immune responses. *Nature Reviews Immunology*, *12*(12), 813–820. https://doi.org/10.1038/nri3339

Kobayashi, M., Fitz, L., Ryan, M., Hewick, R. M., Clark, S. C., Chan, S., Loudon, R., Sherman, F., Perussia, B., & Trinchieri, G. (1989). Identification and purification of natural killer cell stimulatory factor (NKSF), a cytokine with multiple biologic effects on human lymphocytes. *The Journal of Experimental Medicine*, *170*(3), 827–845. https://doi.org/10.1084/jem.170.3.827

Kobelt, G., Thompson, A., Berg, J., Gannedahl, M., Eriksson, J., MSCOI Study Group, & European Multiple Sclerosis Platform. (2017). New insights into the burden and costs of multiple sclerosis in Europe. *Multiple Sclerosis (Houndmills, Basingstoke, England)*, *23*(8), 1123–1136. https://doi.org/10.1177/1352458517694432

Koch, S., Kucharzik, T., Heidemann, J., Nusrat, A., & Luegering, A. (2010). Investigating the role of proinflammatory CD16+ monocytes in the pathogenesis of inflammatory bowel disease. *Clinical and Experimental Immunology*, *161*(2), 332. https://doi.org/10.1111/j.1365-2249.2010.04177.x

Koch-Henriksen, N., & Magyari, M. (2021). Apparent changes in the epidemiology and severity of multiple sclerosis. *Nature Reviews. Neurology*, *17*(11), 676–688. https://doi.org/10.1038/s41582-021-00556-y

Kornek, B., Storch, M. K., Weissert, R., Wallstroem, E., Stefferl, A., Olsson, T., Linington, C., Schmidbauer, M., & Lassmann, H. (2000). Multiple Sclerosis and Chronic Autoimmune Encephalomyelitis: A Comparative Quantitative Study of Axonal Injury in Active, Inactive, and Remyelinated Lesions. *The American Journal of Pathology*, *157*(1), 267–276. https://doi.org/10.1016/S0002-9440(10)64537-3

Kostrominova, T. Y. (2011). Application of WGA lectin staining for visualization of the connective tissue in skeletal muscle, bone, and ligament/tendon studies. *Microscopy Research and Technique*, *74*(1), 18–22. https://doi.org/10.1002/jemt.20865

Kotenko, S. V., Izotova, L. S., Mirochnitchenko, O. V., Esterova, E., Dickensheets, H., Donnelly, R. P., & Pestka, S. (2001). Identification, cloning, and characterization of a novel soluble receptor that binds IL-22 and neutralizes its activity. *Journal of Immunology (Baltimore, Md. : 1950)*, *166*(12), 7096–7103.

Kouris, A., Pistiki, A., Katoulis, A., Georgitsi, M., Giatrakou, S., Papadavid, E., Netea, M. G., Stavrianeas, N., & Giamarellos-Bourboulis, E. J. (2014). Proinflammatory cytokine responses in patients with psoriasis. *European Cytokine Network*, *25*(4), 63–68. https://doi.org/10.1684/ecn.2014.0358

Kreymborg, K., Etzensperger, R., Dumoutier, L., Haak, S., Rebollo, A., Buch, T., Heppner, F. L., Renauld, J.-C., & Becher, B. (2007). IL-22 is expressed by Th17 cells in an IL-23-dependent fashion, but not required for the development of autoimmune encephalomyelitis. *Journal of Immunology (Baltimore, Md.: 1950)*, *179*(12), 8098–8104. https://doi.org/10.4049/jimmunol.179.12.8098

Kubin, M., Chow, J. M., & Trinchieri, G. (1994). Differential regulation of interleukin-12 (IL-12), tumor necrosis factor alpha, and IL-1 beta production in human myeloid leukemia cell lines and peripheral blood mononuclear cells. *Blood*, *83*(7), 1847–1855.

Kulkarni, O. P., Hartter, I., Mulay, S. R., Hagemann, J., Darisipudi, M. N., Vr, S. K., Romoli, S., Thomasova, D., Ryu, M., Kobold, S., & Anders, H.-J. (2014). Toll-Like Receptor 4–Induced IL-22 Accelerates Kidney Regeneration. *Journal of the American Society of Nephrology*, *25*(5), 978–989. https://doi.org/10.1681/ASN.2013050528

La Mantia, L., Munari, L. M., & Lovati, R. (2010). Glatiramer acetate for multiple sclerosis. *The Cochrane Database of Systematic Reviews*, *5*, CD004678. https://doi.org/10.1002/14651858.CD004678.pub2

Laaksonen, H., Guerreiro-Cacais, A. O., Adzemovic, M. Z., Parsa, R., Zeitelhofer, M., Jagodic, M., & Olsson, T. (2014). The multiple sclerosis risk gene IL22RA2 contributes to a more severe murine autoimmune neuroinflammation. *Genes and Immunity*, *15*(7), 457–465. https://doi.org/10.1038/gene.2014.36

Lanz, T. V., Brewer, R. C., Ho, P. P., Moon, J.-S., Jude, K. M., Fernandez, D., Fernandes, R. A., Gomez, A. M., Nadj, G.-S., Bartley, C. M., Schubert, R. D., Hawes, I. A., Vazquez, S. E., Iyer, M., Zuchero, J. B., Teegen, B., Dunn, J. E., Lock, C. B., Kipp, L. B., … Robinson, W. H. (2022). Clonally expanded B cells in multiple sclerosis bind EBV EBNA1 and GlialCAM. *Nature*, *603*(7900), Article 7900. https://doi.org/10.1038/s41586-022-04432-7

Larousserie, F., Bardel, E., Pflanz, S., Arnulf, B., Lome-Maldonado, C., Hermine, O., Brégeaud, L., Perennec, M., Brousse, N., Kastelein, R., & Devergne, O. (2005). Analysis of interleukin-27 (EBI3/p28) expression in Epstein-Barr virus- and human T-cell leukemia virus type 1-associated lymphomas: Heterogeneous expression of EBI3 subunit by tumoral cells. *The American Journal of Pathology*, *166*(4), 1217–1228. https://doi.org/10.1016/S0002-9440(10)62340-1

Lasek, W., Zagożdżon, R., & Jakobisiak, M. (2014). Interleukin 12: Still a promising candidate for tumor immunotherapy? *Cancer Immunology, Immunotherapy: CII*, *63*(5), 419–435. https://doi.org/10.1007/s00262-014-1523-1

Lassmann, H. (2013). Pathology and disease mechanisms in different stages of multiple sclerosis. *Journal of the Neurological Sciences*, *333*(1), 1–4. https://doi.org/10.1016/j.jns.2013.05.010

Lassmann, H. (2018). Multiple Sclerosis Pathology. *Cold Spring Harbor Perspectives in Medicine*, *8*(3), a028936. https://doi.org/10.1101/cshperspect.a028936

Le Page, E., & Edan, G. (2018). Induction or escalation therapy for patients with multiple sclerosis? *Revue Neurologique*, *174*(6), 449–457. https://doi.org/10.1016/j.neurol.2018.04.004

Leinco. (2022). *Sandwich ELISA Protocol*. Leinco Technologies. https://www.leinco.com/sandwich-elisa-protocol/

Lepper, C., Partridge, T. A., & Fan, C.-M. (2011). An absolute requirement for Pax7-positive satellite cells in acute injury-induced skeletal muscle regeneration. *Development (Cambridge, England)*, *138*(17), 3639–3646. https://doi.org/10.1242/dev.067595

Lessard, C. J., Li, H., Adrianto, I., Ice, J. A., Rasmussen, A., Grundahl, K. M., Kelly, J. A., Dozmorov, M. G., Miceli-Richard, C., Bowman, S., Lester, S., Eriksson, P., Eloranta, M.-L., Brun, J. G., Gøransson, L. G., Harboe, E., Guthridge, J. M., Kaufman, K. M., Kvarnström, M., … Sivils, K. L. (2013). Variants at multiple loci implicated in both innate and adaptive immune responses are associated with Sjögren's syndrome. *Nature Genetics*, *45*(11), 1284–1292. https://doi.org/10.1038/ng.2792

Li, J., Yang, F., Wei, F., & Ren, X. (2017). The role of toll-like receptor 4 in tumor microenvironment. *Oncotarget*, *8*(39), 66656–66667. https://doi.org/10.18632/oncotarget.19105

Li, S., Yu, M., Li, H., Zhang, H., & Jiang, Y. (2012). IL-17 and IL-22 in Cerebrospinal Fluid and Plasma Are Elevated in Guillain-Barré Syndrome. *Mediators of Inflammation*, *2012*. https://doi.org/10.1155/2012/260473

Lim, C., Hong, M., & Savan, R. (2016). Human IL-22 binding protein isoforms act as a rheostat for IL-22 signaling. *Science Signaling*, *9*(447), ra95. https://doi.org/10.1126/scisignal.aad9887

Lim, C., & Savan, R. (2014). The role of the IL-22/IL-22R1 axis in cancer. *Cytokine & Growth Factor Reviews*, *25*(3), 257–271. https://doi.org/10.1016/j.cytogfr.2014.04.005

Lindahl, H., Guerreiro-Cacais, A. O., Bedri, S. K., Linnerbauer, M., Lindén, M., Abdelmagid, N., Tandre, K., Hollins, C., Irving, L., Glover, C., Jones, C., Alfredsson, L., Rönnblom, L., Kockum, I., Khademi, M., Jagodic, M., & Olsson, T. (2019). IL-22 Binding Protein

Promotes the Disease Process in Multiple Sclerosis. *Journal of Immunology (Baltimore, Md.: 1950)*, *203*(4), 888–898. https://doi.org/10.4049/jimmunol.1900400

Liu, J. Z., Almarri, M. A., Gaffney, D. J., Mells, G. F., Jostins, L., Cordell, H. J., Ducker, S. J., Day, D. B., Heneghan, M. A., Neuberger, J. M., Donaldson, P. T., Bathgate, A. J., Burroughs, A., Davies, M. H., Jones, D. E., Alexander, G. J., Barrett, J. C., Sandford, R. N., & Anderson, C. A. (2012). Dense fine-mapping study identifies new susceptibility loci for primary biliary cirrhosis. *Nature Genetics*, *44*(10), 1137–1141. https://doi.org/10.1038/ng.2395

Liu, J.-Q., Liu, Z., Zhang, X., Shi, Y., Talebian, F., Carl, J. W., Yu, C., Shi, F.-D., Whitacre, C. C., Trgovcich, J., & Bai, X.-F. (2012). Increased Th17 and regulatory T cell responses in EBV-induced gene 3-deficient mice lead to marginally enhanced development of autoimmune encephalomyelitis. *Journal of Immunology (Baltimore, Md.: 1950)*, *188*(7), 3099–3106. https://doi.org/10.4049/jimmunol.1100106

Liu, L., Cheung, T. H., Charville, G. W., & Rando, T. A. (2015). Isolation of skeletal muscle stem cells by fluorescence-activated cell sorting. *Nature Protocols*, *10*(10), 1612–1624. https://doi.org/10.1038/nprot.2015.110

Liu, X., Yang, J., & Deng, W. (2017). The inflammatory cytokine IL-22 promotes murine gliomas via proliferation. *Experimental and Therapeutic Medicine*, *13*(3), 1087–1092. https://doi.org/10.3892/etm.2017.4059

Liu, Y., & Tang, X. (2018). Depressive Syndromes in Autoimmune Disorders of the Nervous System: Prevalence, Etiology, and Influence. *Frontiers in Psychiatry*, *9*, 451. https://doi.org/10.3389/fpsyt.2018.00451

Lu, R.-M., Hwang, Y.-C., Liu, I.-J., Lee, C.-C., Tsai, H.-Z., Li, H.-J., & Wu, H.-C. (2020). Development of therapeutic antibodies for the treatment of diseases. *Journal of Biomedical Science*, *27*. https://doi.org/10.1186/s12929-019-0592-z

Mabtech. (2022). *ELISA Standard*. https://www.mabtech.com/knowledge-center/tutorials-and-guidelines/elisa-analysis/elisa-standard

Malhotra, J. D., & Kaufman, R. J. (2007). The endoplasmic reticulum and the unfolded protein response. *Seminars in Cell & Developmental Biology*, *18*(6), 716–731. https://doi.org/10.1016/j.semcdb.2007.09.003

Mansilla, M. J., Presas-Rodríguez, S., Teniente-Serra, A., González-Larreategui, I., Quirant-Sánchez, B., Fondelli, F., Djedovic, N., Iwaszkiewicz-Grześ, D., Chwojnicki, K., Miljković, Đ., Trzonkowski, P., Ramo-Tello, C., & Martínez-Cáceres, E. M. (2021). Paving the way towards an effective treatment for multiple sclerosis: Advances in cell therapy. *Cellular & Molecular Immunology*, *18*(6), 1353–1374. https://doi.org/10.1038/s41423-020-00618-z

Markota, A., Endres, S., & Kobold, S. (2018). Targeting interleukin-22 for cancer therapy. *Human Vaccines & Immunotherapeutics*, *14*(8), 2012–2015. https://doi.org/10.1080/21645515.2018.1461300

Martin, Bériou, G., Heslan, M., Bossard, C., Jarry, A., Abidi, A., Hulin, P., Ménoret, S., Thinard, R., Anegon, I., Jacqueline, C., Lardeux, B., Halary, F., Renauld, J.-C., Bourreille, A., & Josien, R. (2016). IL-22BP is produced by eosinophils in human gut and blocks IL-22 protective actions during colitis. *Mucosal Immunology*, *9*(2), 539–549. https://doi.org/10.1038/mi.2015.83

Martin, Bériou, G., Heslan, M., Chauvin, C., Utriainen, L., Aumeunier, A., Scott, C. L., Mowat, A., Cerovic, V., Houston, S. A., Leboeuf, M., Hubert, F. X., Hémont, C., Merad, M., Milling, S., & Josien, R. (2014). Interleukin-22 binding protein (IL-22BP) is constitutively expressed by a subset of conventional dendritic cells and is strongly induced by retinoic acid. *Mucosal Immunology*, *7*(1), 101–113. https://doi.org/10.1038/mi.2013.28

Martin, Wolk, K., Bériou, G., Abidi, A., Witte-Händel, E., Louvet, C., Kokolakis, G., Drujont, L., Dumoutier, L., Renauld, J.-C., Sabat, R., & Josien, R. (2017). Limited Presence of IL-22 Binding Protein, a Natural IL-22 Inhibitor, Strengthens Psoriatic Skin Inflammation. *Journal*

of Immunology (Baltimore, Md.: 1950), *198*(9), 3671–3678. https://doi.org/10.4049/jimmunol.1700021

Marzec, M., Eletto, D., & Argon, Y. (2012). GRP94: An HSP90-like protein specialized for protein folding and quality control in the endoplasmic reticulum. *Biochimica Et Biophysica Acta*, *1823*(3), 774–787. https://doi.org/10.1016/j.bbamcr.2011.10.013

Marzec, M., Hawkes, C. P., Eletto, D., Boyle, S., Rosenfeld, R., Hwa, V., Wit, J. M., van Duyvenvoorde, H. A., Oostdijk, W., Losekoot, M., Pedersen, O., Yeap, B. B., Flicker, L., Barzilai, N., Atzmon, G., Grimberg, A., & Argon, Y. (2016). A Human Variant of Glucose-Regulated Protein 94 That Inefficiently Supports IGF Production. *Endocrinology*, *157*(5), 1914–1928. https://doi.org/10.1210/en.2015-2058

Mattapallil, M. J., Kielczewski, J. L., Zárate-Bladés, C. R., St Leger, A. J., Raychaudhuri, K., Silver, P. B., Jittayasothorn, Y., Chan, C.-C., & Caspi, R. R. (2019). Interleukin 22 ameliorates neuropathology and protects from central nervous system autoimmunity. *Journal of Autoimmunity*, *102*, 65–76. https://doi.org/10.1016/j.jaut.2019.04.017

Mattson, M. P., & Taub, D. D. (2004). Ancient viral protein enrages astrocytes in multiple sclerosis. *Nature Neuroscience*, *7*(10), Article 10. https://doi.org/10.1038/nn1004-1021

Mauro, A. (1961). Satellite cell of skeletal muscle fibers. *The Journal of Biophysical and Biochemical Cytology*, *9*, 493–495. https://doi.org/10.1083/jcb.9.2.493

Mayes, M. D., Bossini-Castillo, L., Gorlova, O., Martin, J. E., Zhou, X., Chen, W. V., Assassi, S., Ying, J., Tan, F. K., Arnett, F. C., Reveille, J. D., Guerra, S., Teruel, M., Carmona, F. D., Gregersen, P. K., Lee, A. T., López-Isac, E., Ochoa, E., Carreira, P., … Martin, J. (2014). Immunochip Analysis Identifies Multiple Susceptibility Loci for Systemic Sclerosis. *The American Journal of Human Genetics*, *94*(1), 47–61. https://doi.org/10.1016/j.ajhg.2013.12.002

Meunier, L., Usherwood, Y.-K., Chung, K. T., & Hendershot, L. M. (2002). A subset of chaperones and folding enzymes form multiprotein complexes in endoplasmic reticulum to bind

nascent proteins. *Molecular Biology of the Cell*, *13*(12), 4456–4469. https://doi.org/10.1091/mbc.e02-05-0311

Mielke, L. A., Jones, S. A., Raverdeau, M., Higgs, R., Stefanska, A., Groom, J. R., Misiak, A., Dungan, L. S., Sutton, C. E., Streubel, G., Bracken, A. P., & Mills, K. H. G. (2013). Retinoic acid expression associates with enhanced IL-22 production by γδ T cells and innate lymphoid cells and attenuation of intestinal inflammation. *The Journal of Experimental Medicine*, *210*(6), 1117–1124. https://doi.org/10.1084/jem.20121588

Mildner, A., Mack, M., Schmidt, H., Brück, W., Djukic, M., Zabel, M. D., Hille, A., Priller, J., & Prinz, M. (2009). CCR2+Ly-6Chi monocytes are crucial for the effector phase of autoimmunity in the central nervous system. *Brain: A Journal of Neurology*, *132*(Pt 9), 2487–2500. https://doi.org/10.1093/brain/awp144

Miltenyi, S., Müller, W., Weichel, W., & Radbruch, A. (1990). High gradient magnetic cell separation with MACS. *Cytometry*, *11*(2), 231–238. https://doi.org/10.1002/cyto.990110203

Mizee, M. R., Nijland, P. G., van der Pol, S. M. A., Drexhage, J. A. R., van het Hof, B., Mebius, R., van der Valk, P., van Horssen, J., Reijerkerk, A., & de Vries, H. E. (2014). Astrocyte-derived retinoic acid: A novel regulator of blood–brain barrier function in multiple sclerosis. *Acta Neuropathologica*. https://doi.org/10.1007/s00401-014-1335-6

Mizoguchi, A., Yano, A., Himuro, H., Ezaki, Y., Sadanaga, T., & Mizoguchi, E. (2018). Clinical importance of IL-22 cascade in IBD. *Journal of Gastroenterology*, *53*(4), 465–474. https://doi.org/10.1007/s00535-017-1401-7

Molinari, M., & Sitia, R. (2005). The Secretory Capacity of a Cell Depends on the Efficiency of Endoplasmic Reticulum-Associated Degradation. In E. Wiertz & M. Kikkert (Eds.), *Dislocation and Degradation of Proteins from the Endoplasmic Reticulum* (pp. 1–15). Springer. https://doi.org/10.1007/3-540-28007-3_1

Mondanelli, G., Volpi, C., Bianchi, R., Allegrucci, M., Talesa, V. N., Grohmann, U., & Belladonna, M. L. (2015). Islet antigen-pulsed dendritic cells expressing ectopic IL-35Ig protect nonobese diabetic mice from autoimmune diabetes. *Cytokine*, *75*(2), 380–388. https://doi.org/10.1016/j.cyto.2015.05.002

Moniuszko, M., Bodzenta-Lukaszyk, A., Kowal, K., Lenczewska, D., & Dabrowska, M. (2009). Enhanced frequencies of CD14++CD16+, but not CD14+CD16+, peripheral blood monocytes in severe asthmatic patients. *Clinical Immunology (Orlando, Fla.)*, *130*(3), 338–346. https://doi.org/10.1016/j.clim.2008.09.011

Murphy, M. M., Lawson, J. A., Mathew, S. J., Hutcheson, D. A., & Kardon, G. (2011). Satellite cells, connective tissue fibroblasts and their interactions are crucial for muscle regeneration. *Development (Cambridge, England)*, *138*(17), 3625–3637. https://doi.org/10.1242/dev.064162

Muzny, D. M., Scherer, S. E., Kaul, R., Wang, J., Yu, J., Sudbrak, R., Buhay, C. J., Chen, R., Cree, A., Ding, Y., Dugan-Rocha, S., Gill, R., Gunaratne, P., Harris, R. A., Hawes, A. C., Hernandez, J., Hodgson, A. V., Hume, J., Jackson, A., … Gibbs, R. A. (2006). The DNA sequence, annotation and analysis of human chromosome 3. *Nature*, *440*(7088), 1194–1198. https://doi.org/10.1038/nature04728

Myoung, J., Kang, H. S., Hou, W., Meng, L., Dal Canto, M. C., & Kim, B. S. (2012). Epitope-specific CD8+ T cells play a differential pathogenic role in the development of a viral disease model for multiple sclerosis. *Journal of Virology*, *86*(24), 13717–13728. https://doi.org/10.1128/JVI.01733-12

Naito, S., Namerow, N., Mickey, M. R., & Terasaki, P. I. (1972). Multiple sclerosis: Association with HL-A3. *Tissue Antigens*, *2*(1), 1–4. https://doi.org/10.1111/j.1399-0039.1972.tb00111.x

Naour, F. L., Hohenkirk, L., Grolleau, A., Misek, D. E., Lescure, P., Geiger, J. D., Hanash, S., & Beretta, L. (2001). Profiling Changes in Gene Expression during Differentiation and

Maturation of Monocyte-derived Dendritic Cells Using Both Oligonucleotide Microarrays and Proteomics. *Journal of Biological Chemistry*, *276*(21), 17920–17931. https://doi.org/10.1074/jbc.M100156200

Niedobitek, G., Päzolt, D., Teichmann, M., & Devergne, O. (2002). Frequent expression of the Epstein-Barr virus (EBV)-induced gene, EBI3, an IL-12 p40-related cytokine, in Hodgkin and Reed-Sternberg cells. *The Journal of Pathology*, *198*(3), 310–316. https://doi.org/10.1002/path.1217

Ohl, K., Tenbrock, K., & Kipp, M. (2016). Oxidative stress in multiple sclerosis: Central and peripheral mode of action. *Experimental Neurology*, *277*, 58–67. https://doi.org/10.1016/j.expneurol.2015.11.010

Okamoto, H., Mizuno, K., & Horio, T. (2003). Circulating CD14+ CD16+ monocytes are expanded in sarcoidosis patients. *The Journal of Dermatology*, *30*(7), 503–509. https://doi.org/10.1111/j.1346-8138.2003.tb00424.x

Olsson, T., Barcellos, L. F., & Alfredsson, L. (2017). Interactions between genetic, lifestyle and environmental risk factors for multiple sclerosis. *Nature Reviews. Neurology*, *13*(1), 25–36. https://doi.org/10.1038/nrneurol.2016.187

OMIM. (2022). *OMIM 2022.* World Wide Web URL: https://omim.org/

Oppmann, B., Lesley, R., Blom, B., Timans, J. C., Xu, Y., Hunte, B., Vega, F., Yu, N., Wang, J., Singh, K., Zonin, F., Vaisberg, E., Churakova, T., Liu, M., Gorman, D., Wagner, J., Zurawski, S., Liu, Y., Abrams, J. S., … Kastelein, R. A. (2000). Novel p19 protein engages IL-12p40 to form a cytokine, IL-23, with biological activities similar as well as distinct from IL-12. *Immunity*, *13*(5), 715–725.

Otero, J. H., Lizák, B., & Hendershot, L. M. (2010). Life and death of a BiP substrate. *Seminars in Cell & Developmental Biology*, *21*(5), 472–478. https://doi.org/10.1016/j.semcdb.2009.12.008

Paijo, J., Döring, M., Spanier, J., Grabski, E., Nooruzzaman, M., Schmidt, T., Witte, G., Messerle, M., Hornung, V., Kaever, V., & Kalinke, U. (2016). CGAS Senses Human Cytomegalovirus and Induces Type I Interferon Responses in Human Monocyte-Derived Cells. *PLOS Pathogens*, *12*(4), e1005546. https://doi.org/10.1371/journal.ppat.1005546

Pakpoor, J., Disanto, G., Gerber, J. E., Dobson, R., Meier, U. C., Giovannoni, G., & Ramagopalan, S. V. (2013). The risk of developing multiple sclerosis in individuals seronegative for Epstein-Barr virus: A meta-analysis. *Multiple Sclerosis Journal*, *19*(2), 162–166. https://doi.org/10.1177/1352458512449682

Palle, P., Monaghan, K. L., Milne, S. M., & Wan, E. C. K. (2017). Cytokine Signaling in Multiple Sclerosis and Its Therapeutic Applications. *Medical Sciences (Basel, Switzerland)*, *5*(4). https://doi.org/10.3390/medsci5040023

Papenfuss, T. L., Powell, N. D., McClain, M. A., Bedarf, A., Singh, A., Gienapp, I. E., Shawler, T., & Whitacre, C. C. (2011). Estriol generates tolerogenic dendritic cells in vivo that protect against autoimmunity. *Journal of Immunology (Baltimore, Md.: 1950)*, *186*(6), 3346–3355. https://doi.org/10.4049/jimmunol.1001322

Patel, A. A., Zhang, Y., Fullerton, J. N., Boelen, L., Rongvaux, A., Maini, A. A., Bigley, V., Flavell, R. A., Gilroy, D. W., Asquith, B., Macallan, D., & Yona, S. (2017). The fate and lifespan of human monocyte subsets in steady state and systemic inflammation. *The Journal of Experimental Medicine*, *214*(7), 1913–1923. https://doi.org/10.1084/jem.20170355

Paton, A. W., Beddoe, T., Thorpe, C. M., Whisstock, J. C., Wilce, M. C. J., Rossjohn, J., Talbot, U. M., & Paton, J. C. (2006). AB5 subtilase cytotoxin inactivates the endoplasmic reticulum chaperone BiP. *Nature*, *443*(7111), 548–552. https://doi.org/10.1038/nature05124

Paton, A. W., Srimanote, P., Talbot, U. M., Wang, H., & Paton, J. C. (2004). A new family of potent AB(5) cytotoxins produced by Shiga toxigenic Escherichia coli. *The Journal of Experimental Medicine*, *200*(1), 35–46. https://doi.org/10.1084/jem.20040392

Pawlikowski, B., Pulliam, C., Betta, N. D., Kardon, G., & Olwin, B. B. (2015). Pervasive satellite cell contribution to uninjured adult muscle fibers. *Skeletal Muscle*, *5*, 42. https://doi.org/10.1186/s13395-015-0067-1

Pelczar, P., Witkowski, M., Perez, L. G., Kempski, J., Hammel, A. G., Brockmann, L., Kleinschmidt, D., Wende, S., Haueis, C., Bedke, T., Witkowski, M., Krasemann, S., Steurer, S., Booth, C. J., Busch, P., König, A., Rauch, U., Benten, D., Izbicki, J. R., … Huber, S. (2016). A pathogenic role for T cell–derived IL-22BP in inflammatory bowel disease. *Science*, *354*(6310).

Pereira, H., Schulze, P. S. C., Schüler, L. M., Santos, T., Barreira, L., & Varela, J. (2018). Fluorescence activated cell-sorting principles and applications in microalgal biotechnology. *Algal Research*, *30*, 113–120. https://doi.org/10.1016/J.ALGAL.2017.12.013

Perriard, G., Mathias, A., Enz, L., Canales, M., Schluep, M., Gentner, M., Schaeren-Wiemers, N., & Du Pasquier, R. A. (2015). Interleukin-22 is increased in multiple sclerosis patients and targets astrocytes. *Journal of Neuroinflammation*, *12*, 119. https://doi.org/10.1186/s12974-015-0335-3

Peterson, J. W., Bö, L., Mörk, S., Chang, A., & Trapp, B. D. (2001). Transected neurites, apoptotic neurons, and reduced inflammation in cortical multiple sclerosis lesions. *Annals of Neurology*, *50*(3), 389–400. https://doi.org/10.1002/ana.1123

Pflanz, S., Timans, J. C., Cheung, J., Rosales, R., Kanzler, H., Gilbert, J., Hibbert, L., Churakova, T., Travis, M., Vaisberg, E., Blumenschein, W. M., Mattson, J. D., Wagner, J. L., To, W., Zurawski, S., McClanahan, T. K., Gorman, D. M., Bazan, J. F., de Waal Malefyt, R., … Kastelein, R. A. (2002). IL-27, a Heterodimeric Cytokine Composed of EBI3 and p28 Protein, Induces Proliferation of Naive CD4+ T Cells. *Immunity*, *16*(6), 779–790. https://doi.org/10.1016/S1074-7613(02)00324-2

Piriyapongsa, J., Polavarapu, N., Borodovsky, M., & McDonald, J. (2007). Exonization of the LTR transposable elements in human genome. *BMC Genomics*, *8*, 291. https://doi.org/10.1186/1471-2164-8-291

Plank, M. W., Kaiko, G. E., Maltby, S., Weaver, J., Tay, H. L., Shen, W., Wilson, M. S., Durum, S. K., & Foster, P. S. (2017). Th22 Cells Form a Distinct Th Lineage from Th17 Cells In Vitro with Unique Transcriptional Properties and Tbet-Dependent Th1 Plasticity. *Journal of Immunology (Baltimore, Md.: 1950)*, *198*(5), 2182–2190. https://doi.org/10.4049/jimmunol.1601480

Pope, R. M., & Shahrara, S. (2013). Possible roles of IL-12-family cytokines in rheumatoid arthritis. *Nature Reviews Rheumatology*, *9*(4), 252–256. https://doi.org/10.1038/nrrheum.2012.170

Popescu, B. F. G., & Lucchinetti, C. F. (2012). Pathology of demyelinating diseases. *Annual Review of Pathology*, *7*, 185–217. https://doi.org/10.1146/annurev-pathol-011811-132443

Popescu, B. F. G., Pirko, I., & Lucchinetti, C. F. (2013). Pathology of multiple sclerosis: Where do we stand? *Continuum (Minneapolis, Minn.)*, *19*(4 Multiple Sclerosis), 901–921. https://doi.org/10.1212/01.CON.0000433291.23091.65

Prineas, J. W., Barnard, R. O., Kwon, E. E., Sharer, L. R., & Cho, E. S. (1993). Multiple sclerosis: Remyelination of nascent lesions. *Annals of Neurology*, *33*(2), 137–151. https://doi.org/10.1002/ana.410330203

Prineas, J. W., Kwon, E. E., Cho, E. S., Sharer, L. R., Barnett, M. H., Oleszak, E. L., Hoffman, B., & Morgan, B. P. (2001). Immunopathology of secondary-progressive multiple sclerosis. *Annals of Neurology*, *50*(5), 646–657. https://doi.org/10.1002/ana.1255

Prinz, M., & Priller, J. (2017). The role of peripheral immune cells in the CNS in steady state and disease. *Nature Neuroscience*, *20*(2), 136–144. https://doi.org/10.1038/nn.4475

Prodromou, C., & Pearl, L. H. (2003). Structure and functional relationships of Hsp90. *Current Cancer Drug Targets*, *3*(5), 301–323. https://doi.org/10.2174/1568009033481877

Puchner, A., Saferding, V., Bonelli, M., Mikami, Y., Hofmann, M., Brunner, J. S., Caldera, M., Goncalves-Alves, E., Binder, N. B., Fischer, A., Simader, E., Steiner, C.-W., Leiss, H., Hayer, S., Niederreiter, B., Karonitsch, T., Koenders, M. I., Podesser, B. K., O'Shea, J. J., … Blüml, S. (2018). Non-classical monocytes as mediators of tissue destruction in arthritis. *Annals of the Rheumatic Diseases*, *77*(10), 1490–1497. https://doi.org/10.1136/annrheumdis-2018-213250

R., R. K., N. S., N., S. P., A., Sinha, D., Veedin Rajan, V. B., Esthaki, V. K., & D'Silva, P. (2012). HSPIR: A manually annotated heat shock protein information resource. *Bioinformatics*, *28*(21), 2853–2855. https://doi.org/10.1093/bioinformatics/bts520

Rangachari, M., & Kuchroo, V. K. (2013). Using EAE to better understand principles of immune function and autoimmune pathology. *Journal of Autoimmunity*, *45*, 31–39. https://doi.org/10.1016/j.jaut.2013.06.008

Relaix, F., Rocancourt, D., Mansouri, A., & Buckingham, M. (2004). Divergent functions of murine Pax3 and Pax7 in limb muscle development. *Genes & Development*, *18*(9), 1088–1105. https://doi.org/10.1101/gad.301004

Robinson, A. P., Harp, C. T., Noronha, A., & Miller, S. D. (2014). The experimental autoimmune encephalomyelitis (EAE) model of MS: Utility for understanding disease pathophysiology and treatment. *Handbook of Clinical Neurology*, *122*, 173–189. https://doi.org/10.1016/B978-0-444-52001-2.00008-X

Robinson, E. K., Covarrubias, S., & Carpenter, S. (2020). The how and why of lncRNA function: An innate immune perspective. *Biochimica et Biophysica Acta (BBA) - Gene Regulatory Mechanisms*, *1863*(4), 194419. https://doi.org/10.1016/j.bbagrm.2019.194419

Romero-Barrios, N., Legascue, M. F., Benhamed, M., Ariel, F., & Crespi, M. (2018). Splicing regulation by long noncoding RNAs. *Nucleic Acids Research*, *46*(5), 2169–2184. https://doi.org/10.1093/nar/gky095

Rossol, M., Kraus, S., Pierer, M., Baerwald, C., & Wagner, U. (2012). The CD14brightCD16+ monocyte subset is expanded in rheumatoid arthritis and promotes expansion of the Th17 cell population. *Arthritis & Rheumatism*, *64*(3), 671–677. https://doi.org/10.1002/art.33418

Roszak, A., Mostowska, A., Sowińska, A., Lianeri, M., & Jagodziński, P. P. (2012). Contribution of IL12A and IL12B polymorphisms to the risk of cervical cancer. *Pathology Oncology Research: POR*, *18*(4), 997–1002. https://doi.org/10.1007/s12253-012-9532-x

Roy, K. C., Bandyopadhyay, G., Rakshit, S., Ray, M., & Bandyopadhyay, S. (2004). IL-4 alone without the involvement of GM-CSF transforms human peripheral blood monocytes to a CD1a(dim), CD83(+) myeloid dendritic cell subset. *Journal of Cell Science*, *117*(Pt 16), 3435–3445. https://doi.org/10.1242/jcs.01162

Ruggieri, M., Avolio, C., Livrea, P., & Trojano, M. (2007). Glatiramer acetate in multiple sclerosis: A review. *CNS Drug Reviews*, *13*(2), 178–191. https://doi.org/10.1111/j.1527-3458.2007.00010.x

Sabat, R., Ouyang, W., & Wolk, K. (2014). Therapeutic opportunities of the IL-22-IL-22R1 system. *Nature Reviews. Drug Discovery*, *13*(1), 21–38. https://doi.org/10.1038/nrd4176

Sadeghi, H. M., Schnelle, J. F., Thoma, J. K., Nishanian, P., & Fahey, J. L. (1999). Phenotypic and functional characteristics of circulating monocytes of elderly persons. *Experimental Gerontology*, *34*(8), 959–970. https://doi.org/10.1016/s0531-5565(99)00065-0

Sallander, E., Wester, U., Bengtsson, E., & Edström, D. W. (2013). Vitamin D levels after UVB radiation: Effects by UVA additions in a randomized controlled trial. *Photodermatology, Photoimmunology & Photomedicine*, *29*(6), 323–329. https://doi.org/10.1111/phpp.12076

Sambasivan, R., Yao, R., Kissenpfennig, A., Van Wittenberghe, L., Paldi, A., Gayraud-Morel, B., Guenou, H., Malissen, B., Tajbakhsh, S., & Galy, A. (2011). Pax7-expressing satellite cells are indispensable for adult skeletal muscle regeneration. *Development*, *138*(17), 3647. https://doi.org/10.1242/dev.067587

Sanes, J. R. (2003). The basement membrane/basal lamina of skeletal muscle. *The Journal of Biological Chemistry*, *278*(15), 12601–12604. https://doi.org/10.1074/jbc.R200027200

San-Juan-Rodriguez, A., Good, C. B., Heyman, R. A., Parekh, N., Shrank, W. H., & Hernandez, I. (2019). Trends in Prices, Market Share, and Spending on Self-administered Disease-Modifying Therapies for Multiple Sclerosis in Medicare Part D. *JAMA Neurology*. https://doi.org/10.1001/jamaneurol.2019.2711

Sattler, H. P., Lensch, R., Rohde, V., Zimmer, E., Meese, E., Bonkhoff, H., Retz, M., Zwergel, T., Bex, A., Stoeckle, M., & Wullich, B. (2000). Novel amplification unit at chromosome 3q25-q27 in human prostate cancer. *The Prostate*, *45*(3), 207–215. https://doi.org/10.1002/1097-0045(20001101)45:3<207::aid-pros2>3.0.co;2-h

Savan, R., McFarland, A. P., Reynolds, D. A., Feigenbaum, L., Ramakrishnan, K., Karwan, M., Shirota, H., Klinman, D. M., Dunleavy, K., Pittaluga, S., Anderson, S. K., Donnelly, R. P., Wilson, W. H., & Young, H. A. (2011). A novel role for IL-22R1 as a driver of inflammation. *Blood*, *117*(2), 575–584. https://doi.org/10.1182/blood-2010-05-285908

Scaramozza, A., Park, D., Kollu, S., Beerman, I., Sun, X., Rossi, D. J., Lin, C. P., Scadden, D. T., Crist, C., & Brack, A. S. (2019). Lineage Tracing Reveals a Subset of Reserve Muscle Stem Cells Capable of Clonal Expansion under Stress. *Cell Stem Cell*, *24*(6), 944-957.e5. https://doi.org/10.1016/j.stem.2019.03.020

Schwarzkopf, K., Rüschenbaum, S., Barat, S., Cai, C., Mücke, M. M., Fitting, D., Weigert, A., Brüne, B., Zeuzem, S., Welsch, C., & Lange, C. M. (2019). IL-22 and IL-22-Binding Protein Are Associated With Development of and Mortality From Acute-on-Chronic Liver Failure. *Hepatology Communications*, *3*(3), 392–405. https://doi.org/10.1002/hep4.1303

Schweitzer, F., Laurent, S., Fink, G. R., Barnett, M. H., Hartung, H. P., & Warnke, C. (2020). Effects of disease-modifying therapy on peripheral leukocytes in patients with multiple sclerosis. *Journal of Neurology*. https://doi.org/10.1007/s00415-019-09690-6

Seale, P., Sabourin, L. A., Girgis-Gabardo, A., Mansouri, A., Gruss, P., & Rudnicki, M. A. (2000). Pax7 is required for the specification of myogenic satellite cells. *Cell*, *102*(6), 777–786. https://doi.org/10.1016/s0092-8674(00)00066-0

Segal, B. M., Constantinescu, C. S., Raychaudhuri, A., Kim, L., Fidelus-Gort, R., Kasper, L. H., & Ustekinumab MS Investigators. (2008). Repeated subcutaneous injections of IL12/23 p40 neutralising antibody, ustekinumab, in patients with relapsing-remitting multiple sclerosis: A phase II, double-blind, placebo-controlled, randomised, dose-ranging study. *The Lancet. Neurology*, *7*(9), 796–804. https://doi.org/10.1016/S1474-4422(08)70173-X

Seidler, S., Zimmermann, H. W., Bartneck, M., Trautwein, C., & Tacke, F. (2010). Age-dependent alterations of monocyte subsets and monocyte-related chemokine pathways in healthy adults. *BMC Immunology*, *11*, 30. https://doi.org/10.1186/1471-2172-11-30

Sertorio, M., Hou, X., Carmo, R. F., Dessein, H., Cabantous, S., Abdelwahed, M., Romano, A., Albuquerque, F., Vasconcelos, L., Carmo, T., Li, J., Varoquaux, A., Arnaud, V., Oliveira, P., Hamdoun, A., He, H., Adbelmaboud, S., Mergani, A., Zhou, J., … Dessein, A. (2015). IL-22 and IL-22 binding protein (IL-22BP) regulate fibrosis and cirrhosis in hepatitis C virus and schistosome infections. *Hepatology*, *61*(4), 1321–1331. https://doi.org/10.1002/hep.27629

Seventer, J. M. van, Nagai, T., & Seventer, G. A. van. (2002). Interferon-β differentially regulates expression of the IL-12 family members p35, p40, p19 and EBI3 in activated human dendritic cells. *Journal of Neuroimmunology*, *133*(1), 60–71. https://doi.org/10.1016/S0165-5728(02)00362-4

Shen, P., Roch, T., Lampropoulou, V., O'Connor, R. A., Stervbo, U., Hilgenberg, E., Ries, S., Dang, V. D., Jaimes, Y., Daridon, C., Li, R., Jouneau, L., Boudinot, P., Wilantri, S., Sakwa, I., Miyazaki, Y., Leech, M. D., McPherson, R. C., Wirtz, S., … Fillatreau, S. (2014). IL-35-producing B cells are critical regulators of immunity during autoimmune and infectious diseases. *Nature*, *507*(7492), Article 7492. https://doi.org/10.1038/nature12979

Shi, L., Lin, H., Li, G., Jin, R.-A., Xu, J., Sun, Y., Ma, W.-L., Yeh, S., Cai, X., & Chang, C. (2016). Targeting Androgen Receptor (AR)→IL12A Signal Enhances Efficacy of Sorafenib plus NK Cells Immunotherapy to Better Suppress HCC Progression. *Molecular Cancer Therapeutics*, *15*(4), 731–742. https://doi.org/10.1158/1535-7163.MCT-15-0706

Shooshtari, P., Huang, H., & Cotsapas, C. (2017). Integrative Genetic and Epigenetic Analysis Uncovers Regulatory Mechanisms of Autoimmune Disease. *American Journal of Human Genetics*, *101*(1), 75–86. https://doi.org/10.1016/j.ajhg.2017.06.001

Simons, B. D., & Clevers, H. (2011). Strategies for homeostatic stem cell self-renewal in adult tissues. *Cell*, *145*(6), 851–862. https://doi.org/10.1016/j.cell.2011.05.033

Sintzel, M. B., Rametta, M., & Reder, A. T. (2017). Vitamin D and Multiple Sclerosis: A Comprehensive Review. *Neurology and Therapy*, *7*(1), 59–85. https://doi.org/10.1007/s40120-017-0086-4

Skrombolas, D., Wylie, I., Maharaj, S., & Frelinger, J. G. (2015). Characterization of an IL-12 p40/p35 Truncated Fusion Protein That Can Inhibit the Action of IL-12. *Journal of Interferon & Cytokine Research*, *35*(9), 690–697. https://doi.org/10.1089/jir.2014.0176

Sonnenberg, G. F., Fouser, L. A., & Artis, D. (2011). Border patrol: Regulation of immunity, inflammation and tissue homeostasis at barrier surfaces by IL-22. *Nature Immunology*, *12*(5), 383–390. https://doi.org/10.1038/ni.2025

Stocki, P., Chapman, D. C., Beach, L. A., & Williams, D. B. (2014). Depletion of cyclophilins B and C leads to dysregulation of endoplasmic reticulum redox homeostasis. *The Journal of Biological Chemistry*, *289*(33), 23086–23096. https://doi.org/10.1074/jbc.M114.570911

Sun, L., He, C., Nair, L., Yeung, J., & Egwuagu, C. E. (2015). Interleukin 12 (IL-12) family cytokines: Role in immune pathogenesis and treatment of CNS autoimmune disease. *Cytokine*, *75*(2), 249–255. https://doi.org/10.1016/J.CYTO.2015.01.030

Sundström, C., & Nilsson, K. (1976). Establishment and characterization of a human histiocytic lymphoma cell line (U-937). *International Journal of Cancer*, *17*(5), 565–577. https://doi.org/10.1002/ijc.2910170504

Sutcu, H. H., & Ricchetti, M. (2018). Loss of heterogeneity, quiescence, and differentiation in muscle stem cells. *Stem Cell Investigation*, *5*, 9. https://doi.org/10.21037/sci.2018.03.02

Tak, T., Drylewicz, J., Conemans, L., de Boer, R. J., Koenderman, L., Borghans, J. A. M., & Tesselaar, K. (2017). Circulatory and maturation kinetics of human monocyte subsets in vivo. *Blood*, *130*(12), 1474–1477. https://doi.org/10.1182/blood-2017-03-771261

Tao, Q., Pan, Y., Wang, Y., Wang, H., Xiong, S., Li, Q., Wang, J., Tao, L., Wang, Z., Wu, F., Zhang, R., & Zhai, Z. (2015). Regulatory T cells-derived IL-35 promotes the growth of adult acute myeloid leukemia blasts. *International Journal of Cancer*, *137*(10), 2384–2393. https://doi.org/10.1002/ijc.29563

Tarlinton, R. E., Martynova, E., Rizvanov, A. A., Khaiboullina, S., & Verma, S. (2020). Role of Viruses in the Pathogenesis of Multiple Sclerosis. *Viruses*, *12*(6), 643. https://doi.org/10.3390/v12060643

Tarrant, T. K., Silver, P. B., Chan, C.-C., Wiggert, B., & Caspi, R. R. (1998). Endogenous IL-12 is required for induction and expression of experimental autoimmune uveitis. *Journal of Immunology*, *161*(1), 122–127. Scopus.

The Human Protein Atlas. (2022). *Tissue Cell Type—IL22RA2*. https://www.proteinatlas.org/ENSG00000164485-IL22RA2/tissue+cell+type

Thermo Fisher Scientific. (2022). *Co-Immunoprecipitation (Co-IP) |—ES*. https://www.thermofisher.com/es/es/home/life-science/protein-biology/protein-biology-learning-center/protein-biology-resource-library/pierce-protein-methods/co-immunoprecipitation-co-ip.html

Thompson, A. J., Baranzini, S. E., Geurts, J., Hemmer, B., & Ciccarelli, O. (2018). Multiple sclerosis. *The Lancet*, *391*(10130), 1622–1636. https://doi.org/10.1016/S0140-6736(18)30481-1

Toosy, A. T., Mason, D. F., & Miller, D. H. (2014). Optic neuritis. *The Lancet. Neurology*, *13*(1), 83–99. https://doi.org/10.1016/S1474-4422(13)70259-X

Trevejo-Nunez, G., Elsegeiny, W., Aggor, F. E. Y., Tweedle, J. L., Kaplan, Z., Gandhi, P., Castillo, P., Ferguson, A., Alcorn, J. F., Chen, K., Kolls, J. K., & Gaffen, S. L. (2019). Interleukin-22 (IL-22) Binding Protein Constrains IL-22 Activity, Host Defense, and Oxidative Phosphorylation Genes during Pneumococcal Pneumonia. *Infection and Immunity*, *87*(11). https://doi.org/10.1128/IAI.00550-19

Trinchieri, G., Pflanz, S., & Kastelein, R. A. (2003). The IL-12 Family of Heterodimeric Cytokines: New Players in the Regulation of T Cell Responses. *Immunity*, *19*(5), 641–644. https://doi.org/10.1016/S1074-7613(03)00296-6

Trowsdale, J., & Knight, J. C. (2013). Major histocompatibility complex genomics and human disease. *Annual Review of Genomics and Human Genetics*, *14*, 301–323. https://doi.org/10.1146/annurev-genom-091212-153455

Tsoi, L. C., Stuart, P. E., Tian, C., Gudjonsson, J. E., Das, S., Zawistowski, M., Ellinghaus, E., Barker, J. N., Chandran, V., Dand, N., Duffin, K. C., Enerbäck, C., Esko, T., Franke, A., Gladman, D. D., Hoffmann, P., Kingo, K., Kõks, S., Krueger, G. G., … Elder, J. T. (2017). Large scale meta-analysis characterizes genetic architecture for common psoriasis associated variants. *Nature Communications*, *8*, 15382. https://doi.org/10.1038/ncomms15382

Uffelmann, E., Huang, Q. Q., Munung, N. S., de Vries, J., Okada, Y., Martin, A. R., Martin, H. C., Lappalainen, T., & Posthuma, D. (2021). Genome-wide association studies. *Nature Reviews Methods Primers*, *1*(1), Article 1. https://doi.org/10.1038/s43586-021-00056-9

van der Lee, R., Buljan, M., Lang, B., Weatheritt, R. J., Daughdrill, G. W., Dunker, A. K., Fuxreiter, M., Gough, J., Gsponer, J., Jones, D. T., Kim, P. M., Kriwacki, R. W., Oldfield, C. J., Pappu, R. V., Tompa, P., Uversky, V. N., Wright, P. E., & Babu, M. M. (2014). Classification of intrinsically disordered regions and proteins. *Chemical Reviews*, *114*(13), 6589–6631. https://doi.org/10.1021/cr400525m

van Velthoven, C. T. J., & Rando, T. A. (2019). Stem Cell Quiescence: Dynamism, Restraint, and Cellular Idling. *Cell Stem Cell*, *24*(2), 213–225. https://doi.org/10.1016/j.stem.2019.01.001

van Zwam, M., Huizinga, R., Melief, M.-J., Wierenga-Wolf, A. F., van Meurs, M., Voerman, J. S., Biber, K. P. H., Boddeke, H. W. G. M., Höpken, U. E., Meisel, C., Meisel, A., Bechmann, I., Hintzen, R. Q., ’t Hart, B. A., Amor, S., Laman, J. D., & Boven, L. A. (2009). Brain antigens in functionally distinct antigen-presenting cell populations in cervical lymph nodes in MS and EAE. *Journal of Molecular Medicine (Berlin, Germany)*, *87*(3), 273–286. https://doi.org/10.1007/s00109-008-0421-4

Vandenbroeck, K. (2012). Cytokine gene polymorphisms and human autoimmune disease in the era of genome-wide association studies. *Journal of Interferon & Cytokine Research : The Official Journal of the International Society for Interferon and Cytokine Research*, *32*(4), 139–151. https://doi.org/10.1089/jir.2011.0103

Vandenbroeck, K., Alvarez, J., Swaminathan, B., Alloza, I., Matesanz, F., Urcelay, E., Comabella, M., Alcina, A., Fedetz, M., Ortiz, M. A., Izquierdo, G., Fernandez, O., Rodriguez-Ezpeleta, N., Matute, C., Caillier, S., Arroyo, R., Montalban, X., Oksenberg, J. R., Antigüedad, A., & Aransay, A. (2012). A cytokine gene screen uncovers SOCS1 as genetic risk factor for multiple sclerosis. *Genes and Immunity*, *13*(1), 21–28. https://doi.org/10.1038/gene.2011.44

Vandiedonck, C., & Knight, J. C. (2009). The human Major Histocompatibility Complex as a paradigm in genomics research. *Briefings in Functional Genomics & Proteomics*, *8*(5), 379–394. https://doi.org/10.1093/bfgp/elp010

Voglis, S., Moos, S., Kloos, L., Wanke, F., Zayoud, M., Pelczar, P., Giannou, A. D., Pezer, S., Albers, M., Luessi, F., Huber, S., Schäkel, K., & Kurschus, F. C. (2018). Regulation of IL-22BP in psoriasis. *Scientific Reports*, *8*(1), 1–8. https://doi.org/10.1038/s41598-018-23510-3

Voskuhl, R. R. (2020). The Effect Of Sex on Multiple Sclerosis Risk And Disease Progression. *Multiple Sclerosis (Houndmills, Basingstoke, England)*, *26*(5), 554–560. https://doi.org/10.1177/1352458519892491

Wade, R., Di Bernardo, M. C., Richards, S., Rossi, D., Crowther-Swanepoel, D., Gaidano, G., Oscier, D. G., Catovsky, D., & Houlston, R. S. (2011). Association between single nucleotide polymorphism-genotype and outcome of patients with chronic lymphocytic leukemia in a randomized chemotherapy trial. *Haematologica*, *96*(10), 1496–1503. https://doi.org/10.3324/haematol.2011.043471

Wallin, M. T., Culpepper, W. J., Campbell, J. D., Nelson, L. M., Langer-Gould, A., Marrie, R. A., Cutter, G. R., Kaye, W. E., Wagner, L., Tremlett, H., Buka, S. L., Dilokthornsakul, P., Topol, B., Chen, L. H., & LaRocca, N. G. (2019). The prevalence of MS in the United States. *Neurology*, *92*(10), e1029–e1040. https://doi.org/10.1212/WNL.0000000000007035

Walton, C., King, R., Rechtman, L., Kaye, W., Leray, E., Marrie, R. A., Robertson, N., La Rocca, N., Uitdehaag, B., van der Mei, I., Wallin, M., Helme, A., Angood Napier, C., Rijke, N., & Baneke, P. (2020). Rising prevalence of multiple sclerosis worldwide: Insights from the Atlas of MS, third edition. *Multiple Sclerosis (Houndmills, Basingstoke, England)*, *26*(14), 1816–1821. https://doi.org/10.1177/1352458520970841

Wang, P., & Heitman, J. (2005). The cyclophilins. *Genome Biology*, *6*(7), 226. https://doi.org/10.1186/gb-2005-6-7-226

Wang, X., Wei, Y., Xiao, H., Liu, X., Zhang, Y., Han, G., Chen, G., Hou, C., Ma, N., Shen, B., Li, Y., Egwuagu, C. E., & Wang, R. (2016). A novel IL-23p19/Ebi3 (IL-39) cytokine mediates

inflammation in Lupus-like mice. *European Journal of Immunology*, *46*(6), 1343–1350. https://doi.org/10.1002/eji.201546095

Wang, Y. X., Dumont, N. A., & Rudnicki, M. A. (2014). Muscle stem cells at a glance. *Journal of Cell Science*, *127*(21), 4543–4548. https://doi.org/10.1242/jcs.151209

Wang, Z., Liu, J.-Q., Liu, Z., Shen, R., Zhang, G., Xu, J., Basu, S., Feng, Y., & Bai, X.-F. (2013). Tumor-Derived IL-35 Promotes Tumor Growth by Enhancing Myeloid Cell Accumulation and Angiogenesis. *The Journal of Immunology*, *190*(5), 2415–2423. https://doi.org/10.4049/jimmunol.1202535

Waschbisch, A., Schröder, S., Schraudner, D., Sammet, L., Weksler, B., Melms, A., Pfeifenbring, S., Stadelmann, C., Schwab, S., & Linker, R. A. (2016). Pivotal Role for CD16+ Monocytes in Immune Surveillance of the Central Nervous System. *Journal of Immunology (Baltimore, Md. : 1950)*, *196*(4), 1558–1567. https://doi.org/10.4049/jimmunol.1501960

Weber, G. F., Schlautkötter, S., Kaiser-Moore, S., Altmayr, F., Holzmann, B., & Weighardt, H. (2007). Inhibition of interleukin-22 attenuates bacterial load and organ failure during acute polymicrobial sepsis. *Infection and Immunity*, *75*(4), 1690–1697. https://doi.org/10.1128/IAI.01564-06

Wei, C.-C., Ho, T.-W., Liang, W.-G., Chen, G.-Y., & Chang, M.-S. (2003). Cloning and characterization of mouse IL-22 binding protein. *Genes & Immunity*, *4*(3), 204–211. https://doi.org/10.1038/sj.gene.6363947

Weiss, B., Wolk, K., Grünberg, B. H., Volk, H.-D., Sterry, W., Asadullah, K., & Sabat, R. (2004). Cloning of murine IL-22 receptor alpha 2 and comparison with its human counterpart. *Genes & Immunity*, *5*(5), 330–336. https://doi.org/10.1038/sj.gene.6364104

Wijeratne, T., Jones, E. C., Grisold, W., & Carroll, W. M. (2022). Global Advocacy in Action: World Brain Day 2021 Dedicated to Stopping Multiple Sclerosis. *Neurology. Clinical Practice*, *12*(1), e1–e2. https://doi.org/10.1212/CPJ.0000000000001151

Wildenberg, M. E., Welzen-Coppens, J. M. C., van Helden-Meeuwsen, C. G., Bootsma, H., Vissink, A., van Rooijen, N., van de Merwe, J. P., Drexhage, H. A., & Versnel, M. A. (2009). Increased frequency of CD16+ monocytes and the presence of activated dendritic cells in salivary glands in primary Sjögren syndrome. *Annals of the Rheumatic Diseases*, *68*(3), 420–426. https://doi.org/10.1136/ard.2008.087874

Williams, D. B. (2006). Beyond lectins: The calnexin/calreticulin chaperone system of the endoplasmic reticulum. *Journal of Cell Science*, *119*(Pt 4), 615–623. https://doi.org/10.1242/jcs.02856

Wirtz, S., Billmeier, U., Mchedlidze, T., Blumberg, R. S., & Neurath, M. F. (2011). Interleukin-35 mediates mucosal immune responses that protect against T-cell-dependent colitis. *Gastroenterology*, *141*(5), 1875–1886. https://doi.org/10.1053/j.gastro.2011.07.040

Witte, E., Witte, K., Warszawska, K., Sabat, R., & Wolk, K. (2010). Interleukin-22: A cytokine produced by T, NK and NKT cell subsets, with importance in the innate immune defense and tissue protection. *Cytokine & Growth Factor Reviews*, *21*(5), 365–379. https://doi.org/10.1016/j.cytogfr.2010.08.002

Wolk, K., Kunz, S., Witte, E., Friedrich, M., Asadullah, K., & Sabat, R. (2004). IL-22 increases the innate immunity of tissues. *Immunity*, *21*(2), 241–254. https://doi.org/10.1016/j.immuni.2004.07.007

Wolk, K., Witte, E., Hoffmann, U., Doecke, W.-D., Endesfelder, S., Asadullah, K., Sterry, W., Volk, H.-D., Wittig, B. M., & Sabat, R. (2007). IL-22 induces lipopolysaccharide-binding protein in hepatocytes: A potential systemic role of IL-22 in Crohn's disease. *Journal of Immunology (Baltimore, Md.: 1950)*, *178*(9), 5973–5981. https://doi.org/10.4049/jimmunol.178.9.5973

Wolk, K., Witte, K., Witte, E., Proesch, S., Schulze-Tanzil, G., Nasilowska, K., Thilo, J., Asadullah, K., Sterry, W., Volk, H.-D., & Sabat, R. (2008a). Maturing dendritic cells are an important source of IL-29 and IL-20 that may cooperatively increase the innate immunity of

keratinocytes. *Journal of Leukocyte Biology*, *83*(5), 1181–1193. https://doi.org/10.1189/jlb.0807525

Wolk, K., Witte, K., Witte, E., Proesch, S., Schulze-Tanzil, G., Nasilowska, K., Thilo, J., Asadullah, K., Sterry, W., Volk, H.-D., & Sabat, R. (2008b). Maturing dendritic cells are an important source of IL-29 and IL-20 that may cooperatively increase the innate immunity of keratinocytes. *Journal of Leukocyte Biology*, *83*(5), 1181–1193. https://doi.org/10.1189/jlb.0807525

Wong, K. L., Tai, J. J.-Y., Wong, W.-C., Han, H., Sem, X., Yeap, W.-H., Kourilsky, P., & Wong, S.-C. (2011). Gene expression profiling reveals the defining features of the classical, intermediate, and nonclassical human monocyte subsets. *Blood*, *118*(5), e16-31. https://doi.org/10.1182/blood-2010-12-326355

Wong, K. L., Yeap, W. H., Tai, J. J. Y., Ong, S. M., Dang, T. M., & Wong, S. C. (2012). The three human monocyte subsets: Implications for health and disease. *Immunologic Research*, *53*(1–3), 41–57. https://doi.org/10.1007/s12026-012-8297-3

Wooliscroft, L., Silbermann, E., Cameron, M., & Bourdette, D. (2019). Approaches to Remyelination Therapies in Multiple Sclerosis. *Current Treatment Options in Neurology*, *21*(7), 34. https://doi.org/10.1007/s11940-019-0574-1

Wosczyna, M. N., & Rando, T. A. (2018). A Muscle Stem Cell Support Group: Coordinated Cellular Responses in Muscle Regeneration. *Developmental Cell*, *46*(2), 135–143. https://doi.org/10.1016/j.devcel.2018.06.018

Wu, S., Hong, F., Gewirth, D., Guo, B., Liu, B., & Li, Z. (2012a). The molecular chaperone gp96/GRP94 interacts with Toll-like receptors and integrins via its C-terminal hydrophobic domain. *The Journal of Biological Chemistry*, *287*(9), 6735–6742. https://doi.org/10.1074/jbc.M111.309526

Wu, S., Hong, F., Gewirth, D., Guo, B., Liu, B., & Li, Z. (2012b). The molecular chaperone gp96/GRP94 interacts with Toll-like receptors and integrins via its C-terminal hydrophobic

domain. *The Journal of Biological Chemistry*, *287*(9), 6735–6742. https://doi.org/10.1074/jbc.M111.309526

Xiao, B.-G., Ma, C.-G., Xu, L.-Y., Link, H., & Lu, C.-Z. (2008). IL-12/IFN-gamma/NO axis plays critical role in development of Th1-mediated experimental autoimmune encephalomyelitis. *Molecular Immunology*, *45*(4), 1191–1196. https://doi.org/10.1016/j.molimm.2007.07.003

Xu, W., Li, R., Dai, Y., Wu, A., Wang, H., Cheng, C., Qiu, W., Lu, Z., Zhong, X., Shu, Y., Kermode, A. G., & Hu, X. (2013). IL-22 secreting CD4+ T cells in the patients with neuromyelitis optica and multiple sclerosis. *Journal of Neuroimmunology*, *261*(1–2), 87–91. https://doi.org/10.1016/j.jneuroim.2013.04.021

Xu, W., Presnell, S. R., Parrish-Novak, J., Kindsvogel, W., Jaspers, S., Chen, Z., Dillon, S. R., Gao, Z., Gilbert, T., Madden, K., Schlutsmeyer, S., Yao, L., Whitmore, T. E., Chandrasekher, Y., Grant, F. J., Maurer, M., Jelinek, L., Storey, H., Brender, T., … Foster, D. C. (2001). A soluble class II cytokine receptor, IL-22RA2, is a naturally occurring IL-22 antagonist. *Proceedings of the National Academy of Sciences of the United States of America*, *98*(17), 9511–9516. https://doi.org/10.1073/pnas.171303198

Yamasaki, R., Lu, H., Butovsky, O., Ohno, N., Rietsch, A. M., Cialic, R., Wu, P. M., Doykan, C. E., Lin, J., Cotleur, A. C., Kidd, G., Zorlu, M. M., Sun, N., Hu, W., Liu, L., Lee, J.-C., Taylor, S. E., Uehlein, L., Dixon, D., … Ransohoff, R. M. (2014). Differential roles of microglia and monocytes in the inflamed central nervous system. *The Journal of Experimental Medicine*, *211*(8), 1533–1549. https://doi.org/10.1084/jem.20132477

Yamazaki, H., Hiramatsu, N., Hayakawa, K., Tagawa, Y., Okamura, M., Ogata, R., Huang, T., Nakajima, S., Yao, J., Paton, A. W., Paton, J. C., & Kitamura, M. (2009). Activation of the Akt-NF-kappaB pathway by subtilase cytotoxin through the ATF6 branch of the unfolded protein response. *Journal of Immunology (Baltimore, Md.: 1950)*, *183*(2), 1480–1487. https://doi.org/10.4049/jimmunol.0900017

Yang, J., Zhang, L., Yu, C., Yang, X.-F., & Wang, H. (2014). Monocyte and macrophage differentiation: Circulation inflammatory monocyte as biomarker for inflammatory diseases. *Biomarker Research*, *2*(1), 1. https://doi.org/10.1186/2050-7771-2-1

Yates, A. D., Achuthan, P., Akanni, W., Allen, J., Allen, J., Alvarez-Jarreta, J., Amode, M. R., Armean, I. M., Azov, A. G., Bennett, R., Bhai, J., Billis, K., Boddu, S., Marugán, J. C., Cummins, C., Davidson, C., Dodiya, K., Fatima, R., Gall, A., … Flicek, P. (2020). Ensembl 2020. *Nucleic Acids Research*, *48*(D1), D682–D688. https://doi.org/10.1093/nar/gkz966

Yue, T., Zheng, X., Dou, Y., Zheng, X., Sun, R., Tian, Z., & Wei, H. (2016). Interleukin 12 shows a better curative effect on lung cancer than paclitaxel and cisplatin doublet chemotherapy. *BMC Cancer*, *16*, 665. https://doi.org/10.1186/s12885-016-2701-7

Zenewicz, L. A. (2018). IL-22: There Is a Gap in Our Knowledge. *ImmunoHorizons*, *2*(6), 198–207. https://doi.org/10.4049/immunohorizons.1800006

Zenewicz, L. A., & Flavell, R. A. (2011). Recent advances in IL-22 biology. *International Immunology*, *23*(3), 159–163. https://doi.org/10.1093/intimm/dxr001

Zhang, J., & Herscovitz, H. (2003). Nascent lipidated apolipoprotein B is transported to the Golgi as an incompletely folded intermediate as probed by its association with network of endoplasmic reticulum molecular chaperones, GRP94, ERp72, BiP, calreticulin, and cyclophilin B. *The Journal of Biological Chemistry*, *278*(9), 7459–7468. https://doi.org/10.1074/jbc.M207976200

Zhu, B., Buttrick, T., Bassil, R., Zhu, C., Olah, M., Wu, C., Xiao, S., Orent, W., Elyaman, W., & Khoury, S. J. (2013). IL-4 and retinoic acid synergistically induce regulatory dendritic cells expressing Aldh1a2. *Journal of Immunology (Baltimore, Md.: 1950)*, *191*(6), 3139–3151. https://doi.org/10.4049/jimmunol.1300329

Ziegler-Heitbrock, L., Ancuta, P., Crowe, S., Dalod, M., Grau, V., Hart, D. N., Leenen, P. J. M., Liu, Y.-J., MacPherson, G., Randolph, G. J., Scherberich, J., Schmitz, J., Shortman, K., Sozzani, S., Strobl, H., Zembala, M., Austyn, J. M., & Lutz, M. B. (2010). Nomenclature of

monocytes and dendritic cells in blood. *Blood*, *116*(16), e74-80. https://doi.org/10.1182/blood-2010-02-258558

Zindl, C. L., Lai, J.-F., Lee, Y. K., Maynard, C. L., Harbour, S. N., Ouyang, W., Chaplin, D. D., & Weaver, C. T. (2013). IL-22-producing neutrophils contribute to antimicrobial defense and restitution of colonic epithelial integrity during colitis. *Proceedings of the National Academy of Sciences of the United States of America*, *110*(31), 12768–12773. https://doi.org/10.1073/pnas.1300318110

ANNEX. INTERNATIONAL RESEARCH STAY

I. Introduction

Musculoskeletal conditions are the leading contributor to disability worldwide, with low back pain being the single leading cause of disability globally (GBD 2017 Disease and Injury Incidence and Prevalence Collaborators, 2018). Musculoskeletal conditions and injuries are not just conditions of older age; they are prevalent across the life span, 20-30% of people (including children) live with a musculoskeletal pain conditions. Musculoskeletal conditions limit mobility and dexterity increasing the risk of developing other chronic health conditions. However, skeletal muscle is renowned for its capacity for regeneration (Wosczyna & Rando, 2018) and thus, a better understanding of the regenerative process could lead to the development of clinical strategies to treat diseases that affect skeletal muscle in order to stop, or even reverse, muscular degeneration.

Tissue homeostasis and regeneration depend on tissue-specific populations of stem cells (Simons & Clevers, 2011), some of which maintain a quiescent state for prolonged periods of time to preserve key functional features (Cheung & Rando, 2013). Skeletal muscle has a population of stem cells for which the quiescent state is essential to their maintenance (Bjornson 2012, Mourikis 2012) and these stem cells are absolutely required for skeletal muscle's ability to regenerate (Lepper et al., 2011; Murphy et al., 2011; Sambasivan et al., 2011).

Muscle Stem Cells (MuSCs) were first described by Alexander Mauro as satellite cells (SCs) because anatomically they appear wedged between basal lamina and the sarcolemma (Mauro, 1961). The basal lamina serves as a scaffold for MuSCs and functions to limit and orient their migration during injury (Sanes, 2003). MuSCs are marked by the expression of Pax7 (Seale et al., 2000) and, in contrast to many tissue-specific stem cells, such as those in blood or brain, which are multipotent, MuSCs are unipotent and generate only muscle cells (van Velthoven & Rando, 2019).

The process to efficiently regenerate an appropriate muscle after injury is highly orchestrated (Figure I.1). MuSCs rapidly activate in response to injury and proliferate, generating myoblast that will ultimately fuse to form new skeletal fibers within a few days (Sambasivan et al., 2011), while a subset of MuSCs is able return to quiescence and replenish the quiescent satellite cell pool (Collins et al., 2005).

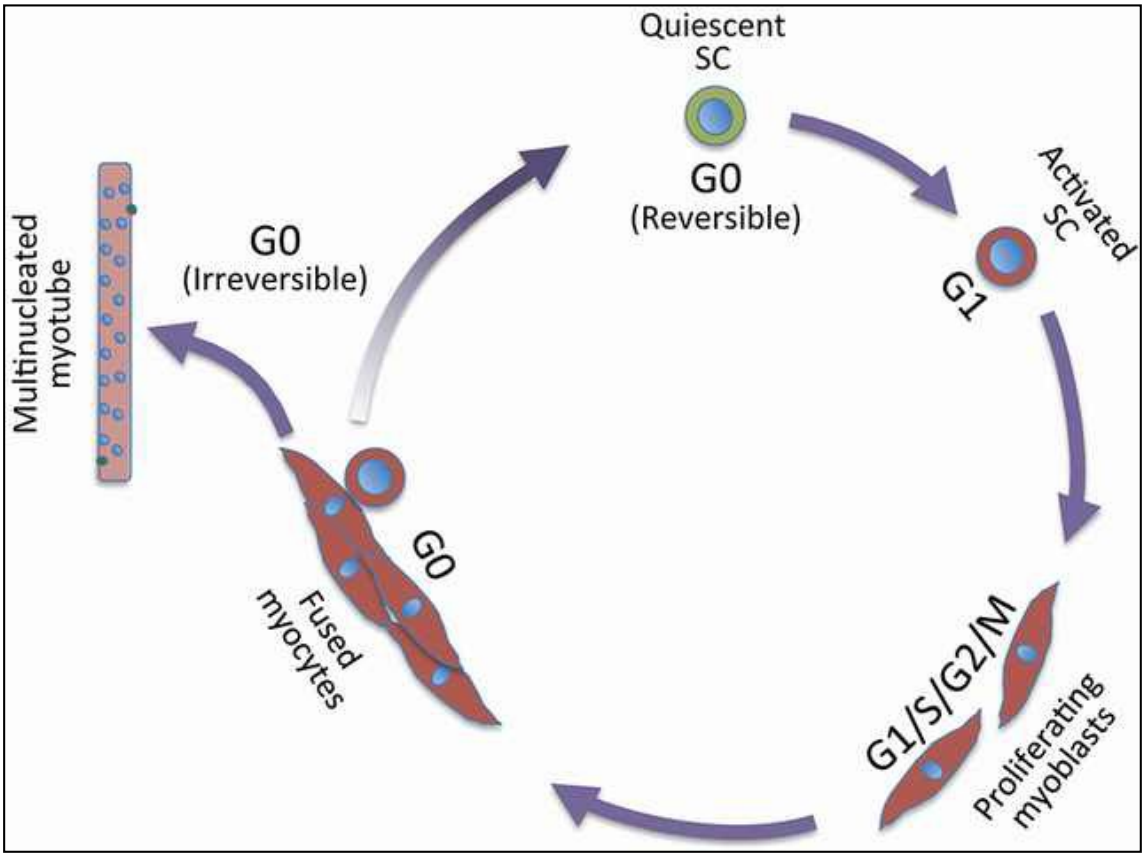

Figure I.1. The adult satellite cell (SC) cell cycle and myogenesis. Satellite cells are in a non-proliferative quiescent state, the G0 phase. Upon activation, they enter G1 phase that commits cells to enter the cell cycle and prepares them to duplicate their DNA during the S phase. After DNA duplication, cells enter G2 phase that prepares for mitosis (M phase), where chromatids and daughter cells separate. After the division, some cells go back to G0 phase to self-renew the satellite cell pool, ready to re-enter the cell cycle under activation stimuli. The rest of the cells keep proliferating and differentiate into muscle cells that would eventually fuse with existing fibers or create new ones, regenerating the muscle and re-establishing muscle function. *Adapted from:* (Sutcu & Ricchetti, 2018).

Whereas the role of MuSCs in regeneration is well established, it is less clear whether MuSCs have a role during homeostasis. Two recent studies have investigated the role of MuSCs during homeostatic conditions. One reported that depleting MuSCs from 6 month old adult mice did not change the myofiber cross-sectional area of uninjured muscles by the time the mice were 20 months old, but a mild atrophy in the diaphragm by the time the mice were 12 months old (Keefe et al., 2015). The other reported a higher than previously estimated level MuSCs fusion into the uninjured adult skeletal muscle (up to 100% in the diaphragm) and raised the possibility of a functional role for MuSCs fusion into adult muscle fibers (myofibers) possibly as part of muscle maintenance (Pawlikowski et al., 2015). Either way, both reports observed muscle and age dependent differences, with high levels of MuSCs contribution in diaphragm muscles and low levels in lower hindlimb muscles (Keefe et al., 2015; Pawlikowski et al., 2015) and raised interesting questions about the role of MuSCs during homeostasis.

The present research is part of a Research Project developed at the Rando Laboratory at Stanford University that aimed to better understand the functional role of MuSCs during homeostasis. The project identified a complex mechanism by which Pax3 expression controls spontaneous activation and cell cycle entry of MuSCs under homeostatic conditions and offered implications for a role for Pax3 in regulating MuSC fusion to myofibers.

II. Aim

To explore the regulation and the functional relevance of Pax3 in MuSCs *in vivo* during homeostasis.

III. Material and methods

A. Animals

Animal procedures were approved by the Administrative Panel on Laboratory Animal Care of the VA Palo Alto Health Care System. C57BL6 mice (strain 000664) and R26YFP mice on C57BL6 background (strain 006148) mice were purchased from The Jackson Laboratory. Pax7CreERT2 mice on the C57BL6 background were kindly provided by Dr. Charles Keller (Oregon Health & Science University). $Pax3^{fl/fl}$ mice were kindly provided by Dr. Conway. Mice were bred to create the necessary experimental mice. $Pax3^{fl/fl}$ mice were bred with $Pax7^{CreERT2/CreERT2}$ mice to create conditional MuSC-specific Pax3 knockout mice ($Pax3^{cKO}$) and the wild type littermates (Pax3wt): $Pax7^{CreERT2/CreERT2}$; $Pax3^{fl/fl}$ and $Pax7^{CreERT2/CreERT2}$; $Pax3^{wt/wt}$. For lineage tracing, YFP was added to MuSCs using $R26^{YFP/YFP}$ mice to get the following genotypes: $R26^{YFP/YFP}$; $Pax7CreERT2^{/CreERT2}$; $Pax3fl^{fl/fl}$ ($Pax3^{cKO;YFP+}$) and $R26^{YFP/YFP}$;$Pax7^{CreERT2/CreERT2}$;$Pax3^{wt/wt}$ ($Pax3^{wt;YFP+}$).

Mice were housed in specific pathogen-free conditions in barrier-protected rooms under a twelve-hour light-dark cycle and were fed ad libitum. Male and female mice were used for analyses. All genotypes were confirmed by PCR. Wild-type littermate controls were used for all studies testing the effects of genetic deletions. All studies were done with mice aged 8-12 weeks unless otherwise noted. Tamoxifen (Sigma) was administered at the ages indicated via intraperitoneal injection at 80 mg/kg in 100% corn oil every other day for ten days.

B. MuSCs isolation

MuSCs isolation was performed following established protocol (L. Liu et al., 2015) with minor modifications. Lower hind-limb muscles or diaphragms were dissected and minced for about 5 minutes. Then each muscle was separately digested two times for the isolation of MuSCs, first with collagenase II for 30 minutes and then with collagenase II and dispase for 20 minutes.

In between digestions, tissues were washed and spun down. To further ensure homogenization and avoid clogging in the cell sorter, digested tissue was passed through a 20-gauge needle 10 times and then through 40 um Nylon cell strainer, washing the cells after each step. The resultant mononucleated cell suspension was stained for 15 minutes with antibodies (all from BD-Pharmingen) against cell surface antigens specific to the different cell types present in the sample. Antibodies were used to stain and negatively select endothelial cells (anti-CD31), leukocytes (anti-CD45), and mesenchymal stem cells (anti-Sca-1). MuSCs are negative for the mentioned 3 markers, they were stained for positive selection with anti-VCAM antibody and their purity was confirmed by re-sort or by Pax7 stain. Cells were sorted using a BD-FACS Aria II and III.

C. EdU incorporation

MuSCs (2–5 × 10^5 cells per chamber) were cultured on ECM (Sigma)-coated eight-well chamber slides (BD Biosciences) in Ham's F-10 medium with 10% horse serum. EdU (Thermo Fisher) was added to cell cultures at a concentration of 10 μM and refreshed every 12 h. Cells were with fixed with 3.7% PFA for 10 minutes. Subsequently, Click-it reaction (Thermo Fisher) was performed. Samples were incubated with 4′-6-diamidino-2-phenylindole (DAPI) for 10 minutes and imaged. Cell counting was performed manually.

D. Quantitative RT-PCR

Total RNA from satellite cells was isolated by using RNeasy Micro Kit (QIAGEN) for mRNA or mirVana miRNA Isolation Kit (Invitrogen) for miRNA. For mRNA analysis, isolated RNA was reverse transcribed, and qPCR was carried out on a LightCycler 480 system (Roche) using SYBR Green (Roche) and primers listed (Invitrogen). For miRNA analysis, mirVana qRT-PCR Primer Sets (Invitrogen) for miRNA specific reverse transcription including U6 snRNA as endogenous control were utilized according to the manufacturer's protocol, the reaction carried out on a LightCycler 480 system (Roche). Relative quantification of gene expression was calculated using the delta-CT method.

E. Immunohistochemistry

Freshly isolated tissues were fixed for 6 hours in 0.5% PFA, dehydrated overnight in 20% sucrose in PBS and cryoprotected with Tissue-Tek O.C.T. (Sakura, #4583) and frozen in cooled isopentane. 10 µm sections were obtained in a cryostat. Different primary antibodies (Table III.1) and secondary antibodies and fluorescent reagents (Table III.2) were used.

An antibody against the matrix protein laminin was used to mark the myofiber outline. Muscle matrix was stained with wheat germ agglutinin (WGA) (Kostrominova, 2011). For MuSCs staining, an antibody against the defining transcription factor of MuSCs, Pax7 (Y. X. Wang et al., 2014) was used. For the enhanced yellow fluorescent protein (eYFP) lineage tracer detection, anti-GFP antibodies were used because eYFP signal is too weak for direct detection. Different protocols were followed depending on the protein of interest.

Target	Species	Clonality	Dilution	Catalog #	Company
Pax7	Ms	Polyclonal	1 in 50	Pax7-c	DSHB
GFP	Rb	Polyclonal	1 in 500	A11122	Life Technologies
GFP	Ch	Polyclonal	1 in 200	Ab13970	Abcam
Laminin	Rt	Monoclonal	1 in 1000	Ab11576	Abcam

Table III.1. Primary antibodies. Ms for mouse; Rb for Rabbit; Ch for chicken; Rt for rat.

Target	Species	Conjugate	Dilution	Catalog #	Company
Mouse	Hs	Biotin	1 in 250	MKB-2225-.1	Vector
Rabbit	Dk	Biotin	1 in 500	65-614-0	Thermo Fisher
Chicken	Dk	Biotin	1 in 500	PA128657	Thermo Fisher
Rat	Dk	Biotin	1 in 500	A18749	Invitrogen
Streptavidin		A647	1 in 500	S32357	Invitrogen
WGA		A488	1 in 100	W11261	Thermo Fisher
DAPI			1 in 15000	D1306	Invitrogen

Table III.2. Secondary antibodies and fluorescent reagents. Hs for Horse; Dk for Donkey.

For Laminin and Pax7 staining:

9. **Section defrost**

Sections were thawed and dried at room temperature (RT).

10. **Fixation**

Sections were fixed in a 4% Paraformaldehyde (PFA) in Phosphate Buffer Saline (PBS) for 10 minutes at 4ºC.

11. **Wash**

To remove PFA, three washes in PBS for 5 minutes at RT were done.

12. **Permeabilization and blocking**

Section were permeabilized and blocked with 5% bovine serum albumin (BSA) in 0,3% Tween PBS (microscopy buffer) protected from light overnight at 4ºC.

Microscopy Buffer		
PBS	1X	10 mL
BSA	5%	0,5 g
Tween 20	0,3%	30 µL

Table III.3. Microscopy buffer.

13. **Laminin staining**

Primary antibody: sections were incubated with laminin antibody (Table III.1) in microscopy buffer protected from light overnight at 4ºC.

Wash: the excess of antibody was washed, 3 washes in 0,3% Tween in PBS buffer (washing buffer) for 10 minutes at RT.

Secondary antibody: sections were incubated in A647 conjugated anti-rat antibody (Table III.2) in microscopy buffer protected from light overnight at RT.

Wash: three washes in washing buffer for 10 minutes at RT.

Fluorescent labeling and DAPI staining: sections were incubated in Streptavidin and DAPI (Table III.2) in microscopy buffer protected from light for 20 minutes at RT.

Wash: three washes in washing buffer for 10 minutes at RT.

14. **Antigen retrieval**

This procedure allows to expose antigens that otherwise would not be accessible to the antibody. Samples are boiled in 1X HIER buffer for 30 minutes. Let them cold down and dry.

1X HIER buffer is prepared from 10X HIER buffer (stock) diluted in MQ H2O. The recipe for 10X HIER buffer is the following:

- Add 29,4 g sodium citrate in 800 mL of MQ H2O in a baker with a stirrer.
- Allow the citrate to dissolve and adjust the pH to 6.0 with 1N HCl.
- Fill to 995 mL and put it in a bottle.
- Add 5 mL Tween 20.
- Mix well and store at RT.

15. **Block**

Mouse on Mouse (MOM) blocking reagent (Vector, #MKB-2213) was used to block endogenous mouse immunoglobulins in mouse tissue section and allow mouse primary antibody staining. Section was blocked in MOM blocking reagent protected from light for two hours at RT.

16. **Pax7 and DAPI staining**

Primary antibody: sections were incubated with Pax7 antibody (Table III.1) in microscopy buffer protected from light overnight at 4ºC.

Wash: three washes in washing buffer for 10 minutes at RT.

Secondary antibody: sections were incubated in A647 conjugated anti-mouse antibody (Table III.2) in microscopy buffer protected from light overnight at RT.

Wash: three washes in washing buffer for 10 minutes at RT.

Fluorescent labeling and DAPI staining: sections were incubated in Streptavidin and DAPI (Table III.2) in microscopy buffer protected from light for 20 minutes at RT.

17. **Wash**

Three washes in washing buffer for 10 minutes at RT.

18. **Mounting and drying**

Once the staining was finish, a dot of FluorSave mounting medium (#345789, Millipore) was put on the slide. Slides were covered by a coverslip and left to dry protected from light overnight at RT.

For GFP staining:

0. **Section defrost**

Sections were thawed and dried at RT.

1. **Fixation**

Sections were fixed in a 4% PFA in PBS for 10 minutes at 4ºC.

2. **Wash**

To remove PFA, three washes in PBS for 5 minutes at RT.

3. **WGA staining**

Sections were stained with WGA (Table III.1) in PBS for 1 hour at RT.

4. **Wash**

To remove WGA excess, three washes in PBS for 10 minutes at RT.

5. **Permeabilization and blocking**

Sections were permeabilized and blocked in microscopy buffer protected from light overnight at 4ºC

6. **GFP staining**

Primary antibody: Sections were incubated in two GFP antibody (Table III.1) in microscopy buffer protected from light overnight for two days at 4ºC.

Wash: three washes in washing buffer for 10 minutes at RT.

Secondary antibody: sections were incubated in A647 conjugated anti-rabbit and anti-chicken antibodies (Table III.2) in microscopy buffer protected from light overnight at RT.

Wash: three washes in washing buffer for 10 minutes at RT.

Fluorescent labeling and DAPI staining: sections were incubated in Streptavidin and DAPI (Table III.2) in microscopy buffer protected from light for one hour at RT.

7. **Wash**

Three washes in washing buffer for 10 minutes at RT.

8. **Mounting an drying**

Once the staining was finished, a dot of mounting medium was put on the slide, and slides were covered by a coverslip and left to dry protected from light overnight at RT.

Imaging was performed with a Zeiss Observer Z1 fluorescent microscope (Carl Zeiss) with a Zeiss Objective Lens Plan and cooled CCD camera. To assess MuSC pool size, Pax7-positive cells and fiber numbers were quantified manually using Volocity (Quorum Technologies). Average myofiber diameters were determined by automatically quantifying the minimum Feret's diameter with the SIOX segmentation plugin for ImageJ and manually counting the number of fibers. IF stainings were performed and quantified blindly.

F. Treadmill running

Mice were trained for three consecutive days for ten minutes, running at a speed of 13 m/min. On the fourth day, mice were tested for 30 minutes, running at a speed of 13 m/min, with subsequent increments of 1 m/min every 30 min. Mice were removed from the treadmill at the point of exhaustion, which was defined at staying four seconds on the electric grid (Laker et al 2017). Mice that ran less than 30 minutes were removed from the analysis.

IV. Results

A. Pax3 increases the propensity of quiescent MuSCs to exit quiescent state

MuSCs in the diaphragm express the transcription factor Pax3, whereas MuSCs in most limb muscles do not (Boutet et al., 2012). Given the established role of Pax3 in driving cell proliferation during embryogenesis (Relaix et al., 2004) and in response to stress (Der Vartanian et al., 2019; Scaramozza et al., 2019), we investigated whether Pax3 might regulate the process of MuSC activation out of the quiescent state and into the cell cycle under homeostatic conditions in the adult.

To test directly whether Pax3 plays a role in the balance between MuSC quiescence and activation under homeostatic conditions, we conditionally deleted Pax3 from adult MuSCs using a Pax7-CreERT2 driver ($Pax3^{cKO}$ mice).

The three-month age was selected for the adult conditional deletion for two reasons. First, because Pax3 is expressed during development of skeletal muscle, central nervous system and neural crest derivatives (Boudjadi et al., 2018) and complete Pax3 knock out mice does not survive (Buckingham & Relaix, 2015). The second reasons is that postnatal MuSCs are actively dividing and lose their proliferative activity progressively, while adult MuSCs are quiescent (Buckingham & Relaix, 2015) and previous report showed that hindlimb muscles reached a steady state level of MuSCs cell fusion by 12 weeks of age (Pawlikowski et al., 2015). For those, reasons, in order to study adult MuSC behavior, and avoid any interference with skeletal muscle development and growth processes that occur thru adulthood, 3-month-old fully developed adult mice were used. The efficiency of $Pax3^{cKO}$ was tested in isolated MuSCs after recombination and the median reduction in Pax3 mRNA obtained was of 96% and 88% in diaphragm and hindlimb MuSCs respectively (de Morree et al., 2019).

In order to understand the mechanisms that determine the extent of MuSCs contribution to adult myofibers, we measured whether any MuSCs activate and enter the cell cycle in different skeletal muscles in the absence of injury. For that purpose 5-ethynyl-2′-deoxyuridine (EdU), a thymidine analogue which is incorporated into the DNA of dividing cells (Chehrehasa et al., 2009), was used. Mice were pulsed for three days with EdU, before we isolated the MuSCs and quantified the number of EdU positive cells. We observed higher levels of EdU incorporation in diaphragm, gracilis, and triceps MuSCs, which are known to express Pax3, compared to EDL MuSCs, which are known to not express Pax3. Pax3 deletion resulted in a significant decrease in EdU incorporation *in vivo* in MuSCs in the diaphragm and gracilis, a non-significant reduction in triceps and a much smaller decline in limb muscle MuSCs (Figure VI.1).

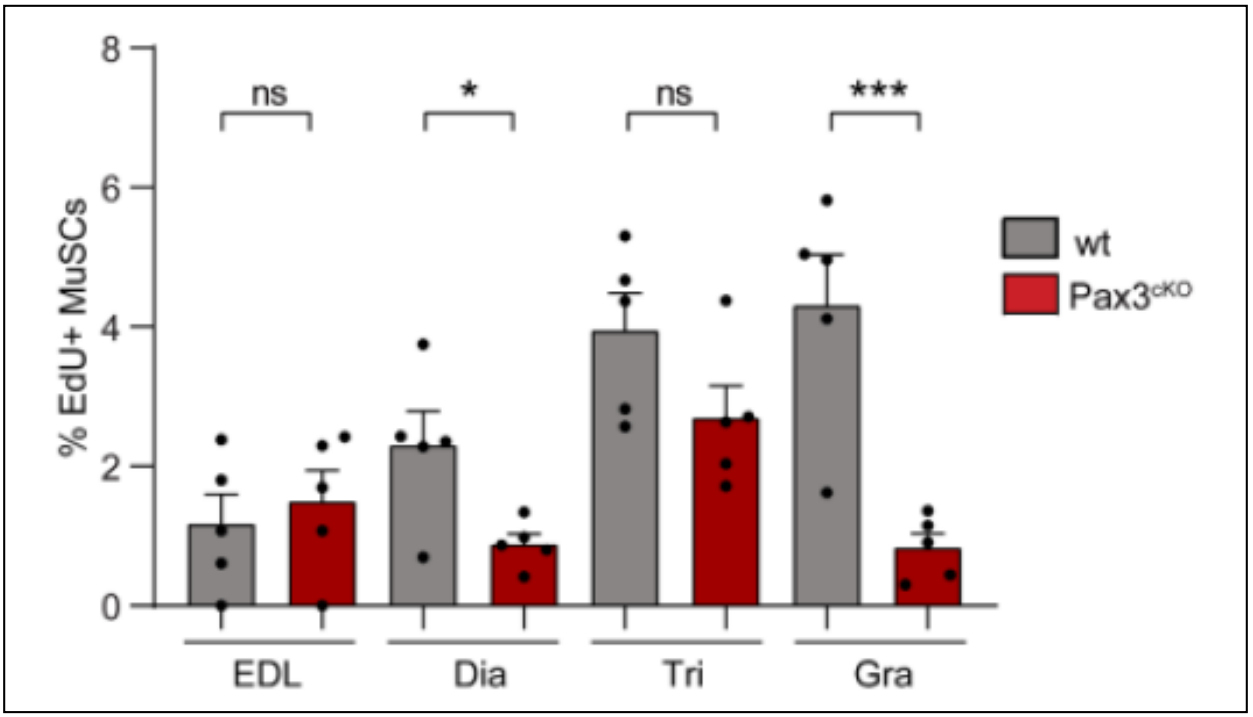

Figure IV.1. Percentage of EdU-positive cells for different muscles in WT and Pax3cKo mice. MuSCs were isolated from mice treated with EdU for three days, stained for EdU and counterstained with DAPI (n=5, mean + SEM, paired two-tailed t-test, *p<0.05). Dia: diaphragm; Tri: triceps; Gra: gracilis; TA: tibialis anterior; EDL extensor digitorum longus.

To further test the role of Pax3 in MuSC activation, we sought to increase Pax3 expression *in vivo*. Prior work from the Rando lab showed that the microRNA miR206 inhibits Pax3 expression in MuSCs isolated from hindlimb muscles (Boutet et al., 2012).

We therefore, analyzed miR206$^{-/-}$ mice for Pax3 expression, finding that although loss of miR206 does not lead to changes in Pax3 mRNA levels (Figure IV.2A), miR206$^{-/-}$ mice have increased levels of Pax3 protein in the limb but not in the diaphragm (Figure IV.2B), suggesting that, *in vivo*, miR206 inhibits Pax3 expression at the translational level.

Pax3 protein increases corresponded with increases in EdU incorporation in limb MuSCs, comparable to levels seen in the diaphragm (Figure IV.2C). In contrast, MuSCs in the diaphragm did not show increased Pax3 levels in the absence of miR206, consistent with prior findings (Boutet et al).

We conclude that Pax3 levels regulate the propensity of quiescent MuSCs to exit the quiescent state and enter the cell cycle.

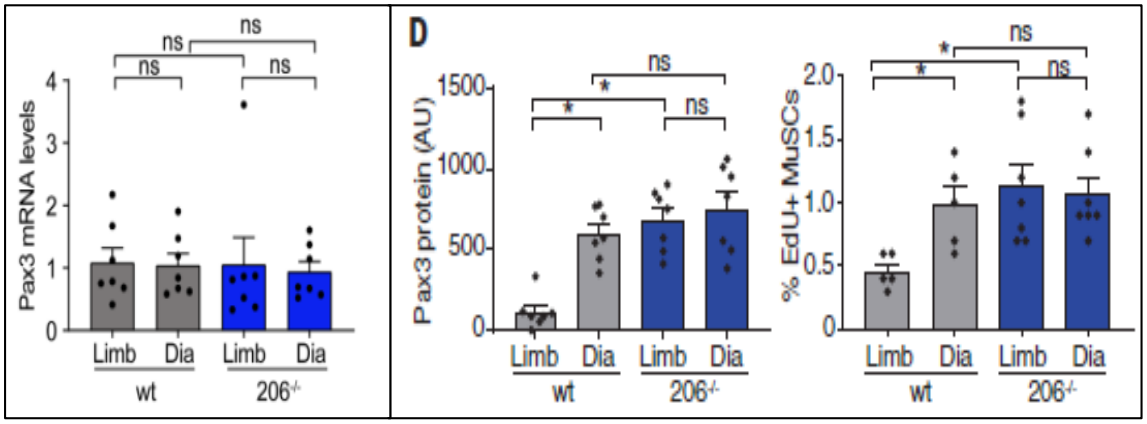

Figure IV.2. *Pax3* mRNA levels, Pax3 protein quantity and percentage of EdU-positive MuSCs for different muscles in WT and miR206-/- mice. *Pax3* mRNA levels values are relative to *Gapdh* and normalized to WT (A; n=8). MuSCs were isolated from mice treated with EdU for three days, stained for Pax3 protein (B; n=7) or EdU and counterstained with DAPI (C; n=5). Mean + SEM, paired 2-tailed test, *p<0.05. Dia: diaphragm; AU: arbitrary units.

B. The complex mechanism of alternative polyadenylation of Pax3 that controls muscle stem cell fate

The extent of miR206 regulation of Pax3 depends on the expression of different Pax3 mRNA isoforms. Previous results from the Rando Lab showed that longer Pax3 mRNAs are generated through the use of a distal polyadenylation site. These longer isoforms are subject to miR206-mediated translational repression, whereas shorter isoforms are produced when proximal polyadenylation sites are used, which produce a mRNA isoforms that do not contain miR206 targeting sequences and are therefore not susceptible to miR206 (Boutet et al., 2012).

In agreement with previous work, as explained in the previous section, we found that MuSCs isolated from hindlimb muscles express long *Pax3* transcripts whose expression is inhibited by miR206, while MuSCs isolated from diaphragm that express short *Pax3* transcripts are not affected. We also found that the level of Pax3 protein is directly related to the level of EdU incorporation (MuSCs activation).

mRNA length is controlled through polyadenylation, the addition of a polyadenosine tail to the 3' untranslated region (UTR) of an mRNA at polyadenylation signal sequences. To elucidate the underlying mechanisms that regulate differential polyadenylation of Pax3 mRNAs, we compared the expression of known alternative polyadenylation factors in MuSCs from hindlimb (which contain longer Pax3 mRNAs and lower PAX3 protein expression) and diaphragm (shorter Pax3 mRNAs and higher PAX3 protein expression). We observed increased levels of the small nucleolar RNA (snRNA) U1 in limb MuSCs compared to diaphragm MuSCs, but comparable levels of other known alternative polyadenylation factors. U1 snRNA is a small nuclear ribonucleoprotein (snRNP) that protects nascent mRNAs against premature transcription termination and polyadenylation (Berg et al., 2012; Kaida et al., 2010). Further experiments demonstrated that U1 snRNA could induce the expression of longer Pax3 transcript isoforms in

MuSCs *in vivo* and that it works through conserved motifs within the Pax3 transcript, modifying Pax3 protein levels and MuSCs activation (de Morree et al., 2019).

Altogether, we demonstrated that higher expression of U1 snRNA favors the use of the distal polyadenylation site in the 3' UTR of the Pax3 mRNA, leading to generation of longer Pax3 mRNAs and lower PAX3 protein expression owing to miR206-mediated repression (Figure IV.3). This is if not the first, one of the first examples of three classes of interacting RNAs, namely small nucleolar RNA, messenger RNA, and microRNA, to control stem cell state. Together, U1 snRNA, miR206, and Pax3 mRNA create a rheostat of Pax3 protein expression that controls spontaneous activation and cell cycle entry of MuSCs under homeostatic conditions.

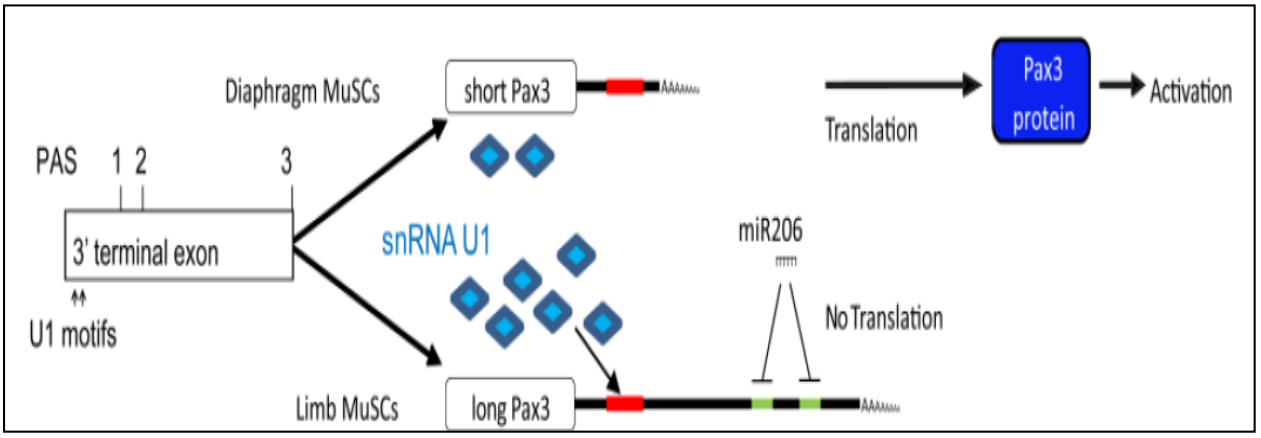

Figure IV.3. Model for Pax3 regulation by U1 snRNA and miR206. The Pax3 3' terminal exon has three functional polyadenylation sites (PAS1-3). MuSCs in the diaphragm express low levels of U1 snRNA, select a proximal polyadenylation site (1 or 2) and express short Pax3 isoforms that are translated into Pax3 protein. MuSCs in the limb express high levels ofU1 snRNA, select the distal polyadenylation site, and express long Pax3 isoforms that are targeted by miR206, leading to translation repression and no Pax3 protein.

C. In muscles in which MuSCs express high levels of Pax3, the conditional loss of Pax3 from MuSCs resulted in reduced MuSCs contribution to mature myofibers and smaller fiber size, and reduced functional performance.

While independent experiments from the Rando lab demonstrated the complex mechanism by which three classes of interacting RNAs control stem cell state, the physiological and functional relevance of Pax3 protein and MuSCs activation levels remained to be investigated.

Given that Pax3 is important for MuSCs activation and that $Pax3^{cKO}$ has reduced MuSCs EdU incorporation, we asked whether deletion of Pax3 from adult MuSCs would over time result in changes in the stem cell pool. To test this, we analyzed the MuSCs number per tissue section area in $Pax3^{cKO}$ muscles compared to WT using Pax7 staining. For that purpose, we induced recombination at 3 months and stained for Pax7 at two time points. First, after two weeks to see whether there was an immediate effect of Pax3 deletion. Secondly, on the long term, nine months after recombination, when mice are 12 months old, because it has been reported that MuSCs contributed to all muscles between 6 and 12 months but between 12 and 20 months MuSCs only continued to contribute to a subset of muscles (Keefe et al., 2015).

The results (Figure IV.1) did not show any differences, suggesting that Pax3 deletion does not affect the numbers of MuSCs during homeostasis.

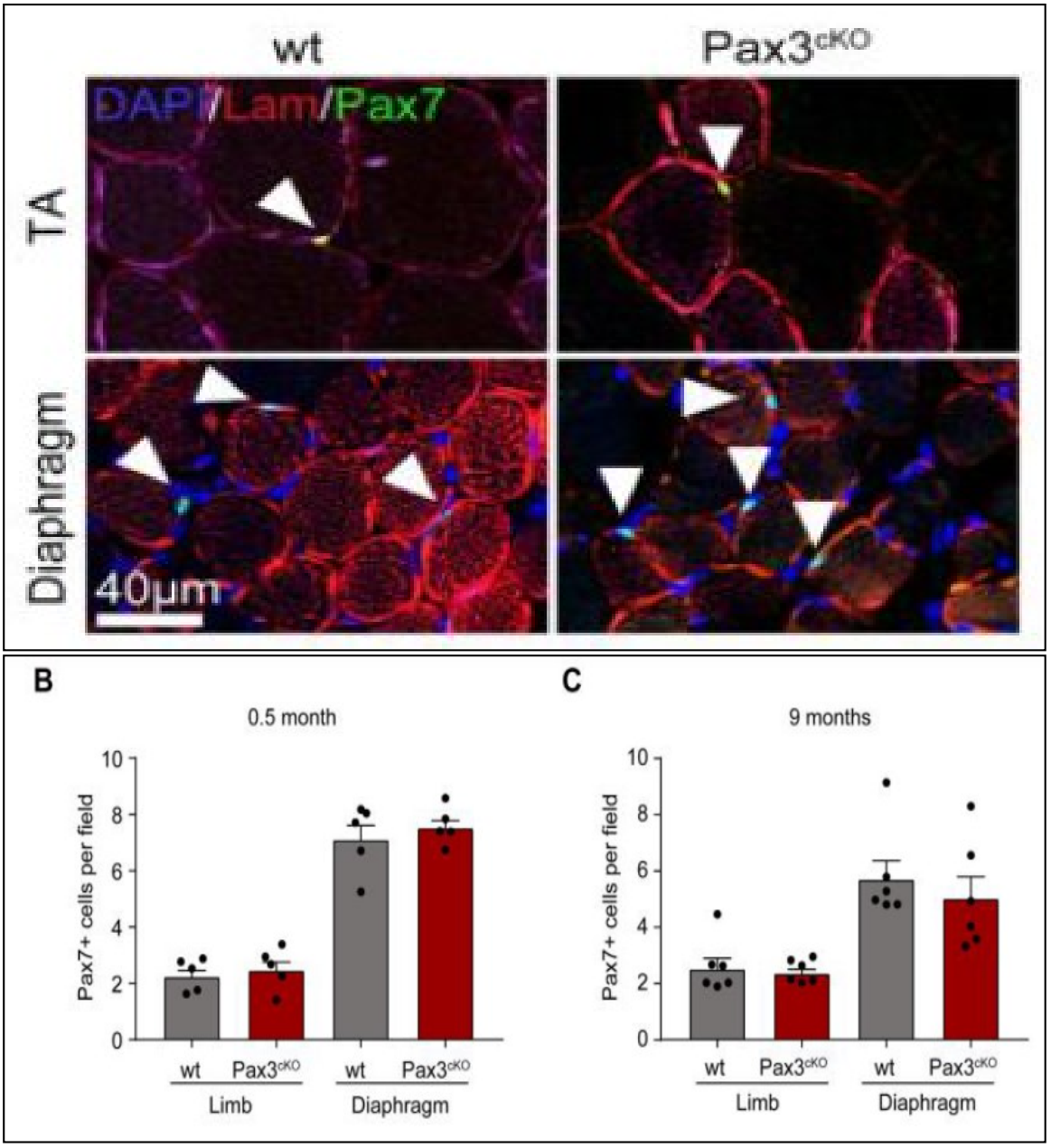

Figure IV.1. Pax7 staining and counts. A) TA and diaphragm muscles of Pax3wt and Pax3cKO stained with laminin (red) and Pax7 (green) and counterstained with DAPI (blue). Representative images are shown. Arrowheads indicated the Pax7-positive MuSCs under the basal lamina. B) and C) Graph of quantifications of Pax7-positive cells per field (n=5; mean + SEM, one-tailed Student's t-test).

Given that deletion of Pax3 reduced the basal activation of MuSCs but did not lead to any change in steady-state MuSC numbers, we asked whether deletion of Pax3 resulted in any change in MuSC fate. In this sense, it has been reported that the ablation of MuSCs led to a

modest atrophy in muscles with high rates of MuSC fusion (Keefe et al., 2015) and that the depletion of MuSCs resulted in reduced voluntary wheel running performance (Jackson et al., 2015), showing the relevance of MuSCs for maintaining skeletal muscle function.

First, the expression of the lineage tracer eYFP, in MuSCs of three-month old mice was tested, showing that over 80% of MuSCs become YFP positive (de Morree et al., 2019), validating the system.

The experiment was repeated, and nine months after induction, animals were sacrificed and the muscles stained for the lineage tracer eYFP (Figure IV.2). Consistent with previous reports (Keefe et al., 2015; Pawlikowski et al., 2015), we observed clear presence of YFP in myofibers, with roughly 60% of fibers positive in the diaphragm and 10% positive in the TA of WT mice. In $Pax3^{cKO;YFP+}$ mice fewer fibers stained positively for eYFP, suggesting that fewer MuSCs have fused with those fibers and therefore that $Pax3^{cKO}$ MuSCs give fewer progeny that can fuse with the fibers. We conclude that Pax3 expression determines the extent of MuSC contribution to mature myofibers during normal homeostatic turnover (Figure IV.3).

Previous work showed that ablation of MuSCs resulted in a mild atrophy in the diaphragm but not the TA (Keefe et al., 2015). We therefore asked whether deleting Pax3 from MuSCs would influence muscle fiber size. Indeed, after long-term deletion of Pax3 from MuSCs in adult mice, we observed a significant decrease in myofiber size in diaphragm muscles, which are high in Pax3-positive MuSCs, but not in TA muscles, which are low in Pax3 protein expression MuSCs (Figure IV.4).

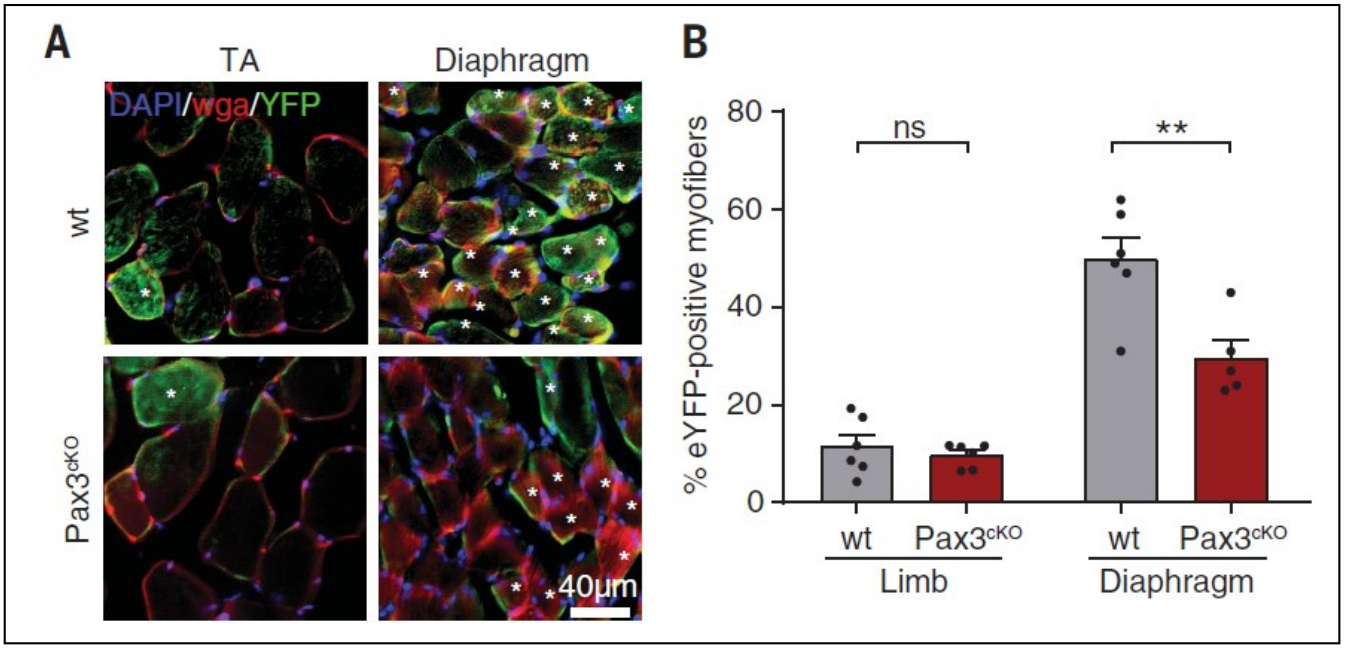

Figure IV.2. eYFP staining and counts. A) TA and diaphragm muscles of Pax3wt and Pax3cKO stained with WGA (red) and eYFP (green) and counterstained with DAPI (blue). Representative images are shown. Asterisks indicated eYFP-positive myofibers. B) Graph of quantifications of eYFP-positive myofibers (n=6; mean + SEM, two-tailed Student's test, **p< 0.01).

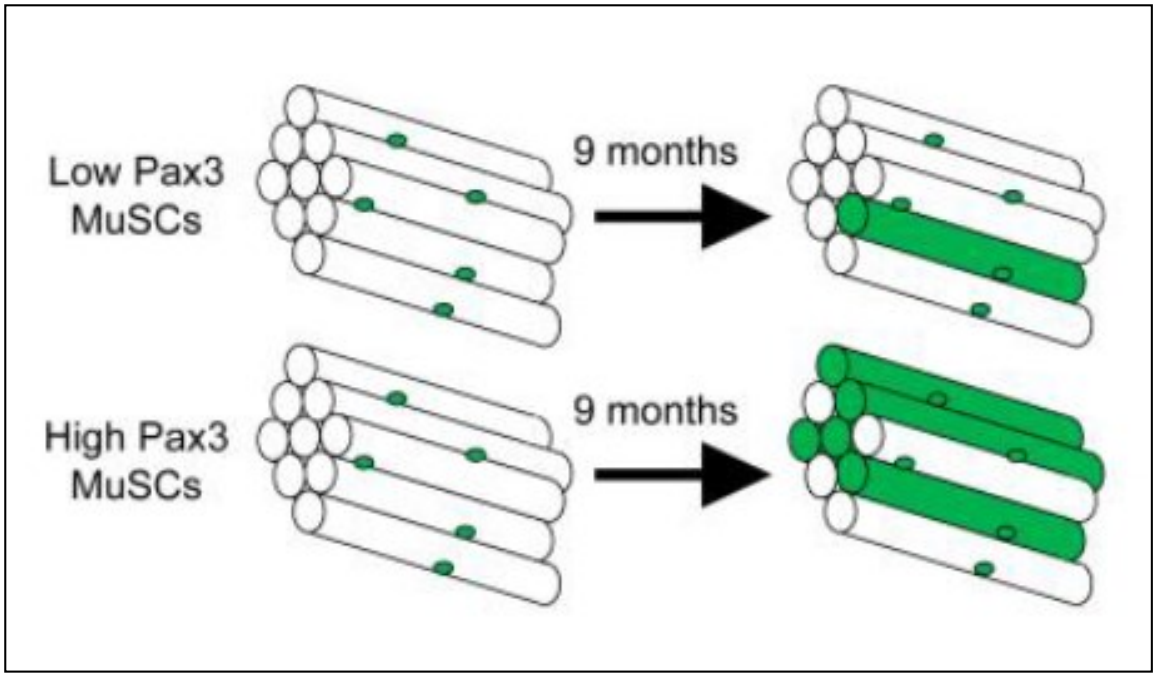

Figure IV.3. Schematic model of MuSC contribution to myofibers. Muscles with low Pax3 expression in the MuSCs give rise over time to a fewer progeny that fuse with existing myofibers than muscles with high Pax3 expression.

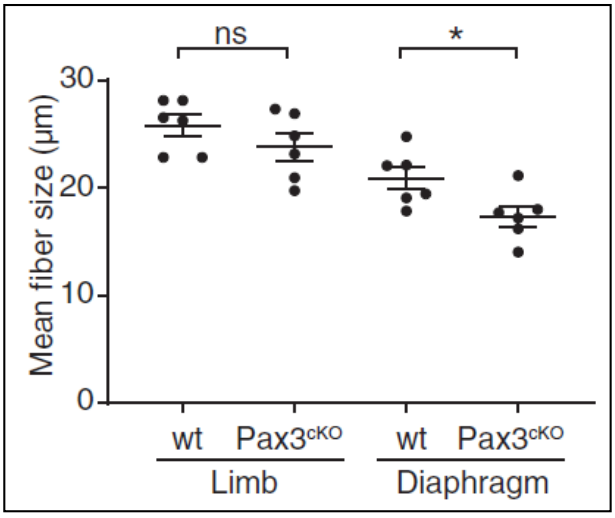

Figure IV.4. Graph of mean fiber diameter. n=6; mean + SEM, two-tailed Student's t test, *p<0.05.

We next asked whether this decrease in myofiber size impacts the physiology of the muscles. The loss or reduction of myofiber diameter is the hallmark histopathological feature of skeletal muscle atrophy. It results in functional impairment of the muscles and can be induced by a diversity of pathophysiologic conditions such as hereditary muscular disorder, disuse, denervation, aging, sepsis, cachexia or cancer (Dumitru et al., 2018). We assessed muscle function by measuring running distance in an endurance treadmill running assay. Pax3^{cKO} mice showed reduced performance with shorter distances run (Figure IV.5). Pax3^{cKO} mice also displayed a decrease in grip strength (de Morree et al., 2019). We conclude that in muscles in which MuSCs express high levels of Pax3, Pax3 expression in MuSCs is critical for structural and functional homeostasis of the tissue.

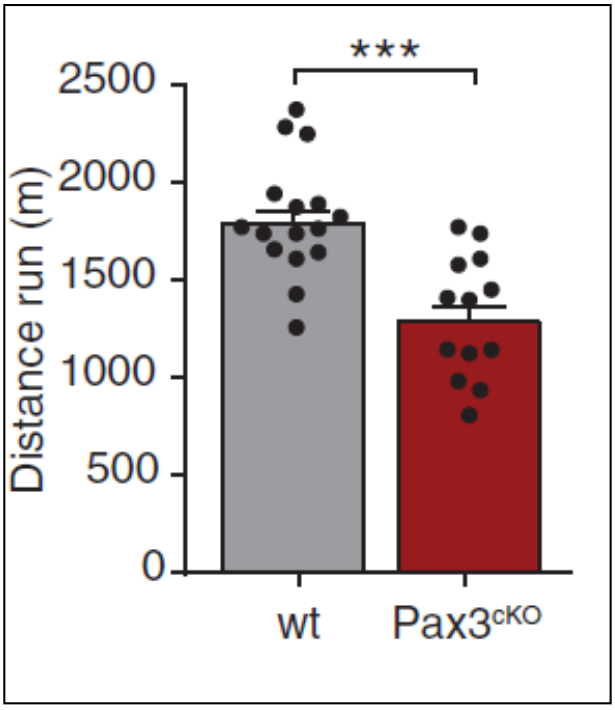

Figure IV.4. Results of endurance running protocol. Total distance was plotted for individual mice (n=15; mean + SEM). ***P < 0.001.

V. Discussion

The different experiments performed allowed us to understand Pax3 regulation, its effects in the MuSCs activation in different muscles and gave evidence of the functional relevance of Pax3 in MuSCs in vivo during homeostasis.

Our results on the EdU incorporation of MuSCs of different muscles showed that different muscles have different incorporation rates, in line with previous work that revealed widespread fusion of MuSCs with mature myofibers, with large differences in the levels of fusion between various muscles across the body (Keefe et al., 2015). The Pax3 deletion also resulted in muscle specific differences with a significant decrease in EdU incorporation *in vivo* in MuSCs in the diaphragm and gracilis, a non-significant reduction in triceps and a much smaller decline in limb muscle MuSCs.

Those different effects of Pax3 deletion in MuSCs activation in different muscles is the result of the muscle specific Pax3 isoform expression and regulation. Continuing previous work from the lab (Boutet et al., 2012) we have shown that when comparing wild type and miR206$^{-/-}$ mice, in tissues in which the MuSCs express long Pax3 isoforms, like hindlimb muscles, the Pax3 isoforms are susceptible of translational repression by miR206 but in tissues in which the MuSCs express short Pax3 isoforms, like the diaphragm, the isoforms are not affected by translational repression. The results showed again that Pax3 protein is directly related to the level of EdU incorporation (MuSCs activation). Independent experiments from the lab have demonstrated that U1 snRNA is responsible for alternative polyadenylation of Pax3, inducing long isoforms that are inhibited by miR206. Those results are in line with a previous report that demonstrated U1 snRNP ability to determine mRNA length and regulate isoform expression (Berg et al., 2012).

MuSCs in different muscles have different Pax3 isoforms expression that leads to different miR206 regulation of the protein expression. Muscles, such as the limb, expressing long isoforms have miR206 inhibition of Pax3 protein expression and low MuSCs activation. On the contrary, in MuSCs expressing short isoforms, such as in the diaphragm, do not suffer miR206 inhibition and express high levels Pax3 protein and have higher MuSCs activation. The $Pax3^{cKO}$ has no or little effect on MuSCs activation on the limb because Pax3 protein levels are already inhibited. Conversely, activation of MuSCs in the diaphragm, that have naturally higher levels of Pax3 protein, is significantly affected by $Pax3^{cKO}$ compared to wt.

Our results exploring the functional relevance of Pax3 in adult MuSCs in vivo during homeostasis using $Pax3^{cKO}$ mice revealed significant changes in the mature muscle, including reduced MuSC fusion and smaller myofibers after long-term deletion of Pax3 and point to a dominant role for Pax3 in driving MuSC fusion with mature myofibers to maintain muscle homeostasis. Our results are consistent with previous reports that ablation of MuSCs led to a reduction of myofiber size in muscles with high rates of MuSC fusion (Keefe et al., 2015). However, for a definitive proof of MuSCs fusion to adult myofibers to be a requirement for active maintenance of the muscle, the experiments should be repeated in a model of myoblast fusion. In this regard, there are available linage tracers, such us luciferase, that would make it possible to take quantitative measurements of MuSCs and their progeny by *in vivo* imaging. This kind of approach would allow the study of MuSC contribution to muscle fibers over time, increasing the understanding of the homeostatic maintenance of the muscle, and could also be employed for addressing the effects on regeneration and disease progression *in vivo*.

The smaller myofibers produced by Pax3 deletion led to impaired muscle function. The results of the forced treadmill assay and grip strength assay showed reduced performance levels in $Pax3^{cKO}$ mice. The forced treadmill is a short-term physiology assay we used because it is an easy to perform and controlled running test, that allowed us to evaluate running performance

without inducing changes in the muscles but further experiments should consider the use voluntary wheel-running test. As their names suggest, forced treadmill assay allows deciding the time and the intensity of the exercise while in the voluntary wheel running, mice were free to run at chosen time and intensity. A recent study comparing the metabolic effects of both assays (Y. J. Kim et al., 2020) has shown that compared with a 5 days/week forced treadmill regime mice, voluntary wheel mice run roughly 20-40 times longer. Mice exercised in the voluntary wheel also showed increased grip strength, muscle weight per total body weight and food intake than forced treadmill mice. Although both mouse groups showed a decreased body weight and fat mass, the mice exercised on treadmills showed increased levels of cortisol induced by stress. That report increases the interest to repeat the experiment using the voluntary wheel assay, and suggests that the observed effects may be even more marked than with the forced treadmill. A previous report studied the effect of MuSCs depletion on muscle function and showed reduced running speed and running distance in voluntary wheel running experiments that let to reduced grip strength in MuSCs depleted mice (Jackson et al., 2015). Those results suggest again that the lack of MuSC fusion to myofibers during homeostasis may be responsible for the observed muscle function impairments both induced by Pax3 deletion or MuSCs depletion. Altogether our results demonstrated that that MuSCs are not only required for skeletal muscle regeneration (Lepper et al., 2011; Murphy et al., 2011; Sambasivan et al., 2011) but also very relevant for homeostasis and maintenance of muscle function and Pax3 controls MuSC fate and function during homeostasis.

Based on those results future research should further investigate the observed changes in the uninjured mature muscle. It would be of interest to further investigate the link between muscle function and molecular changes resulting from long term Pax3 deletion. In line with that, conducting direct force measurements or comparing the forced treadmill versus the voluntary wheel running, would provide further insights in the nature and extent of the changes induced by

Pax3 deletion. In addition, it is well established that muscles have different fiber types. It will be interesting to correlate Pax3 expression to Myosin expression and fiber type abundance in the different muscles. However, future research shall not limit to the study of the effect of Pax3 deletion in an uninjured muscle but it needs also to elucidate its role in the context of muscle regeneration (injury) and disease.

All this could be combined with the *in vivo* pharmacological interventions like the ones described by de Morree et al. (de Morree et al., 2019), that are able to tune Pax3 protein expression through blocking different polyadenylation sites, and thereby modify MuSC proliferation. It would be of great interest to address if such interventions have an impact on muscle function *in vivo* and mimic the one observed by Pax3 deletion. If they would, they could potentially emerge as future therapeutic interventions.